

Chronic inflammatory pain

New molecules & mechanisms

Hanneke Willemen

The publication of this thesis has been kindly supported by Gilles Hondius Foundation, Patiëntenvereniging Complex Regionaal Pijn Syndroom (CRPS), Reumafonds, Fibromyalgie en Samenleving (F.E.S.); de Nationale Vereniging voor Fibromyalgie-patiënten, Harlan Laboratories, IITC Life Science.

Chronic inflammatory pain: New molecules & mechanisms
Dissertation, University of Utrecht, Utrecht, The Netherlands

Etch on cover v./v. V.V.? by Ad Willemen

Lithography Inducopy, Moerdijk

Printing Optima Grafische Communicatie, Rotterdam

ISBN 978-94-6169-355-6

Hanneke Willemen, Utrecht, The Netherlands, 2013. All Rights reserved. No part of this publication may be reproduced or transmitted in any form or by any means, electronic or mechanical, including photocopy, recording, or any information storage and retrieval system, without permission from the copyright owner.

Chronic inflammatory pain

New molecules & mechanisms

Chronische ontstekingspijn

Nieuwe moleculen & mechanismes

(met een samenvatting in het Nederlands)

Proefschrift

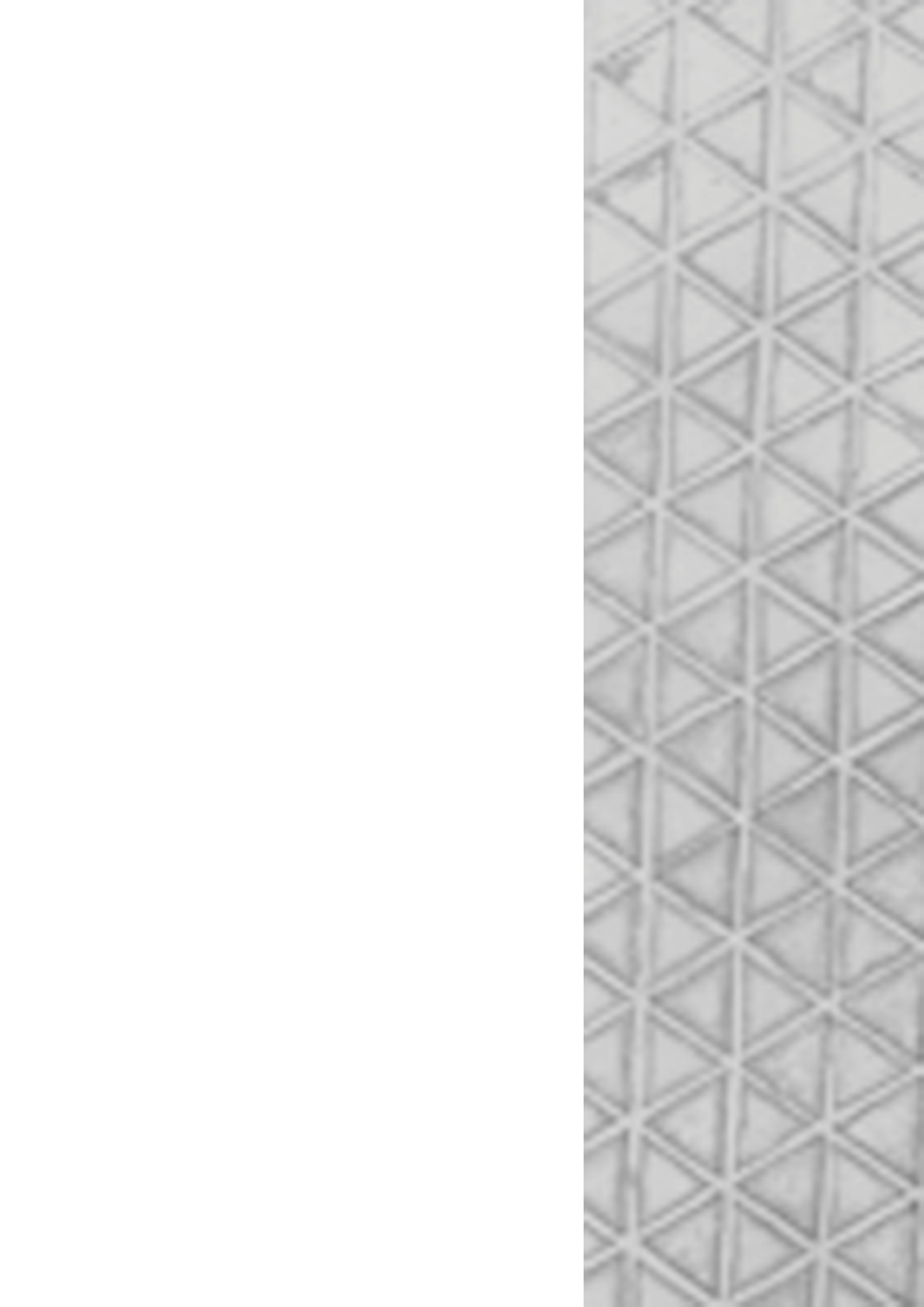
ter verkrijging van de graad van doctor aan de Universiteit Utrecht
op gezag van de rector magnificus, prof.dr. G.J. van der Zwaan,
ingevolge het besluit van het college voor promoties
in het openbaar te verdedigen op
woensdag 10 april 2013 des ochtends te 10.30 uur

door

Hanneke Lucia Dorothea Maria Willemen

geboren op 21 maart 1982 te 's-Hertogenbosch

Promotoren: Prof.dr. C.J. Heijnen
Prof.dr. A. Kavelaars
Co-promotor: Dr. N. Eijkelkamp



CONTENTS

Chapter 1	General introduction	1
Chapter 2	Microglial/macrophage GRK2 determines duration of peripheral IL-1 β -induced hyperalgesia: contribution of spinal cord CX3CR1, p38 and IL-1 signaling <i>PAIN (2010) 150: 550-560</i>	11
Chapter 3	MicroRNA-124 as a novel treatment for persistent hyperalgesia <i>Journal of Neuroinflammation (2012) 9: 143</i>	31
Chapter 4	Peripheral monocytes/macrophages control resolution of inflammatory pain <i>Submitted</i>	47
Chapter 5	A novel p38 MAPK docking groove-targeted compound is a potent inhibitor of inflammatory hyperalgesia <i>Submitted</i>	63
Chapter 6	Genome-wide association study meta-analysis of chronic widespread pain: evidence for involvement of the 5p15.2 region <i>Annals of the Rheumatic Diseases (2012)</i>	81
Chapter 7	Summary and discussion	119
	References	135
	Nederlandse samenvatting	149
	Dankwoord–Acknowledgements	155
	List of publications	161
	Curriculum Vitae	165

1

General introduction

Pain perception

Pain is an important self-protecting signal. The pain system detects and reacts to (withdrawal reflex) the presence of an acute potentially injurious stimulus such as heat, pressure, tissue damage or inflammation to avoid possible (further) tissue damage. However, after inflammation or tissue damage has resolved, persistent pain can develop without further protective or restorative goal. Persistent or chronic pain has become a major health problem in many countries, especially because there is no effective medication available to prevent or combat chronic pain states. Chronic pain involves spontaneous pain in the absence of a pain-inducing stimulus, but is also often associated with an increased pain response to a painful stimulus (*hyperalgesia*). In addition, patients suffering from chronic pain frequently report that pain is experienced in response to a stimulus that normally does not evoke pain, such as light touch or a slight increase in temperature (not heat); this phenomenon is known as *allodynia*. Examples of chronic pain are neuropathic pain or inflammatory pain. Neuropathic pain is a consequence of nerve trauma and can develop in patients with spinal cord injury, diabetic mellitus, carpal tunnel syndrome, multiple sclerosis or it can develop after chemotherapy¹⁸⁴. Inflammatory pain is often observed in patients with rheumatoid arthritis, inflammatory bowel diseases and fibromyalgia^{57,261}. However, inflammatory pain can also be initiated during neuropathic disorders, since during nerve injury chemokines are produced to recruit leukocytes/granulocytes. These leukocytes/granulocytes locally produce inflammatory mediators that can contribute to both pain and may afflict damage to nerve terminals¹⁵⁵. In addition, people can develop chronic pain even when the inflammation has resolved, known as post-inflammatory pain. For example, the human herpes virus Varicella zoster induces primary infections and produces localized skin lesions and damage to sensory nerves, leading to development of neuropathic pain. However, when the lesions are healed and the inflammation has resolved, chronic pain can develop and post-herpetic neuralgia will develop as a chronic pain state⁷⁶. World-wide chronic pain is a major clinical problem and effective pain-killers are urgently needed. However, pain is a complex trait since many neurobiological processes based on genetic and environmental characteristics play a role in the aetiology of chronic pain. Moreover, there is limited understanding of the mechanisms leading to transition from acute to chronic pain. In this thesis I mainly focused on the investigation of *neurobiological mechanisms underlying transition from acute to chronic inflammation-induced pain* (Chapter 2-5) and in addition the investigation on the genetic contribution to chronic pain (Chapter 6).

Nociceptors

All painful stimuli are detected by the peripheral terminal of specialized sensory neurons (nociceptors). When nociceptors are triggered by noxious stimuli (heat, cold, mechanical stress, certain chemical agents), sensory nerve fibers become activated and transmit information via the cell body in the dorsal root ganglion (DRG) to a central nerve terminal in the spinal cord. Nociceptive neurons can be divided in medium or small sized neurons with axons belonging to A δ or C-fibers, respectively. A δ -fibers are fast-conducting myelinated fibers and are mostly involved in transmitting signals from mechanical noxious stimuli and produce the well-known feeling of sharp pain. However, the majority of nociceptors exist of unmyelinated C-fibers, which have a relatively low conduction velocity. These fibers respond to noxious temperatures (cold < 5°C and heat > 45°C) and to mechanical or chemical stimulation, and generate a burning type of pain¹⁸⁷. The A δ and C-fibers terminate mainly inside the dorsal horn of the spinal cord where they transmit the pain signal to the so called “wide dynamic range” neurons. These neurons transport the pain signal via the spino-thalamic tract (STT) to the thalamus; a site in the brain

where a behavioral response is coordinated⁴⁶. Under certain conditions the main area to control pain perception is in the spinal cord. For example, when a person touches a hot object a rapid withdrawal (< 0.5 seconds) movement is initiated to protect against possible tissue damage²¹⁴. In this example mainly C-fibers are activated and transmit pain signals to the spinal cord. Motor neurons in the spinal cord are activated to control the contraction of the muscles in the affected area. The spinal cord is the main area to control the withdrawal reflex, rather than the brain, and is therefore also known as spinal reflex⁷.

Pain hypersensitivity

Peripheral sensitization

During tissue damage or inflammation, a large variety of mediators (including cytokines, chemokines, histamines, prostaglandins, ATP, growth factors) are released to modify the nociceptor so that the threshold for activation reduces and/or signaling intensity increases. This phenomenon is known as peripheral sensitization (i.e., occurring in the peripheral nervous system)⁸¹. Under noxious stimulation, this process can lead to an increased responsiveness (hyperalgesia) and a reduced threshold (allodynia) of the nociceptors involved²⁶². Normally, nociceptors recover from this sensitization soon after the tissue heals or the inflammation resolves. However, the acute transient hyperalgesia does not always resolve and subsequently chronic pain may develop.

Peripheral sensitization mechanisms

Two processes are important for the development of peripheral sensitization. Firstly, post-translational modifications of the signaling proteins and/or ion channels in the nociceptors may occur as a response. The majority of these modifications involve kinases (which can be activated by different inflammatory mediators) that phosphorylate the various proteins. This can have dramatic consequences for the properties of the protein. For example, nociceptors express different ion channels (Na⁺, Ca⁺, K⁺), which define the excitability of the nociceptor terminal. When ion channels are activated, they will open rapidly and initiate a specific signaling cascade. Phosphorylation of sodium channels lowers the threshold allowing a lower threshold for opening of the channel or longer duration of opening of the channel. Consequently, a stimulus to the nociceptor terminal will evoke a larger response⁶³. The second process that can contribute to peripheral sensitization is dependent of changes in protein expression and reorganization of the cell⁸. Signals initiated by inflammatory mediators can be transmitted from the nociceptor terminal along the axon or nerve fiber to the cell body in the DRG. In the DRG, the expression of particular genes can be increased (increase in transcription) and/or more protein can be produced (increase in translation). The newly synthesized proteins are transported back to the nociceptor terminal, where they will contribute to peripheral sensitization. For example, transient receptor potential vanilloid type 1 (TRPV1) is an ion channel that is activated by noxious heat, acid and capsaicin (compound in hot chili peppers). During inflammation or tissue damage inflammatory mediators (e.g. prostaglandins, bradykinin, nerve growth factor (NGF) and chemokines) result in increased expression of TRPV1 in the DRG, leading to increased expression of the receptor in the nociceptor terminal^{109,270}. There it contributes to increased responsiveness of the nociceptor terminal after a noxious (hyperalgesia) or innocuous (allodynia) stimulus. In addition, changes in ion channels can also cause an increase in the excitability of the nociceptor terminal in the absence of a stimulus resulting in spontaneous firing of the neuron. Furthermore, A- and C-fibers can be injured after peripheral nerve injury,

which results in spontaneous firing of the peripheral neuron and in turn initiates the development of chronic pain¹⁰¹. It is known that the development of chronic pain is not only dependent on peripheral mechanisms but is also mediated by the central nervous system.

Central sensitization

Peripheral sensitization can lead to central sensitization, since the output from primary afferent nociceptors is affected. In addition, the sensitivity of the wide dynamic range neurons located inside the spinal cord can be altered, which leads to an increase in the excitability of those neurons contributing to central sensitization. As a result, those sensitized neurons are activated and start producing inflammatory substances which can induce a pain response by directly activating the neuron and/or start activation of microglia and astrocytes. Many different mechanisms can contribute to the phenomenon of central sensitization and thereby the development of chronic pain. Some important aspects will be discussed below.

Central sensitization mechanisms

Neuronal-dependent sensitization mechanisms

In response to peripheral sensitization, the central terminals of the nociceptors release signaling molecules (e.g. glutamate, substance P, CGRP, BDNF). These signaling molecules act on the specific neuronal receptors in the spinal cord thereby initiating and activating signaling cascades leading to phosphorylation of receptors and ion channels. For example, the neurotransmitter glutamate is released from the primary afferent neuron and mainly binds to the N-methyl-D-aspartate (NMDA) receptor (Ca²⁺channel), the α -amino-3-hydroxy-5-methyl-4-isoxazole-propionic acid (AMPA) receptor and kainate receptor (both ion channels for Na⁺) expressed on wide dynamic range neurons in the spinal cord. This leads to phosphorylation of the channels, consequently lowering the threshold for opening of these channels and thereby increasing the excitability of these neurons, which results in increased responsiveness to noxious stimulation^{126,253}. Beside neurons also non-neuronal cells, like glia inside the spinal cord, can become activated via these mediators.

Glia-dependent

It has long been thought that the main function of glia cells was to physically support neurons, transport nutrients to neurons, destroy pathogens, remove cell debris and/or neurotransmitters and to maintain the integrity of the blood-brain barrier. However, there is increasing evidence that glia activation also regulates neuronal signaling and responsivity and is thus crucial for the development of chronic pain. The two main subtypes of glia cells are microglia and astrocytes.

Microglia

During inflammation or tissue damage, spinal cord microglia activation is initiated by neuronal signals (e.g. ATP, glutamate, chemokines, cytokines) which results in the production and release of substances that act on neurons and microglia, contributing to the development of chronic pain. Under normal circumstances, microglia are in a quiescent state. It has been suggested that neurons produce a so called “off-signal” (e.g. TGF- β , CX3CL1, BDNF) to keep microglia in a “resting” phenotype¹⁰. Similar to macrophages, microglia change their phenotype when they are activated as a consequence of a loss of inhibitory signals (e.g. CD200-CD200R interaction) and/or increase in activating signals (e.g. ATP, glutamate, pro-inflammatory cytokines)^{10,152}. Activation status of microglia/macrophages can be subdivided into two main subtypes, known as pro-inflammatory (M1-type) and anti-inflammatory (M2-type). These two activated types can

be discriminated by the expression of specific markers on their cell surface, and are characterized by expression of pro-inflammatory factors such as inducible nitric oxide synthase (iNOS) and interleukin (IL)-1 β (in M1 microglia/macrophages), or anti-inflammatory cytokines including transforming growth factor (TGF)- β and IL-10 (in M2 microglia/macrophages)^{69,120}. The factors released during both activation states have an important effect on the neurons and consequently the pain response. For example, activated microglial cells release pro-inflammatory factors (M1-factors), like IL-1 β , tumor necrosis factor (TNF)- α and prostaglandin E2 (PGE2) that interact with their receptors expressed on neurons. This will increase neuronal excitability and chronic pain can develop^{38,133,255}. On the other hand, the effects of M2-factors (IL-10 and TGF- β) are thought to regulate the neuronal response indirectly, by inhibiting the production of pro-inflammatory mediators by glial cells. It has been suggested that the initiation of the fractalkine pathway is a cause for the production of inflammatory mediators and consequently for the maintenance of chronic pain. The fractalkine pathway is an important mechanism for neuro-microglia communication since fractalkine is expressed on neurons, whereas its receptor CX3CR1 is mainly expressed on microglia/macrophages in the spinal cord^{38,249}. It has been hypothesized that under conditions of pain primary afferent neurons produce high extracellular ATP levels to induce the release of the lysosomal cysteine protease cathepsin S (CatS) located in spinal microglia. Subsequently, CatS cleaves and liberates fractalkine expressed on neuronal membranes. The soluble fractalkine interacts with the fractalkine receptor (CX3CR1), which is only expressed on microglia and initiates the p38 MAPK-pathway. p38 MAPK activation promotes the release of pro-inflammatory mediators (e.g. nitric oxide (NO), IL-1 β) which in turn sensitize the sensory system and maintain microglia activation, resulting in chronic pain³⁸. Therefore, the activation of the p38MAPK signaling pathway is an important source for the production of inflammatory mediators. It has been shown in several animal models of chronic pain, that p38 MAPK is upregulated and that pain hypersensitivity can be transiently blocked by p38 MAPK inhibitors^{61,111}. Furthermore, the development of chronic pain can be suppressed by pretreating the animals with minocycline (an inhibitor of microglia / macrophage activation), indicating a crucial role for microglia in the regulation of chronic pain^{61,136,198}.

Not only neuronal signals are the regulators of microglia activation. There are studies that suggest that under certain pathological conditions, peripheral monocytes/macrophages access the CNS to regulate the microglia activation state. Some of those studies investigated the role of monocytes/macrophages on the injury or repair on the damaged spinal cord or nerve. However, those studies described contradictory results and the effect of peripheral monocytes/macrophages on pain response is still unclear.

Astroglia

The exact role of astroglia (astrocytes) in the context of pain has been less studied than that of microglia. It is known, however, that astrocytes also contribute to chronic pain, and have a different role than the microglia. In general, it is thought that microglial cells play an important role in the early phase of central sensitization, providing a fast response to nerve damage or chronic inflammation. Astrocytes, however, have a slower and more permanent activation profile, suggesting that activated astrocytes have a role in the maintenance of the hyperalgesia. There is also some speculation that astrocytes can contribute to the termination of hyperalgesia by expressing immunosuppressive factors, which in turn inhibit microglia activation^{83,166,180}.

SNP's in pain genes

Recent research shows that genetic factors can also play an important role in the development of chronic pain. It has been demonstrated that pain hypersensitivity can be initiated by mutations in specific “pain genes”. A mutation in a gene can be caused by a change of one single nucleotide, also known as single-nucleotide polymorphism (SNP). During the past several years, SNP's have been found in genes involved in both the peripheral and the central nervous system. The most studied gene in relation to pain is COMT (catechol-O-methyltransferase); an enzyme that degrades neurotransmitters including dopamine, adrenaline and noradrenaline. A particular SNP (SNP rs4680) in this gene can result in a COMT enzyme with a reduced thermostability, and decreased enzymatic activity. This has been associated with reduced opioid activity and increased pain sensitivity^{146,199}. Furthermore, SNP's in genes that encode for ion channels (e.g. SCN9A, TRPA1 and TRPV1), opioid receptors (e.g. OPRM1 and OPRD1), enzymes (e.g. GCH1 and MAOA) and transcription factors (NRSF and NRSE) have been described, all related to pain perception^{72,171}. So in recent years progress has been made to understand pain genetics. However, there is still enough to be investigated, since there are many complex interactions between environmental and genetic factors that can potentially contribute to the development of chronic pain.

GPCRs and GRKs

G protein-coupled receptors (GPCRs)

Numerous pain signaling molecules (e.g. chemokines, neurotransmitters and neuropeptides) signal through G protein- coupled receptors (GPCRs). GPCR signaling plays an essential role during pain perception. Proper termination of GPCR signaling is essential to protect cells against overstimulation (sensitization). Upon GPCR stimulation, G protein-coupled receptor kinases (GRKs) are important to turn off (desensitization) the responsiveness of the GPCR. In general, GPCRs are bound to heterotrimeric G-proteins, composed of $G\alpha$, $G\beta$ and $G\gamma$ subunits that are in an inactive GDP bound state. Upon receptor stimulation, conformational changes in the GPCR occur, which allows it to act as a guanine nucleotide exchange factor (GEF). This GEF activity promotes the exchange of bound GDP on $G\alpha$ for GTP and the activated $G\alpha$ subunit dissociates from the $G\beta\gamma$ subunit. Depending on the $G\alpha$ subtype ($G_{\alpha s}$, $G_{\alpha i/o}$, $G_{\alpha q/11}$, $G_{\alpha 12/13}$) specific intracellular signaling cascades will initiate, such as the cAMP signaling pathway and the phosphatidylinositol signaling pathway^{202,254}. Furthermore, phosphorylation sites on the activated GPCR are unmasked which will allow GRKs to phosphorylate the receptor. In turn, those phosphorylated sites act as binding sites for members of the β -arrestin family. After binding of β -arrestin to the GPCR, the G-protein will be uncoupled from the receptor, thereby terminating receptor signaling (desensitization). Proper termination of GPCR signaling is crucial to prevent the cell against over activation. Further desensitization is achieved by internalization of the receptor; consequently the receptor will be recycled and transported back to the membrane. In addition β -arrestin acts as a scaffold protein and can initiate intracellular signaling pathways. In conclusion, GRKs are crucial in controlling GPCR signaling, by preventing cells from overstimulation^{70,127,192}.

GRK2

The GRK family consists of seven members (GRK1-7) grouped in 3 subfamilies based on sequence homology. The first group is that of the rhodopsin kinases or visual GRKs, GRK1 and GRK7, which are expressed in retinal rods and cones, respectively. Second, the GRK2-like subfamily, first known as β -adrenergic receptor kinase includes GRK2 and GRK3. Third, the GRK4-like family, consisting of GRK4, GRK5 and GRK6^{1,64,151,188}.

Interestingly, GRK2 is expressed in all tissues examined so far with specially high levels of expression in cells of the immune and nervous system^{149,243}. GRK2 is the most studied member of the GRK family and regulates desensitization of several GPCRs. Cells with reduced GRK2 levels display prolonged and/or more pronounced signaling in response to activation of GPCRs²⁴³. More recent evidence indicates that GRK2 cannot only regulate cellular signaling at the level of GPCRs, but also by direct interaction with non-GPCR substrates, such as members of the MAP kinase family (e.g. p38 MAPK and MEK1/2), components of the PI3kinase signaling pathway (e.g. PI3 kinase and Akt), cytoskeletal elements (e.g. tubulin and ezrin) and the cAMP sensor EPAC^{60,112,124,185}. Thus GRK2 can have many functions in regulating intracellular signaling.

GRK2 expression levels can be up-regulated or down-regulated, which has been observed in different pathological conditions. For example, patients with the inflammatory disease rheumatoid arthritis or multiple sclerosis have reduced GRK2 protein levels in peripheral blood mononuclear cells^{147,242}. In line with these findings, GRK2 present in leukocytes was reduced in response to inflammation in animal models of these diseases (adjuvant arthritis and EAE)^{148,240}. In cell culture, pro-inflammatory mediators have been shown to reduce GRK2 in several cell types^{123,147,150,200}. Therefore increased levels of inflammatory mediators may reduce GRK2 levels in conditions of chronic inflammation.

GRK2 and pain

The first evidence that GRK2 was associated with pain perception came after the finding that spinal cord GRK2 levels were decreased in a rodent model of neuropathic pain¹²³. To investigate more in detail the contribution of GRK2 in pain perception, special GRK2 knockout mice were generated. A homozygous knockout model for deletion of GRK2 in all cells is not available, since homozygous GRK2 knockout mice die in utero. However, heterozygous GRK2 knockout mice (GRK2^{+/-} mice) are available. In these mice, the level of GRK2 is reduced by approximately 35-55% in all tissues examined so far^{61,107,242}.

In the first study examining the contribution of GRK2 to inflammatory pain, the development of thermal and mechanical hyperalgesia in response to an acute peripheral inflammatory stimulus in control wild type (WT) and GRK2^{+/-} mice was investigated. Injection of carrageenan (seaweed extract) in the paw of WT mice induces acute thermal hyperalgesia which lasts for 2-3 days. Interestingly, the same injection in GRK2^{+/-} mice resulted in increased and markedly prolonged hyperalgesia; in GRK2-deficient mice it takes approximately 3 weeks to completely resolve the hyperalgesia^{61,123}. Carrageenan induces an inflammatory soup, so a large number of different receptors for inflammatory mediators on nociceptors are activated, which in turn activates multiple intracellular signaling cascades. This makes it more difficult to understand the underlying mechanisms that contribute to the development of chronic pain. Further evidence that low GRK2 promotes the transition from acute to chronic pain comes from studies using a single injection of an inflammatory mediator (e.g. PGE2, CCL3, epinephrine, IL-1 β) to induce hyperalgesia or allodynia. All tested inflammatory mediators markedly prolonged the hyperalgesia in GRK2^{+/-} mice^{60,61,245}.

The development of chronic hyperalgesia is not only the result of a complex interaction between different signaling cascades. As mentioned above, the interplay between different cell types including peripheral neurons, wide dynamic range neurons, microglia and astrocytes contribute to the development and maintenance of hyperalgesia. Therefore, cell specific GRK2 knockout mice were generated to understand at which level of pain processing GRK2 deficiency is contributing to the transition to chronic pain. Results of studies in mice with a cell specific reduction in one of the main players in the pain response have allowed more detailed understanding of the mechanisms contributing to transition to chronic pain. For example, a selective reduction of GRK2 in nociceptors increased acute hyperalgesia and prolonged hyperalgesia induced by carrageenan. However, this prolongation was not sufficient to mimic the 3 weeks of carrageenan-induced hyperalgesia observed in mice with low GRK2 in all cells. Conversely, low GRK2 levels in LysM-positive cells (i.e. microglia/macrophages/granulocytes) does not have any effect on acute carrageenan-induced hyperalgesia, but significantly prolongs its duration. In the carrageenan model, the reduced level of GRK2 in microglia/macrophages of LysM-GRK2^{+/-} mice is sufficient to cause the transition to chronic hyperalgesia with a duration similar to that of observed in mice with low GRK2 in all cells. Low GRK2 levels in astrocytes did not affect the course of inflammatory-induced hyperalgesia. In addition, GRK2 levels are reduced in microglia/macrophages isolated from lumbar spinal cord in a rodent model of neuropathic pain⁶¹. Collectively, these previous findings all indicate that GRK2 is an important regulator of spinal cord microglia/macrophage activation and thereby can regulate the duration of inflammatory-induced hyperalgesia.

Outline of the thesis

The main aim of the studies described in this thesis was to investigate the role of GRK2 in inflammatory hyperalgesia and to unravel neurobiological downstream mechanisms (**Chapter 2-4**). Furthermore, we developed and tested a potential therapeutic drug to alleviate chronic pain (**Chapter 5**) and investigated genetic variants in patients with chronic widespread pain (**Chapter 6**).

In **Chapter 2** we determined whether ongoing inflammation changes GRK2 expression in spinal microglia/macrophages. Subsequently, we investigated whether and how reduced GRK2 in microglia/macrophages regulates the duration of hyperalgesia induced by a single peripheral injection of IL-1 β and which signaling cascades are involved.

In **Chapter 3** we investigated the contribution of microRNA-124 to regulation of hyperalgesia and microglia/macrophage activation in GRK2-deficient mice. Subsequently, we determined whether low GRK2 is associated with the expression of the M1 and M2 phenotype in spinal-cord microglia. In addition, we investigated the effect of miR-124 treatment in chronic inflammatory and neuropathic pain in WT mice.

In **Chapter 4** we investigated whether peripheral monocytes/macrophages contribute to the course of IL-1 β -induced hyperalgesia. In addition we determined whether adoptive transfer of WT, GRK2^{+/-} and IL-10 bone marrow-derived monocytes can prevent the transition to persistent IL-1 β -induced hyperalgesia in LysM-GRK2^{+/-} mice.

In **Chapter 5** we developed a novel p38 MAPK compound as a potential therapeutic drug to treat inflammation-induced chronic hyperalgesia. Subsequently, we tested whether this new compound can attenuate carrageenan-induced chronic pain.

In **Chapter 6** we identified genetic variants in patients with chronic widespread pain by a large-scale hypothesis-free genome-wide association study (GWAS). Subsequently we studied expression levels of the nearest two genes in mice with inflammatory-induced chronic pain.

In **Chapter 7** all findings are summarized and discussed. Furthermore, concluding remarks and implications for future research are presented.

A large, white, serif-style number '2' is centered on a vertical strip. The strip has a repeating geometric pattern of triangles and diamonds in a light gray color. The rest of the page is white.

2

Microglial/macrophage GRK2 determines duration of peripheral IL-1 β -induced hyperalgesia: Contribution of spinal cord CX3CR1, p38 and IL-1 signaling

Hanneke L.D.M. Willemen^{1*}

Niels Eijkelkamp^{1,2*}

Huijing Wang¹

Robert Dantzer²

Gerald W. Dorn II³

Keith W. Kelley²

Cobi J. Heijnen^{1,2}

Annemieke Kavelaars^{1,2}

* These authors contributed equally to this manuscript

¹ Laboratory of Neuroimmunology and Developmental Origins of Disease (NIDOD), University Medical Center Utrecht, 3584 EA Utrecht, The Netherlands.

² Integrative Immunology and Behavior Program, College of ACES and College of Medicine, University of Illinois at Urbana-Champaign, Urbana, IL 61801, USA

³ Center for Pharmacogenomics, Washington University, St. Louis, MI 63110, USA.

Abstract

Chronic pain associated with inflammation is a major clinical problem, but the underlying mechanisms are incompletely understood. Recently, we reported that GRK2^{+/-} mice with a ~50% reduction of GRK2 develop prolonged hyperalgesia following a single intraplantar injection of the pro-inflammatory cytokine interleukin-1 β (IL-1 β). Here we show that spinal microglia/macrophage GRK2 is reduced during chronic inflammation-induced hyperalgesia. Next, we applied CRE-Lox technology to create mice with low GRK2 in microglia/macrophages/granulocytes (LysM-GRK2^{f/+}), or sensory neurons or astrocytes. Only mice deficient in microglial/macrophage/granulocyte GRK2 display prolonged IL-1 β -induced hyperalgesia that lasts up to 8 days. Two days after intraplantar IL-1 β , increased microglial/macrophage activity occurs in the lumbar but not thoracic spinal cord of GRK2-deficient mice. Intrathecal pre-treatment with minocycline, an inhibitor of microglia/macrophage activation, accelerates resolution of hyperalgesia independent of genotype and prevents transition to chronic hyperalgesia in GRK2^{+/-} mice. *Ongoing* hyperalgesia in GRK2^{+/-} mice is reversed by minocycline administration at days 1 and 2 after IL-1 β injection. Similarly, IL-1 β -induced hyperalgesia in LysM-GRK2^{f/+} mice is attenuated by intrathecal administration of anti-CX3CR1 to abrogate fractalkine-signaling, the p38 inhibitor SB239063 and the IL-1 antagonist IL-1ra. These data establish that chronic inflammatory hyperalgesia is associated with reduced GRK2 in microglia/macrophages and that low GRK2 in these cells is sufficient to markedly prolong hyperalgesia after a single intraplantar injection of IL-1 β . Ongoing hyperalgesia is maintained by spinal microglial/macrophage activity, fractalkine signaling, p38 activation and IL-1 signaling. We propose that chronic inflammation decreases spinal microglial/macrophage GRK2, which prevents silencing of microglia/macrophage activity and thereby contributes to prolonged hyperalgesia.

Introduction

Pain associated with inflammation is an important clinical issue and can persist long after resolution of inflammation^{155,216}. Peripheral inflammation increases the response to painful stimuli via direct actions of inflammatory mediators such as interleukin-1 β (IL-1 β) on primary sensory neurons^{11,100,216}. This peripheral sensitization rapidly but transiently increases excitability of primary nociceptors and leads to a transient increase in the response to noxious stimulation¹⁰⁰. Modulation of inflammatory hyperalgesia also takes place at the level of the spinal cord, and glial cells have been implicated in this process^{55,166}. However, the neurobiological mechanisms underlying inflammation-associated pain have only begun to be unraveled. Very little is currently known about the intra- and intercellular pathways that contribute to *resolution* of inflammatory hyperalgesia.

G protein-coupled receptor kinase 2 (GRK2) belongs to a family of seven G protein-coupled receptor kinases^{188,202}. GRK2 phosphorylates agonist-activated G protein-coupled receptors (GPCRs), leading to receptor desensitization and internalization^{202,244}. GRK2 can also interact with elements of several intracellular signaling pathways, including Akt, MEK1/2, phosphoinositide-3 kinase (PI3 kinase) and p38 MAPK, as well as various cytoskeletal elements^{185,205}. These two pathways allow GRK2 to regulate intracellular signaling not only in response to GPCR activation but also independent of GPCRs. An example of this last mechanism is the enhanced *in vitro* cytokine response of macrophages or microglia from GRK2^{+/-} mice following Toll-like receptor (TLR)4 stimulation^{177,185}. During the past several years, we have developed evidence for a role of GRK2 in regulating chronic pain. At the correlational level, we established that GRK2 in neurons of the spinal cord dorsal horn is reduced in two models of neuropathic pain, i.e. chronic constriction injury in rats and partial spinal nerve transection in mice^{123,125}. In addition, GRK2 levels are reduced in microglia/macrophages isolated from the lumbar spinal cord in the L5 spinal transection model of neuropathic pain in rats⁶¹. Moreover, thermal hyperalgesia induced by transient inflammatory stimuli, such as carrageenan, the GPCR-binding chemokine CCL3 and the pro-inflammatory cytokine IL-1 β , is markedly prolonged in GRK2^{+/-} mice that express only 40-60% of normal GRK2 levels⁶¹. These data strongly suggest GRK2 to be a crucial molecule in actively suppressing events that are associated with thermal prolonged hyperalgesia.

The aim of experiments reported here was to test the hypothesis that reduced GRK2 in microglia/macrophages is critical for prolonging the duration of inflammatory pain and to investigate the underlying mechanisms. We first determined whether ongoing inflammation changes GRK2 expression in spinal cord microglia/macrophages. Subsequently, we investigated whether and how reduced GRK2 in microglia/macrophages regulates the duration of hyperalgesia induced by a single peripheral injection of IL-1 β . For this purpose, we compared mice heterozygous for deletion of GRK2 only in microglia/macrophage generated using CRE-Lox technology and littermate controls. As a control, we used mice with low GRK2 specifically in primary sensory neurons or in astrocytes.

Materials and Methods

Animals

Female C57Bl/6 mice (12-14 weeks) heterozygous for targeted deletion of the GRK2 gene (GRK2^{+/-}) and their WT littermates were used^{61,107}. In addition, mice with cell-specific reduction of GRK2 were generated using CRE-Lox technology; GFAP-GRK2^{f/+}, LysM-GRK2^{f/+}, Na_v1.8-

GRK2^{f/+} and control GFAP-GRK2^{+/+}, LysMGRK2^{+/+} or Na_v1.8-GRK2^{+/+} offspring were generated by breeding heterozygous GFAP-CRE (Jackson laboratories, Bar Harbor, ME, USA), homozygous LysM-CRE (Jackson laboratories) or homozygous Na_v1.8-CRE transgenic mice²²⁴ with heterozygous GRK2-Lox mice (GRK2^{f/+})¹⁵⁶. Heterozygous floxed GRK2 mice were used to obtain a similar reduction in GRK2 levels as in GRK2^{+/-} mice. LysM-GRK2^{f/f} mice were generated by breeding LysM-GRK2^{f/+} with homozygous GRK2-Lox mice. The mice were genotyped by PCR analysis on genomic DNA. They were bred and maintained in the animal facility of the University of Utrecht (The Netherlands). All experiments were performed in accordance with international guidelines and approved by the Experimental Animal Committee of University Medical Center Utrecht.

Carrageenan paw inflammation, spinal microglia/macrophage isolation and immunohistochemical staining

The mice received an intraplantar injection of 20 µl λ-carrageenan (2 % (w/v), Sigma-Aldrich, St. Louis, MO, USA) in saline in both hind paws. At day 6 after carrageenan, they were sacrificed and spinal cord lumbar enlargements of 4 mice were pooled. Spinal cords were ground briefly using a glass Potter in 4 ml ice-cold Hanks' balanced salt solution (HBSS, Gibco, Carlsbad, CA, USA), containing 15 mM *N*-2-hydroxyethylpiperazine-*N'*-2-ethanesulfonic acid (Gibco) and 0.5% glucose (Sigma-Aldrich). Suspensions were passed through a 70-µm cell strainer (BD Biosciences, Alphen aan de Rijn, The Netherlands), the cells were centrifuged at 400*g* for 7 min. at 10°C and resuspended in 75% Percoll (GE Healthcare, Uppsala, Sweden) in HBSS. A density gradient consisting of 4 ml cells in 75% Percoll, 3 ml 50% Percoll, 3 ml 35% Percoll, and 2 ml dPBS (Gibco) was centrifuged (1000*g* for 20 min. at 10°C). The cells at the 50/75% interface were collected, washed in ice-cold DPBS, and resuspended in DPBS containing 1% Bovine Serum Albumin. The cells were rapidly centrifuged onto a microscope slide using a cytospin centrifuge.

The cells were fixed in acetone at -20°C for 5 minutes. Slides were blocked in PBS containing 0.1% saponin and 2% BSA and 2% normal goat serum and incubated with rabbit-anti-GRK2 (1:100, Santa Cruz Biotechnology, Santa Cruz, CA) and rat-anti-CD11b (1:200, BD Biosciences). The specificity of GRK2 staining was controlled by using primary anti-GRK2 antibody blocked with a GRK2 blocking peptide (Santa Cruz Biotechnology). Specificity of CD11b staining was controlled by using isotype control antibody. Staining was visualized using alexa488-conjugated goat-anti-rabbit antibody and alexa594-conjugated goat-anti-mouse (1:200, Invitrogen, Paisley, UK) and slides were stained with Dapi (Sigma-Aldrich). Using this procedure, more than 95% of the isolated cells were CD11b positive. The cells were photographed with a Zeiss Apotome Microscope (Zeiss, Oberkochen, Germany) and GRK2 levels in CD11b+ cells were analyzed with ImageJ software.

IL-1β-induced hyperalgesia

The mice received an intraplantar injection in the hind paw of 5 µl recombinant mice IL-1β (200 ng/ml or 20 ng/ml; Peprotech, Rocky Hill, NJ, USA) diluted in saline. Heat withdrawal latency times were determined using the Hargreaves (IITC Life Science, Woodland Hills, CA) test as described⁸⁹. Intensity of the light beam was chosen to induce a heat withdrawal latency time of approximately 8 s at baseline. Mechanical allodynia was measured with von Frey hairs (Stoelting, Wood Dale, USA) and the 50% paw withdrawal thresholds were calculated as described²⁸. Baseline withdrawal latencies were determined on three consecutive days. On the third day, the mice received an intraplantar injection of IL-1β. Intraplantar injection of saline did

not induce detectable hyperalgesia in any of the genotypes. All behavioral experiments were performed by an experimenter blinded to treatment and in a randomised set up.

Drug administration

Intrathecal (i.t) injections were performed as described by Hylden and Wilcox¹⁰³ under light isoflurane/O₂ anesthesia. The following drugs were injected i.t. in a volume of 5 µl: minocycline (30 µg in PBS^{61,233}; Sigma-Aldrich), mouse recombinant fractalkine (1 ng in saline³⁵; R&D systems, Minneapolis, MN, USA), rabbit anti-rat CX3CR1 (1 µg in saline³⁵; Torrey Pines Biolabs, NJ, USA) or normal rabbit IgG (1 µg in saline; Upstate, Millipore, MA, USA), p38 inhibitor SB239063 (5 µg in 10% DMSO in saline²⁵; Sigma-Aldrich), PI3 kinase inhibitor LY294002 (5 µg in saline²⁶⁴; Sigma-Aldrich), IL-1ra (10 ng in saline¹³⁵; R&D systems).

Intraperitoneal administrations of minocycline (50 mg/kg¹⁹⁸) were performed at day 1 and day 2 after intraplantar IL-1β injection.

Immunohistochemistry spinal cord slices and paw biopsies

Two days after intraplantar IL-1β mice were deeply anesthetized with sodium pentobarbital (50 mg/kg, i.p.), and perfused intracardially with saline followed by 4% paraformaldehyde in PBS. Spinal cords were removed, post-fixed in 4% paraformaldehyde for 6 hours at 4°C, equilibrated in 30% sucrose, and mounted in OCT compound (Optimal Cutting Temperature compound; Sakura, Zoeterwoude, The Netherlands). Transverse spinal cord sections (10 µm) of thoracic segments T8-T10 and lumbar segments L2-L4 were cut using a cryostat. The sections were blocked in 5% normal goat serum (NGS) and 0.1% Triton X-100 in PBS. They were then incubated overnight at 4°C with 1:200 rabbit anti-Iba-1 (Wako Pure Chemical Industries, Japan) and binding was visualized using alexa488-conjugated goat-anti-rabbit antibody (1:200; Invitrogen). The slides were analyzed for Iba-1⁺ cells with a Leica TCS-NT confocal microscope.

Paw biopsies were fixed in 4% paraformaldehyde, embedded in paraffin, blocked with 5% NGS in PBS/0.5% Triton X. The sections were incubated with 1:200 rabbit anti-Iba-1 (Wako) monoclonal antibody followed by incubation with 1:200 goat-anti-rabbit biotin (Vector Laboratories, Burlingame, CA, USA). Staining was visualized using Vectastatin ABC kit (Vector Laboratories) and diaminobenzamide (DAB) (Sigma-Aldrich).

Primary microglia and macrophage isolation

To control for effective cell-specific deletion or reduction of GRK2 expression, we analyzed GRK2 protein levels in peritoneal macrophages and primary microglia. The macrophages were collected from the peritoneal cavity after intraperitoneal injection of 3 ml RPMI-1640 (Gibco) using CD11b micro beads and a MACS column (Miltenyi Biotec, Bergisch Gladbach, Germany). Mixed primary cultures of cortical astrocytes and microglia were obtained from 1-day-old mice. Cortices were dissected after removal of meninges and blood vessels, minced and incubated with 0.25% trypsin for 15 min. in Grey's balanced salt solution containing 100 U/ml penicillin, 100 µg/ml streptomycin and 30 mM D(+)-glucose. The cells were dissociated and cultured in poly-L-ornithine (15 µg/ml)-coated culture flasks in DMEM/Ham's F10 (1:1) supplemented with 10% FCS, 2 mM glutamine and antibiotics as stated above. After 10-12 days, the flasks were shaken for 3 h at 37°C to collect microglia.

Total cell lysates were prepared in RIPA buffer (20 mM Hepes pH 7.5, 1% Triton X-100, 150 mM NaCl, 10 mM EDTA and protease inhibitors (Sigma-Aldrich)) for 30 min. at 4°C followed by 15 min. centrifugation at 13,000 rpm.

Western Blotting

Protein concentrations of the total cell lysates were determined using a protein assay (Bradford assay, Bio-Rad, Alphen a/d Rijn, The Netherlands). Protein samples (20 µg) were separated by 10% SDS-PAGE and transferred to nitrocellulose membranes (Hybond-C, Amersham Biosciences, Roosendaal, The Netherlands). The membranes were stained with 1:300 rabbit anti-GRK2 or 1:2000 goat anti-β-actin (both Santa Cruz Biotechnology) followed by incubation with 1:5000 donkey anti rabbit-HRP (Amersham Biosciences) or 1:5000 donkey-anti-goat-HRP (Santa Cruz Biotechnology). Specific bands were visualised by chemiluminescence (ECL, Amersham Biosciences) with X-ray film exposure. The films were scanned with a GS-700 Imaging Densitometer and analyzed with Quantity One Software (Bio-Rad).

Real-time RT-PCR

Total RNA was isolated from thoracic and lumbar spinal cord or paw biopsies with Trizol (Invitrogen). One microgram of total RNA was used to synthesize cDNA with SuperScript Reverse Transcriptase (Invitrogen). The real-time PCR reaction was performed with iQ5 Real-Time PCR Detection System (Bio-Rad) using the following primers:

- CatS forward: CggCgTCTCATCTgggAAAAG, reverse: gAgCACCCATCCgACACAAg
- Fractalkine forward: gCgAgTgACTACTAggAg, reverse: gATTCgTgAggTCATCTTg
- CX3CR1 forward: TgTCCACCTCCTTCCCTgAA, reverse: TCgCCCAAATAACAggCC
- IL-1β forward: CAACCAACAAGTgATATTCTCCATg, reverse: gATCCACACTCTCCAgCTgCA

Data were normalized for GAPDH expression. GAPDH forward: TgAAgCaggCATCTgAggg, reverse CgAAggTggAAgAgTgggAg.

MPO-activity

MPO-activity in paw biopsies was determined as described before⁵⁹. Briefly, frozen paw biopsies were homogenized in 50 mM Hepes buffer (pH 8.0) using a Potter homogenizer. Homogenates were centrifuged for 30 min at 10,000g at 4°C, the pellets were used to determine myeloperoxidase (MPO) activity.

Statistical Analysis

All data are presented as mean ± SEM. Two-way ANOVA with Bonferroni post-tests was used to analyze the effect of time or location and genotype.

Results

GRK2 levels are decreased in spinal cord microglia/macrophages during inflammatory hyperalgesia

The first question we addressed is whether ongoing peripheral inflammation is associated with changes in GRK2 expression in spinal cord microglia/macrophages. The rationale to perform these experiments was to determine whether GRK2 in spinal cord microglia/macrophages is reduced under pathophysiological conditions. To answer this question, we used the high dose carrageenan model of paw inflammation¹⁰⁰. WT mice received an intraplantar injection of carrageenan at a dose that induces prolonged inflammation and hyperalgesia (20 μ l, 2%⁹⁸). At 6 days after intraplantar carrageenan, thermal sensitivity (heat withdrawal latency at baseline 8.5 ± 0.2 s) was increased indicating ongoing hyperalgesia (decrease in heat withdrawal latency;

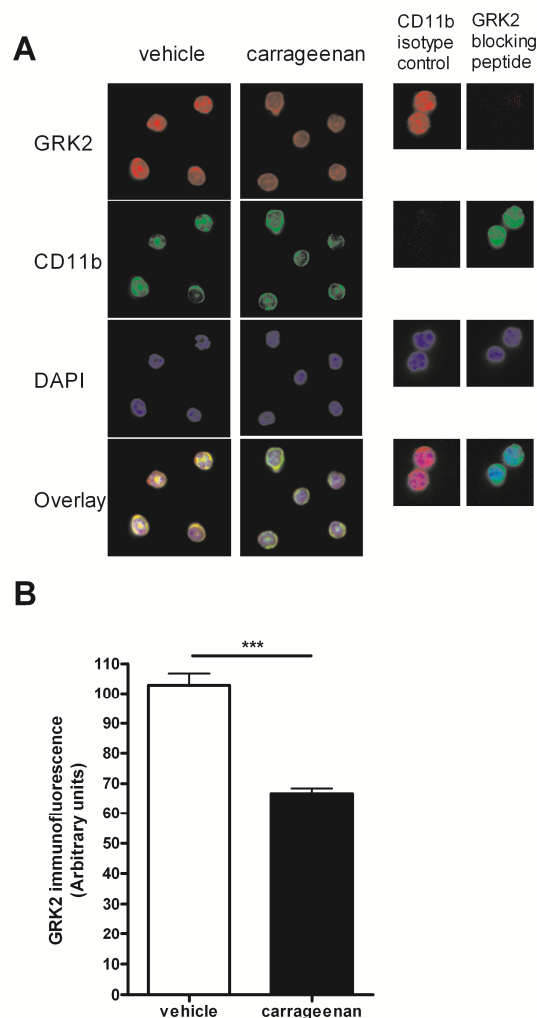


Figure 2.1: GRK2 levels in spinal microglia/macrophages during inflammatory hyperalgesia. (A) GRK2 expression in microglia/macrophages isolated from lumbar spinal cord at 6 days after intraplantar carrageenan or saline administration was compared by immunofluorescence analysis. Representative pictures of GRK2, CD11b and DAPI-staining of isolated microglia/macrophages. (B) GRK2 expression was quantified in approximately 60 cells per group on three different slides each containing microglia/macrophages from spinal cord of 4 mice per group. Data are expressed as mean SEM. *** $p < 0.001$.

vehicle $1.34 \pm 2.14\%$; carrageenan: $39.33 \pm 2.92\%$, $n = 12$ per group; $p < 0.01$) and paw thickness (baseline 1.47 ± 0.02 mm) was increased (vehicle: $0.94 \pm 5.72\%$, carrageenan: $48.69 \pm 8.37\%$, $n = 4$ per group; $p < 0.001$) indicative of ongoing inflammatory activity. At this time point, the mice were sacrificed and microglia/macrophages were isolated from lumbar spinal cord to determine the level of GRK2 protein by immunohistochemistry. We used this approach because our earlier studies showed that GRK2 levels in microglia/macrophages cannot be determined reliably in tissue sections due to the high level of expression of GRK2 in spinal cord neurons that masks the microglial/macrophage signal^{123,125}. As is shown in figure 2.1, GRK2 protein level in microglia/macrophages isolated from lumbar spinal cord of carrageenan-treated mice was reduced by approximately 40% as compared to microglia/macrophages from spinal cord of saline-treated controls. These findings indicate that ongoing peripheral inflammation and the associated ongoing hyperalgesia co-occur with a reduction in GRK2 protein levels in spinal cord microglia/macrophages. In the next set of experiments we focused on the effect of reduced GRK2 in microglia/macrophages on hyperalgesia induced by the cytokine IL-1 β .

IL-1 β -induced hyperalgesia and mechanical allodynia are prolonged in GRK2-deficient mice

Homozygous GRK2 knockout mice die in utero and therefore we used GRK2^{+/-} mice and WT littermate controls to determine the contribution of GRK2 to the regulation of hyperalgesia. We have shown before that the level of GRK2 in tissues from heterozygous GRK2^{+/-} mice is reduced by 40-60%^{61,125,177}. The cytokine interleukin-1 β was used to induce hyperalgesia because this cytokine is known to induce transient hyperalgesia in WT animals¹¹.

As expected, IL-1 β -induced hyperalgesia was transient in WT mice and completely disappeared within 1 day (Figure 2.2A). In GRK2^{+/-} mice, the acute phase of hyperalgesia was similar to that observed in control mice until 6 h after IL-1 β . However, the hyperalgesic response of GRK2^{+/-} mice lasted significantly longer than that of WT mice. Baseline thermal sensitivity was not affected by reduced GRK2⁶¹. To investigate whether the lack of effect of low GRK2 on *acute* hyperalgesia during the first 6 h after intraplantar IL-1 β was due to a ceiling effect, a lower dose of IL-1 β (0.1 ng/paw) was injected intraplantarly. Also at this lower dose, the magnitude of acute hyperalgesia was similar in WT and GRK2^{+/-} mice (Figure 2.2B).

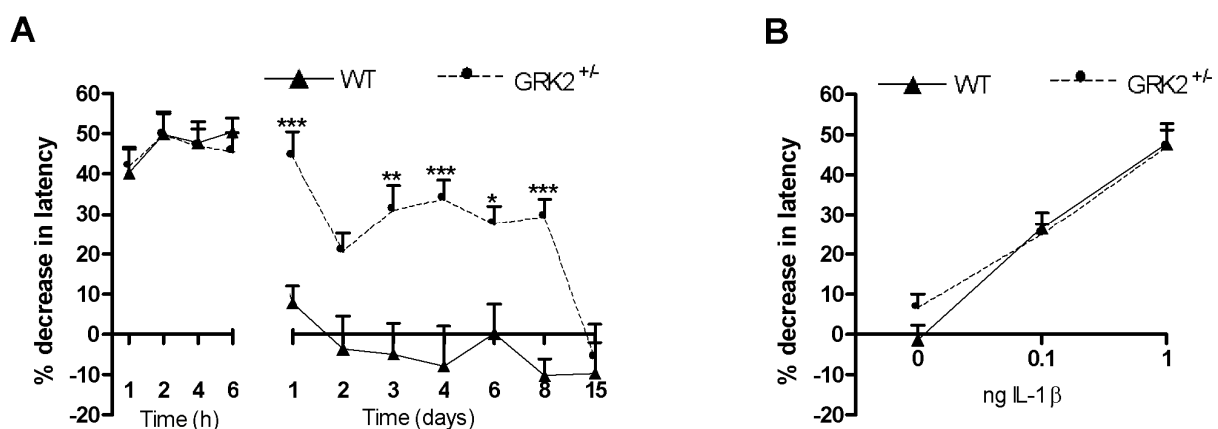


Figure 2.2: GRK2 regulates duration of peripheral IL-1 β -induced hyperalgesia. Percentage decrease in heat withdrawal latency in WT and GRK2^{+/-} mice (A) after intraplantar IL-1 β at a dose of 1 ng ($n = 8$), (B) 4 hours after intraplantar injection of 0 (saline), 0.1 or 1 ng IL-1 β ($n = 8$). Data are expressed as mean \pm SEM. * $p < 0.05$, ** $p < 0.01$, *** $p < 0.001$.

Next, we compared IL-1 β -induced hyperalgesia in LysM-GRK2^{f/+} mice with a ~40% reduction in GRK2 only in microglia/macrophages (Figure 2.3A) and littermate control LysM-GRK2^{+/+} mice. The course of IL-1 β -induced hyperalgesia was similar in mice with reduced GRK2 only in microglia/macrophages (Figure 2.3B) and in mice with reduced GRK2 in all cells (Figure 2.2A), indicating that GRK2 in microglia/macrophages is critical for determining the duration of hyperalgesia in this model. Baseline thermal sensitivity was not affected by low GRK2 in microglia/macrophages (heat withdrawal latency LysM-GRK2^{f/+} mice 8.1 \pm 0.1 s vs. control LysM-GRK2^{+/+} mice 8.2 \pm 0.2 s; n = 22). To determine whether a gene dosage effect of GRK2 exists, we generated homozygous LysM-GRK2^{f/f} mice. GRK2 expression in microglia or

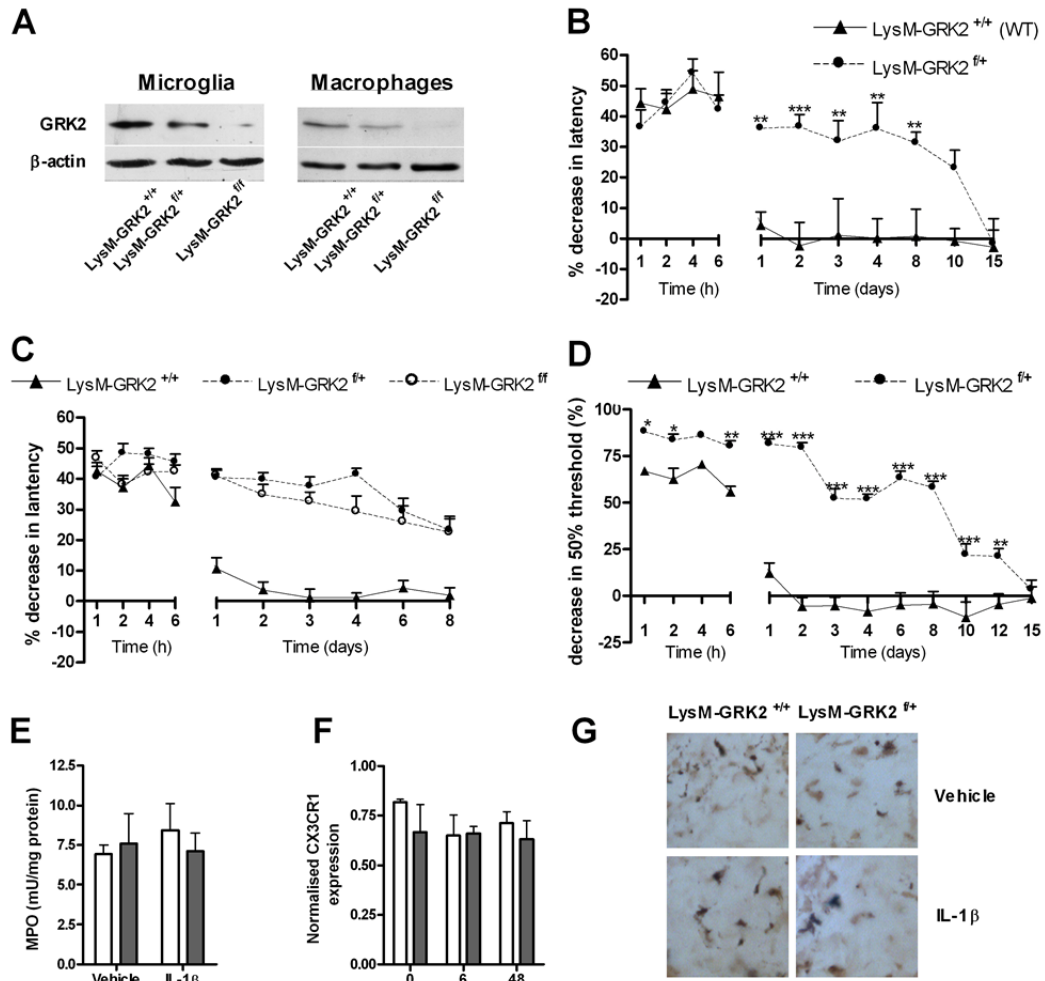


Figure 2.3: Gene dosage effect and cellular specificity of the effect of low GRK2 on thermal hyperalgesia and mechanical allodynia. (A) GRK2 expression in primary microglia and in CD11b⁺ peritoneal macrophages from LysM-GRK2^{+/+} (WT), LysM-GRK2^{f/+} and LysM-GRK2^{f/f} mice was determined by Western blot analysis. (B) Percentage decrease in heat withdrawal latency after intraplantar IL-1 β (1 ng) injection in control LysM-GRK2^{+/+} (WT) and LysM-GRK2^{f/+} mice (n = 8) (C) Change in heat withdrawal latency in control LysM-GRK2^{+/+} (WT) (n = 18), heterozygous LysM-GRK2^{f/+} (n = 12) and homozygous LysM-GRK2^{f/f} mice (n = 14) after intraplantar injection of 1 ng IL-1 β . (D) Decrease in 50% threshold for withdrawal in response to mechanical stimulation after intraplantar IL-1 β (1 ng) in LysM-GRK2^{+/+} (WT) and LysM-GRK2^{f/+} mice (n = 8). (E) MPO-content of paw biopsies as a measure of neutrophil infiltration at 2 days after intraplantar IL-1 β injection (n = 8). (F-G) As a measure of macrophage infiltration after intraplantar IL-1 β administration, samples were analyzed for (F) CX3CR1 mRNA expression in paw biopsies at 0, 6 and 48 hours after injection of IL-1 β (n = 6), (G) Iba-1 staining in paw biopsies at 2 days after injection of IL-1 β . Data are expressed as mean \pm SEM. * p<0.05, ** p<0.01, *** p<0.001.

peritoneal macrophages from LysM-GRK2^{f/f} mice was decreased by >95% compared to LysM-GRK2^{+/+} controls (Figure 2.3A). The residual GRK2 expression in LysM-GRK2^{f/f} that was observed in Western blot analysis might be due to incomplete removal of the floxed genes in some cells. Residual GRK2 expression may also be derived from contaminating astrocytes in the microglial preparation or lymphocytes in the macrophage enriched fraction. The data in figure 2.3C demonstrate that the magnitude and duration of IL-1 β -induced hyperalgesia was similar in mice heterozygous or homozygous for deletion of GRK2 in LysM-positive cells.

Low GRK2 in microglia/macrophages also affects mechanical allodynia as determined using von Frey hairs. In control LysM-GRK2^{+/+} mice, intraplantar injection of IL-1 β induces a transient increase in sensitivity to mechanical stimulation (Figure 2.3D). At 1 day after intraplantar IL-1 β , mechanical sensitivity in control mice has returned to baseline levels (Figure 2.3D), whereas LysM-GRK2^{f/f} mice continue to display mechanical allodynia until at least 12 days after the intraplantar injection of IL-1 β .

Neutrophil influx into the paw was determined by measuring MPO activity (Figure 2.3E) and macrophage influx was determined by expression of CX3CR1 mRNA (Figure 2.3F) and Iba-1-staining (Figure 2.3G) in paw biopsies of LysM-GRK2^{f/f} and LysM-GRK2^{+/+} mice. The findings indicate that the genotype-related differences in IL-1 β -induced thermal hyperalgesia and allodynia are not caused by genotype-related differences in the influx of neutrophils and macrophages into the paw (Figure 2.3E-G).

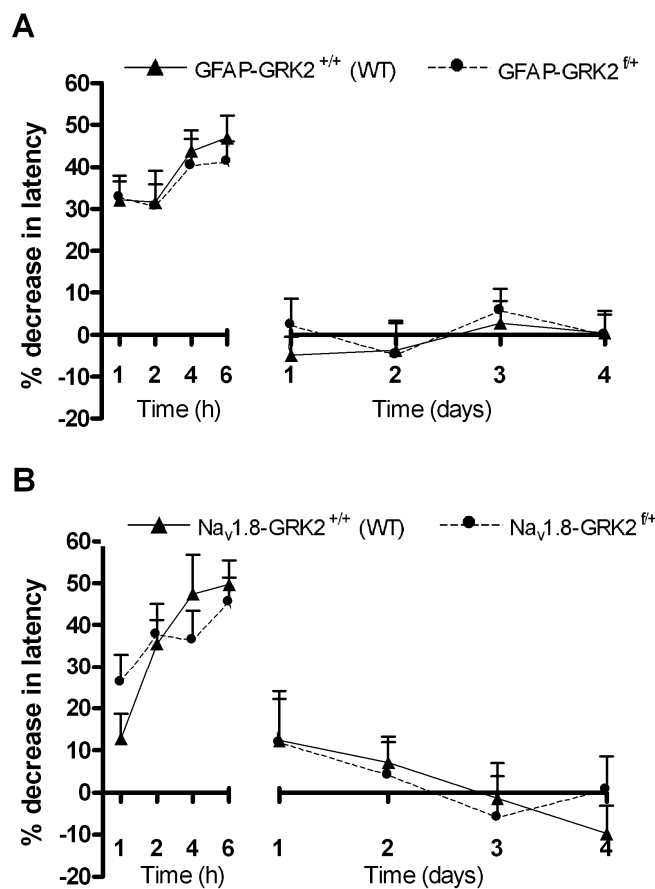


Figure 2.4: Contribution of GRK2 in astrocytes and primary sensory neurons to IL-1 β -induced hyperalgesia. Percentage decrease in heat withdrawal latency after intraplantar IL-1 β (1 ng) in (A) control GFAP-GRK2^{+/+} (WT) and GFAP-GRK2^{f/f} mice (n = 8), (B) control Nav1.8-GRK2^{+/+} (WT) and Nav1.8-GRK2^{f/f} mice (n = 8).

Contribution of GRK2 in astrocytes and primary sensory neurons to IL-1 β -induced hyperalgesia

We also examined the effect of reduction of GRK2 in GFAP-positive astrocytes. Previously, we showed that the level of GRK2 in astrocytes from GFAP-GRK2^{f/+} mice was approximately 60% lower than in WT control mice⁶¹. The data in figure 2.4A demonstrate that changes in astrocyte GRK2 did not affect the course of intraplantar IL-1 β -induced hyperalgesia. Similarly, the reduction of GRK2 in Nav1.8-positive peripheral sensory neurons that occurs in Nav1.8-GRK2^{f/+} mice⁶¹ had no effect on IL-1 β -induced hyperalgesia (Figure 2.4B).

Spinal cord microglial/macrophage activation plays a key role in IL-1 β -induced chronic hyperalgesia in GRK2-deficient mice

Next, we determined whether ongoing hyperalgesia in mice with low GRK2 in microglia/macrophages was associated with signs of ongoing activation of these cells in the spinal cord. We observed an increased number of lumbar but not thoracic spinal cord Iba-1⁺ microglia/macrophages with an activated phenotype in LysM-GRK2^{f/+} mice compared to control LysM-GRK2^{+/+} mice at day 2 after intraplantar IL-1 β (Figure 2.5A).

As a measure of spinal cord microglial/macrophage activity, we also analyzed mRNA expression of the fractalkine receptor CX3CR1, the fractalkine-releasing enzyme cathepsin S³⁵ and IL-1 β that are all expressed by microglia/macrophages. The data in figure 2.5B-E indicate that IL-1 β , cathepsin S and CX3CR1 mRNA expression were all significantly increased in lumbar spinal cord of GRK2^{+/-} mice as compared to WT mice. No changes were observed in thoracic spinal cord that was analyzed as a control. In contrast, mRNA expression for fractalkine that is produced by neurons was not affected by low GRK2.

To determine whether *ongoing* microglial/macrophage activity was required for maintaining hyperalgesia in GRK2^{+/-} mice, we used the inhibitor of microglial/macrophage activation minocycline^{198,233}. We examined whether we could reverse *ongoing* thermal hyperalgesia in mice with reduced GRK2 by treatment with minocycline at day 1 and 2 after intraplantar IL-1 β . The data in figure 2.6 demonstrate that this treatment reversed the ongoing hyperalgesia in GRK2^{+/-} mice. Minocycline treatment at these time points did not have any effect on thermal sensitivity in WT mice that had returned already to baseline. These data indicate that ongoing spinal cord microglial/macrophage activity is required to maintain the hyperalgesic state that developed in GRK2^{+/-} mice after a single intraplantar injection of IL-1 β .

Spinal cord pathways contributing to ongoing IL-1 β -hyperalgesia in GRK2-deficient mice

The data in figure 2.5 indicate that ongoing hyperalgesia in GRK2-deficient mice was associated with increased spinal cord expression of the fractalkine releasing enzyme cathepsin S and upregulation of the fractalkine receptor CX3CR1 that was detectable at 2 days after IL-1 β . To determine the contribution of fractalkine signaling to ongoing hyperalgesia in LysM-GRK2^{f/+} mice, the mice were treated with a neutralizing antibody against CX3CR1 at day 2 after intraplantar IL-1 β . Intrathecal injection of anti-CX3CR1 (1 μ g/mouse) during the prolonged phase of IL-1 β hyperalgesia blocked ongoing hyperalgesia in LysM-GRK2^{f/+} mice as determined from 1 h after anti-CX3CR1 injection. The same dose of normal rabbit IgG did not have any effect and anti-CX3CR1 did not affect thermal sensitivity in control LysM-GRK2^{+/+} mice (Figure 2.7A).

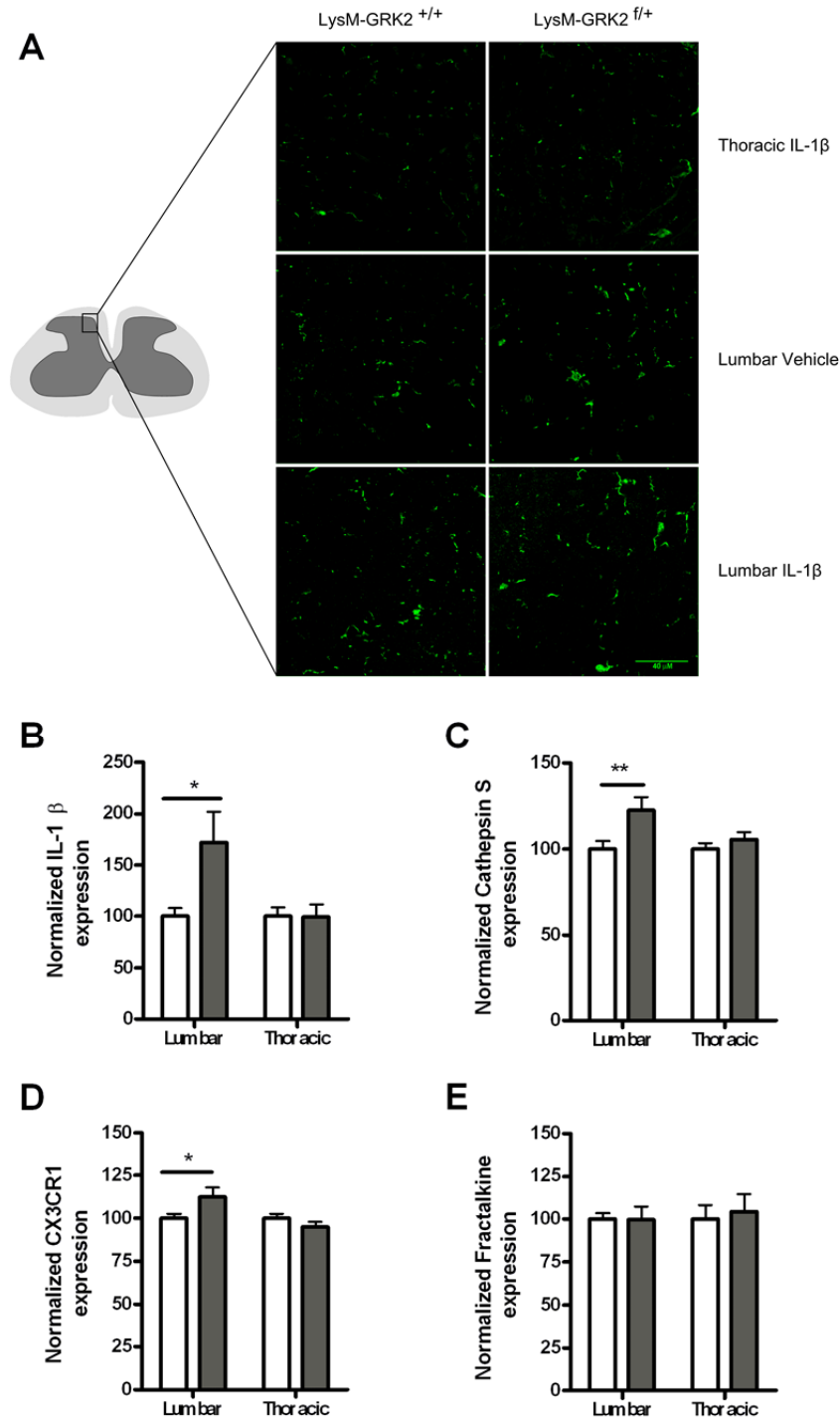


Figure 2.5: Spinal cord microglia/macrophage activity. (A) LysM-GRK2^{+/+} (WT) and LysM-GRK2^{f/+} mice received an intraplantar injection of IL-1 β or saline. At 2 days after injection, spinal cord was collected and frozen sections of lumbar spinal cord (L2-L4) and as a control thoracic spinal cord (T8-T10) were stained with Iba-1 to visualize microglia/macrophages. Representative example of morphology of Iba-1-positive cells in the dorsal horn (see drawing for exact location) of one of three mice per group is displayed. (B-D) WT (white bars) and GRK2^{+/-} mice (grey bars) received an intraplantar injection of IL-1 β (1 ng) and lumbar and as a control thoracic spinal cord was collected 2 days later. Samples were analyzed for mRNA encoding (B) IL-1 β ; (C) Cathepsin S; (D) CX3CR1 and (E) fractalkine. n = 10 per group. * p<0.05.

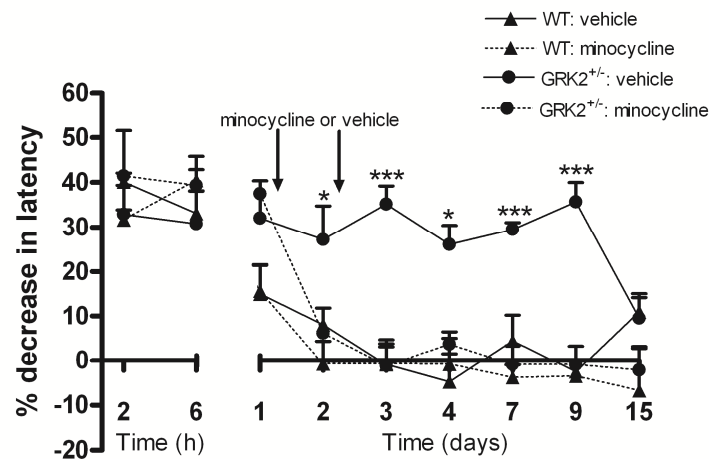


Figure 2.6: Effect of minocycline treatment at day 1 and 2 after intraplantar IL-1 β on hyperalgesia.

WT and GRK2^{+/+} mice received an intraplantar injection of IL-1 β (1 ng) and the percentage decrease in heat withdrawal latency was determined. At 1 and 2 days after IL-1 β , minocycline (50 mg/kg) or vehicle was administered (n = 4 per group). Data are expressed as mean \pm SEM. * p<0.05, ** p<0.01, *** p<0.001 vs. vehicle.

Activation of CX3CR1 on microglia is thought to activate p38 leading to increased production of pro-inflammatory cytokines such as IL-1 β and subsequent central sensitization via a direct effect on sensory neurons. The possible contribution of this pathway was tested by intrathecal injection of the p38 inhibitor SB239063 at day 2 after intraplantar IL-1 β . This treatment reversed ongoing thermal hyperalgesia in mice with low GRK2 in microglia/macrophages (Figure 2.7B). Intrathecal SB239063 at day 2 after IL-1 β did not affect thermal sensitivity in control LysM-GRK2^{+/+} mice.

The phosphatidylinositol-3 kinase (PI3 kinase) pathway can also be triggered by soluble and membrane-bound fractalkine, leading to modulation of microglial/macrophage activity^{153,201}. However, intrathecal administration of the PI3 kinase inhibitor LY294002 at day 2 after intraplantar IL-1 β injection did not have any effect on ongoing hyperalgesia in LysM-GRK2^{f/+} mice (Figure 2.7C).

As mentioned above, fractalkine signaling to microglial p38 is thought to enhance IL-1-release leading to neuronal sensitization and hyperalgesia. To examine the contribution of ongoing spinal cord IL-1-signaling to the prolonged hyperalgesia that we observed in LysM-GRK2^{f/+} after intraplantar IL-1 β , we used the IL-1 antagonist IL-1ra. Intrathecal administration of IL-1ra at day 2 after intraplantar IL-1 β reversed ongoing hyperalgesia in LysM-GRK2^{f/+} mice (Figure 2.7D) within 1 h after administration. No effect of intrathecal IL-1ra was observed in control LysM-GRK2^{+/+} mice.

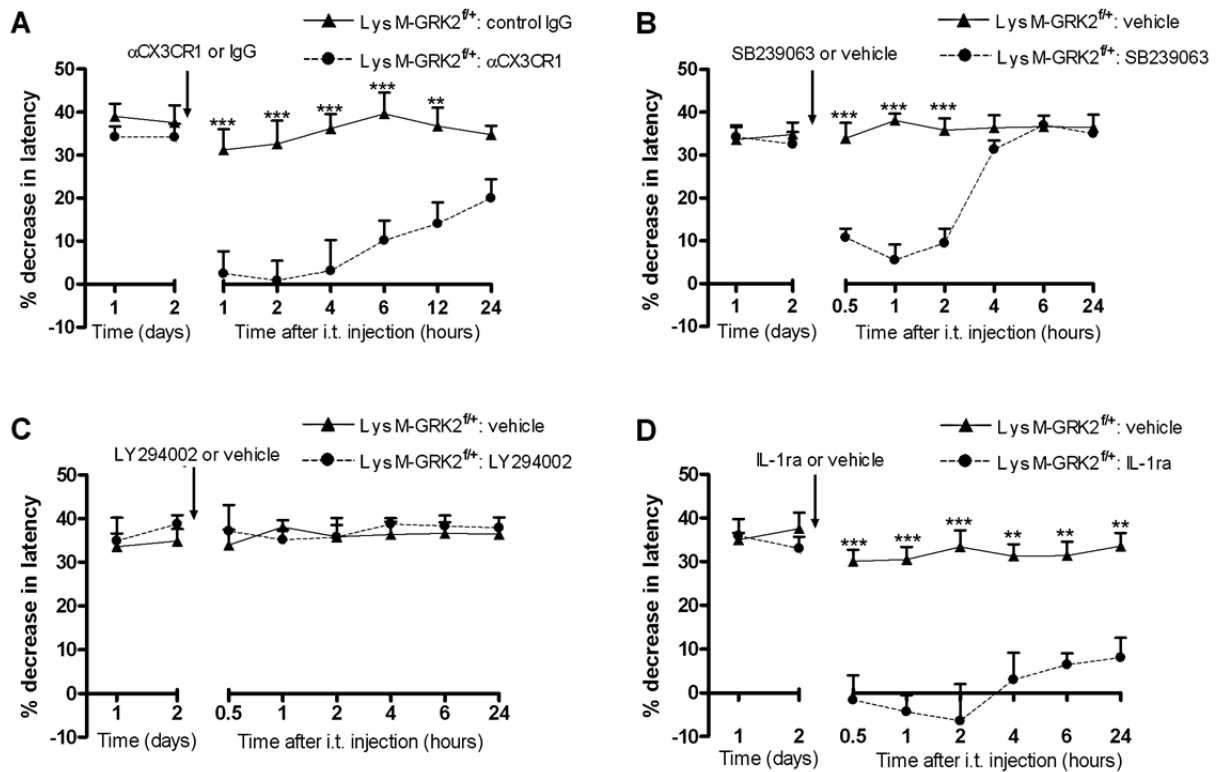


Figure 2.7: Factors contributing to ongoing hyperalgesia in GRK2-deficient mice. LysM-GRK2^{fl/fl} mice received an intraplantar injection of IL-1 β and the percentage decrease in heat withdrawal latency was determined. At day 2 after intraplantar IL-1 β , mice received an intrathecal injection of (A) α CX3CR1 (1 μ g/mouse) or rabbit IgG (1 μ g/mouse) (n = 6 per group), (B) p38 inhibitor SB239063 (5 μ g/mouse; n = 8) or vehicle (n = 4), (C) PI3 kinase inhibitor LY294002 (5 μ g/mouse) or vehicle (n = 4 per group), (D) IL-1ra (10 ng/mouse; n = 6) or vehicle (n = 4). Heat sensitivity in IL-1 β -treated LysM-GRK2^{+/+} (WT) mice had already returned to baseline at day 2 after injection and was not affected by any of the treatments (data not shown). The inhibitors did not affect heat sensitivity in naïve mice of either genotype. Data are expressed as mean \pm SEM. * p<0.05, ** p<0.01, *** p<0.001 vs. vehicle or control IgG.

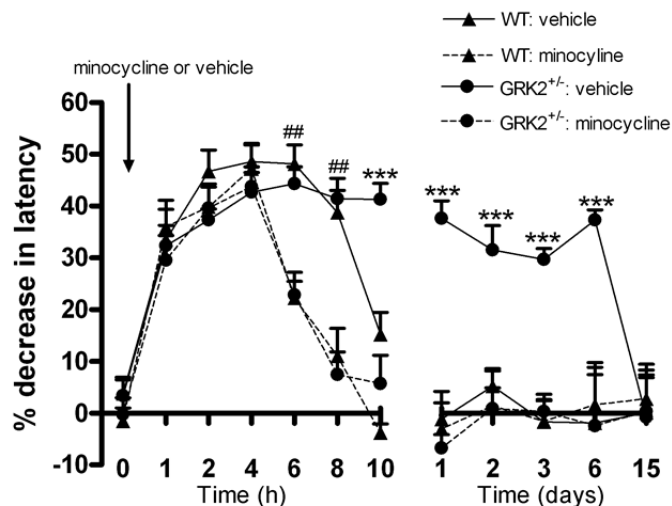


Figure 2.8: Contribution of early spinal cord microglial/macrophage activity to IL-1 β -induced hyperalgesia. WT and GRK2^{+/-} mice (n = 8 per group) received an intrathecal injection of minocycline (30 μ g) or vehicle 60 min prior to intraplantar IL-1 β and the percentage change in heat withdrawal latency was determined. Data are expressed as mean \pm SEM. * p<0.05, ** p<0.01, *** p<0.001 for GRK2^{+/-} mice/minocycline vs. GRK2^{+/-} mice/vehicle. ## p<0.01 for both genotypes with minocycline vs. saline.

Contribution of early spinal cord microglial/macrophage activity

To address the question whether early spinal cord microglial activity contributed to the *transition* from acute to prolonged IL-1 β hyperalgesia in GRK2-deficient mice, we now administered minocycline (30 μ g) intrathecally at 60 min before intraplantar IL-1 β . This pre-treatment did not have any effect on acute IL-1 β hyperalgesia at 1 - 4 h after intraplantar IL-1 β injection in either genotype. However, hyperalgesia at 6 h and 8 h after IL-1 β injection was significantly reduced by pre-emptive minocycline treatment to the same extent in WT and GRK2^{+/-} mice. Moreover, in GRK2^{+/-} mice the development of the chronic phase of hyperalgesia was completely prevented by minocycline pre-treatment (Figure 2.8).

Contribution of fractalkine signaling to prolonged hyperalgesia in response to intraplantar IL-1 β

The fractalkine receptor CX3CR1 is a member of the G protein-coupled receptor family and in the spinal cord CX3CR1 is mainly expressed on microglia/macrophages. GRK2 regulates a wide array of GPCRs via desensitization of these receptors. Although it is not known whether CX3CR1 is a substrate for this kinase, low GRK2 may contribute to transition from acute to prolonged IL-1 β -hyperalgesia by facilitating fractalkine signaling as a result of impaired CX3CR1 desensitization. To determine whether mice with low GRK2 in microglia/macrophages are more sensitive to fractalkine-induced hyperalgesia, we compared the effect of intrathecal administration of fractalkine on thermal sensitivity in LysM-GRK2^{f/+} and control LysM-GRK2^{+/+} mice. In line with data in the literature^{35,163}, intrathecal injection of fractalkine (1 ng/mouse) in WT mice induced hyperalgesia that was first detectable at 2 h after fractalkine injection (Figure 2.9A). During the first 6 h after injection, fractalkine-induced hyperalgesia was identical in LysM-GRK2^{f/+} and control LysM-GRK2^{+/+} mice. Also at lower doses of fractalkine (10-100 pg/mouse), acute hyperalgesia in control and LysM-GRK2^{f/+} mice was indistinguishable (data not shown). Notably, however, fractalkine-induced hyperalgesia did become chronic in mice with reduced GRK2 in microglia/macrophages, whereas it was only transient in control LysM-GRK2^{+/+} littermates (Figure 2.9A).

Next, we investigated whether the transition from acute to prolonged peripheral IL-1 β -induced hyperalgesia is dependent on spinal cord fractalkine signaling. The mice received an intraplantar injection of IL-1 β and we examined the effect of intrathecal injection of anti-CX3CR1 before or at 4 h after intraplantar IL-1 β . As is shown in figure 2.8B and C, this early administration of anti-CX3CR1 did not have any effect on IL-1 β -induced hyperalgesia in LysM-GRK2^{+/+} mice or LysM-GRK2^{f/+} mice (Figure 2.9B and C), suggesting that fractalkine signaling is not involved in the transition from acute to chronic hyperalgesia.

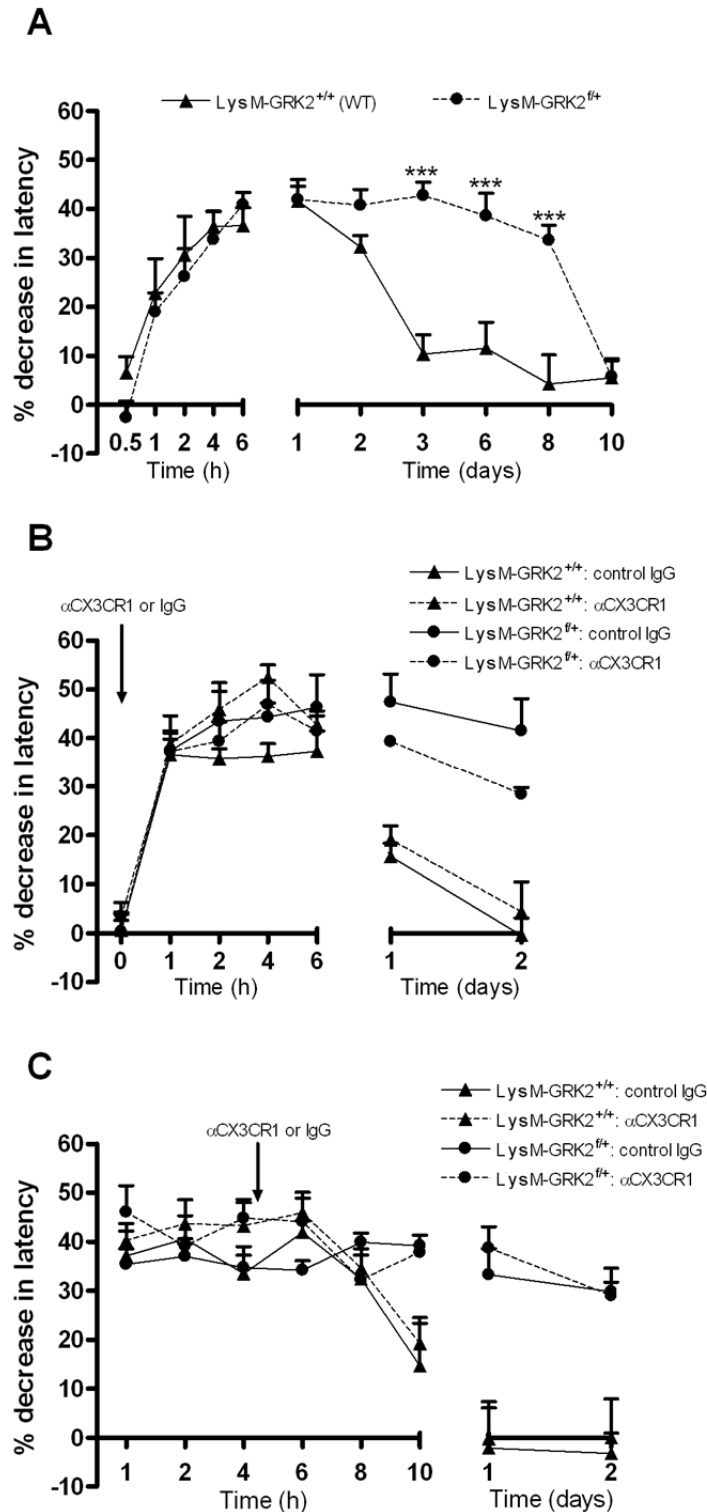


Figure 2.9: Contribution of fractalkine to prolonged IL-1 β -induced hyperalgesia in GRK2-deficient mice. (A) Mice received an intrathecal injection of fractalkine (1 ng) and the percentage decrease in heat withdrawal latency was determined in LysM-GRK2^{+/+} (WT) and in LysM-GRK2^{fl/fl} mice (n = 8 per group). (B and C) Mice received an intraplantar injection of IL-1 β . The effect of intrathecal administration of anti-CX3CR1 (1 μ g/mouse) or rabbit IgG (1 μ g/mouse) (B) before or (C) 4 hours after intraplantar IL-1 β administration on hyperalgesia in LysM-GRK2^{+/+} (WT) and LysM-GRK2^{fl/fl} mice (n = 4 per group) was determined. Data are expressed as mean \pm SEM. *** p < 0.001.

Discussion

The present study assessed the contribution of GRK2 in microglia/macrophages to the neurobiology of inflammation-induced hyperalgesia using mice with low GRK2 only in microglia/macrophages that were generated using CRE-Lox technology. The level of microglia/macrophage GRK2 appeared to play a crucial role in determining the duration of hyperalgesia. Thermal hyperalgesia or mechanical allodynia induced by one single intraplantar injection of IL-1 β lasted at least 8 days in LysM-GRK2^{f/+} mice whereas in WT LysM-GRK2^{+/+} mice IL-1 β hyperalgesia and allodynia resolved within 24 h. These genotype-related differences in the duration of hyperalgesia and allodynia were not associated with genotype differences in the influx of neutrophils or macrophages. Prolonged thermal hyperalgesia in GRK2-deficient mice was dependent on ongoing microglial/macrophage activity, fractalkine signaling, p38 activity and IL-1 β signaling in the spinal cord. We propose that normal levels of microglial/macrophage GRK2 are important to ensure adequate termination of the activity of spinal cord microglia/macrophages and resolution of hyperalgesia. The pathophysiological relevance of these findings is strengthened by the recent finding that spinal cord microglia/macrophage GRK2 is reduced by ~35% in a rat model of chronic neuropathic pain⁶¹ and in a model of ongoing inflammatory pain as is shown here.

The maximal effect of low microglial/macrophage GRK2 on prolongation of IL-1 β -induced hyperalgesia was already obtained in heterozygous LysM-GRK2^{f/+} mice with a 40-60% reduction in microglial/macrophage GRK2. The only previous study using mice homozygous for cell-specific deletion of GRK2 showed that neither partial nor total GRK deletion in cardiac myocytes had any consequences for the end point investigated (cardiac development)¹⁹⁵. Therefore, we do not know whether the lack of gene dosage effect is specific for microglial/macrophage GRK2 or represents a general phenomenon. We previously described a similar lack of gene dosage effect for GRK6; experimental colitis was prolonged to the same extent in mice that were heterozygous or homozygous for deletion of GRK6⁵⁹.

IL-1 β acts directly on peripheral sensory neurons to increase excitability leading to a rapid increase in thermal sensitivity^{11,162} via enhancement of TTX-resistant sodium currents¹¹. Consistent with direct sensitization of sensory neurons by IL-1 β , we show that intrathecal administration of the microglial/macrophage inhibitor minocycline did not affect hyperalgesia during the first 4 h after intraplantar IL-1 β . However, this treatment reduced hyperalgesia as determined at 6-8 h after IL-1 β and this effect was irrespective of genotype. These findings indicate that spinal cord microglial/macrophage activity contributes to the late phase of acute IL-1 β -induced hyperalgesia, a process which is not altered by lowering GRK2. In addition, the acute phase of hyperalgesia after activation of spinal microglia by intrathecal administration of fractalkine was indistinguishable in LysM-GRK2^{+/+} and LysM-GRK2^{f/+} mice. Moreover, spinal cord fractalkine signaling was not required for the initial activation of microglia/macrophages in our model, since early inhibition of fractalkine signaling by administration of anti-CX3CR1 before or at 4 h after intraplantar IL-1 β did not affect the course of hyperalgesia. These findings imply that although microglial/macrophage activity is contributing to hyperalgesia at 6-8 h after IL-1 β , fractalkine signaling is not yet involved in microglial/macrophage activation. Moreover, GRK2-deficiency does not affect the initial hyperalgesic response to fractalkine stimulation of microglia/macrophages.

It is well established that spinal cord microglia/macrophage activity contributes to chronic hyperalgesia in response to complete Freund's adjuvant or carrageenan models of chronic inflammation-induced hyperalgesia^{34,55,166}. What is not known, however, is which factors

contribute to *terminating* spinal cord microglial/macrophage activity after resolution of peripheral inflammation. In WT mice microglial/macrophage-dependent central sensitization is a self-limiting process as hyperalgesia completely resolves within 12-24 h after intraplantar IL-1 β or 3 days after intrathecal fractalkine. In contrast, the mice with low GRK2 in microglia/macrophages hyperalgesia did not resolve until 7-8 days after intraplantar IL-1 β or 8-10 days after intrathecal fractalkine. The prolonged phase of hyperalgesia in GRK2-deficient mice was reversed by minocycline treatment at 24-48 h after intraplantar IL-1 β , indicating that low GRK2 facilitates *ongoing* microglial/macrophage activity. The prolonged hyperalgesic state in GRK2-deficient mice is dependent on spinal cord fractalkine signaling, since intrathecal administration of anti-CX3CR1 at 2 days after intraplantar IL-1 β attenuated ongoing hyperalgesia. Activation of CX3CR1 on microglia/macrophages is thought to lead to activation of p38 and release of pro-inflammatory cytokines including IL-1 β ³⁵. We propose that in LysM-GRK2^{f/+} mice the prolonged hyperalgesia in response to peripheral IL-1 β is maintained via a loop involving fractalkine signaling, p38 activation and IL-1 β production. This hypothesis is based on our findings that inhibition of either fractalkine signaling, p38 activity or IL-1 β signaling attenuated the ongoing hyperalgesic response in GRK2-deficient mice.

The model of IL-1 β -induced hyperalgesia that we used here is acute and transient in WT animals. However, we show that a ~50% reduction in GRK2 in microglia/macrophages is sufficient to markedly prolong IL-1 β -hyperalgesia and allodynia. Thus, our data strongly underline the importance of microglia/macrophages in determination of *duration* of hyperalgesia and allodynia and identify a central role for GRK2 in this process.

Fractalkine signaling not only contributes to microglial activity, but may also serve to keep cerebral microglia in a quiescent state via a PI3 kinase dependent pathway¹⁵³. Since inhibition of spinal cord PI3 kinase activity did not have any effect in our model of peripheral inflammatory hyperalgesia, spinal cord fractalkine signaling probably does not serve to suppress spinal cord microglial activation in this model. This may be due to site-specific differences in mechanisms operative in brain vs. spinal cord microglia.

We previously showed that acute hyperalgesia induced by the GPCR-binding chemokine CCL3 as determined within the first 3 h after intraplantar injection was more pronounced in GRK2^{+/-} than in WT mice. Increased acute CCL3 hyperalgesia was also observed in mice deficient for GRK2 only in peripheral sensory neurons⁶¹. In contrast, our present data show that IL-1 β hyperalgesia was completely normal in mice with low GRK2 only in peripheral sensory neurons. CCL3 signals via CCR1 and CCR5 and these receptors are sensitive to GRK2-dependent desensitization^{61,182,241}. IL-1 β signaling is mediated by receptors that are not GPCR. This might explain why IL-1 β -hyperalgesia is not affected by low GRK2 in primary sensory neurons. However, IL-1 β -induced sensitization of peripheral sensory neurons is mediated via a p38-dependent pathway¹¹ and GRK2 can regulate p38 activation. Direct interaction of GRK2 with p38 can result in phosphorylation of Thr-123 in the docking groove which reduces binding of upstream kinases like MKK6 as well as down stream targets¹⁸⁵. GRK2 has been shown to reduce LPS-induced cytokine production by microglia/macrophages via this mechanism^{61,177,185}. However, since a ~50% reduction in GRK2 was not sufficient to enhance IL-1 β -induced *acute* hyperalgesia, a possible interaction between GRK2 and p38 in peripheral sensory neurons does not appear to contribute to regulation of acute IL-1 β hyperalgesia.

Previously, we described that spinal cord neuronal GRK2 was reduced in rat or mouse models of neuropathic pain^{123,125}. Moreover, our recent data showed that GRK2 levels in microglia/macrophages isolated from ipsilateral lumbar spinal cord of rats at day 14 after L5

spinal nerve transection were decreased by ~35% as compared to cells from contralateral spinal cord or from sham control rats⁶¹. Here we show that the high dose carrageenan paw inflammation model of prolonged hyperalgesia is also associated with reduced spinal cord microglial/macrophage GRK2. Thus, *in vivo*, in models of chronic pain, spinal microglial/macrophage GRK2 levels are reduced. Our findings that reduced microglial/macrophage GRK2 prolongs hyperalgesia indicate that the reduced levels of GRK2 that occur in these cells may well contribute to the chronic pain that develops in these models of chronic inflammation. *In vitro*, culture of various cell types with inflammatory mediators including cytokines can decrease GRK2 levels^{66,147}. Clinically, we have shown that GRK2 protein levels in peripheral blood mononuclear cells from patients with rheumatoid arthritis or multiple sclerosis were reduced as compared to healthy controls^{147,242}. These observations indicate that in humans GRK2 can be down regulated in immune cells during chronic inflammation. It is unclear, however, whether painful inflammatory conditions in humans are also associated with reduced GRK2 in spinal cord microglia/macrophages and this question is subject of our current investigations.

Collectively, our data indicate that inflammatory hyperalgesia is associated with reduced spinal cord microglial/macrophage GRK2. The pathophysiological significance of low GRK2 in these cells is attested by our finding that peripheral IL-1 β -induced hyperalgesia was markedly prolonged in mice with reduced microglial/macrophage GRK2. We propose that the ongoing hyperalgesia observed in mice with low GRK2 is maintained via a positive feedback loop that involves fractalkine signaling, p38 activation, IL-1 release and ongoing microglial/macrophage activity in the spinal cord. Taken together our data indicate that microglial/macrophage GRK2 may be crucial for resolution of inflammatory hyperalgesia. Future studies should aim at determining the mechanism how spinal cord microglia/macrophage activity is terminated in the context of inflammatory pain.

Acknowledgements

The authors thank Dr. J. N. Wood, University College London, London, UK for sharing the Na_v1.8-CRE mice and Mrs. Ilona den Hartog, UMC Utrecht, for excellent technical assistance.

3

MicroRNA-124 as a novel treatment for persistent hyperalgesia

Hanneke L.D.M. Willemen¹

Xiao-Jiao Huo²

Qi-Liang Mao-Ying²

Jitske Zijlstra¹

Cobi J Heijnen¹

Annemieke Kavelaars^{2,1}

¹ Laboratory of Neuroimmunology and Developmental Origins of Disease (NIDOD), University Medical Center Utrecht, Utrecht 3584 EA, The Netherlands

² Integrative Immunology and Behavior Program, College of ACES and College of Medicine, University of Illinois at Urbana-Champaign, Urbana, IL 61801, USA

Abstract

Background

Chronic pain is often associated with microglia activation in the spinal cord. We recently showed that microglial levels of the kinase G protein-coupled receptor kinase (GRK)2 are reduced in models of chronic pain. We also found that mice with a cell-specific reduction of around 50% in GRK2 level in microglia/macrophages (LysM-GRK2^{+/-} mice) develop prolonged inflammatory hyperalgesia concomitantly with ongoing spinal microglia/macrophage activation. The microRNA miR-124 is thought to keep microglia/macrophages in brain and spinal cord in a quiescent state. In the present study, we investigated the contribution of miR-124 to regulation of hyperalgesia and microglia/macrophage activation in GRK2-deficient mice. In addition, we investigated the effect of miR-124 on chronic inflammatory and neuropathic pain in wild-type (WT) mice.

Methods

Hyperalgesia was induced by intraplantar IL-1 β in WT and LysM-GRK2^{+/-} mice. We determined spinal cord microglia/macrophage miR-124 expression and levels of pro-inflammatory M1 and anti-inflammatory M2 activation markers. The effect of intrathecal miR-124 treatment on IL-1 β -induced hyperalgesia and spinal M1/M2 phenotype, and on carrageenan-induced and spared nerve injury-induced chronic hyperalgesia in WT mice was analyzed.

Results

Transition from acute to persistent hyperalgesia in LysM-GRK2^{+/-} mice is associated with reduced spinal cord microglia miR-124 levels. In our LysM-GRK2^{+/-} mice, there was a switch towards a pro-inflammatory M1 phenotype together with increased pro-inflammatory cytokine production. Intrathecal administration of miR-124 completely prevented the transition to persistent pain in response to IL-1 β in LysM-GRK2^{+/-} mice. The miR-124 treatment also normalized expression of spinal M1/M2 markers of LysM-GRK2^{+/-} mice. Moreover, intrathecal miR-124 treatment reversed the persistent hyperalgesia induced by carrageenan in WT mice and prevented development of mechanical allodynia in the spared nerve injury model of chronic neuropathic pain in WT mice.

Conclusions

We present the first evidence that intrathecal miR-124 treatment can be used to prevent and treat persistent inflammatory and neuropathic pain. In addition, we show for the first time that persistent hyperalgesia in GRK2-deficient mice is associated with an increased ratio of M1/M2 type markers in spinal cord microglia/macrophages, which is restored by miR-124 treatment. We propose that intrathecal miR-124 treatment might be a powerful novel treatment for pathological chronic pain with persistent microglia activation.

Background

Micro (mi) RNAs regulate expression of multiple genes by promoting degradation of mRNA or by preventing translation of target genes. It has recently been reported that high levels of the miRNA miR-124 are present in resident microglia in brain and spinal cord. Ponomarev *et al.* showed that microglia activated *in vitro* and *in vivo* have low levels of miR-124. In addition, peripheral macrophages, which have an activated phenotype, express low levels of miR-124 compared with isolated naive microglia from brain and spinal cord. Based on such findings, it has been suggested that high levels of miR-124 are required to keep microglia in a quiescent state¹⁸⁹.

Microglia/macrophages in the spinal cord play a key role in the development of chronic pain in rodent models of neuropathic pain, diabetic neuropathy, and chronic inflammatory pain^{37,51,166,204,250,274}. However, it is not known whether microglial miR-124 contributes to chronic pain.

Recently, we reported that chronic inflammatory hyperalgesia and neuropathic pain are associated with decreased levels of the serine–threonine kinase G protein receptor kinase (GRK)2 in spinal microglia/macrophages^{61,257}. GRK2 regulates cellular signaling by promoting desensitization of agonist-occupied G protein-coupled receptors and by direct interaction with multiple downstream signaling pathways^{60,112,124,185,243}. Our recent functional studies indicated a key role for GRK2 in regulating the transition from acute to persistent hyperalgesia. In mice with a 50% reduction of GRK2 in microglia/macrophages (LysM-GRK2^{+/-} mice), thermal and mechanical hyperalgesia induced by intraplantar injection of inflammatory mediators were markedly prolonged^{60,61,119,257}. For example, thermal hyperalgesia induced by a single intraplantar injection of the pro-inflammatory cytokine IL-1 β resolved within 24 hours in wild type (WT) mice, but lasted for at least 8 days in LysM-GRK2^{+/-} mice. Similarly, low-dose carrageenan-induced hyperalgesia was prolonged from 3 to 4 days in WT mice to 20 days in LysM-GRK2^{+/-} mice. This prolongation of hyperalgesia in LysM-GRK2^{+/-} mice was reversible by intrathecal administration of the microglial/macrophage inhibitor minocycline, indicating a decisive role for spinal cord microglia/macrophage activity in regulating the transition to persistent hyperalgesia in these models^{61,257}.

It is now well known that macrophage activation can induce development of two functional subtypes known as pro-inflammatory (M1-type) and anti-inflammatory (M2-type) macrophages. These two activated types of macrophages can be discriminated by the expression of specific markers on their cell surface, and are characterized by expression of pro-inflammatory factors such as interleukin 1 β , and inducible nitrous oxide (iNOS) (in M1 macrophages) or anti-inflammatory cytokines including transforming growth factor (TGF)- β (in M2 macrophages). In addition, there is evidence that microglial activation can also lead to development of either the M1 or M2 phenotype^{69,161}. However, it is not known whether or how these distinct macrophages/microglia phenotypes contribute to regulation of pain responses.

In this study we investigated whether low levels of microglial/macrophage GRK2 promote the transition to chronic hyperalgesia via a miR-124-mediated pathway in spinal microglia/macrophages, and whether low GRK2 is associated with the expression of the M1 and M2 phenotype in spinal cord microglia. We also determined whether miR-124 can be used to treat persistent hyperalgesia in models of chronic inflammatory and neuropathic pain in WT mice.

Methods

Experiments were performed in accordance with international guidelines and approved by the experimental animal committee of UMC Utrecht.

Animals

We used female mice (aged 12 to 14 weeks) with cell-specific reduction of GRK2 in microglia/macrophages (LysM-GRK2^{+/-}), and control LysM-GRK2^{+/+} mice^{61,257} (WT littermates bred and maintained in the animal facility of the University of Utrecht, The Netherlands). LysM-Cre mice and GRK2-flox mice were obtained from Jackson Laboratories.

Mice received an intraplantar injection in the hind paw of 5 μ l recombinant murine IL-1 β (200 ng/ml; Peprotech, Rocky Hill, NJ, USA) or 20 μ l λ -carrageenan (2% w/v; Sigma-Aldrich, St. Louis, MO, USA) diluted in saline. Heat-withdrawal latency times were determined using the Hargreaves test (IITC Life Science, Woodland Hills, CA) as described previously⁸⁹. Intraplantar injection of saline did not induce detectable hyperalgesia in any of the genotypes.

Spared nerve injury (SNI) was performed in male C57BL/6 mice (Harlan Laboratories) as described previously⁵³. Briefly, under 2% isoflurane anesthesia, the sciatic nerve and its three terminal branches were exposed carefully with minimal damage. Leaving the sural nerve intact, the common peroneal and the tibial nerves were tightly ligated with 6-0 silk surgical sutures and cut 2 to 4 mm distal to the ligation. Sham controls underwent anesthesia, incision, and exposure of the nerve only.

Mechanical allodynia was measured using von Frey hairs as described previously²⁵⁷. The 50% paw-withdrawal threshold was calculated using the up-and-down method²⁸. In brief, animals were placed on a wire-grid base, through which the von Frey hairs (Stoelting, Wood Dale, IL, USA) were applied (bending force range from 0.02 to 1.4 g, starting with 0.16 g). The hair force was increased or decreased depending on the response. Clear paw withdrawal, shaking, or licking were considered as nociceptive-like responses. Ambulation was considered an ambiguous response, and in such cases, the stimulus was repeated.

Spontaneous locomotor activity (LMA) was determined 3 days after SNI in a clean, novel cage similar to the home cage, but devoid of bedding or litter. The cage was divided into four virtual quadrants, and LMA was measured by counting the number of line crossings over a five-min period.

All behavioral experiments were performed by an experimenter blinded to treatment and in a randomized fashion.

The miRNA-124 (2 μ g in 50 μ l PBS, PM10691 Applied Biosystems, Carlsbad, CA, USA) or control miRNA (2 μ g in 50 μ l PBS, AM17110; Applied Biosystems) was mixed with transfection reagent (Lipofectamine 2000; Invitrogen, Paisley, UK), diluted to the appropriate concentration (3 μ l in 50 μ l PBS) and applied intrathecally (5 μ l/mouse) while the animals were under light isoflurane anesthesia.

Spinal microglia and peripheral macrophage isolation

At 24 hours after intraplantar IL-1 β injection, lumbar enlargements (L2-L5) or thoracic (T6-T10) spinal cord of four mice were pooled and the microglia were isolated by Percoll density gradient centrifugation as described previously²⁵⁷.

Peripheral macrophages were isolated from peritoneal lavages using CD11b magnetic beads, in accordance with the manufacturer's instructions (BD IMag, San Diego, CA, USA).

MicroRNA-124 and mRNA expression analysis

Total RNA was isolated using a commercial kit (RNeasy Mini Kit; Qiagen, Hilden, Germany). Specific reverse transcriptase and Taqman miRNA assays (Applied Biosystems) were carried out in accordance with the manufacturer's instructions. The miR-124 expression (mmu-miR-124a, 001182) was normalized for snoRNA55 (001228) expression.

Real-time reverse transcriptase PCR

cDNA was processed from total RNA using reverse transcriptase (SuperScript; Invitrogen), and real-time PCR was performed (iQ5 Real-Time PCR Detection System; Bio-Rad, Alphen a/day Rijn, The Netherlands) using the primers shown in table 3.1. Data were normalized for GAPDH and actin expression.

Immunohistochemistry

Mice were perfused intracardially with PBS 15 hours after intraplantar IL-1 β injection, followed by 4% paraformaldehyde in PBS. Spinal cords were post-fixed in 4% paraformaldehyde for 6 hours at 4°C, and cryoprotected in sucrose. Cryosections (10 μ m) of thoracic segments T6 to T10 and lumbar segments L2 to L5 were incubated with 1:100 goat anti-mouse CD206 (R&D Systems, Minneapolis, MN, USA), 1:200 goat anti-mouse aginase I (Santa Cruz Biotechnology, Santa Cruz, CA, USA) or 1:500 rat anti-mouse CD16/32 (BD Biosciences) followed by alexa flour 488-conjugated secondary antibodies. Sections were viewed under a fluorescence microscope (Axio Observer; Zeiss, Jena, Germany). M1 and M2 expression was quantified in approximately 10 to 15 dorsal horns of spinal cords per group (four mice per group). The level of expression in the lumbar or thoracic part from control WT mice was set at 100%.

Table 3.1 Primers used for real-time reverse transcriptase PCR.

Name	Direction	Primer sequence 5'→3'
C/EBP- α	Forward	AgCTTACAACAggCCAaggTTTC
	Reverse	CggCTggCgACATACAgTAC
TGF- β	Forward	CAGAgCTgCgCTTgCAGAg
	Reverse	gTCAGCAGCCggTTACCAAg
iNOS	Forward	ACCCACATCTggCAGAAAg
	Reverse	AgCCATgACCTTTCgCATTAg
IL-1 β	Forward	CAACCAACAAGTgATATTCTCCATg
	Reverse	gATCCCACTCTCCAgCTgCA
GAPDH	Forward	TgAAgCAGgCATCTgAggg
	Reverse	CgAAggTggAAgAgTgggAg
Actin	Forward	AgAgggAAATCgTgCgTgAC
	Reverse	CAATAgTgATgACCTggCCgT

Abbreviations: C/EBP, CCAAT-enhancer-binding protein; GAPDH, glyceraldehyde 3-phosphate dehydrogenase; IL, interleukin; iNOS, inducible nitrous oxide; TGF, transforming growth factor.

Statistical analysis

All data are presented as mean \pm SEM. Measurements were compared using Student's *t*-test or two-way ANOVA with Bonferroni post-hoc tests using Prism 4 software.

Results

MicroRNA-124 expression in spinal cord microglia and in peripheral macrophages

First, we examined whether the transition from acute IL-1 β -induced hyperalgesia to persistent hyperalgesia in LysM-GRK2^{+/-} mice is associated with changes in the level of miR-124 in spinal cord microglia. We isolated lumbar spinal cord microglia at baseline and 24 hours after intraplantar IL-1 β injection from WT and LysM-GRK2^{+/-} mice. At this time point, intraplantar IL-1 β -induced hyperalgesia had resolved completely in the WT mice, whereas the LysM-GRK2^{+/-} mice were still hyperalgesic (Figure 3.1A). These data confirm our earlier results²⁵⁷.

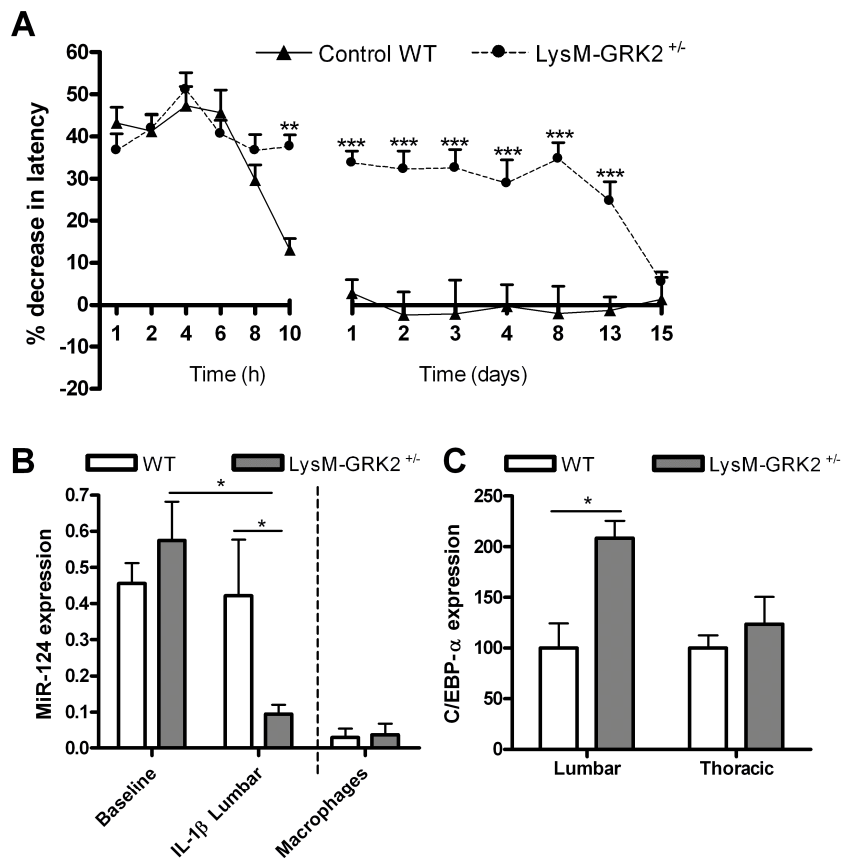


Figure 3.1: MicroRNA-124 and CCAAT-enhancer-binding protein (C/EBP)- α expression after intraplantar interleukin (IL)-1 β in wild-type (WT) and LysM G protein-coupled receptor kinase (GRK)2^{+/-} mice. Control WT and LysM-GRK2^{+/-} mice received an intraplantar injection of 1 ng IL-1 β . (A) Percentage decrease in heat withdrawal latency after the injection in control WT and LysM-GRK2^{+/-} mice (n = 12). At baseline (n = 9) and 24 hours (n = 6) after IL-1 β injection, lumbar (L2 to L5) spinal cord microglia were isolated to determine (B) miR-124 expression (normalized for small nucleolar (sno)RNA55) and (C) the lumbar and thoracic mRNA expression of C/EBP- α normalized for glyceraldehyde-3-phosphate dehydrogenase (GAPDH) and actin) in control WT (n = 6) and LysM-GRK2^{+/-} (n = 6) mice. n = One sample contains isolated microglia from four mice. Data are expressed as means \pm SEM. *p<0.05, ** p<0.01, *** p<0.001.

At 24 hours after intraplantar injection of IL-1 β , the level of miR-124 in microglia isolated from the lumbar spinal cord of LysM-GRK2^{+/-} mice was significantly lower than that of spinal microglia from WT mice (Figure 3.1B). At baseline (without stimulus), no difference was seen between WT and LysM-GRK2^{+/-} mice in miR-124 expression in microglia from spinal cord or in macrophages from the peritoneal cavity (Figure 3.1B). In line with data in the literature, the basal expression of miR-124 was lower in peripheral macrophages than in spinal cord microglia¹⁸⁹. There was no significant difference in miR-124 between microglia isolated from thoracic spinal (T6 to T10) cord of WT and LysM-GRK2^{+/-} mice after intraplantar IL-1 β (data not shown). Therefore, thoracic spinal cord was used as a control in subsequent experiments.

It is thought that miR-124 regulates microglia/macrophage activity by downregulating the expression of CCAAT-enhancer-binding protein (C/EBP)- α , a transcription factor regulating myeloid cell differentiation^{68,189,268}. Consistent with this notion, we found a significant increase in C/EBP- α mRNA in microglia isolated from the lumbar spinal cord of LysM-GRK2^{+/-} mice compared with microglia from control WT mice after intraplantar IL-1 β (Figure 3.1C). C/EBP- α expression was similar in microglia isolated from control thoracic spinal cord of LysM-GRK2^{+/-} and control WT mice injected intraplantarly with IL-1 β (Figure 3.1C).

Spinal cord M1/M2 markers in interleukin-1 β -induced persistent hyperalgesia

We next addressed the question of whether low GRK2 and decreased expression of miR-124 in spinal cord microglia are related to differences in the expression of microglia/macrophage activation markers in the spinal cord. We examined the expression of the markers of the classically activated (M1) microglia/macrophages CD16/32 and the alternatively activated (M2) cells arginase-I and CD206 by immunohistochemistry. After intraplantar injection of IL-1 β , expression of the M1 marker CD16/32 in lumbar spinal cord was higher in LysM-GRK2^{+/-} mice than in WT mice. There were no differences in M1 marker expression between thoracic spinal cord of WT and LysM-GRK2^{+/-} (Figure 3.2A-C). Conversely, the level of expression of the M2 markers CD206 and arginase-I after intraplantar IL-1 β injection was lower in lumbar spinal cord of LysM-GRK2^{+/-} mice compared with that of WT mice. Thoracic spinal cord of both genotypes did not differ in M2 marker expression (Figure 3.2A-C). In control thoracic spinal cord, no genotype-related differences were seen in the expression of M1 and M2 markers (Figure 3.2B and C).

As a functional correlate of the M1 and M2 phenotype, we quantified mRNA encoding the pro-inflammatory (M1) cytokine IL-1 β , the M1-related enzyme iNOS, and the anti-inflammatory (M2) cytokine TGF- β ^{17,74,120,129}. We injected LysM-GRK2^{+/-} or WT mice with intraplantar IL-1 β , and isolated microglia from lumbar spinal cord 24 hours later. Compared with control WT mice, freshly isolated microglia from LysM-GRK2^{+/-} mice contained significantly more mRNA for pro-inflammatory IL-1 β and iNOS, and less mRNA for anti-inflammatory TGF- β (Figure 3.3). As a control, we isolated microglia from the thoracic spinal cord of the same animals, and did not observe any difference in cytokine expression between genotypes in these cells (Figure 3.3).

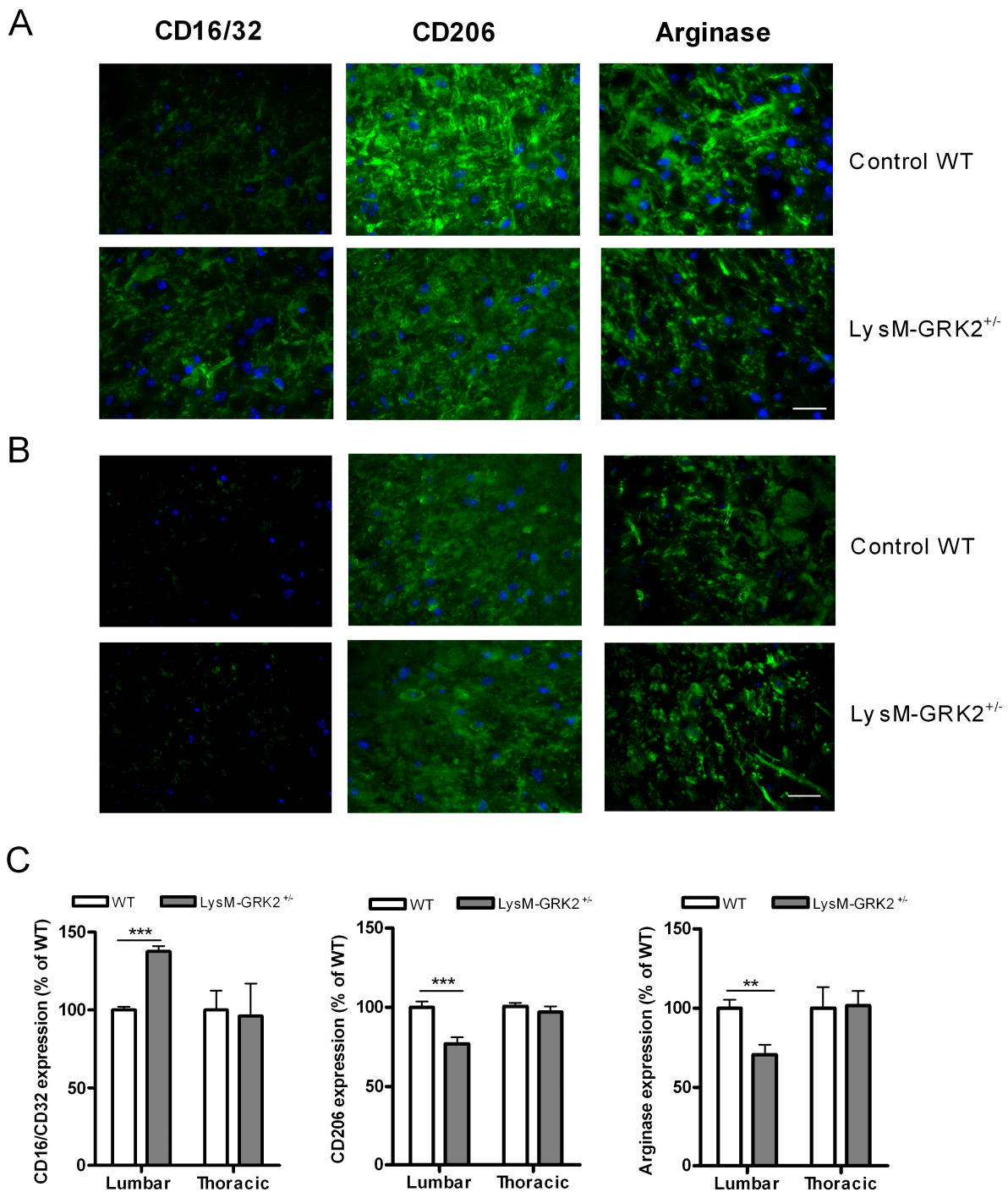


Figure 3.2: M1 and M2 phenotype in spinal cord after intraplantar IL-1 β . Wild-type (WT) and LysM G protein-coupled receptor kinase (GRK2)^{+/-} mice received an intraplantar injection of 1 ng IL-1 β . At 15 hours after injection, spinal cord was collected, and frozen sections of (A) lumbar spinal cord (L2 to L5) and as control (B) thoracic spinal cord (T6 to T10) were stained for M1 (CD16/32) and M2 (CD206 and arginase-I) phenotypic markers. A representative example of M1 and M2 staining in the dorsal horn of one of the four mice per group is displayed. Scale bar indicates 20 μ m. (C) Quantification of microglia/macrophages expressing M1 and M2 phenotypic markers in spinal cord from WT and LysM-GRK2^{+/-} mice. Expression was quantified in approximately 10 to 15 dorsal horns of spinal cords per group (4 mice per group). The level of expression in the lumbar or thoracic area from control WT mice was set at 100%. Data are expressed as means \pm SEM. ** $p < 0.01$, *** $p < 0.001$.

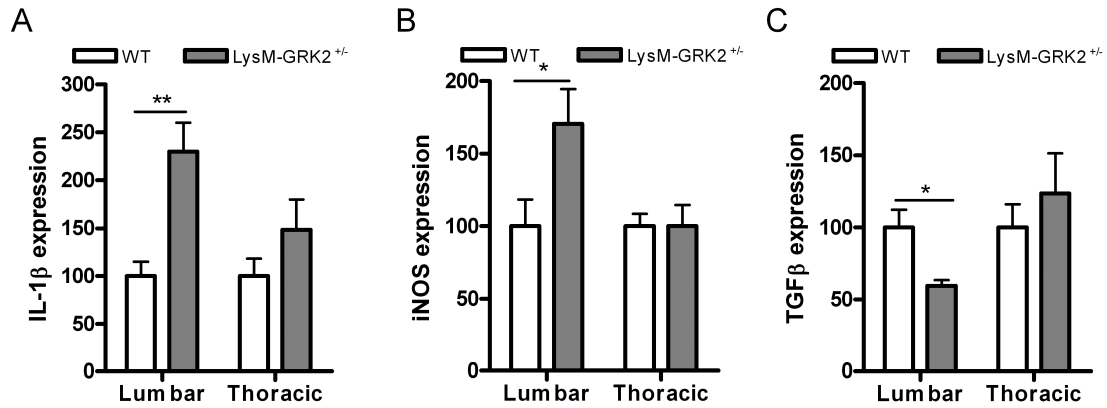


Figure 3.3: Gene expression of M1-associated and M2-associated genes in spinal microglia after intraplantar injection of interleukin (IL)-1β. Wild-type (WT) and LysM-G protein-coupled receptor kinase (GRK)2^{+/-} mice received an intraplantar injection of 1 ng IL-1β into the hind paws. At 24 hours after injection lumbar (L2 to L5) spinal cord and (as a control) thoracic (T6 to T10) spinal cord was collected from WT and LysM-GRK2^{+/-} mice, and microglia were isolated for analysis of mRNA expression by quantitative RT-PCR of (A) IL-1β, (B) inducible nitrous oxide synthase (iNOS) and (C) transforming growth factor (TGF)-β (n = 6 quantitative PCR samples per group; one sample contains isolated microglia from 4 mice). Data are expressed as means ± SEM. * p<0.05, ** p<0.01.

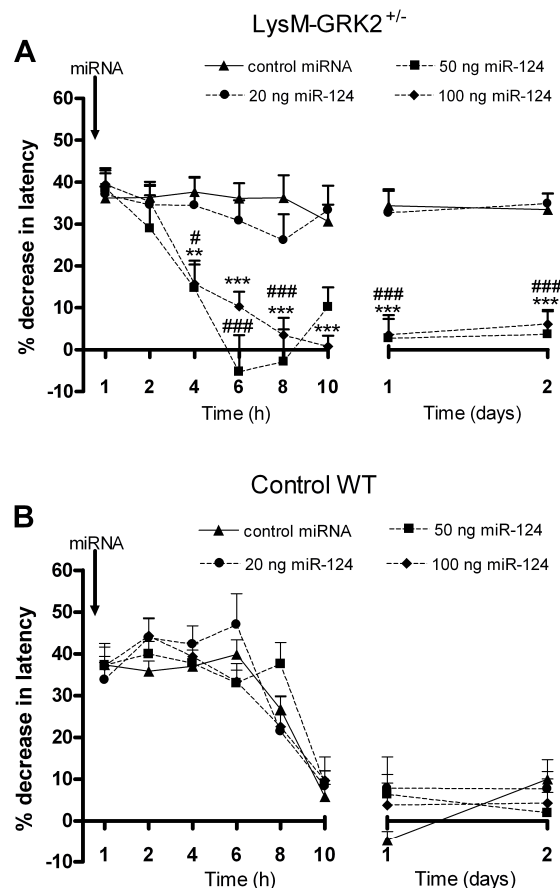


Figure 3.4: Effect of microRNA (miR)-124 treatment on interleukin (IL)-1β-induced hyperalgesia. (A) LysM G protein-coupled receptor kinase (GRK)2^{+/-} and (B) wild-type (WT) mice received an intrathecal injection of 20, 50 or 100 ng miR-124 per mouse or 100 ng negative control miRNA 1 day before intraplantar injection of 1 ng IL-1β and the percentage change in heat-withdrawal latency was determined (n = 4 to 10 per group). Data are expressed as means ± SEM. ** p<0.01, *** p<0.001 for 50 ng miR-124 versus control miRNA; # p<0.05, ### p<0.001 for 100 ng miR-124 versus control miRNA.

MicroRNA-124 treatment prevents transition to persistent hyperalgesia in LysM-GRK2^{+/-} mice

To examine the contribution of miR-124 to the course of hyperalgesia, we treated WT and LysM-GRK2^{+/-} mice with an intrathecal injection of miR-124, and monitored its effect on intraplantar IL-1 β -induced hyperalgesia. Intrathecal administration of 50 ng and 100 ng miR-124 completely prevented the transition from acute to persistent IL-1 β -induced hyperalgesia in LysM-GRK2^{+/-} mice (Figure 3.4A). Whereas intrathecal administration of 100 ng negative control miRNA or the lowest dose of miR-124 tested (20 ng) did not have any effect on the course of hyperalgesia in LysM-GRK2^{+/-} mice (Figure 3.4A). In WT mice, intrathecal administration of 20 to 100 ng miR-124 did not have any effect on IL-1 β -induced hyperalgesia (Figure 3.4B). In addition, baseline thermal sensitivity was not affected by miRNA administration either (decrease in heat withdrawal latency; WT plus control miRNA $2.6 \pm 1.9\%$; WT plus miR-124 $1.8 \pm 3.7\%$; LysM-GRK2^{+/-} plus control miRNA $2.0 \pm 3.25\%$; LysM-GRK2^{+/-} plus miR-124 $0.7 \pm 3.2\%$; $n = 4$).

Role of miR-124 in regulating spinal cord M1/M2 phenotype

After intraplantar IL-1 β injection, expression of M1 marker was increased and the expression of M2 marker was significantly decreased in LysM-GRK2^{+/-} mice compared with WT mice (Figure 3.2). We hypothesized that miR-124 treatment would normalize the expression of the M1 and M2 markers in LysM-GRK2^{+/-} mice. Indeed, the data clearly showed that miR-124 treatment regulates the M1/M2 balance; the intrathecal miR-124 reversed the difference in the expression of M1 and M2 phenotypic markers between WT and LysM-GRK2^{+/-} mice in response to intraplantar IL-1 β injection (Figure 3.5).

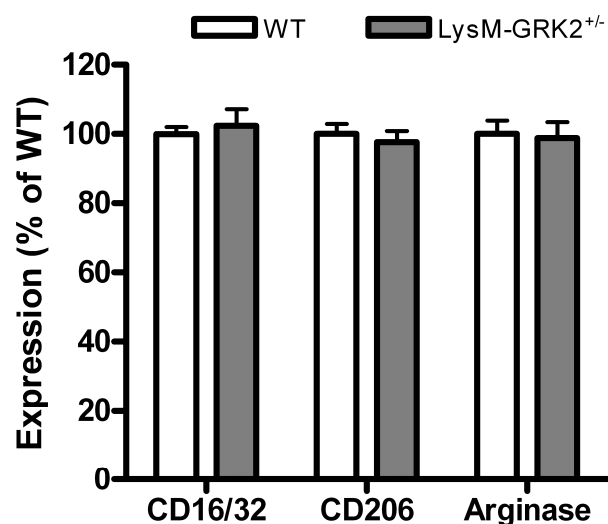


Figure 3.5 MicroRNA-124 treatment influences the M1/M2 balance and abolishes the genotype differences after interleukin (IL)-1 β injection. Mice received an intrathecal injection of 100 ng miR-124 the day before intraplantar injection of 1 ng IL-1 β . At 15 hours after IL-1 β injection, the spinal cord was collected, and frozen sections of lumbar spinal cord (L2 to L5) were stained for M1 and M2 phenotypic markers. M1 and M2 marker expressions were compared in wild-type (WT) versus LysM G protein-coupled receptor kinase (GRK)2^{+/-} mice, and expression was quantified in 18 dorsal and 18 lumbar spinal-cord sections per group from 4 mice per group. The level of expression in IL-1 β -treated WT mice was set at 100%. Data are expressed as means \pm SEM.

Effect of microRNA-124 on carrageenan-induced inflammatory hyperalgesia in wild-type mice

The next question we addressed is whether intrathecal miR-124 treatment can also reverse the persistent hyperalgesia that develops in WT mice after intraplantar injection of carrageenan^{6,61,98,257}. WT mice were still hyperalgesic 6 days after an intraplantar injection of high-dose λ -carrageenan. Intrathecal treatment with miR-124 at day 6 rapidly attenuated this persistent carrageenan-induced thermal hyperalgesia (Figure 3.6).

Effect of microRNA-124 in a model of neuropathic pain

We used the SNI model of chronic neuropathic pain in WT mice to investigate the effect of intrathecal miR-124 treatment on mechanical allodynia as assessed by von Frey filaments. The miR-124 or control miRNA was injected intrathecally once every day, starting 1 day after SNI surgery. Mice treated with control miRNA developed unilateral mechanical allodynia (Figure 3.7A). The miR-124 treatment completely prevented the mechanical allodynia that develops in the ipsilateral paw in response to SNI (Figure 3.7A), but did not affect mechanical sensitivity in the contralateral paw (Figure 3.7B). The miR-124 treatment did not affect spontaneous locomotor activity of SNI mice as determined in an open field 3 days after SNI (Figure 3.7C).

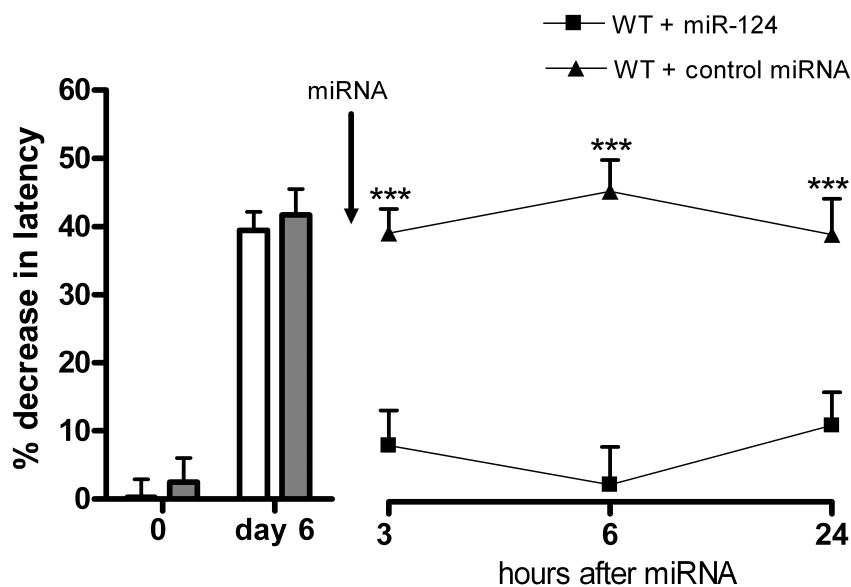


Figure 3.6 Effect of microRNA(miR)-124 treatment on carrageenan-induced persistent hyperalgesia in wild-type (WT) mice. Wild-type (WT) mice received an intraplantar injection of 20 μ l 2% λ -carrageenan. At day 6, mice were still hyperalgesic. At this time point, mice received an intrathecal injection of 100 ng miR-124 or control miRNA, and the percentage change in heat withdrawal latency was determined (miR-124 n = 8; control miRNA n = 4). Data are expressed as means \pm SEM. *** p<0.001.

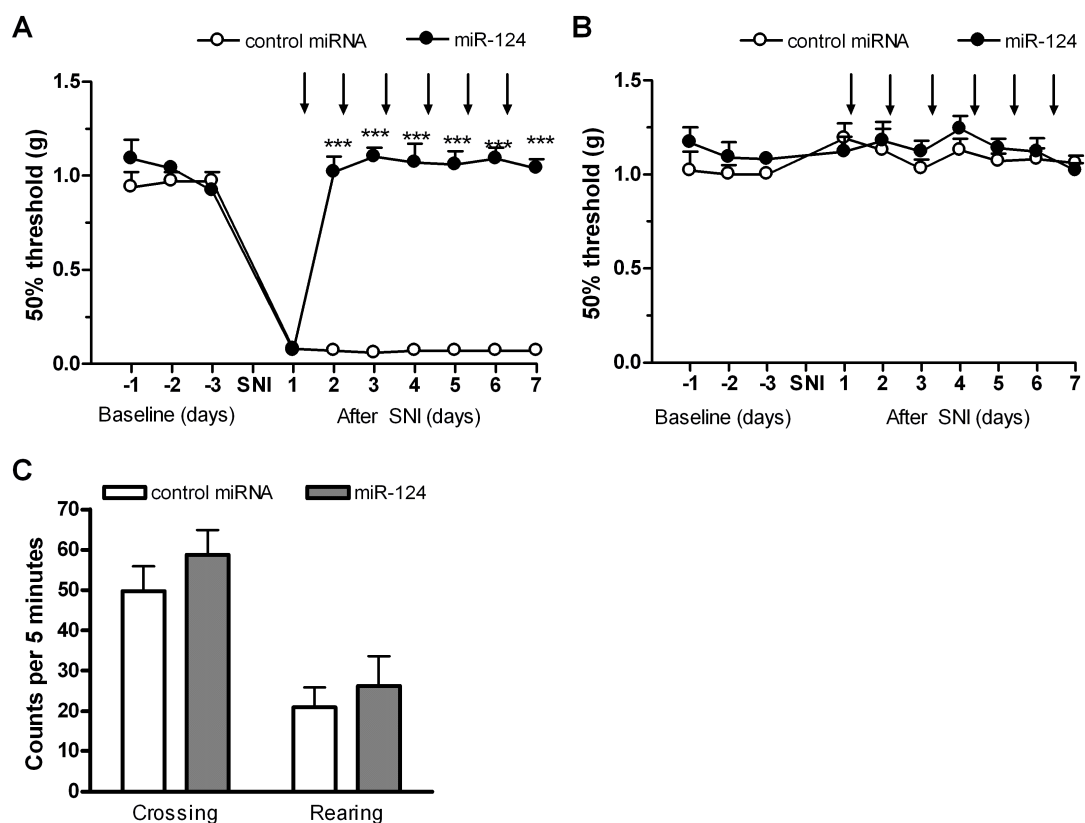


Figure 3.7: Effect of miR-124 treatment on SNI-induced mechanical allodynia in WT mice. Spared nerve injury was performed on WT mice and were treated daily with 100 ng miR-124 or control miRNA intrathecally (n = 7 per group). Mechanical allodynia was monitored in (A) ipsi- and (B) contralateral paw and is depicted as force needed for 50% withdrawal determined in accordance with the up and down method. Arrows indicate miRNA injection. (C) Spontaneous locomotor activity in an open field was monitored at day three after SNI to control for a potential effect of miR-124 treatment on motor function. Data are expressed as mean \pm SEM. *** p<0.01.

Discussion

In this paper, we present a previously unreported role of miR-124 in the regulation of chronic inflammatory and neuropathic pain. We found that intraplantar IL-1 β administration to LysM-GRK2 $^{+/-}$ mice, which induces persistent hyperalgesia, decreased the level of miR-124 in spinal cord microglia, increased expression of M1 type phenotypic markers and pro-inflammatory cytokines, and decreased expression of anti-inflammatory cytokines and M2 markers. We also showed that intrathecal administration of miR-124 normalized the M1/M2 ratio and prevented transition to persistent IL-1 β -induced hyperalgesia in GRK2-deficient mice. Moreover, this is the first study, to our knowledge, to show that intrathecal miR-124 treatment reverses persistent carrageenan-induced hyperalgesia in WT mice. Finally, we found that miR-124 treatment completely inhibits mechanical allodynia in the SNI model of chronic neuropathic pain. Collectively, our findings indicate that miR-124 could represent a novel treatment for chronic pain.

We showed previously that chronic carrageenan-induced paw inflammation in WT mice is associated with a decrease in GRK2 in spinal cord microglia²⁵⁷. In addition, in the spinal nerve transection model of chronic neuropathic pain in rats, spinal-cord microglial GRK2 levels are also reduced by approximately 50%⁶¹. In the current study, we found that intraplantar IL-1 β

injection in mice with low microglial/macrophage GRK2 levels induced a reduction in miR-124 expression, leading to a change in the M1/M2 balance towards a more pro-inflammatory phenotype and persistent hyperalgesia. Collectively, our current and previous findings indicate that the mechanisms involved in transition from acute to persistent hyperalgesia in the heterozygous GRK2 knockout model may well be applicable to the chronic pain that develops in more classic models of chronic pain. Indeed, our present findings show that miR-124 treatment also abrogates the existing persistent hyperalgesia induced by carrageenan in WT mice. The clinical relevance is further supported by the current data showing that miR-124 treatment inhibited the development of hyperalgesia in the SNI model of neuropathic pain supports.

It has been shown recently that intracranial injection of a miR-124 antisense oligonucleotide inhibitor induced activation of cerebral microglia¹⁸⁹. In addition, *in vitro* bone marrow-derived macrophages transfected with miR-124 produced reduced levels of iNOS and increased levels of TGF- β in conjunction with decreased C/EBP- α expression. The current study is the first, to our knowledge, to show that miR-124 treatment prevents transition to persistent hyperalgesia in mice with low GRK2 levels in microglia/macrophages. We also found that treatment with miR-124 reversed the increased M1/M2 ratio that occurred in response to intraplantar IL-1 β in the spinal cord of LysM-GRK2^{+/-} compared with WT mice. At the functional level, we showed that the decrease in miR-124 in LysM-GRK2^{+/-} spinal cord microglia in response to intraplantar IL-1 β was associated with increased expression of the pro-inflammatory cytokine IL-1 β and the pro-inflammatory enzyme iNOS, and with decreased expression of the anti-inflammatory cytokine TGF- β in spinal-cord microglia. At the same time, C/EBP- α , a 'master' transcription factor regulated by miR-124, was increased in spinal cord microglia from LysM-GRK2^{+/-} mice after intraplantar injection of IL-1 β . Collectively, our findings support the notion that the decreased miR-124 expression seen in conditions of low GRK2 promotes spinal cord microglial/macrophage activation, leading to an increased M1/M2 ratio and prolonged inflammatory hyperalgesia.

The current *in vivo* data are in line with the results from *in vitro* studies reported by Ponomarev *et al*, who found that *in vitro* miR-124 treatment reduces expression of iNOS and increases TGF- β , arginase I and Fizz expression by activated bone marrow-derived macrophages¹⁸⁹. Therefore, we propose that miR-124 treatment reverses hyperalgesia by restoring the ratio of M1/M2 microglia/macrophages.

To our knowledge, this is the first study to describe a beneficial effect of miR-124 treatment on inflammatory pain and a decrease in spinal cord microglial miR-124 in a model of persistent hyperalgesia. A few recent studies investigated miR-124 expression in other pain models. Bai *et al*. showed that miR-124 levels were significantly reduced in the trigeminal ganglion in a model of carrageenan-induced muscle pain, indicating that inflammatory activity regulates miR-124 in multiple pain models⁶. Brandenburger *et al*. reported that total spinal cord miR-124 was not changed in the chronic constriction injury model of neuropathic pain¹⁹; however, because miR-124 is expressed at a high level in neurons, a potential change in microglial miR-124 may well have been masked in that study. In the present study, by contrast, miR-124 levels were quantified in isolated spinal microglia.

Because we injected miR-124 intrathecally, we cannot completely exclude that miR-124 also directly affects other cells in the spinal cord, including sensory neurons. Notably, however, in control WT mice we did not observe any effect of miR-124 treatment on the magnitude or duration of IL-1 β -induced hyperalgesia. Moreover, intrathecal administration of miR-124 did not affect thermal sensitivity at baseline or mechanical sensitivity in the contralateral paw in the

SNI model and did not affect spontaneous locomotor activity. A study using a conditional Dicer knockout mice found that nociceptor miRNA transcripts are required for lowering peripheral pain thresholds in inflammatory hyperalgesia; nociceptor specific deletion of Dicer, an enzyme required for generation of miRNAs, prevents the development of inflammatory hyperalgesia²⁷². Based on these and our present findings it is unlikely that the inhibition of persistent hyperalgesia by miR-124 treatment in our study is mediated by inhibition of neuronal hypersensitivity or by impaired motor function.

Intraplantar IL-1 β administration did not have any effect on miR-124 expression in spinal cord microglia from control WT mice, whereas it significantly reduced miR-124 levels in microglia from LysM-GRK2^{+/-} mice. This finding indicates that low GRK2 in microglia/macrophages sensitizes these cells for an intraplantar IL-1 β -induced decrease in miR-124 expression in spinal cord microglia. The question arises how intraplantar administration of IL-1 β induces a decrease in microglial miR-124 levels. Interestingly, *in vitro* it has been shown that co-culture of bone marrow derived macrophages with primary neurons reduces the level of macrophage miR-124¹⁸⁹. These findings indicate that neuronal signals can directly regulate the expression of miR-124 in macrophage-like cells. It is known that peripheral nociceptors express IL-1 β receptors and triggering of these receptors results in direct sensitization of the nociceptor⁶². Therefore, it is conceivable that concomitantly, neuronal signals transmitted to the spinal cord induce a reduction in miR-124 and thereby induce a M1 type spinal cord microglia activation. Our finding that only in mice with low GRK2 in microglia/macrophages miR-124 levels in spinal cord microglia are reduced in response to intraplantar IL-1 β may point to a contribution of a GPCR-mediated signal to nociceptor-to-microglia signaling. However, GRK2 is also known to regulate cellular signaling at various levels downstream of the membrane receptors. Thus, also increased signaling independently of GPCRs in GRK2-deficient spinal cord microglia/macrophages may contribute to the seen decrease in miR-124 expression in microglia/macrophages from LysM-GRK2^{+/-} mice after intraplantar IL-1 β .

Conclusions

We propose that low spinal microglia/macrophage GRK2 levels promote a transition to persistent hyperalgesia via impaired microglial miR-124 regulation, and consequently an impaired spinal M1/M2 balance. This model is supported by our findings that treatment with intrathecal administration of miR-124 normalized the expression of M1 and M2 markers in LysM-GRK2^{+/-} mice and inhibited the development of IL-1 β -induced persistent hyperalgesia in these mice. The broader relevance of our results is supported by our finding that miR-124 treatment reversed persistent hyperalgesia induced by a high dose of carrageenan and prevented development of hyperalgesia in the SNI model of chronic neuropathic pain. In conclusion, miR-124 might represent a novel option for the treatment of chronic pain.

Acknowledgements

This study was supported by NIH grants R01 NS 073939 and R01 NS 074999 to AK.

A large, bold, white number '4' is centered on a vertical strip. The strip has a repeating geometric pattern of overlapping triangles, creating a mesh-like structure. The background to the left of the strip is plain white.

4

Peripheral monocytes/macrophages control resolution of inflammatory pain

Hanneke L.D.M. Willemen¹

Niels Eijkelkamp¹

Anibal Garza Carbajal^{1,4}

Huijing Wang¹

Matthias Mack²

Jitske Zijlstra¹

Cobi J. Heijnen^{3,1}

Annemieke Kavelaars^{3,1}

¹ Laboratory of Neuroimmunology and Developmental Origins of Disease (NIDOD), University Medical Center Utrecht, Utrecht, The Netherlands

² Department of Internal Medicine II, University Hospital Regensburg, Regensburg, Germany

³ Department of Symptom Research, University of Texas MD Anderson Cancer Center, Houston, TX

⁴ Department for Molecular Human Genetics, Max Planck Institute for Molecular Genetics, Berlin, Germany

Abstract

Insights into mechanisms governing resolution of inflammatory pain are of interest for many chronic pain associated diseases. Peripheral monocyte/macrophage depletion delayed resolution of transient IL-1 β -induced inflammatory hyperalgesia (<1 day) with more than 1 week in WT mice. Cell-specific reduction in G protein-coupled receptor kinase 2 (GRK2) in LysM-positive macrophages prolonged IL-1 β -induced hyperalgesia. Depleting peripheral monocyte/macrophages in LysM-GRK2^{+/-} mice did not reduce prolonged hyperalgesia. Adoptive transfer of WT but not GRK2^{+/-} bone marrow-derived monocytes (BMDM) to LysM-GRK2^{+/-} mice prevented development of persistent IL-1 β -induced hyperalgesia. Mechanistically, we show that GRK2^{+/-} macrophages produce less IL-10 *in vitro* and intrathecal IL-10 attenuated IL-1 β -induced hyperalgesia in LysM-GRK2^{+/-} mice. In WT mice intrathecal anti-IL10 prolonged IL-1 β -induced hyperalgesia. Adoptive transfer of IL-10^{-/-} BMDM did not prevent IL-1 β -induced persistent hyperalgesia in LysM-GRK2^{+/-} mice. Our data indicate a key role for peripheral monocytes/macrophages in promoting resolution of inflammatory hyperalgesia via a mechanism dependent of IL-10 signaling and GRK2 levels.

Introduction

According to a recent study of the Institute of Medicine approximately 100 million Americans suffer from chronic pain (www.iom.edu/relievingpain). One of the limitations for development of novel interventions identified in this report is the limited understanding of the mechanisms governing the transition from acute to chronic pain.

Studies in rodents have revealed that spinal cord microglia, the resident macrophages of the central nervous system, play an important role in the development of chronic pain in models of nerve damage-induced neuropathic pain, diabetic neuropathy and chronic inflammatory pain^{37,55,166,204,250,274}. In addition, it has been hypothesized that infiltration of peripheral macrophages into the spinal cord enhances the hyperalgesia in models of chronic pain⁵⁸. A common finding is that pro-inflammatory cytokines released by activated spinal cord microglia and/or infiltrating macrophages contribute to the chronic hyperalgesia that is a hallmark of these animal models of chronic pain^{51,166,216}.

We recently showed that mice with a cell-specific 50% reduction of the kinase GRK2 in lysozyme (Lys)M-positive macrophages/microglia develop markedly prolonged hyperalgesia in response to an intraplantar injection of a cytokine, chemokine or carrageenan. For example, thermal hyperalgesia and mechanical allodynia induced by a single intraplantar injection of the pro-inflammatory cytokine IL-1 β resolves within one day in WT mice, but lasts at least 8 days in LysM-GRK2^{+/-} mice^{257,258}. Intrathecal administration of the microglial/macrophage inhibitor minocycline reversed this prolongation of hyperalgesia in LysM-GRK2^{+/-} mice, indicating a contribution of spinal cord and/or dorsal root ganglion (DRG) microglia/macrophages in the transition to persistent hyperalgesia^{61,257}. The pathophysiological relevance of a reduced level of GRK2 in microglia/macrophages is exemplified by our recent findings that spinal cord microglia/macrophage GRK2 levels are reduced by approximately 40% during chronic inflammatory hyperalgesia and neuropathic pain in WT mice^{61,257}. In addition, in patients with the painful chronic inflammatory disease rheumatoid arthritis the level of GRK2 in circulating mononuclear cells is reduced by 40-60%¹⁴⁷.

Here we investigated the contribution of peripheral monocyte/macrophages using depletion and adoptive transfer strategies on acute intraplantar IL-1 β induced hyperalgesia in WT mice and the transition to persistent hyperalgesia in LysM-GRK2^{+/-} mice.

Materials and Methods

Animals

We used female (aged 10-14 weeks) mice with cell-specific reduction of GRK2 in LysM-positive cells (LysM-GRK2^{+/-}) and control LysM-GRK2^{+/+} mice (WT littermates)^{61,258}. For adoptive transfer experiments WT and GRK2-deficient green fluorescent protein (GFP) positive bone marrow-derived monocytes (BMDM) were obtained by breeding GRK2^{+/-} mice with CX3CR1^{gfp/gfp} mice (Jackson Laboratories). In addition, BMDM from IL-10^{-/-} mice (Jackson Laboratories) were used. Mice were housed at the Utrecht University animal facility. Experiments were performed in accordance with international guidelines and approved by the UMC Utrecht experimental animal committee.

Mice received an intraplantar injection in the hind paw of 5 μ l recombinant murine IL-1 β (200 ng/ml in saline; Peprotech). Heat withdrawal latency times were determined by an experimenter blinded to treatment using the Hargreaves test (IITC Life Science)⁸⁹.

Drug administration

Intrathecal (i.t.) injections (5 μ l) with goat anti-mouse IL-10 (10 μ g in PBS; Sigma-Aldrich), normal goat IgG (10 μ g in PBS; R&D systems) or human recombinant IL-10 (0.5 μ g in PBS; Sigma-Aldrich) were performed under light isoflurane anaesthesia as described previously⁶¹.

Cell depletion

Mice received intraperitoneal injections with 100 μ l anti-CCR2 (MC21; 0.2 μ g/ μ l¹⁵⁴) or IgG2b control (BD Biosciences) at 24 h and 0.5 h before and 10 h after intraplantar IL-1 β . Alternatively, mice received intraperitoneal injections with 200 μ l (7 mg/ml) clodronate-liposomes²³⁶ or PBS-liposomes at 30 min before and 10 h after intraplantar IL-1 β .

Adoptive transfer

Bone marrow-derived monocytes (BMDM) were isolated as described recently²¹⁷. Following Ficoll (GE Healthcare) density gradient centrifugation of bone marrow from femora and tibiae, CD115⁺ monocytes were isolated with biotin labelled anti-CD115 antibodies and streptavidin-coupled magnetic beads following manufactures instructions (Miltenyi Biotec). IL10^{-/-}, WT-CX3CR1^{gfp/+} or GRK2^{+/-}-CX3CR1^{gfp/+} monocytes were intravenously injected (3.5 \times 10⁶ cells per mouse).

Flow cytometry

BMDM, blood leukocytes and cells isolated from the peritoneum were stained with anti-CD115 (eBioscience), anti-CCR2 (R&D systems) and anti-CD45. Cells were analyzed on a FACSCanto II flowcytometer using FACS Diva software (BD Biosciences).

In vitro culture

Peritoneal macrophages (0.2 \times 10⁶ cells per well) were cultured in RPMI-1640 with 10% FCS, 2 mM glutamine and 50 μ M β -mercaptoethanol (all Gibco) and stimulated with 10 ng/ml LPS (Sigma-Aldrich) for 18 h (RNA) or 24 h (protein). IL-10 and TNF- α concentration in the supernatant was determined with ELISA (Ucytech). To determine IL-1 β with ELISA (BD OpTEIA) cultured cells were exposed for 60 min to 3 mM ATP to induce IL-1 β secretion.

Immunohistochemistry

Spinal cord and dorsal root ganglia (DRG) were post-fixed in 4% paraformaldehyde and cryoprotected in sucrose. Cryosections (10 μ m) of DRG and of lumbar segments L2-L5 were incubated with 1:100 rabbit anti-GFP (GeneTex) and 1:200 rat anti-CD45-PE (BD Bioscience) followed by alexa fluor 594-conjugated secondary antibody. Photographs were taken with a Zeiss Axio Observer microscope (Zeiss).

Statistical Analysis

All data are presented as mean \pm SEM and were analyzed using Student's t-test or two-way ANOVA with Bonferroni post-hoc tests.

Results

Effect of peripheral monocyte/macrophage depletion

To investigate the contribution of peripheral monocytes/macrophages to the course of intraplantar IL-1 β -induced thermal hyperalgesia, we utilized two different monocyte/macrophage depletion strategies. First, we administered anti-CCR2 monoclonal antibody intraperitoneally (i.p.) at 24 h and 30 min before and 10 h after intraplantar IL-1 β . In WT mice, anti-CCR2 treatment prolonged IL-1 β -induced hyperalgesia to at least 8 days (Figure 4.1A). In WT mice treated with control IgG, IL-1 β -induced hyperalgesia resolved within 24 h, which is consistent with our earlier findings in WT mice receiving intraplantar IL-1 β only^{61,257}. In LysM-GRK2^{+/-} mice IL-1 β -induced hyperalgesia was prolonged compared to WT mice^{61,257}. Here we show that this prolonged hyperalgesia in LysM-GRK2^{+/-} mice was not affected by anti-CCR2 mediated monocyte/macrophage depletion (Figure 4.1A). Baseline thermal sensitivity was not affected by antibody injections as well (Table 4.1). FACS analysis of peritoneal lavage and peripheral blood confirmed monocyte/macrophage depletion in both WT-CX3CR1^{gfp/+} and GRK2^{+/-}-CX3CR1^{gfp/+} mice (Figure 4.1B and C).

In a second set of experiments mice received i.p. injections of clodronate-liposomes which are known to deplete peritoneal macrophages/monocyte without affecting microglial numbers^{179,213,236}. Clodronate-mediated depletion of peripheral monocytes/macrophages prolonged the hyperalgesic response to intraplantar IL-1 β -injection in WT mice from less than 24 h to at least two days (Figure 4.1C). Clodronate-treatment did not have any effect on the persistent IL-1 β -induced hyperalgesia in LysM-GRK2^{+/-} mice (Figure 4.1D). Baseline sensitivity was not affected by clodronate treatment (Table 4.2).

Table 4.1: Baseline heat withdrawal latency times (in seconds) after antibody injections.

	WT (n = 4)	LysM-GRK2 ^{+/-} (n = 4)
IgG	7.66 \pm 0.15	7.71 \pm 0.12
Anti-CCR2	7.88 \pm 0.17	7.77 \pm 0.18

Table 4.2: Baseline heat withdrawal latency times (in seconds) after liposome injections.

	WT (n = 8)	LysM-GRK2 ^{+/-} (n = 8)
PBS-liposomes	7.99 \pm 0.44	8.02 \pm 0.22
Clodronate-liposomes	8.32 \pm 0.15	7.96 \pm 0.18

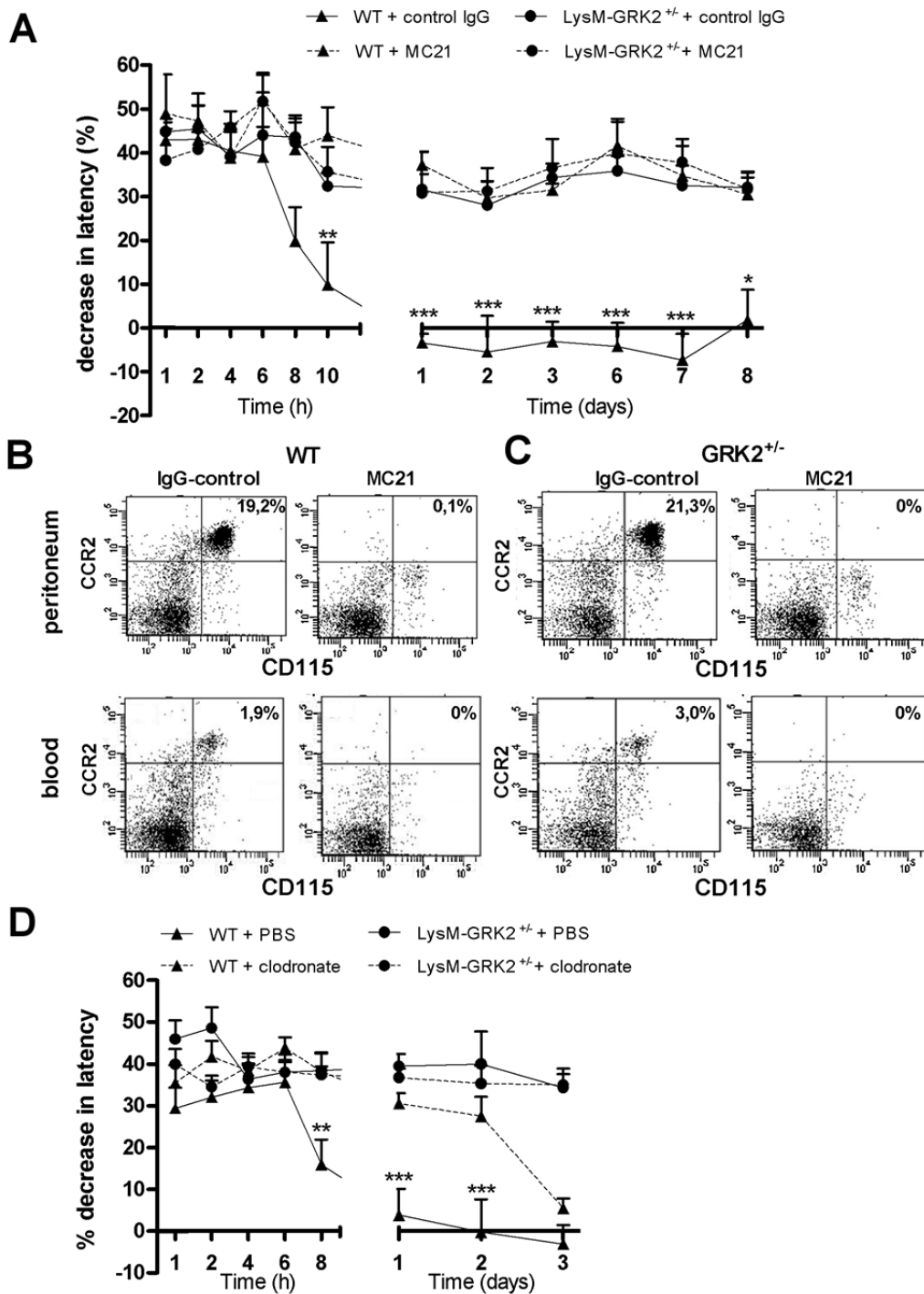


Figure 4.1: Effect of peripheral monocyte/macrophage depletion on the duration of IL-1 β -induced hyperalgesia. (A) The percentage decrease in heat withdrawal latency was assessed over time after intraplantar injection of 1 ng IL-1 β in WT and LysM-GRK2^{+/-} mice. To deplete monocytes/macrophages, mice received intraperitoneal injections of 20 μ g anti-CCR2 antibody (MC21) or control IgG at 24 h and 0.5 h before as well as 10 h after intraplantar IL-1 β (n = 4 per group). (B-C) Flow cytometric analysis shows successful depletion of CD115⁺/CCR2⁺ monocytes in peritoneal cavity washes and peripheral blood from (B) WT and (C) GRK2^{+/-} mice. (D) Mice received i.p. injections of 200 μ l (7 mg/ml) clodronate-liposomes or PBS-liposomes at 15 min before and 10 h after intraplantar IL-1 β (n = 8 per group). The percentage decrease in heat withdrawal latency was followed over time after intraplantar injection of IL-1 β (1 ng) in WT and LysM-GRK2^{+/-} mice. Data are expressed as mean \pm SEM. * p<0.05, ** p<0.01, *** p<0.001.

Adoptive transfer of WT BMDM to LysM-GRK2^{+/-} mice

The findings in figure 4.1 indicate that in WT mice, peripheral monocytes/macrophages are key to promoting the resolution of IL-1 β -induced hyperalgesia. To test the contribution of peripheral monocytes/macrophages to transition to persistent hyperalgesia in LysM-GRK2^{+/-} mice, we adoptively transferred WT BMDM. LysM-GRK2^{+/-} mice were injected intravenously (i.v.) with 3.5×10^6 WT BMDM (based on ²¹⁷) 10 min prior intraplantar IL-1 β injection. Transfer of WT BMDM to LysM-GRK2^{+/-} mice completely prevented the development of persistent IL-1 β hyperalgesia and led to resolution of IL-1 β hyperalgesia in LysM-GRK2^{+/-} mice within a time frame similar to that observed in WT mice (Figure 4.1A vs 4.2A). Transfer of GRK2-deficient BMDM to LysM-GRK2^{+/-} did not have any effect on IL-1 β -induced hyperalgesia (Figure 4.2B). FACS analysis showed that the percentage of CD115⁺/CD45⁺ and CCR2⁺ cells in BMDM was similar in WT and GRK2^{+/-} mice (see Supplementary Figure 4.1). Transfer of WT BMDM to WT mice prior to intraplantar IL-1 β did not affect the spontaneous resolution of hyperalgesia in these mice (Figure 4.2C).

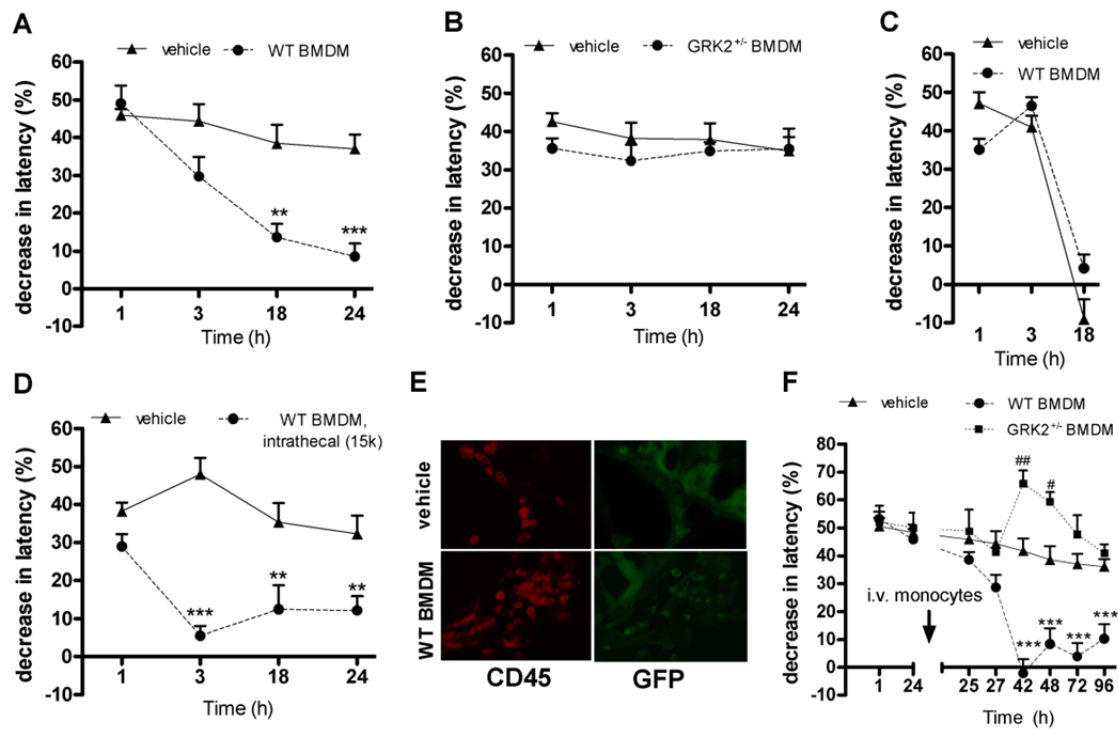


Figure 4.2: Adoptive transfer of WT BMDM prevents and treats persistent IL-1 β -induced hyperalgesia in LysM-GRK2^{+/-} mice. (A-D) The percentage decrease in heat withdrawal latency was assessed over time after intraplantar IL-1 β . (A-B) LysM-GRK2^{+/-} mice were injected intravenously (i.v.) with (A) WT BMDM (3.5×10^6 cells per mouse; $n = 10$), (B) GRK2^{+/-} BMDM (3.5×10^6 cells per mouse; $n = 8$) or vehicle ($n = 8$) 10 min before intraplantar IL-1 β . (C) WT mice received i.v. WT BMDM (3.5×10^6 cells per mouse) or vehicle ($n = 10$ per group) 10 min before intraplantar IL-1 β . (D) LysM-GRK2^{+/-} received WT BMDM (15,000 per mouse) or vehicle intrathecally ($n = 6$ per group) 10 min before intraplantar IL-1 β . (E) Representative pictures of DRG of LysM-GRK2^{+/-} mice treated with vehicle or WT GFP-BMDM (3.5×10^6 cells per mouse) 10 min before intraplantar IL-1 β . DRG were isolated 8 h after intraplantar IL-1 β administration and stained for GFP and CD45 to identify transplanted cells. (F) WT or GRK2^{+/-} BMDM (3.5×10^6 cells per mouse) or vehicle were administered i.v. 24 h after intraplantar IL-1 β , i.e. during already established persistent hyperalgesia in LysM-GRK2^{+/-} mice. The percentage decrease in heat withdrawal latency was assessed over time ($n = 4 - 8$). Data are expressed as mean \pm SEM. ** $p < 0.01$, *** $p < 0.001$ WT BMDM vs. vehicle. # $p < 0.05$, ## $p < 0.01$ GRK2^{+/-} BMDM vs. vehicle.

As compared to intravenous administration (Figure 4.2A), intrathecal administration of 15,000 WT BMDM promoted a more rapid resolution of IL-1 β hyperalgesia in LysM-GRK2^{+/-} mice (Figure 4.2D), indicating that macrophages locally in DRG or spinal cord are likely to contribute. Indeed, we detected GFP⁺-BMDM in lumbar DRG after intravenous administration (Figure 4.2E). However, we did not detect donor GFP⁺-BMDM in lumbar spinal cord.

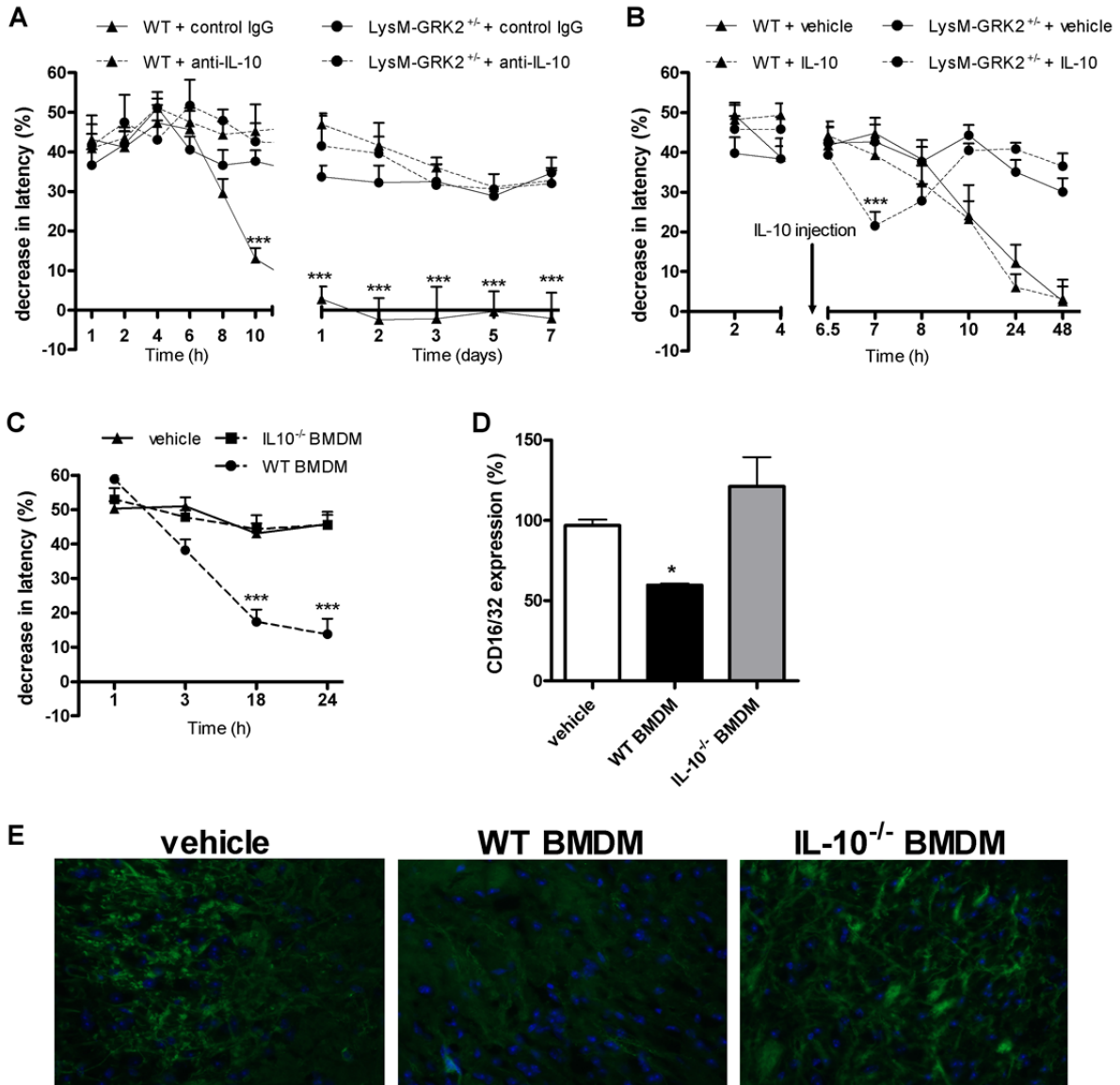


Figure 4.3: Role of IL-10 in the regulation of IL-1 β -induced hyperalgesia. The percentage decrease in heat withdrawal latency was determined over time after intraplantar IL-1 β in WT and LysM-GRK2^{+/-} mice. Mice received an i.t. injection of (A) 10 μ g anti-IL10 or control IgG (n = 12 per group) 15 min prior to intraplantar IL-1 β . (B) WT and LysM-GRK2^{+/-} mice received an intrathecal injection of 0.5 μ g recombinant IL-10 (n = 8) or vehicle (n = 4) 6 h after intraplantar IL-1 β . (C) IL10^{-/-} BMDM or WT BMDM (3.5 \times 10⁶ cells per mouse) were injected i.v. 10 min prior to intraplantar IL-1 β in LysM-GRK2^{+/-} mice (n = 6 - 8 per group). (D-E) 24 h after adoptive transfer of WT or IL-10^{-/-} BMDM lumbar dorsal horn spinal cord sections were stained for the M1-type microglia/macrophage activation marker CD16/32 (D) Quantification of the CD16/32 immunofluorescence (n = 4) and (E) representative sections of lumbar dorsal horn spinal cord stained for CD16/CD32. All data are expressed as mean \pm SEM. * p<0.05 ** p<0.01, *** p<0.001.

The data in figure 4.2F show that intravenous administration of WT BMDM at 24 h after intraplantar IL-1 β also reduces already persistent hyperalgesia (Figure 4.2F). Transfer of GRK2^{+/-} BMDM at 24 h after IL-1 β increased hyperalgesia at 3 and 18 h after transfer (Figure 4.2F).

Role of IL-10 in the regulation of IL-1 β -induced hyperalgesia

Next we tested the hypothesis that monocytes/macrophages control resolution of hyperalgesia via an IL-10 dependent pathway. In WT mice, intrathecal injection of anti-IL-10 antibody significantly prolonged hyperalgesia induced by intraplantar IL-1 β to at least 7 days. In WT mice treated with control IgG, IL-1 β -induced hyperalgesia resolved within 24 h. Notably, i.t. anti-IL-10 did not have any effect on IL-1 β -induced hyperalgesia in LysM-GRK2^{+/-} mice (Figure 4.3A).

Conversely, intrathecal IL-10 injection at 6 h after intraplantar IL-1 β transiently reduced IL-1 β hyperalgesia in LysM-GRK2^{+/-} mice without having any effect in WT mice (Figure 4.3B). This transient effect of IL-10 is likely due to the reported short half-life of IL-10¹⁶⁴.

Transfer of IL-10^{-/-} BMDM into LysM-GRK2^{+/-} mice did not prevent the transition to persistent hyperalgesia induced by IL-1 β , whereas transfer of the same number of WT BMDM completely prevented the transition to persistent hyperalgesia in LysM-GRK2^{+/-} mice (Figure 4.3C).

We previously reported that the persistent IL-1 β -induced hyperalgesia in LysM-GRK2^{+/-} mice is associated with a pro-inflammatory M1 microglia/macrophage phenotype in the spinal cord²⁵⁸. Here we show that transfer of WT monocytes, but not of IL-10^{-/-} monocytes reduces expression of the M1 marker CD16/32 in the spinal cord of intraplantar IL1 β -treated LysM-GRK2^{+/-} mice (Figure 4.3D and E).

Supporting our hypothesis that GRK2-deficiency in peripheral monocytes/macrophages is key to the prolongation of hyperalgesia in LysM-GRK2^{+/-} mice, GRK2 protein levels are reduced by ~50% in macrophages of these mice, whereas GRK2 protein or mRNA levels did not differ between freshly isolated microglia from WT and LysM-GRK2^{+/-} mice (see Supplementary Figure 4.2). We showed earlier that in primary cultures of LysM-GRK2^{+/-} microglia at 14 days GRK2 protein levels are reduced by ~50%. These findings confirm that the LysM promoter is not active in naive freshly isolated microglia but is induced in microglia after *in vitro* culture and is active in peripheral monocytes and macrophages^{31,157}.

Effect of GRK2-deficiency on IL-10 production

Finally we tested the hypothesis that GRK2-deficiency impairs the capacity of GRK2^{+/-} macrophages to produce IL-10. Both the level of IL-10 mRNA as well as the amount of IL-10 secreted was significantly lower in LPS-stimulated cultures of GRK2^{+/-} compared to WT macrophages (Figure 4.4). Conversely, GRK2^{+/-} macrophages released higher levels of the pro-inflammatory cytokines TNF- α and IL-1 β (Figure 4.4 and ¹⁸⁵) after stimulation with LPS.

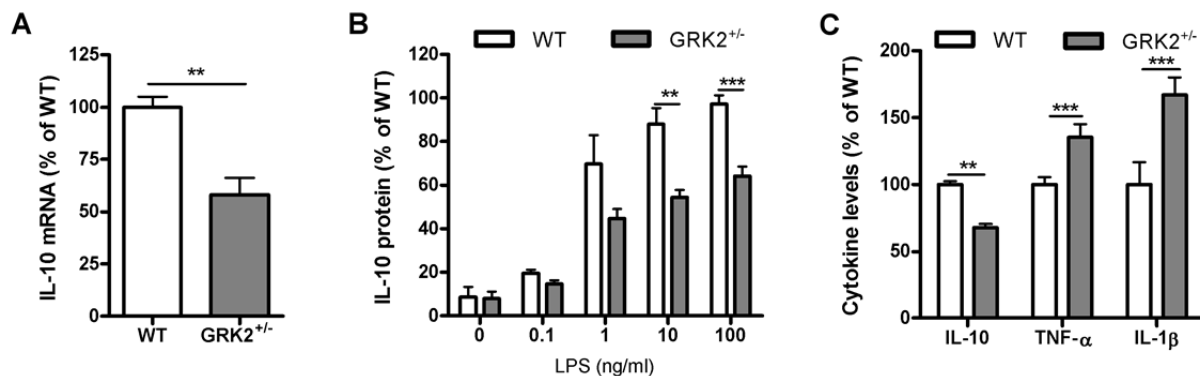


Figure 4.4: IL-10 production by WT and GRK2^{+/-} macrophages. (A) Freshly isolated WT and GRK2^{+/-} peritoneal macrophages were stimulated with 10 ng/ml LPS and after 18 h IL-10 mRNA expression was determined. (B) WT and GRK2^{+/-} macrophages were stimulated for 24 h with different doses of LPS and IL-10 protein content in supernatant was determined. Data were normalised against the maximal response of WT macrophages induced by 100 ng/ml LPS (C) WT and GRK2^{+/-} monocytes were stimulated with 10 ng/ml LPS for 24 h and IL-10, TNF- α and IL-1 β protein content in supernatant was determined (n = 4 – 8 per group). Data are expressed as mean \pm SEM. ** p<0.01, *** p<0.001.

Discussion

Here we present a so far unrecognized and crucial role for peripheral monocytes/macrophages in the resolution of transient inflammatory hyperalgesia. Specifically depletion of peripheral monocytes/macrophages in WT mice causes transition from transient IL-1 β -induced hyperalgesia into persistent hyperalgesia. Moreover, adoptive transfer of WT BMDM, but not of GRK2^{+/-} BMDM, to LysM-GRK2^{+/-} mice prevents and reverses the persistent hyperalgesia that develops in these mice. Adoptive transfer of IL-10^{-/-} monocytes did not have any effect on the persistent hyperalgesia in LysM-GRK2^{+/-} mice and intrathecal administration of anti-IL-10 markedly prolonged hyperalgesia in WT mice. Collectively, our findings identify a crucial role for peripheral monocytes/macrophages with normal GRK2 levels, which produce IL-10 to promote resolution of IL-1 β -induced hyperalgesia.

We are the first to show that peripheral monocytes/macrophages are required for the spontaneous resolution of hyperalgesia in response to a transient inflammatory stimulus. We demonstrate that anti-CCR2- or clodronate-mediated peripheral monocyte/macrophage depletion prolongs hyperalgesia in response to a transient peripheral inflammatory stimulus. This finding indicates that peripheral monocytes/macrophages are key to preventing the transition to chronic pain.

The few earlier studies that used depletion strategies to determine the contribution of peripheral monocytes/macrophages to pain focused mainly on neuropathic pain and results were mixed. Rutkowski et al., described that nerve-injury induced mechanical allodynia was not altered by clodronate liposome-mediated depletion prior to the induction of nerve injury²¹¹. In contrast, Liu et al. showed alleviation of nerve injury-induced allodynia by clodronate liposome-mediated monocyte/macrophage depletion during ongoing neuropathic pain and a reduction in the number of macrophages in the injured nerve¹⁴⁴. Development of diabetic neuropathy was delayed after macrophage depletion¹⁶⁰. Persistent hyperalgesia after intraplantar injection with Freund's adjuvant was not affected by clodronate-liposome-mediated monocyte/macrophage local depletion in the hindpaw¹⁸. In contrast, our study indicates that in the context of transient

hyperalgesia induced by a single injection of a mild inflammatory stimulus (IL-1 β), monocyte/macrophage depletion markedly prolongs hyperalgesia.

In search for the pathway via which peripheral monocytes/macrophages promote resolution of transient inflammatory hyperalgesia, we focused on the anti-inflammatory cytokine IL-10. Our data showing that intrathecal injection of anti-IL-10 in WT mice prolongs the duration of IL-1 β hyperalgesia, indicate that IL-10 signaling in the spinal cord or DRG is required for spontaneous resolution of hyperalgesia in this model of acute inflammatory pain. It has been shown before that intrathecal treatment with IL-10 or local overexpression of IL-10 alleviates hyperalgesia in mouse and rat models of neuropathic pain¹⁶⁴. However, until now it was not known that IL-10 signaling, likely downstream of IL-10 production by peripheral monocytes/macrophages, is required for the spontaneous resolution of hyperalgesia in response to a short-lasting peripheral inflammatory stimulus.

We reported earlier that the transition from acute to persistent IL-1 β -hyperalgesia in LysM-GRK2^{+/-} mice is associated with persistent microglia/macrophage activation in the spinal cord with an M1 or pro-inflammatory phenotype. In addition, after intraplantar IL-1 β isolated spinal cord microglia/macrophages from LysM-GRK2^{+/-} mice express significantly more pro-inflammatory (M1) cytokine and less anti-inflammatory (M2) cytokines compared to cells from WT mice²⁵⁸. Here we show that *in vitro*, GRK2-deficient monocytes/macrophages produce less of the anti-inflammatory M2-type cytokine IL-10 and increased levels of the pro-inflammatory M1-type cytokines IL-1 β and TNF- α . Moreover, transfer of WT, but not IL-10 deficient BMDM promotes resolution of hyperalgesia and reduces the expression of CD16/32, a marker of pro-inflammatory M1 microglia/macrophages in LysM-GRK2^{+/-} spinal cord. Collectively these findings indicate that the transition from acute to persistent hyperalgesia in LysM-GRK2^{+/-} mice is caused by reduced capacity of GRK2-deficient macrophages to produce IL-10 which inhibits the M1-type spinal cord microglia/macrophage activity.

In our previous studies, we showed that GRK2 levels of primary microglia cultures from LysM-GRK2^{+/-} mice were reduced by approximately 50% compared to WT microglia^{177,257}. However, in the present study we show that the level of GRK2 protein or mRNA in freshly isolated microglia from LysM-GRK2^{+/-} mice was not different from WT microglia. This finding is in line with the notion that the LysM promoter is not active in naive freshly isolated microglia but becomes active in these cells after stimulation^{31,157}. The fact that GRK2 is reduced in macrophages, but not microglia from LysM-GRK2^{+/-} further supports the hypothesis that the *peripheral* monocytes/macrophage component are key for regulating the transition from acute to chronic pain.

Our current findings that IL-10-producing BMDM suppress spinal cord inflammatory activity and promote resolution of transient inflammatory hyperalgesia are reminiscent of earlier findings regarding the contribution of BMDM to injury and repair of the damaged spinal cord. In a model of spinal cord injury Shechter et al. demonstrated that peripheral monocytes infiltrate into the damaged central nervous system to regulate recovery. They also showed that adoptive transfer of WT, but not IL-10 deficient BMDM, promoted recovery from spinal cord injury²¹⁷. The model of spinal cord injury is associated with damage to the blood brain barrier which will facilitate the infiltration of BMDM into the spinal cord. Notably, it is unlikely that the blood brain barrier is damaged or more permeable in response to a single intraplantar injection of IL-1 β . Yet, intravenous adoptive transfer of monocytes promotes resolution of hyperalgesia and this effect can be mimicked by intrathecal delivery of a much lower number of BMDM. However, even though the transfer of BMDM reduced the expression of pro-inflammatory microglia marker

CD16/32 in the spinal cord, we did not detect infiltration of donor BMDM into the spinal cord, but only in the DRGs. Based on these results, we propose that the control of resolution of hyperalgesia by BMDM involves IL-10 signaling in the DRG resulting in suppression of nociceptor sensitization and reduction of microglial activation in the spinal cord. However, we cannot exclude that intravenous adoptive transfer of BMDM promotes resolution of hyperalgesia via an effect of transferred cells on the peripheral nerve endings or on local inflammatory activity in the paw.

Earlier studies have shown that chronic constriction injury in rats leads to a decrease in IL-10 protein in the DRG¹⁰⁸. In addition, overexpression of IL-10 in the spinal cord alleviates chronic hyperalgesia in models of chronic neuropathic pain^{165,167}. Successful treatment of neuropathic pain in rats is associated with an increase in IL-10 in the spinal cord²⁵⁶. In line with these observations in animal models, an inverse correlation between pain intensity and plasma IL-10 has been reported in patients with chronic pain receiving opioid therapy. Moreover, plasma IL-10 levels were two-fold higher in patients with painful compared to painless neuropathy²⁷⁶. It remains to be determined whether a decrease in IL-10 production in patients with chronic pain is associated with reduced expression of GRK2 in peripheral monocytes/macrophages. Notably, we showed earlier that the painful autoimmune diseases rheumatoid arthritis and multiple sclerosis are associated with a decrease in the level of GRK2 in peripheral blood mononuclear cells as compared to healthy individuals^{147,242}. Moreover, analysis of cytokine profiles in these patients showed increased pro-inflammatory cytokines such as TNF- α and decreased levels of anti-inflammatory cytokines such as IL-10 and TGF- β ^{44,168,267}.

In conclusion, we propose that IL-10 producing peripheral monocytes/macrophages are key to preventing the transition from acute to chronic inflammatory pain. We also propose that GRK2 deficiency in peripheral monocytes/macrophages is sufficient to promote transition from acute to chronic pain because of the reduced capacity of these cells to produce IL-10. Future studies should elucidate whether low GRK2 expression and/or impaired IL-10 production by peripheral monocytes/macrophages represent biomarkers for the risk of developing chronic pain after inflammation.

Acknowledgements

The authors thank Dr. N. van Rooijen, Vrije Universiteit, VUMC, Amsterdam, The Netherlands, for sharing the clodronate-liposomes. This study was supported by NIH grants R01 NS 073939 and R01 NS 074999.

Supplementary Materials and Methods

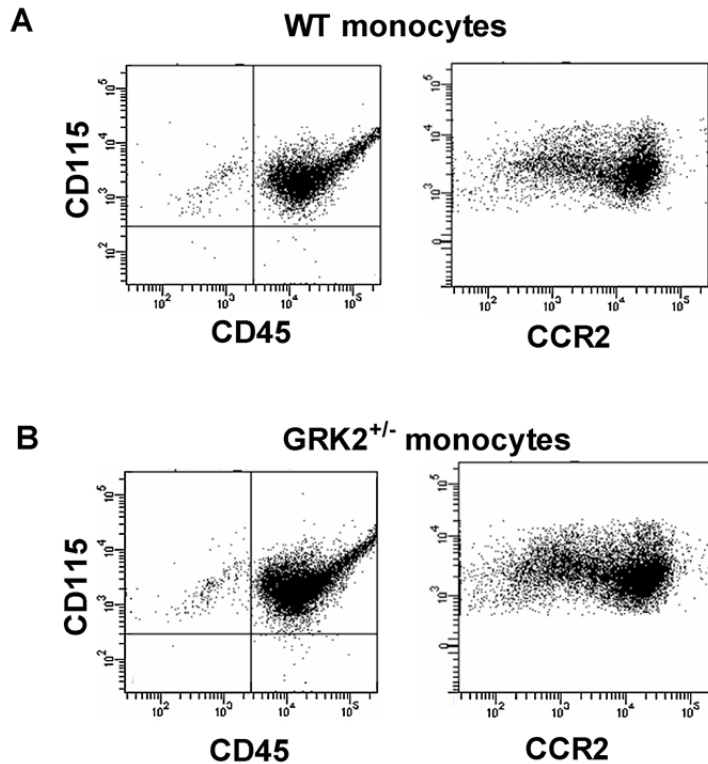
Microglia/macrophage isolation

Microglia were isolated from brains and spinal cord by Percoll (GE Healthcare) density gradient centrifugation as described previously²⁵⁸. CD11b⁺ macrophages were isolated from peritoneal lavage of naive mice followed by magnetic beads separation according to manufactures instructions (BD IMag). GRK2 protein levels in microglia and peritoneal macrophages were determined by Western Blot as described previously²⁵⁷. GRK2 mRNA levels in spinal cord microglia were analyzed by real-time RT-PCR.

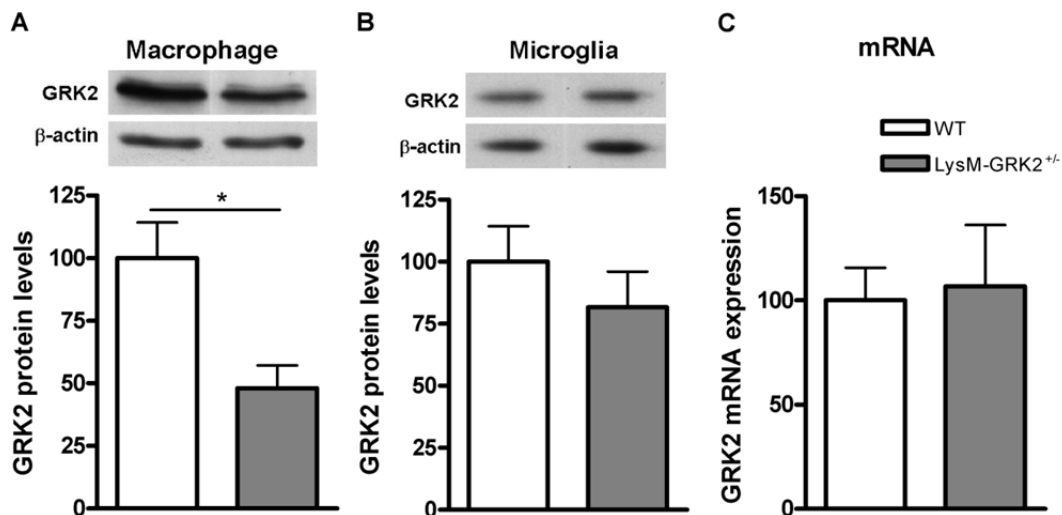
Real-time RT-PCR

Total RNA from freshly isolated microglia was isolated using RNeasy mini kit (Qiagen) and cDNA was synthesized using Superscript Reverse Transcriptase (Invitrogen). Quantitative real-time PCR reaction was performed with an I-cycler iQ5 (Bio-Rad) using the following primers: GRK2 forward: CgggACTTCTgCCTgAACCATCTg, reverse: CTCggCTgCggACCACACg. Data were normalized for GAPDH and β -actin expression. GAPDH forward: TgAAgCaggCATCTgAggg, reverse: CgAAggTggAAgAgTgggAg, Actin forward: AgAgggAAATCgTgCgTgAC, reverse: CAATAgTgATgACCTggCCgT.

Supplementary Figures



Supplementary figure 4.1: Flow cytometric analysis of WT and GRK2^{+/-} BMDM. (A) WT and (B) GRK2^{+/-} CD115⁺ BMDM were isolated for adoptive transfer studies. Flow cytometric analysis shows that the vast majority of BMDM were CD45⁺/CD115⁺. No differences in the percentage CCR2⁺ BMDM were observed between WT and GRK2^{+/-} BMDM.



Supplementary figure 4.2: GRK2 expression levels in peripheral macrophages and freshly isolated microglia. GRK2 protein expression levels were determined by Western blot in (A) isolated peritoneal macrophages (n = 4) and (B) freshly isolated adult brain microglia (n = 8) from WT and LysM-GRK2^{+/-} mice. (C) Spinal cord microglia were isolated from WT and LysM-GRK2^{+/-} mice (n= 6 per group) for direct analysis of mRNA expression by qRT-PCR of GRK2. Data are expressed as mean \pm SEM. * p<0.05.

5

A novel p38 MAPK docking groove-targeted compound is a potent inhibitor of inflammatory hyperalgesia

Hanneke L.D.M. Willemen^{1,\$}

Pedro M. Campos^{2,3,\$}

Elisa Lucas^{2,4}

Antonio Morreale⁵

Rubén Gil-Redondo^{5,7}

Juan Agut⁶

Florenci González⁶

Paula Ramos^{2,4}

Federico Mayor Jr.^{2,4}

Cobi Heijnen^{1,8}

Annemieke Kavelaars^{1,8*}

Cristina Murga^{2,4*}

^{\$} equal contribution to this work

¹ Laboratory of Neuroimmunology and Developmental Origins of Disease, University Medical Center Utrecht, Utrecht, The Netherlands

² Departamento de Biología Molecular and Centro de Biología Molecular “Severo Ochoa” UAM-CSIC, Madrid, Spain

³ current address: Allinky Biopharma, Madrid, Spain.

⁴ Instituto de Investigación Sanitaria La Princesa, Madrid, Spain

⁵ Centro de Biología Molecular “Severo Ochoa”, UAM-CSIC, Madrid, Spain

⁶ Departament de Química Inorgànica i Orgànica, Universitat Jaume I, Castelló, Spain

⁷ current address: SmartLigs Bioinformática S.L., Fundación Parque Científico de Madrid, Campus de Cantoblanco UAM, Madrid, Spain

⁸ Department of Symptom Research, University of Texas MD Anderson Cancer Center, Houston, TX, USA

Abstract

The mitogen activated protein kinase (MAPK) p38 is a well-established mediator of inflammation and contributes to inflammatory and neuropathic pain. Pharmaceutical companies generated p38 MAPK inhibitors targeting the ATP binding site without positive therapeutic results. Here, we developed and investigated a novel p38 MAPK compound as a potential therapeutic drug to treat chronic pain. We recently demonstrated that docking- groove dependent interactions are important for p38 MAPK-mediated signal transduction. Here, we performed a virtual screening procedure with a one million compound library in order to identify putative docking groove targeted p38 MAPK inhibitors. Of the candidates identified, several compounds of the benzooxadiazol family showed low micromolar inhibitory activity both *in vitro* in a p38 MAPK activity assay using MEK2 phosphorylation and in cells using inhibition of LPS-induced TNF- α secretion by THP-1 monocytic cells as read-outs. Substituting positions 2 and 5 in the phenyl ring of the compounds was essential for the described inhibitory activity, and a compound bearing a chloride at position 5 and a methyl at position 2 (FGA-19) yielded the best inhibitory activity with a 2 μ M IC₅₀. The *in vivo* effect of FGA-19 was analyzed in a mouse model of persistent inflammatory hyperalgesia induced by intraplantar injection of carrageenan. A single intrathecal injection of FGA-19 at seven days after carrageenan completely resolved hyperalgesia. The minimal effective dose was 0.5 μ g per mouse and we did not detect peripheral anti-inflammatory effects. FGA-19 also reversed persistent hyperalgesia in the LysM-GRK2^{+/-} mouse, a model of post-inflammatory hyperalgesia. The analgesic effect of FGA-19 lasted much longer than that of the established p38 MAPK inhibitor SB239063. Our data identify the family of benzooxadiazol-based compounds as good p38 MAPK docking-site targeted inhibitors, and FGA-19 as a potential novel candidate for the treatment of inflammatory hyperalgesia.

Introduction

The mitogen activated protein kinase (MAPK) p38 is a key intracellular kinase involved in regulation of the production of multiple inflammatory mediators. p38 MAPK has been the target of intensive basic research performed in academic groups and of programs of drug development by many different pharmaceutical companies⁴⁵. p38 belongs to the MAPK family of serine/threonine kinases that share a common overall structure and also a similar mode of activation through phosphorylation at the activation lip by upstream activators, in the case of p38 including MKK3 and MKK6 although alternative mechanisms of activation exist (reviewed in⁴⁸). Of the four p38 MAPK isoforms, p38 α and β are ubiquitously expressed and, in inflammatory cells, p38 α is the most prominent. Many different extracellular stimuli activate p38 MAPK, among them inflammatory cytokines, lipopolysaccharide (LPS) or other bacterial products, and different stressors such as thermal, mechanical or hypoxic insults⁴². In turn, p38 MAPK directly phosphorylates important transcription factors including myocyte enhancer factor 2 (MEF-2) and activating transcription factor 2 (ATF-2). p38 MAPK also controls the activation state of downstream kinases such as MAPK-activated protein kinases 2 and 3 (MK2 and 3) that in turn phosphorylate heat shock protein-27 (Hsp-27) and other cellular proteins. In the inflammatory pathway, p38 MAPK regulates the stability and expression of multiple mRNAs including those coding for TNF α , IL-1 β , IL-6, and IL-8¹³². It has been shown in several models of chronic pain, that p38 MAPK is upregulated and that pain hypersensitivity can be transiently blocked by commercially available p38 MAPK inhibitors^{11,61,62,110,138,257}. These findings indicate that p38 MAPK may be an interesting target for the development of therapeutic drugs to treat chronic inflammatory pain. However, so far human clinical trials using p38 MAPK inhibitors, such as a trial in patients with rheumatoid arthritis have been disappointing³⁹.

p38 MAPK is able to specifically interact with upstream regulators and also with downstream substrates by virtue of a specific domain called docking domain that lays opposite to the catalytic cleft and the activation loop surface⁴⁸. The specific features of these interactions have been characterized in detail and the structure of p38 α co-crystallized with peptides derived from the interacting motifs in MKK3b and MEF-2A has been resolved²⁷. Interestingly, the interactions mediated by this docking domain can be regulated by means of, for example, phosphorylation of either the substrate or the p38 kinase itself¹⁸⁵. This event provides a feasible mechanism of intervention into the p38 MAPK route, by providing a protein surface that can be more specific as a target of therapeutic drugs than the currently most used pocket: the ATP binding site of p38 MAPK, which shares a high overall homology with that of other protein kinases¹⁴. Along these lines, a major effort has been invested in the development of specific p38 MAPK inhibitors given the failure, during human clinical trials, of the first and second generation ATP-site targeted compounds⁴⁵. Consequently, the need for novel strategies aimed at targeting the p38 MAPK by different mechanisms or utilizing unexplored interactive domains is a venue that certainly deserves further research. Recently we described that p38 MAPK can be phosphorylated in the docking groove (at Thr-123) resulting in reduced binding of upstream kinases and downstream targets and thereby reduced activation of p38 MAPK¹⁸⁵. With this knowledge, we performed a virtual screening of a chemical library of compounds to search for potential novel p38 MAPK inhibitors targeting the docking groove.

Materials and Methods

Virtual Screening (VS)

All VS calculations were performed within the automated platform VSDMIP²³. For the sake of clarity, we briefly describe here the main steps comprising the protocol.

Receptor preparation. The three-dimensional structure of p38 MAPK as found in complex with MEF2A peptide (PDB: 1LEW)²⁷ was used as the receptor. All atoms other than those from the receptor were removed. AMBER ff99 force field²⁴⁷ was then used to assign atom types and charges for each atom in the receptor. Addition of missing hydrogen atoms and computation of the protonation state of ionizable groups at pH 6.5 were carried out using the H++ Web server⁸², which relies on AMBER parameters and finite difference solutions to the Poisson–Boltzmann equation. A salt concentration of 0.15 M and an internal and external dielectric constant of 4 and 80, respectively, were used.

Binding site definition and characterization. To delimit the binding site we selected MEF2A as the core around which to build the docking box by adding a 5.0 Å cushion to the maximum dimensions of the peptide. An equally spaced grid of 0.5 Å was then built, and CGRID¹⁸⁶ calculated protein interaction fields (a 12–6 Lennard-Jones term and an electrostatic term modeled with a sigmoidal dielectric screening function) using common atom probes (C, N, O, S, P, H, F, Cl, Br, and I) at each grid point. Next, benzene, water and methanol probes were docked with CDOCK¹⁸⁶ to generate intermolecular interaction energy maps aimed at capturing the most likely areas of interest for hydrophobic, hydrophilic and hydrogen bond interactions, respectively. These areas were further compressed into gaussian functions using GAGA algorithm²⁴⁸ producing a sort of a negative image of the interaction site. The putative active ligands in the library must conform to this approximate shape.

Chemical library preparation. Ligands for VS consisted on a selection of ~1 million non-redundant molecules obtained from the publicly available ZINC database¹⁰⁶, mainly from ChemBridge and ASINEX companies, in SMILES format²⁵¹. Multiple protonation states and tautomeric forms were considered as implemented by default in ZINC. The molecules were then processed within VSDMIP as usually: (a) conversion from SMILES to 3D MOL2 using Corina Molecular Networks, (b) atomic charge calculations with MOPAC²²³ (MNDO ESP method) on every single structure provided by CORINA; and (c) atom type assignment according to the AMBER ff99 force field and conformational analysis using ALFA⁷⁸.

Filter 1. An initial filter was performed with the docking program DOCK to quickly discard those molecules that do not geometrically fit within the binding site. The spheres needed by DOCK were those previously generated with GAGA. We used DOCK contact as the scoring function, normalizing the score values ($score_i$) by converting them into ZScore using mean (average score) and standard deviation (σ) values ($ZScore_i = (score_i - \text{average score})/\sigma$). Only those molecules with a ZScore beyond a cut off value of 2.5 were selected (45,488) and passed onto the next step.

Filter 2. Selected molecules from the previous step were docked with the more accurate docking algorithm CDOCK. CDOCK exhaustively docks each molecule within the binding site of the receptor using the interaction energy grids previously calculated with CGRID. This was achieved by an exhaustive exploration of the location and orientation of each molecule by positioning its center of mass on grid points and performing discrete rotations of 27° on each axis (poses). Finally, the energy of the poses was evaluated by the molecular mechanics force-field scoring

function implemented in CDOCK, which beside including a 12–6 Lennard-Jones term and an electrostatic term modeled with a sigmoidal dielectric screening function, also accounts for ligand and receptor desolvations as well as for hydrogen bonding interactions¹⁷⁰.

Molecular dynamics simulations and MM-GBSA calculations. The top ranked 200 molecules according to CDOCK's scoring function were subjected to better binding free energy estimation by a combination of molecular dynamics (MD) trajectories and MM-GBSA¹²⁸ calculation on these trajectories. The 200 complexes were hydrated by using boxes containing explicit water molecules with added counter ions to maintain electro neutrality, energy minimized, heated (20 ps), and equilibrated (100 ps). After equilibration, MD trajectories were continued for 200 ps. From this last part, structures were homogeneously sampled each 10 ps and stored for post-processing. All the simulations were performed at constant pressure and temperature (1 atm and 300 K) with an integration time step of 2 fs. SHAKE²¹² was used to constrain all the bonds involving H atoms at their equilibrium distances. Periodic boundary conditions and the Particle Mesh Ewald methods were used to treat long-range electrostatic effects⁵⁰. AMBER ff99 and TIP3P¹¹⁵ force-fields were used in all cases. Finally, the effective binding free energies were qualitatively estimated using the MM-GBSA approach, which calculates the free energy of binding as a sum of a Molecular Mechanics (MM) interaction term, a solvation contribution thorough a Generalized Born (GB) model and a Surface Area (SA) contribution to account for the non-polar part of desolvation. A 12–6 Lennard-Jones term was used to model de MM contribution. For GB, the solute dielectric constant was set to 4 while that of the solvent was set to 80, and the dielectric boundary was calculated using a solvent probe radius of 1.4 Å. The SA contribution was approximated as a linear relationship to the change in SASA (Solvent Accessible Surface Area):

$$\Delta G_{np} = a + b \cdot \Delta SASA$$

where a is 0.092 kcal·mol⁻¹, b is 0.00542 kcal·mol⁻¹·Å⁻², ΔG_{np} is the SA contribution, and the change in SASA refers to the complex SASA minus the sum of that of the protein and the ligand alone. In addition, interaction energy analysis between the ligands and the more relevant residues in the binding site were computed (with MM-GBSA). All the trajectories and analysis were performed using the AMBER 8 computer program and associated modules²⁶.

Selection of candidates. Averaged structures along the trajectories were obtained and energy minimized in vacuum with the ff99 force field, without periodic boundary conditions and during 1000 steps (the first 500 with the steepest descent method and the rest with the conjugated gradient) solely to alleviate the possible clashes that may be originated by averaging the coordinates. These structures were used for graphical representation and comparison of the binding modes. From the highest scoring compounds, and upon visual examination, 18 candidates were finally selected, purchased (see below), and tested experimentally. All visualizations were done within the molecular graphics program PyMOL⁵⁴ Unfortunately, not all the compounds were available from the vendors. In these cases similarity search was performed employing two complementary strategies based on: (a) the 2D topological representation of the molecules and the search/compare engine implemented in ZINC; and (b) the 3D structure of the molecules, the shape-matching algorithm implemented in the program ROCS²⁰⁸, and the ZINC database as implemented in VSDMIP. The similarity between structures was assessed by the Tanimoto coefficient (T_c), selecting only those candidates with a $T_c \geq 0.9$ to be docked into the receptor and further analysis. The final goal was to choose one or two purchasable analogues for each not-found compound presenting as similar interactions as possible when compared to the originally selected molecules.

Hit to lead optimization (H2L)

The scheme for the H2L optimization cycle is shown in figure 5.1. A typical optimization step involves a finer docking study of the best compounds from the experimental assays over an energy minimized MD-averaged structure followed by MD simulation and MM-GBSA analysis. In brief, for every docked molecule we: (a) selected the 100 best docking solutions; (b) clustered them according to their structural resemblance; (c) selected a representative structure from each of the cluster based on its CDock energy; (d) run a MD simulation for a period of up to 10 ns; (e) estimated their free energy of binding *via* MM-GBSA method; (f) selected the best pose based on MM-GBSA energy; and (g) visually inspected and analyzed the structures from (f). This last analysis consisted in determining the essential ligand-receptor interactions to suggest possible chemical modification as to enhance its binding towards the receptor. These suggestions represent new candidates to be passed on to our synthetic colleagues. Following synthesis, the compounds are experimentally assayed and the theoretical models revised. This process (a)-(f) was performed twice resulting in two final lead compounds.

Chemical Synthesis

N-(5-chloro-2-methylphenyl)-7-nitrobenzo[*c*][1,2,5]oxadiazol-4-amine (FGA-19) was synthesized as follows: a solution of 4-chloro-7-nitrobenzofurazan (NBD-Cl) (798.2 mg, 4 mmol) and 5-chloro-2-methylaniline (1.26 g, 8 mmol) in *N,N*-dimethylformamide (50 mL) was refluxed for 24 h. Then the reaction mixture was allowed to warm up to room temperature and was quenched with a saturated aqueous sodium bicarbonate solution, then extracted with ethyl ether (3 x 30 mL), the combined organic layers were washed with brine and dried (sodium sulfate), filtered and concentrated to afford a crude oil which was purified using chromatography over silica-gel and hexanes:ethyl acetate (7:3) as eluent. The desired compound was obtained as a red oil (608 mg, yield = 50%) which was crystallized (MeOH:H₂O (1:1)) to afford pure compound FGA-19 as red crystals.

Chemical Synthesis

Compounds FGA-17, FGA-19, FGA-20, FGA-23, FGA-25, FGA-27, FGA-28, FGA-29, FGA-30, FGA-31, FGA-32 and FGA-34 were synthesized as follows: a solution of 4-chloro-7-nitrobenzofurazan (NBD-Cl) (798.2 mg, 4 mmol) and the corresponding aniline (8 mmol) in ethyl acetate (50 mL) was refluxed for 48 h. Then the reaction mixture was allowed to warm up to room temperature and was quenched with a saturated aqueous sodium bicarbonate solution (30 mL), then extracted with ethyl ether (3 x 30 mL), the combined organic layers were washed with brine and dried (sodium sulfate), filtered and concentrated under vacuum to afford a crude oil which was purified using chromatography over silica-gel and hexanes:ethyl acetate mixture as eluent. The desired compounds were obtained as coloured oils (yield = 50-85%) which were crystallized (MeOH:H₂O (1:1)) to afford pure compounds as coloured crystals.

Compound FGA-21 was synthesized as follows: a solution of 4-chloro-7-nitrobenzofurazan (NBD-Cl) (3 g, 15 mmol) in acetic acid (60 mL), ethyl acetate (30 mL) and H₂O (6 mL) was heated at 50°C and treated with iron powder (4.2 g, 753 mmol). Then the reaction mixture was heated at 80°C for 30 minutes and then allowed to cool down to room temperature and was filtered through celite eluting with ethyl acetate, the filtrate was washed with a saturated aqueous sodium bicarbonate solution, then dried (sodium sulfate), filtered and concentrated under vacuum to afford a red solid which was purified using chromatography over silica-gel and

hexanes:ethyl acetate (7:3) as eluent. The desired compound was obtained as red crystals (2.1 g, yield = 82%).

Compound FGA-22 was synthesized as follows: a solution of 3-chlorobenzaldehyde (56 mL, 0.49 mmol), FGA-21 (85 mg, 0.5 mmol) and sodium sulfate (17 mg, 0.14 mmol) in tetrahydrofuran (2 mL) was stirred at room temperature under nitrogen atmosphere for 48 h. Then sodium borohydride (22 mg, 0.59 mmol) was added in one portion. Then the resulting mixture was stirred at room temperature for 5 h. Then ethyl ether (10 mL) and water (10 mL) were added, the organic layer was separated and the aqueous layer was extracted with ethyl ether (2 x 10 mL), the combined organic layers were washed with brine and dried (sodium sulfate), filtered and concentrated under vacuum to afford an orange oil which was purified using chromatography over silica-gel and hexanes:ethyl acetate (8:2) as eluent. The desired compound was obtained as an orange solid (12 mg, yield = 8%).

Compounds FGA-24 and FGA-26 were synthesized as follows: to a -78°C cold solution of FGA-21 (102 mg, 0.6 mmol) in tetrahydrofuran (1 mL) was added n-butyllithium (1.6 M in hexanes) (0.4 mL, 0.61 mmol), then the solution mixture turned black. After 10 min the corresponding acyl chloride (previously prepared starting from 5-chloro-2-methoxybenzoic acid for FGA-24 or 3-chlorobenzoic acid for FGA-26 and thionyl chloride in benzene under reflux) (0.66 mmol of the corresponding carboxylic acid) in tetrahydrofuran (0.5 mL). Then the resulting mixture was stirred at -78°C under nitrogen atmosphere for 30 min and allowed to warm up to room temperature for additional 30 min. Then saturated aqueous ammonium chloride solution was added (15 mL) and solvent was evaporated under vacuum and the resulting aqueous solution was extracted with dichloromethane (2 x 15 mL), the combined organic layers were washed with 1 M sodium hydroxide aqueous solution, then washed with brine and dried (sodium sulfate), filtered and concentrated under vacuum to afford crude oils which were purified using chromatography over silica-gel and hexanes:ethyl acetate (7:3) as eluent. The desired compounds were obtained as yellowish solids (yield = 60%).

Animals

Female C57Bl/6 mice (aged 12 to 14 weeks) and female mice with cell-specific reduction of GRK2 in LysM-positive microglia/macrophages (LysM-GRK2^{+/-}) were used²⁵⁷. LysM-Cre mice and GRK2-fLox mice were obtained from Jackson Laboratories (Jackson Laboratories, Bar Harbor, ME, USA) to generate LysM-GRK2^{+/-} and control LysM-GRK2^{+/+} mice (WT littermates). All mice were bred and maintained in the animal facility of the University of Utrecht, The Netherlands. Experiments were performed in accordance with international guidelines and approved by the experimental animal committee of UMC Utrecht.

Mice received an intraplantar injection in the hind paw of 20 µl λ-carrageenan (2% w/v; high dose; Sigma-Aldrich, St. Louis, MO, USA) or 5 µl λ-carrageenan (1% w/v; low dose; Sigma-Aldrich) diluted in saline. Heat withdrawal latency times were determined using the Hargreaves (IITC Life Science, Woodland Hills, CA) test as described⁴². Paw Thickness was measured using a Digimatic Micrometer (Mitutoyo, Veenendaal, the Netherlands). Different concentrations of FGA-19 were applied intrathecally (5 µl/mouse) while the animals were under light isoflurane anesthesia. All behavioral experiments were performed by an experimenter blinded to treatment and in a randomized fashion.

Fluoro-Jade B staining

Two days after intrathecal FGA-19 mice were deeply anesthetized with sodium pentobarbital (50 mg/kg, i.p.) and perfused intracardially with 4% paraformaldehyde in PBS. Spinal cords were removed and paraffin-embedded. Spinal cord sections were, deparaffinized, pretreated with 0.06% potassium permanganate and stained with 0.001% Fluoro-Jade B solution (Millipore Bioscience Research Reagents, Hampshire, UK) in 0.1% acetic acid.

TNF- α determination in tissue lysates

Spinal cords were homogenated in PBS and centrifuged at 13,000g for 15 min at 4°C. TNF- α content in the supernatant was determined by ELISA (R&D systems, San Diego, CA, USA).

Electrophoresis and Western Blot

Proteins were resolved by SDS-PAGE, and transfer to nitrocellulose membranes for western blotting analysis. The antibodies used were as follows: anti-p-p38(TGY)(#9211), anti-p38(#9212), anti-p-MK2(T334)(#3041), anti-MK2(#3042), anti-p-Hsp-27 (2405) and anti-MEF2A(#9736) were purchased from Cell Signaling. Anti-p-MEF2A(T312)(#ab30644) was obtained from Abcam.

In vitro inhibition of p38 MAPK activation and activity with small molecules

p38 α (75 nM) was preincubated for 15 minutes at 30°C with the small molecule at concentration between 0.1 and 100 μ M in buffer (25 mM Tris pH 7.5, 50 μ M EGTA, 50 μ M NaVO₄ and 0.05% β -ME). After that, constitutively active MKK6 (10 nM), magnesium acetate (2.5 mM) and ATP (25 μ M) were added and kinase reaction was performed in 15 minutes at 30°C. Reaction was terminated with Laemli buffer and proteins were resolved by SDS-PAGE and phospho-p38 (TGY) was detected by western blot.

In vitro activity assays were also performed. Recombinant activated p38 α (1 nM) was preincubated for 15 minutes at 30°C with the small molecule in the same buffer. MEF2A (10 nM), magnesium acetate and ATP were added and kinase reaction was performed. Phospho-MEF2A was detected by western blot.

Inhibition of TNF- α secretion by small molecules

THP-1 cells, growing in log phase, were centrifuged and resuspended in RPMI-1640 to a final concentration of 2×10^6 cells/ml and distributed in 24-well plates. Molecules were added to the wells to a final concentration ranging from 10 nM to 100 μ M and plates were incubated at 37°C and 5% CO₂ in humidified atmosphere. Cells were stimulated 1h later with LPS to a final concentration of 0.5-2 μ g/ml and incubated for 3h followed by centrifugation to pellet the cells. Supernatants were collected and stored at -20°C for further analysis. TNF- α secretion was measured by ELISA following manufacturer's indications. TNF- α concentration was determined making a standard curve with known concentration of recombinant TNF- α .

Cell viability

Toxicity of the molecules was quantified with Propidium Iodide (PI) which specifically label dying cells. Cells were resuspended in buffer (PBS, 1% BSA, 1% FBS, 0,01% NaN₃ and 1 μ g/ml PI) and kept in ice for 30-60 minutes and then analyzed by flow cytometry with A FACSCalibur (Becton Dickinson). Results were obtained with Cell Quest Pro Software (Becton Dickinson).

Statistical analysis

All data are presented as mean \pm SEM. Measurements were compared using one-way ANOVA followed up by post-hoc Tukey or two-way ANOVA with Bonferroni post-hoc tests using Prism 5 software.

Results

Virtual screening and identification of a lead compound

The virtual screening (VS) protocol employed here is summarized in figure 5.1A and 5.1B and briefly described in the methods section. An essential part of the procedure is to characterize the shape of the active site. For this purpose we used the space occupied by the MEF2A peptide co-crystallized with the p38 MAPK receptor and the GAGA algorithm to obtain a sort of a negative image of the binding site. Although different X-ray structures were available to be used as the receptor for the VS, we selected the one contained in the PDB ID 1LEW because of its high resolution, in particular in the area where the docking was going to be performed. Moreover, superimposition of several structures (PDB IDs 1LEW, 3P4K, 1P38, 2FSL, 2FSM, 2FSO and 2FSZ) showed a very low RMSD values considering equivalent C α carbon atoms. This fact is reassuring taking into account that the protein flexibility is not explicitly considered during the docking process.

Upon characterizing the binding site, a library of around 1 million compounds was first screened using DOCK and the negative image of the binding site. After applying a ZScore cut off value of 2.5 on the DOCK ranked list, 45,488 molecules passed onto the next step. These molecules were then re-docked with CDOCK and scored with its molecular mechanics energy function which explicitly included solvent and hydrogen bonding terms. The 200 highest scoring compounds were submitted to MD simulation in explicit solvent and their binding energies estimated and pair-wise decomposed by MM-GBSA calculation over a large collection of snapshots homogeneously sampled along the trajectories.

Finally, from the top scoring compounds, and upon visual examination, 18 candidates were selected, purchased, and tested experimentally. The most promising candidate, the highly symmetrical compound 978604, was not available from the vendor. Besides, and according to Lipinski's rule of five (RoF)¹⁴³, this compound presented a very high logP value²³² (\sim 8.00). Therefore, a similarity search was performed resulting in a new compound, 5380, that was found to be structurally one half of the original one due to its symmetry. On the one hand, 5380 due to its reduced size is better suited for chemical modifications; on the other its logP value was drastically reduced being within the RoF (5.00) criteria. This compound was purchased, experimentally tested and submitted to two optimization rounds. From the first one a lead candidate was obtained, FGA-19, with enhanced pharmacological profile and logP value (4.35). Finally, upon studying FGA-19 binding mode, in the second optimization cycle, a second lead was discovered, FGA-29, which simply consisted in replacing the methyl group in FGA-19 with an hydroxyl moiety, reducing even more its logP value (3.68) although with a slightly different experimental behavior (Figures 5.1B and 5.1C).

FGA-19 and FGA-29, due to their structural resemblance, display a common interaction pattern with residues Ile112, Leu118 and Leu126, or His122, Phe125, Val154, and Cys157. Besides, the interaction with residue Gln116 is favorable to FGA-29, and in almost the same amount, residue Gln129 interacts with FGA-19, counterbalancing the former. Finally, there are some subtle differences in their binding modes (Figure 5.1D). In particular, the interactions with residues

Asn155 and Glu156, which are geometrically optimized in FGA-29 as compared to FGA-19, are mainly hydrophobic in nature and account for a total energy difference of about 2 kcal·mol⁻¹. However, this magnitude is of the order of the error found in their calculations. Therefore, no firm conclusions can be drawn up to their activity, which is in agreement with the experimental observations.

***In vitro* effects of FGA-19 on p38 MAPK activation and inhibition of the p38 MAPK route in human monocytic cells**

We next set out to investigate the possible effects of the FGA-19 compound on p38 MAPK in an *in vitro* kinase activity assay using purified p38 MAPK-dependent phosphorylation of a well-characterized docking-dependent p38 MAPK substrate; i.e. the MEF2A protein. When adding increasing doses of the FGA-19 molecule to the reaction mix containing the active kinase and a saturating amount of substrate in the presence of ATP, we observed a dose-dependent inhibition of p38 MAPK-mediated phosphorylation of MEF2A at the specific site targeted by this kinase (T312) (Figure 5.2A and 5.2B). Quantification by densitometric analysis of the Western Blot data of the decrease phosphorylated MEF2A in the presence of increasing amounts of FGA-19 in several experiments, revealed an estimated mean inhibitory concentration (IC₅₀) of 6.31 ± 2.32 μM an almost full inhibition of p38 kinase activity towards MEF2A was observed at the 50 μM dose (Figures 5.2A and 5.2B).

The effects of FGA-19 were then analyzed in a well-established cellular system of cytokine secretion by a monocytic human cell line (THP-1) stimulated with LPS¹³². Secretion of TNF-α by these cells is p38 MAPK-dependent, and thus this system has been broadly utilized to study the effects of different p38 MAPK inhibitors. As shown in figure 5.2C, FGA-19 has a dose-dependent inhibitory effect on TNF-α secretion in this cell system with an IC₅₀ of 1.8 ± 0.006 μM reaching an almost maximal inhibition at the 10 μM concentration. As a comparison, the IC₅₀ for SB203580 (commercially available p38 MAPK inhibitor targeting the ATP binding site) in the same system was 1 μM (data not shown), and the effect at the 10 μM dose was similar to that obtained for FGA-19. Of note, we did not detect significant cell death as determined by FACS analysis of propidium iodine staining at concentrations up to 100 μM, indicating that there was no cellular toxicity (Figure 5.2C).

Next we set out to analyze the effects of the FGA-19 compound on the p38 MAPK signaling route in this monocytic cell line. As can be seen in figure 5.2D, in the presence of FGA-19 we detected clear inhibition of p38 MAPK phosphorylation at the activation loop by upstream kinases. As expected, an even clearer inhibitory effect was observed on the activity of p38 MAPK in THP1 monocytic cells as measured by phosphorylation of downstream substrates of this kinase such as MK-2, and further downstream on Hsp-27 phosphorylation. Quantification of these inhibitory effects of the FGA-19 revealed a ~80% inhibition for phosphorylation of p38 MAPK and ~100% inhibition in the case of p-MK2 phosphorylation at the 5 μM dose of FGA-19 (Figure 5.2E).

Identification of the structural determinants of the inhibitory effect

Comparative analysis of FGA-19 and several structurally-related compounds, all belonging to the benzooxadiazol family, allowed us to conclude that the substituents in positions 2 and 5 of the phenyl ring are essential for the inhibitory activity towards p38 MAPK. When the substituents in positions 2 and 5 present in the FGA-19 molecule (namely a chloride and a methyl group) are located in other positions of the phenyl ring (as happens in the FGA-17, FGA-20 and FGA-23 compounds), the IC₅₀ for the inhibition of TNF-α secretion by monocytic cells decreased at least

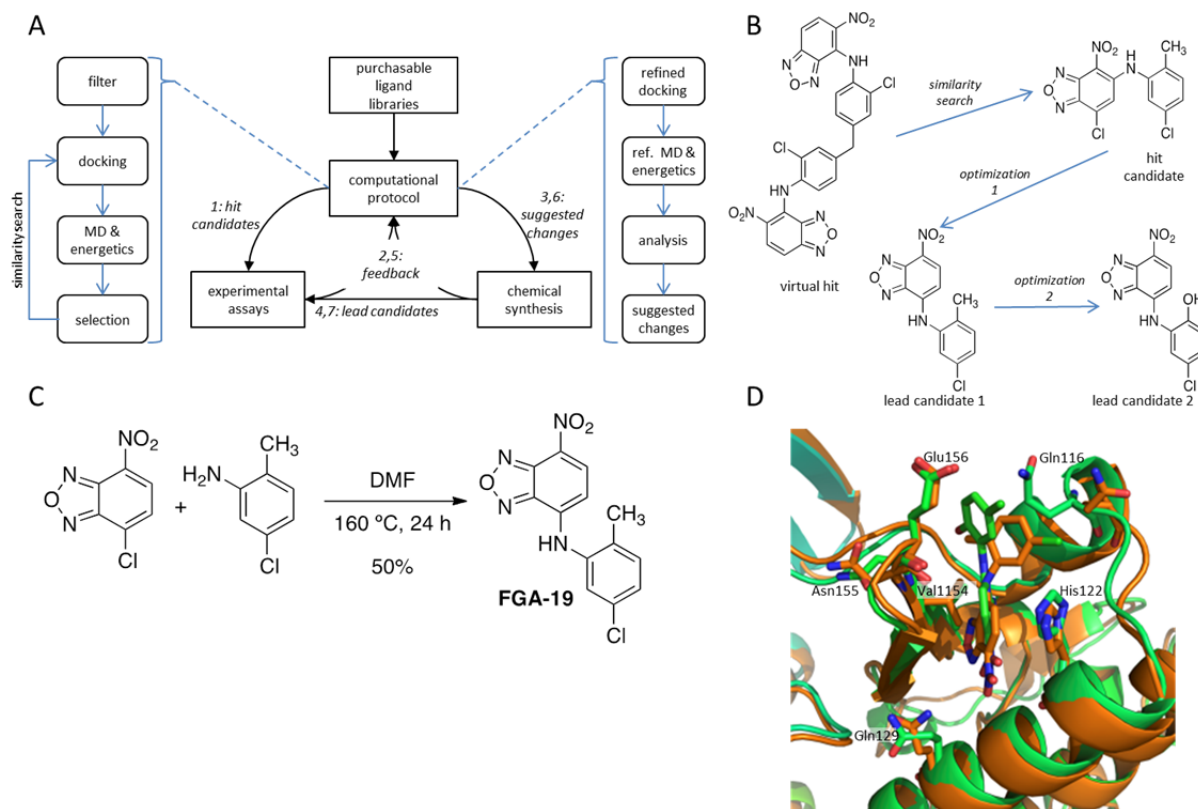


Figure 5.1: Virtual screening and identification of a lead compound. (A) Schematic representation of the computational protocol employed in this study (left and right panels) and the drug design cycle established with the experimental counterpart (central panel); (B) Structural pathway from the identified virtual hit 978604 to the hit candidate 5380 and to the lead compounds FGA-19 and FGA-29 after two rounds of optimization; (C) Chemical reaction for the preparation of FGA-19 starting from 4-chloro-7-nitrobenzofurazan and 5-chloro-2-methylaniline; (D) proposed binding modes for FGA-19 and FGA-29. The receptor is represented in cartoons (orange in FGA-19 complex and green in FGA-29 complex), whereas the ligands are shown in sticks with the following atom coloring scheme: for FGA-19 carbon atoms are in orange, nitrogen atoms in blue, oxygen atoms in red and the chloride atom in pink; for FGA-29, carbon atoms are in green, nitrogen atoms in blue, oxygen atoms in red and the chloride atom in pink. In both cases hydrogen atoms have been omitted for clarity.

by a logarithmic unit (Figure 5.3 and Table 5.1). This was the case for Cl and CH₃ located in positions 4 and 5 (FGA-17), or 4 and 6 (FGA-20), with the IC₅₀ shifting from 1.8 μM to 17 μM and 28 μM respectively, or for OH and CH₃ at positions 2 and 4 (FGA-23, IC₅₀ higher than 100 μM). The presence of a single substituent at different positions of the ring also resulted in IC₅₀ higher than 100 μM in at least three other compounds (data not shown). On the other hand, when other substituents are placed in the same positions of the ring where the chloride and the methyl are located in the FGA-19 molecule, an IC₅₀ similar to that obtained for FGA-19 is detected. This is the case for the substitution of positions 2 and 5 by OH and Cl (in FGA-29), for Cl and OCH₃ (in FGA-34) and for F (FGA-32). All three compounds yielded IC₅₀s in the low micromolar range (3.5 μM, 3.2 μM and 2.8 μM, respectively), which is very comparable to that achieved by FGA-19 (1.8 μM) (Table 5.1). Altogether, these results establish that substituting positions 2 and 5 in the phenyl ring is essential for the described inhibitory activity and, furthermore, that a chloride at position 5 and a methyl at position 2 are the best chemical groups among those tested so far.

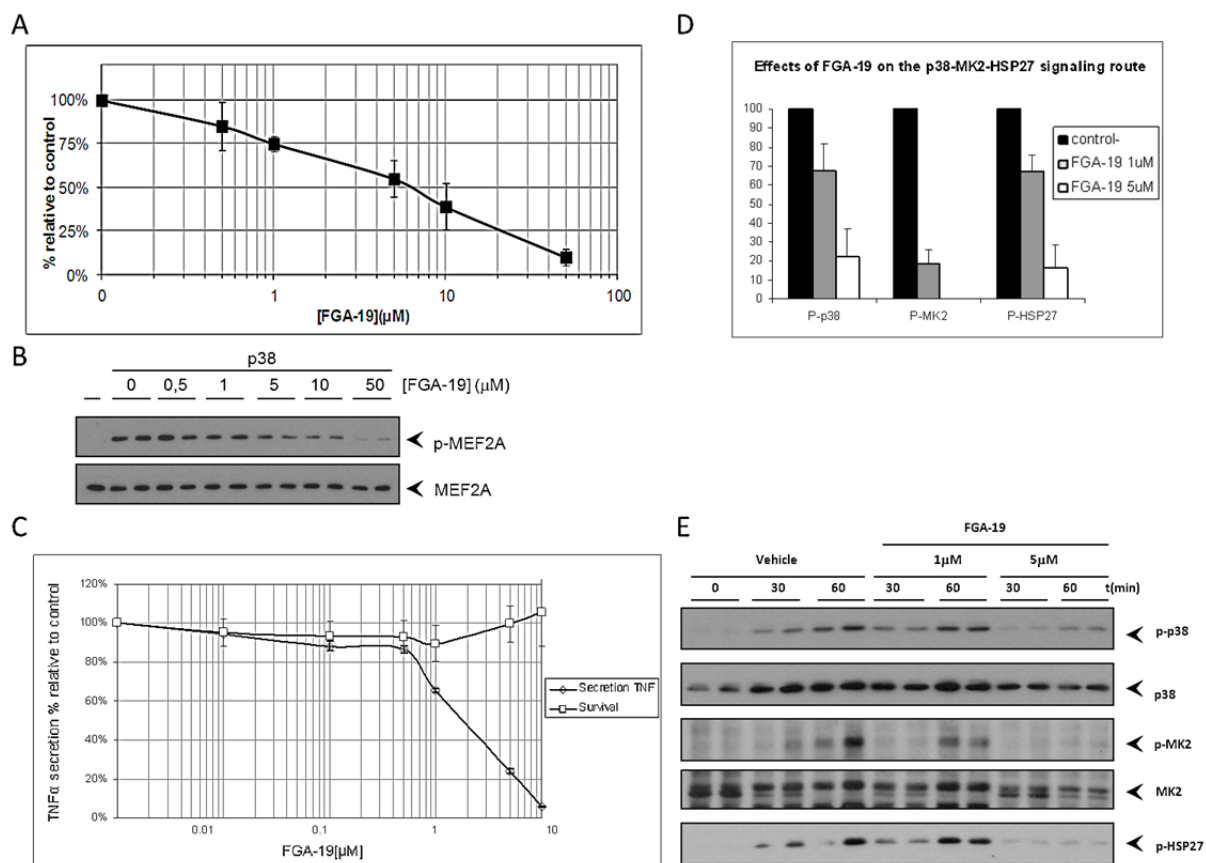


Figure 5.2: Effects of FGA-19 on the activity of p38 MAPK *in vitro* and on the p38-MK2-Hsp-27 signaling route. (A) Recombinant active p38 (1 nM) and MEF2A (10 nM) were incubated with different concentrations of FGA-19 in kinase buffer for 5 minutes. Proteins were resolved by SDS-PAGE and p38 MAPK activity was measured as phosphorylated MEF2A using p-MEF2A (T312) specific antibody. Average results are plotted as percent phosphorylation relative to controls (DMSO) of two independent experiments performed in duplicate. (B) Autoradiogram of a representative experiment. (C) THP-1 cells were preincubated with indicated doses of FGA-19 for 1 hour and stimulated with LPS for 3 hours. Cells were stained with Propidium Iodide and surviving cells were counted with a FACS Calibur cytometer. TNF- α secretion in cell supernatants was quantified using a TNF- α ELISA kit and referred to control (DMSO). Results are average of 3 independent experiments each in duplicate. (D) THP-1 cells were preincubated with indicated doses of FGA-19 for 1 hour and stimulated with LPS for 30 or 60 minutes. Cell lysates were resolved by SDS-PAGE and proteins were detected with specific antibodies and films quantified by densitometric analysis. Average results of two independent experiments with duplicates are plotted as percent phosphorylation relative to cells with vehicle. (E) An autoradiogram of a representative experiment is shown.

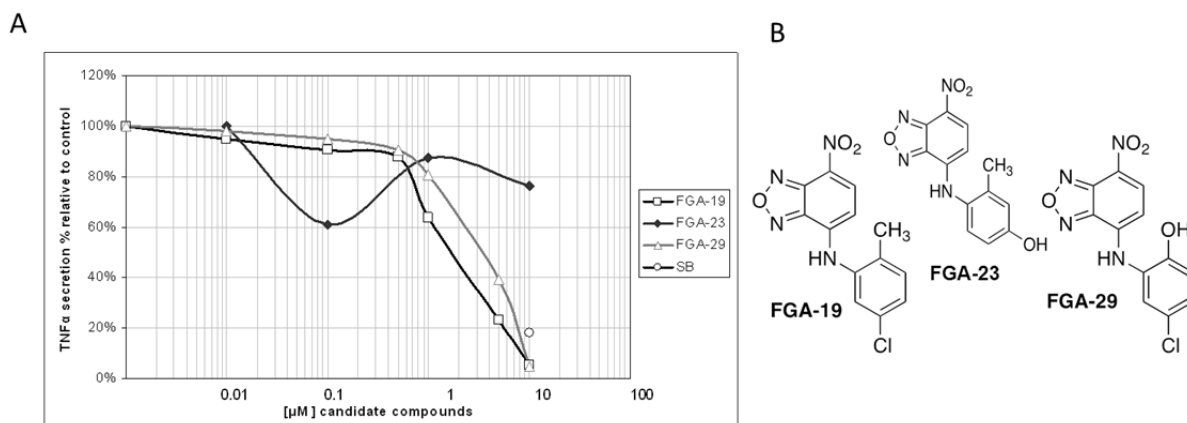


Figure 5.3: Inhibition of TNF- α secretion by FGA-19, FGA-23 and FGA-29. (A) THP-1 cells growing in log phase were preincubated for 1 hour with indicated doses of compounds or with 10 μ M SB203580 (SB) as a control. Cells were stimulated with LPS for 3 hours and supernatants were analyzed for TNF- α secretion by ELISA. Results are the mean of 2 independent experiments performed in duplicate and are referred to controls with DMSO (vehicle). (B) FGA-19 and structurally-related compounds.

Table 5.1: Comparative analysis of the effects on TNF- α secretion of FGA-19 and several structurally-related compounds belonging to the benzooxadiazol family. THP-1 cells were preincubated with indicated doses of several benzooxadiazol-derived compounds for 1 hour and stimulated with LPS for 3 hours. TNF- α secretion in cell supernatants was quantified using a TNF- α ELISA kit and referred to control (DMSO). Values were used to approximate graphically an IC₅₀ value in μ M units. When the substituents in positions 2 and 5 present in the FGA-19 molecule (namely a chloride and a methyl group) are located in other positions of the phenyl ring, the IC₅₀ for the inhibition of TNF- α secretion by monocytic cells decreases.

	FGA-17	FGA-19	FGA-20	FGA-23	FGA-29	FGA-32	FGA-34
2D molecular structure							
^aIC₅₀	17	1.8	28	>100	3.5	2.8	3.2

^aUnits in mM; TNF α secretion in LPS-stimulated THP1 cells.

In vivo effect of FGA-19 on inflammatory hyperalgesia

To determine the *in vivo* efficacy of FGA-19, we examined its effect in the high dose carrageenan model of persistent inflammatory hyperalgesia in C57Bl/6 mice. In response to intraplantar injection of 20 μ l 2% carrageenan, mice develop thermal hyperalgesia that lasts at least 11 days (Figure 5.4A). We injected increasing doses of FGA-19 intrathecally at day 6 after intraplantar carrageenan. The data show that hyperalgesia completely resolved in response to a single injection of 1 μ g FGA-19. A lower dose of 0.5 μ g FGA-19 transiently inhibited carrageenan-induced hyperalgesia (Figure 5.4A). For comparison, we used the established p38 MAPK inhibitor SB239063. At the maximal dose that could be injected using 20 % DMSO as a solvent, i.e. 5 μ g SB239063, carrageenan-induced hyperalgesia was only transiently attenuated (Figure 5.4A). Thermal sensitivity was not affected by FGA-19 in control saline-treated mice (Figure 5.4B). The structurally similar FGA-23 compound, that *in vitro* has an IC₅₀ of > 100 μ M, did not have any effect on the course of carrageenan-induced hyperalgesia (Figure 5.4B).

The inhibition of hyperalgesia by FGA-19 was not associated with cellular damage in the spinal cord as we did not observe Fluoro-Jade positive cells in the spinal cord at 48 hrs after 1 μg FGA-19 (Figure 5.4C).

Our cell culture experiments showed that FGA-19 inhibits LPS-induced TNF- α production (Figure 5.2C) and spinal cord production of pro-inflammatory cytokines such as TNF- α is known to contribute to the persistent hyperalgesia in this model^{13,32,102}. To investigate whether *in vivo* FGA-19-treatment affects TNF- α levels, we injected carrageenan or saline intraplantarly, followed by intrathecal FGA-19 or vehicle on day 6 and isolated spinal cord 2 days later for analysis of TNF- α levels by ELISA. Intraplantar carrageenan causes a significant increase in spinal TNF- α (Figure 5.4D) and intrathecal FGA-19 treatment significantly inhibits this carrageenan induced rise in spinal TNF α . FGA-19 alone does not have any effect on TNF- α expression (Figure 5.4D).

Six days after intrathecal FGA-19 treatment mice have still increased paw thickness and redness, indicating that intrathecal FGA-19 treatment did not directly affect peripheral inflammatory activity (Figure 5.4E).

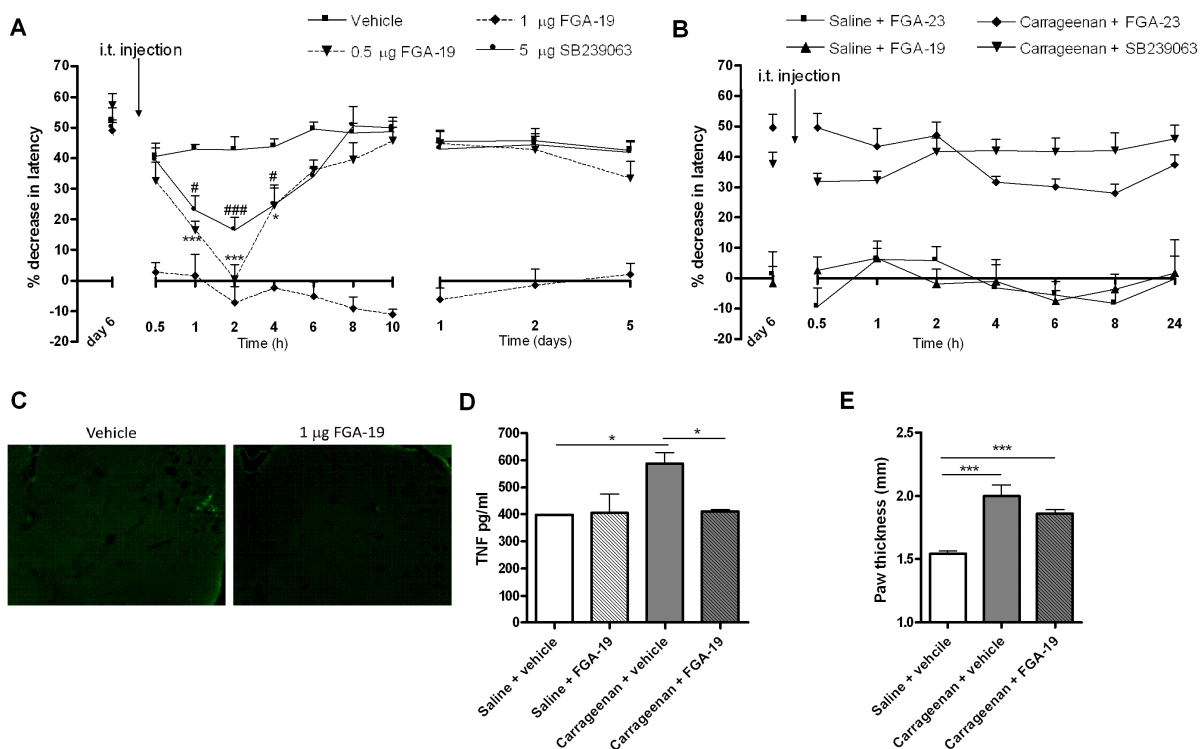


Figure 5.4: Effect of FGA-19 treatment on high-dose carrageenan-induced persistent hyperalgesia in WT mice. Mice received an intraplantar injection of 20 μl 2% λ -carrageenan or saline. At day 6, carrageenan-treated mice were still hyperalgesic. At this time point, mice received an intrathecal injection of (A) different doses of FGA-19 or (B) 1 μg of the inactive compound FGA-23, and the percentage change in heat withdrawal latency was determined ($n = 4$ to 8 per group). Two days after intrathecal injection, lumbar spinal cord was collected and (C) sections were stained for Fluoro-Jade B to investigate the potential neurotoxicity of FGA-19 and (D) TNF- α levels were determined by ELISA ($n = 4$). (E) As a measure for paw-inflammation, the effect of FGA-19 treatment on the paw thickness was determined ($n = 8$). Data are expressed as means \pm SEM. * or # $p < 0.05$, *** or ### $p < 0.001$ (Figure A: * for 0.5 μg FGA-19 versus vehicle; # for 5 μg SB239063 versus vehicle).

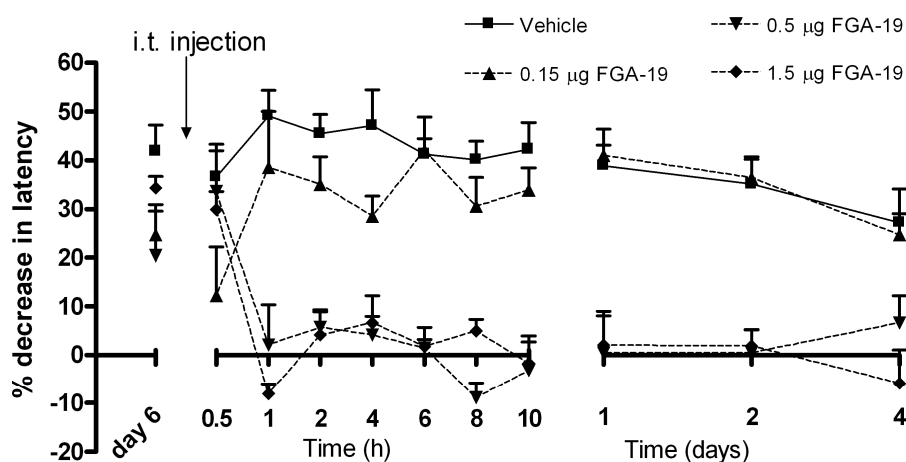


Figure 5.5: Effect of FGA-19 treatment on low dose carrageenan-induced persistent hyperalgesia in LysM-GRK2^{+/-} mice. LysM-GRK2^{+/-} mice received a low dose of carrageenan (5 µl of 1% λ-carrageenan) and at day 6 mice were still hyperalgesic. At this time point, mice received an intrathecal injection with different doses of FGA-19 and the percentage in heat withdrawal latency was determined (n = 4). Data are expressed as means ± SEM.

As we have previously described, in response to an intraplantar injection of a low dose of carrageenan (5 µl of 1%) LysM-GRK2^{+/-} mice (with a ~40% reduction in GRK2 in macrophages) develop persistent hyperalgesia lasting at least 20 days. In this low-dose carrageenan model of transient hyperalgesia, WT control mice develop only transient hyperalgesia that resolves within 2 days²⁵⁷. The LysM-GRK2^{+/-} mice can be considered as a model of persistent post-inflammatory hyperalgesia as we do not observe ongoing peripheral inflammation (no redness or thick paws, no detectable increase in inflammatory cytokines in comparison to control paws⁶¹). As depicted in figure 5.5, intrathecal administration of FGA-19 completely attenuates hyperalgesia in this model of post-inflammatory hyperalgesia. The lowest effective dose in this model was established in 0.5 µg of FGA-19 as well, since a 0.15 µg dose did not provide a long lasting analgesic effect).

Discussion

The search for inhibitors of p38 MAPK has rendered, so far, no fruitful therapeutic results. The reasons underlying this lack of success include low efficacy in some cases and the identification of certain toxicities during the development of human clinical trials that were not uncovered in animal models of the different diseases tested⁸⁸. These toxicities can have several etiologies. On the one hand, first and second generation p38 MAPK inhibitors were all designed to target the ATP binding pocket of p38 MAPK, thus exploiting a common domain found in many different kinases. Since the off target effects of this particular type of inhibitors are likely to affect other signaling pathways apart from p38 MAPK that are important for cell survival or proliferation, they may cause cells to undergo apoptosis as a side effect⁴⁵. On the other hand, even when new allosteric site inhibitors were developed to overcome these type of off-target effects, it became apparent that a strong downregulation of the p38 MAPK pathway can trigger the upregulation of other signaling pathways by virtue of the concomitant stimulation of interconnecting feedback mechanisms (see below), and these final undesired consequences may have been underestimated⁴². Lastly, the systemic administration of p38 MAPK inhibitors has been proven to provoke toxicities in organs other than those important for the disease they were meant to

combat, such as liver or brain among others⁸⁸. For all these reasons, in this study we set out to characterize a novel family of inhibitors that take advantage of the existence of docking domains in the p38 MAPK protein providing the possibility of modulating the activity and activation of this kinase independently of its intrinsic catalytic activity in a more subtle but yet possibly more efficacious manner. Our strategy relied on our previous results showing that p38 MAPK can be phosphorylated at the docking domain, precisely at T123 of murine p38 α . This phosphorylation subsequently leads to the loss of interaction with different partners and thereby to reduced activation and activity of p38 MAPK¹⁸⁵. On this basis, we performed a virtual screening of a chemical library of compounds over a model based on pre-existing structures of p38 MAPK bound to peptides derived from upstream regulators or downstream substrates²⁷. This search yielded the identification of compounds of different chemical nature that were analyzed for their *in vitro* activity of inhibiting either phosphorylation of p38 MAPK as a measure of activation of the kinase or cytokine secretion induced by LPS in a human monocytic cell line model as a measure of cellular p38 MAPK activity. Only some molecules were effective in the micromolar range of concentrations in inhibiting any of those events. Out of these, the family of benzooxadiazol-based compounds described in this study, FGA-19 as a lead candidate, it has been determined to be effective both in cells and in an animal model, bearing several putative sites susceptible of chemical modifications that make of this molecule a good lead compounds to perform further drug development strategies.

The *in vivo* effects of this compound surpass those detected for other well established p38 MAPK inhibitors in our inflammatory-based hyperalgesia model system both in potency and in terms of duration of the pharmacologic effect detected. Of note, our molecule, FGA-19 is almost ten times as potent as the SB239063 inhibitor, since a 0.5 μg dose of FGA-19 is able to exert the same acute analgesic effect as 5 μg of SB239063 while both molecules have similar molecular weights (368.40 g/mol for SB239063 and 304.45 g/mol for FGA-19). Moreover, longer-lasting effects are detected in mice treated intrathecally with FGA-19, with a 1 μg dose abrogating hyperalgesia for at least 5 days post-injection while the duration of the pharmacological effect of SB239063 at the highest dose that can be injected did not last longer than 6 hours. These results suggest a very promising family of molecules could be derived from the benzooxadiazol structure to specifically target ongoing inflammation-based chronic pain, and these results surely deserve further investigation. Interestingly, recent studies have shown that mice with a reduction level of GRK2 in macrophages develop chronic hyperalgesia in response to inflammatory mediators that induce only transient hyperalgesia in WT mice (reviewed in ¹¹⁹). We used these mice to test whether FGA-19 is also a potent inhibitor in this model of post-inflammatory hyperalgesia. We show that the persistent hyperalgesia that develops in *LysM-GRK2^{+/-}* mice is completely reversed by a single intrathecal injection of FGA-19. Collectively, our findings indicate that FGA-19 is a potential candidate for the treatment of inflammatory hyperalgesia.

Clinical trials performed for p38 MAPK in the contexts of chronic inflammation have been so far unsuccessful due to both lack of efficacy and toxic effects⁸⁸. However, although the importance of p38 MAPK in regulating hyperalgesia responses is well established in mice and in humans¹¹¹, few studies have been conducted so far that try to assess the efficacy of p38 inhibition in pain therapeutics. In particular, different laboratories have shown that phosphorylated p38 MAPK is increased in spinal cord microglia after nerve ligation or spinal cord injury, and more importantly, that intrathecal infusion of p38 MAPK inhibitors attenuates neuropathic pain in different animal models (see references in ¹¹¹). A small study has described a potent analgesic effect of p38 MAPK inhibition in post-surgical dental pain in humans²⁰³ and several recent studies have described in animal models the importance of p38 MAPK not only for neuropathic

post-surgical pain, but also for cancer-derived allodynia and for chronic mechanical hypersensitivity¹⁷³. It is also well established that increased levels of phosphorylated p38 MAPK are detected in microglia of inflammatory pain animal models (see references in ¹¹⁹). In accordance with this, in already published studies in murine models and in our own results, inhibition of spinal cord p38 MAPK by intrathecal administration of specific inhibitors efficiently reversed ongoing hyperalgesia (⁶¹ and this work). However, the effect observed using these classic p38 MAPK inhibitors was much more transient than that observed using the FGA-19 inhibitor, which at a 1 µg dose shows a perdurable effect that lasted along the 5 days of the experimental setup.

The strategy hereby utilized to identify and analyze FGA-19 has been based on interfering with docking interactions between p38 MAPK and substrates or activators of p38 MAPK¹⁸⁵, but was not meant to completely ablate its kinase activity or fully block its activation. This particular characteristic of the drug discovery strategy that was followed, could in principle yield a different mode of action leading to a less potent input on the pathway flow and to, at least theoretically, less toxic effects. For instance, one of the off-target effects described to occur for classical p38 MAPK inhibitors consists in that, as a consequence of completely downregulating p38 MAPK activity, the JNK route appears to become hyperactivated. This is caused by such a strong inhibition of p38 MAPK that is able to cancel some negative feedback loops that this kinase maintains towards upstream kinase such as MLK2/MLK3 or TAK1 which also sit upstream of JNK³⁰. Thus, abolition of the negative feedback control exerted by the p38 MAPK branch redirects the pathway flow towards a higher activation of the JNK pathway. However, in our case, preliminary data indicates that no activation of JNK was detected by the presence of FGA-19 in our cells (data not shown). On the contrary, JNK pathway was either unchanged or inhibited to a lesser extent than the p38 MAPK route by FGA-19, thus suggesting that these types of effects may not happen for docking-based inhibitors or for inhibitors that do not fully ablate p38 MAPK catalytic activity. The possibility that a more refined, less potent inhibition of p38 MAPK such as obtained by FGA-19 can prevent undesired side effects such as the hyperactivation of cell death routes certainly deserves further investigation.

In conclusion, we present evidence that a novel small compound targeting the docking groove of p38 MAPK, FGA-19, is a potent inhibitor of chronic inflammatory and post-inflammatory hyperalgesia. In addition, we show that FGA-19 inhibits cytokine production in monocytic cells. We propose that this novel compound can form the basis for further investigation of similar compounds for their specificity and potency in these models and ultimately for clinical translation.

Ethics of Animal Experiments

All experiments adhere to the guidelines of the Committee for Research and Ethical Issues of IASP and were reviewed by an institutional animal care and use committee of the institutions involved.

Acknowledgements

We acknowledge grants from Ministerio de Educación y Ciencia (SAF2011-23800), The Cardiovascular Network (RECAVA) of Ministerio Sanidad y Consumo-Instituto Carlos III (RD06-0014/0037), Comunidad de Madrid (S2010/BMD-2332) to F.M and Instituto Carlos III (PS09/01208) and UAM-Grupo Santander to C.M. The work of A.K. is supported by grants #RO1 NS074999 and #RO1 NS073939 from the National Institute of Health and a STARS award from the University of Texas System.

6



Genome-wide association study meta-analysis of chronic widespread pain: evidence for involvement of the 5p15.2 region

Hanneke L.D.M. Willemen^{1*}

Marjolein J. Peters^{2,3*}

Linda Broer^{4*}

45 others

Annemieke Kavelaars^{1&}

Cornelia M. van Duijn^{4&}

Frances M. K. Williams^{5&}

Joyce B. J. van Meurs^{2,3&}

* shared first authors

& shared last authors

¹ Laboratory of Neuroimmunology and Developmental Origins of Disease, University Medical Center Utrecht, the Netherlands.

² Department of Internal Medicine, Erasmus Medical Center Rotterdam, the Netherlands

³ The Netherlands Genomics Initiative-sponsored Netherlands Consortium for Healthy Aging (NGI-NCHA), Leiden / Rotterdam, the Netherlands.

⁴ Department of Epidemiology, Erasmus Medical Center Rotterdam, the Netherlands.

⁵ Department of Twin Research and Genetic Epidemiology, King's College London, UK.

Abstract

Background and objectives Chronic widespread pain (CWP) is a common disorder affecting ~10% of the general population and has an estimated heritability of 48-52%. In the first large-scale genome-wide association study (GWAS) meta-analysis, we aimed to identify common genetic variants associated with CWP.

Methods We conducted a GWAS meta-analysis in 1308 female CWP cases and 5791 controls of European descent, and replicated the effects of the genetic variants with suggestive evidence for association in 1480 CWP cases and 7989 controls ($p < 1 \times 10^{-5}$). Subsequently, we studied gene expression levels of the nearest genes in two chronic inflammatory pain mouse models, and examined 92 genetic variants previously described associated with pain.

Results The minor C-allele of rs13361160 on chromosome 5p15.2, located upstream of chaperonin-containing-TCP1-complex5 gene (CCT5) and downstream of FAM173B, was found to be associated with a 30% higher risk of CWP (minor allele frequency=43%; OR=1.30, 95% CI 1.19 to 1.42, $p = 1.2 \times 10^{-8}$). Combined with the replication, we observed a slightly attenuated OR of 1.17 (95% CI 1.10 to 1.24, $p = 4.7 \times 10^{-7}$) with moderate heterogeneity ($I^2 = 28.4\%$). However, in a sensitivity analysis that only allowed studies with joint-specific pain, the combined association was genome-wide significant (OR=1.23, 95% CI 1.14 to 1.32, $p = 3.4 \times 10^{-8}$, $I^2 = 0\%$). Expression levels of Cct5 and Fam173b in mice with inflammatory pain were higher in the lumbar spinal cord, not in the lumbar dorsal root ganglions, compared to mice without pain. None of the 92 genetic variants previously described were significantly associated with pain ($p > 7.7 \times 10^{-4}$).

Conclusions We identified a common genetic variant on chromosome 5p15.2 associated with joint-specific CWP in humans. This work suggests that CCT5 and FAM173B are promising targets in the regulation of pain.

Introduction

Chronic widespread pain (CWP) is a common disorder, affecting about 10% of the general population⁴⁷. The prevalence of CWP increases with age for both men and women, but is more common in women at any age⁴⁷. CWP represents a major underestimated health problem and is associated with substantial impairment and a reduced quality of life. It has been related to a number of physical and affective symptoms such as fatigue, psychological distress and somatic symptoms^{47,260}. Chronic musculoskeletal pain is one of the most common conditions seen in rheumatology clinics and accounts for 6.2% of the total healthcare costs in the Netherlands every year¹⁵⁹. Further research is needed to be able to understand the causal mechanisms and optimal treatment for CWP patients.

CWP causally relates to an initial local pain stimulus, such as an acute injury or athletic injuries or another pain state such as low back pain or local pain due to osteoarthritis (OA) or rheumatic arthritis (RA)^{22,104,139}. However, most injured subjects do not develop CWP, and only a proportion of patients with OA or RA develop CWP. We therefore hypothesize that several discrete stimuli may initiate CWP via a common final pathway that involves the generation of a central pain state through the sensitization of second order spinal neurons.

CWP is a complex trait since both environmental and genetic factors play a role in the etiology. Heritability estimates of twin studies suggest that 48%-52% of the variance in CWP occurrence is due to genetic factors, implying a strong genetic component¹¹⁸. A number of studies have examined genetic variants for CWP. These candidate gene studies examined polymorphisms in genes involved in both the peripheral and the central nervous system¹⁴¹. In particular, genes involved in neurotransmission (pathway of dopamine and serotonin^{15,21,40,73,84,85,175,181,190,225,229}), and genes important for the hypothalamic-pituitary-adrenal axis have been considered⁹⁷. A number of genetic variants in these candidate genes were found to be associated with CWP, individual pain sites, or experimental pain. However, no consistent significant associations have been demonstrated.

The most studied gene in relation to pain is catechol-O-methyltransferase (COMT), an enzyme that degrades neurotransmitters including dopamine. The variant allele of rs4680 (or V158M) results in reduced enzymatic activity due to its effect on thermostability²²⁸, and has been associated with reduced opioid activity in response to painful stimuli resulting in increased pain sensitivity²⁷⁷. But also for COMT, no consistent results have been observed in genetic association studies^{41,86,87,94,174,229,235,237}.

Overall, the results have been conflicting which is likely due to the modest sample sizes used and paucity of replication. In general, candidate studies are biased by previous knowledge of the aetiology of the disease under study. Since knowledge about the pathophysiology of CWP is poor, the chances of success using this approach are low. Therefore our objective was to identify genetic variants involved in CWP by means of a large-scale hypothesis-free genome-wide association study (GWAS) meta-analysis including 2788 cases and 13780 controls. To our knowledge, this is the first study presenting a large-scale GWAS meta-analysis of chronic pain. The prevalence of CWP is approximately two times higher in women than in men and there is strong evidence that women tolerate less thermal and pressure pain than men¹⁹⁷. Therefore only women were included in this study to reduce heterogeneity and thereby increase power.

Materials and Methods

We performed a meta-analysis (stage 1) of GWAS data of 1308 female Caucasian CWP cases and 5791 female Caucasian controls, derived from five studies, and focused our follow-up efforts on the single-nucleotide polymorphisms (SNPs) with suggestive evidence of association ($p < 1 \times 10^{-5}$) with CWP (stage 2). The study outline is summarized in figure 6.1.

Phenotype

CWP was defined as subjects having pain in the left side of the body, in the right side of the body, above waist, below waist, and in the axial skeleton (following the Fibromyalgia Criteria of the American College of Rheumatology²⁶⁰). Controls were defined as subjects not having CWP. Subjects using analgesics (ATC-code: N02²¹⁹) were excluded from the control group. Detailed descriptions of the study specific inclusion criteria are presented in supplementary table S6.1.

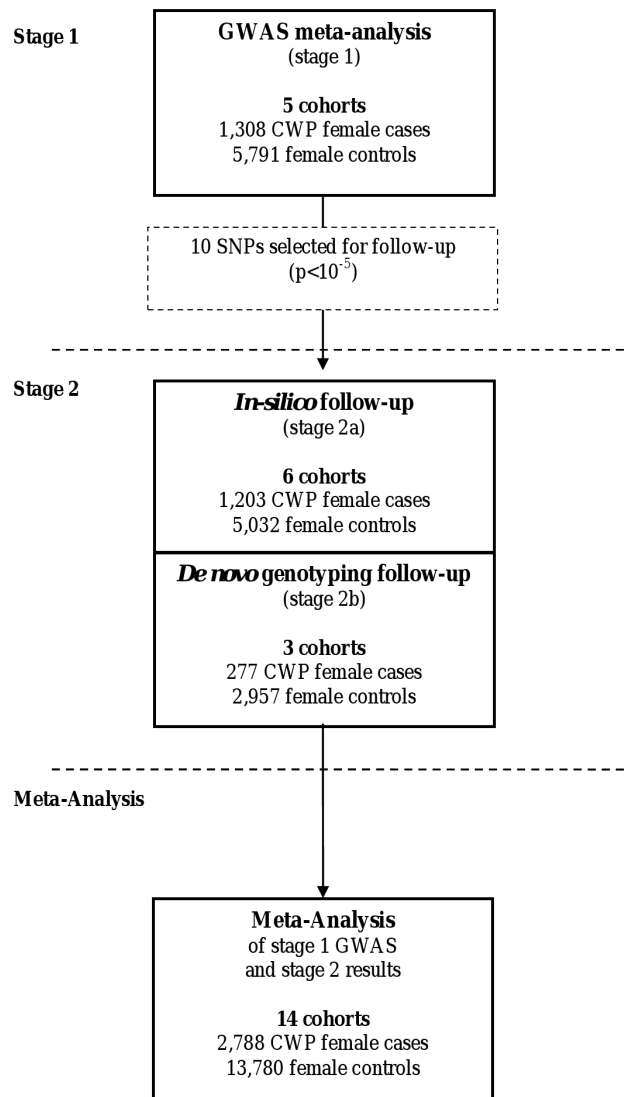


Figure 6.1: Study Outline. CWP, chronic widespread pain; GWAS, genome-wide association study.

Table 6.1: Overview of all participating studies.

Study (stage)	Reference article	Study design	Ethnic origin	Country of origin	Medication	Age/BMI	Mean age (y)	# CWP cases	# CWP controls
<i>Stage 1</i>									
ERF study	3	Family Based Cohort	Caucasian	the Netherlands	Y	Y	46.4	149	665
RS-I	95	Population Based Cohort	Caucasian	the Netherlands	Y	Y	69.4	563	1892
RS-II	95	Population Based Cohort	Caucasian	the Netherlands	Y	Y	67.9	110	668
RS-III	95	Population Based Cohort	Caucasian	the Netherlands	Y	Y	56.3	85	868
TWINSUK	221,222	Twins Based Cohort	Caucasian	United Kingdom	Y	Y	51.9	401	1698
Total # samples							59.7	1308	5791
<i>Stage 2a</i>									
1958BC	43,94,191,252	Prospective Birth Cohort	Caucasian	United Kingdom	N	Y (born in 1958)	NA	315	2206
AGES	90	Population Based Cohort	Caucasian	Iceland	Y	Y	76.5	173	1204
DSDBAG	196	Population Based Cohort	Caucasian	United Kingdom	Y	Age only	80.1	81	219
FOA	67	Population Based Cohort	Caucasian	United States	Y	Y	59.3	384	814
GARP	207	Case Control Based	Caucasian	the Netherlands	Y	Y	58.5	67	925*
SHIP	113,239	Population Based Cohort	Caucasian	Germany	Y	Y	57.6	183	589
<i>Stage 2b</i>									
CHINGFORD	91,92	Population Based Cohort	Caucasian	United Kingdom	Y	Y	56.6	48	337
EPIFUND	97	Population Based Cohort	Caucasian	United Kingdom	N	Age only	49.0	139	503
HCS	227	Population Based Cohort	Caucasian	United Kingdom	Y	Y	66.4	90	2117
Total # samples								1480	7989

*GARP consists of clinical and radiographically confirmed osteoarthritis case only; therefore we used 925 randomly chosen Rotterdam Study samples as controls. Age/BMI Y, age and BMI data are available; Age only, no BMI data are available; AGES, Age, Gene/Environment Susceptibility study Reykjavik; BMI, body mass index; CWP, chronic widespread pain; CHINGFORD, Chingford 1000 Women Study; DSDBAG, Dyne Steel DNA Bank for Ageing and Cognition; ERF study, Erasmus Rucpen Family study; EPIFUND, Epidemiological study of FUNCTIONal Disorders study; HCS, Hertfordshire Cohort Study. FOA, Framingham Osteoarthritis Study; GARP, Genetics OsteoArthritis and Progression study Leiden; Medication Y, information about medication use available; Medication N, medication use not available; RS, Rotterdam Study; SHIP, Study of Health In Pomerania; TwinsUK, the U Adult Twin Registry; 1958BC, 1958 Birth Cohort.

Study design summary

We combined the summary statistics of GWAS in a meta-analysis comprising 1308 CWP female Caucasian cases and 5791 female Caucasian controls (stage 1). We focused our follow-up efforts on the SNPs with suggestive evidence of association ($p < 1 \times 10^{-5}$) with CWP in 1480 CWP cases and 7989 controls available for replication (stage 2).

Subjects

A full detailed description of all study cohorts is presented in table 6.1 and in the supplementary methods section. For the stage 1 analysis, we included studies from the Netherlands (the Erasmus Rucphen Family study (ERF study))³, Rotterdam Study I, II and III (RS-I, RS-II and RS-III)⁹⁵, and the UK (TwinsUK^{221,222}). All studies were approved by their institutional ethics review committees and all participants provided written informed consent. For our stage 2 analysis, we sought follow-up samples with pre-existing GWAS *in-silico* data (stage 2a) as well as *de novo* genotyping (stage 2b). The studies are from the UK (the British 1958 Birth Cohort (1958BC))^{43,94,191,252}, the Chingford Study (CHINGFORD)^{91,92}, the Dyne Steel DNA Bank for Aging and Cognition (DSDBAG)¹⁹⁶, the EPIdemiological study of FUNctional Disorders (EPIFUND)⁹⁷, and the Hertfordshire Cohort Study (HCS)²²⁷; from Iceland (the Age, Gene/Environment Susceptibility Study (AGES))⁹⁰; from the USA (Framingham Osteoarthritis Study (FOA))⁶⁷; from the Netherlands (the Genetics osteoARthritis and Progression Study (GARP))²⁰⁷; and from German (the Study of Health In Pomerania (SHIP))^{113,239}. All studies were approved by the local ethics committees and all participants provided written informed consent.

Genotyping, quality control and imputation

Genotyping of the stage 1 cohorts was done by Illumina Infinium HumanHap550 Beadchip (RS-I and RS-II), the Illumina Infinium HumanHap610 (RS-II, RS-III, and TwinsUK), or the Illumina Infinium HumanHap300 (ERF and TwinsUK). More details about the genotyping, quality control (QC), and imputation are shown in the supplementary methods section. Complete information on genotyping protocols and QC measures for all stage 1 cohorts is described in the supplementary material (Table S6.2). Detailed descriptions of the QC and imputation procedures are provided in the supplementary material (Table S6.3).

Genotypes of the stage 2a studies (1958BC, AGES, DSDBAG, FOA, GARP and SHIP) were obtained from SNP arrays and imputed data. Where unavailable, proxy SNPs were selected based on high linkage disequilibrium (LD). The stage 2b studies (CHINGFORD, EPIFUND and HCS) performed *de novo* genotyping, using both Sequenom iPLEX and TaqMan-based assays (supplementary methods). Genotyping platforms, calling algorithms, quality control before imputation, imputation methods and analysis software used were all study-specific (see supplementary tables S6.4 and S6.5). The explicit number of follow-up SNPs genotyped in the different studies and whether the original or a proxy SNP was used is summarized in supplementary table S6.6.

GWAS-analysis in the stage 1 studies

CWP was analyzed as a binary trait (cases vs controls) using logistic regression under an additive model with adjustment for age and body mass index (see supplementary table S6.7). To adjust for population substructure, we included the four most important PCs as covariates in the regression analysis of RS-I, RS-II, and RS-III. These PCs were derived from an multidimensional

scaling analysis of identity-by-state distances, using PLINK software¹⁹⁴. Detailed descriptions of the GWAS methods are provided in supplementary table S6.8).

Stage 1 GWAS meta-analysis

p Values for association were combined using the Meta-Analysis Tool for genome-wide association scans (METAL)²⁵⁹. The genomic control method⁵⁶ as implemented in METAL was used to correct for any residual population stratification or relatedness not accounted for by the four most important PCs. A p value $< 5 \times 10^{-8}$ was considered genome-wide significant while a p value $< 1 \times 10^{-5}$ was considered suggestive¹⁸³. Power calculations were performed using CaTS software (www.sph.umich.edu/csg/abecasis/CaTS/). Using Bonferroni correction ($p < 5 \times 10^{-8}$), power calculations showed that we had approximately 80% power to detect an odds ratio (OR) of 1.30 for SNPs with a minor allele frequency (MAF) of 0.43, given a disease prevalence of 10% for 1308 cases and 5791 controls in the discovery group. Using a p value $< 1 \times 10^{-5}$, we had 80% power to detect an OR of 1.25.

SNP selection for replication

We aimed to select SNPs for replication (stage 2) that were enriched for signals of association with CWP. All SNPs with suggestive evidence for association in the stage 1 analyses were selected and separated into independent loci by taking the most significantly associated SNP and eliminating all SNPs that have a HapMap CEU pair-wise correlation coefficient $r^2 > 0.8$ with that SNP using the PLINK software.

Meta-analysis of stage 1 and stage 2 results

We combined the stage 1 and stage 2 association results to derive a combined meta-analysis for the suggestively associated loci. METAL was used to conduct a fixed-effects meta-analysis as in stage 1. Estimated heterogeneity variance and forest plots were generated using comprehensive meta-analysis (www.meta-analysis.com).

Functional analysis of associated SNPs

To determine whether the associated SNPs have any regulatory effect on gene expression levels, we checked their effect (and the effect of the linked SNPs) on the expression levels of their neighbouring genes. We used the 1000 genomes data in the SNAP software^{77,114} to identify those SNPs having LD thresholds of $r^2 > 0.1$. We searched two publicly available eQTL databases: the NCBI GTEx (Genotype-Tissue Expression) eQTL Browser (<http://www.ncbi.nlm.nih.gov/gtex/GTEX2/gtex.cgi>) and the expression Quantitative Trait Loci database (<http://eqtl.uchicago.edu/cgi-bin/gbrowse/eqtl/>). We used SIFT¹³¹ to predict whether the coding non-synonymous variant causing an amino acid substitution affects protein function.

RNA expression analyses in mice

For functional follow-up, two independent mouse models of inflammatory pain were studied. The first model was based on carrageenan injections; female C57Bl/6 mice received an intraplantar injection of 20 μ l λ -carrageenan (2% (w/v), Sigma-Aldrich, Zwijndrecht, the Netherlands) in saline in both hind paws²⁵⁷. The second model was based on Complete Freund's Adjuvant (CFA) injections; male C57Bl/6 mice (Harlan Laboratories) received an intraplantar injection of 20 μ l CFA (Sigma-Aldrich) in saline in both hind paws²⁷¹. Controls were injected with saline only. At day 3 (after CFA injection) or day 6 (after carrageenan injection), thermal sensitivity (heat withdrawal latency time) was measured using the Hargreaves (IITC Life

Science, Woodland Hills, California, USA) test as described⁸⁹. Intensity of the light beam was chosen to induce heat withdrawal latency time of approximately 8 s at baseline.

After measurement the mice were sacrificed and the lumbar (L2-L5) spinal cord and the dorsal root ganglions (DRG) (L2-L5) were isolated. These areas of spinal cord and DRG were selected because pain transmission from the hind paws is mediated via primary sensory neurons that have their cell bodies in the lumbar DRG, and transmit the signal to the lumbar spinal cord through sensory fibres in the dorsal roots. Total RNA was isolated and mRNA levels of *Cct5* and *Fam173b* were measured in the spinal cord and the DRG. For more details, see the supplementary methods section.

All experiments were performed in accordance with international guidelines and approved by the experimental animal committee of University Medical Center Utrecht (carrageenan experiment) or the UK Home Office Animals (Scientific Procedures) Act 1986 (CFA experiment). Mice used for the carrageenan experiment were bred and maintained in the animal facility of the University of Utrecht (the Netherlands).

Systemic review of genetic variants previously described

We systematically searched for associations earlier reported with pain in the Hugenavigator PhenoPedia Database²⁶⁶. We used the search term “pain” and checked all publications for genes and SNPs associated with pain at least twice. Genes and SNPs associated with drug therapy, facial pain, migraine, and postoperative pain were excluded. For all reported SNPs, we examined their association with CWP in our stage 1 meta-analysis. The significance threshold was set at $p < 8 \times 10^{-4}$ using Bonferroni correction for 65 independent genetic loci. Again, power calculations were performed using CaTS software (www.sph.umich.edu/csg/abecasis/CaTS/). With an α level of 8×10^{-4} , power calculations showed that we had approximately 80% power to detect an OR of 1.22 for SNPs with an minor allele frequency of 20% or higher.

Results

GWAS meta-analysis for CWP

The Manhattan plot and quantile-quantile (QQ) plot of the initial stage 1 meta-analysis are presented in figure 6.2. In total, 2224068 SNPs (directly genotyped or imputed) were tested for association. The overall genomic control lambda (λ_{GC}) was 1.007, indicating no significant population stratification. We identified two SNPs which were genome-wide significant ($p < 5 \times 10^{-8}$), and another 39 SNPs with suggestive evidence for association ($p < 1 \times 10^{-5}$) located in 10 independent genomic regions. The most significant association was observed for two imputed highly correlated SNPs ($r^2 = 0.97$) located upstream of the chaperonin-containing-TCP1-complex-5 gene (*CCT5*) and downstream of the FAMily with sequence similarity 173, member B gene (*FAM173B*) (rs13361160, $p = 1.2 \times 10^{-8}$ and rs2386592, $p = 2.6 \times 10^{-8}$). For both SNPs, the minor allele (MAF=43%) was associated with a 30% higher risk for CWP (OR=1.30, 95% CI 1.19 to 1.42).

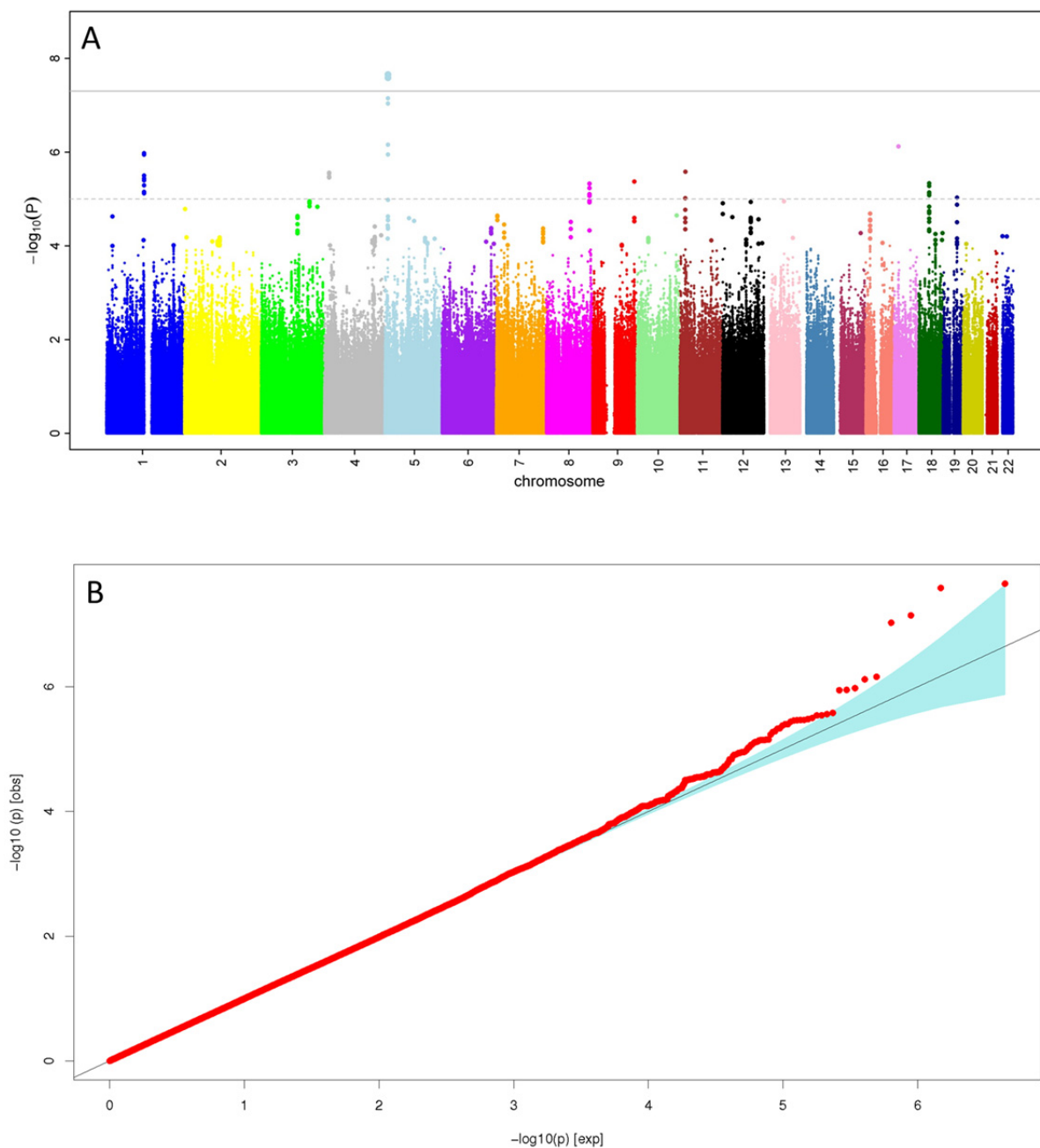


Figure 6.2: Genome-wide association results for chronic widespread pain (CWP) (stage 1). (A) Manhattan plot showing the p value of association tests for about 2 million SNPs with CWP in the stage 1 meta-analysis. SNPs are plotted on the x-axis according to their position on each chromosome. On the y-axis, the association p values with CWP are shown (as $-\log_{10}$ p values). The grey solid horizontal line represents the p value threshold of 5×10^{-8} (genome-wide significance). The grey dashed horizontal line represents the p value threshold of 1×10^{-5} (the level for suggestive evidence): SNPs in loci reaching 1×10^{-5} were tested for replication. (B) Quantile-Quantile (QQ) plot of SNPs. The blue area represents the 95% CI around the test statistics. A QQ plot compares the additive model statistics to those expected under the null distribution using fixed effects for all analyzed HapMAP CEU imputed SNPs passing quality control criteria.

	Nr cases	Nr controls	OR and 95% CI	p-Value
DISCOVERY				
ERF	149	665	1.42 (1.09-1.85)	8.30E-3
RS-I	563	1892	1.35 (1.18-1.56)	1.98E-5
RS-II	110	668	1.23 (0.92-1.65)	1.66E-1
RS-III	85	868	1.27 (0.93-1.74)	1.37E-1
TWINSUK	401	1698	1.20 (1.02-1.41)	2.48E-2
Overall Effect Discovery	1308	5791	1.30 (1.19-1.42)	1.18E-8
<i>(Fixed-effects: I² = 0%)</i>				
REPLICATION				
1958BC	315	2206	1.05 (0.88-1.26)	5.85E-1
AGES	173	1204	1.07 (0.85-1.34)	5.55E-1
CHINGFORD	48	337	1.23 (0.80-1.89)	3.57E-1
DSDBAC	81	219	1.03 (0.70-1.50)	8.98E-1
EPIFUND	139	503	0.94 (0.74-1.20)	6.34E-1
FOA	384	814	1.08 (0.89-1.31)	4.36E-1
GARP	67	925*	1.16 (0.82-1.64)	4.02E-1
HCS	90	2117	1.47 (1.08-2.00)	1.54E-2
SHIP	183	589	0.93 (0.73-1.20)	5.89E-1
Overall Effect Replication	1480	7989	1.07 (0.98-1.16)	1.24E-1
<i>(Fixed-effects: I² = 0%)</i>				
Overall Effect All Studies	2788	13780	1.17 (1.10-1.24)	4.67E-7
<i>(Fixed-effects: I² = 28.4%)</i>				

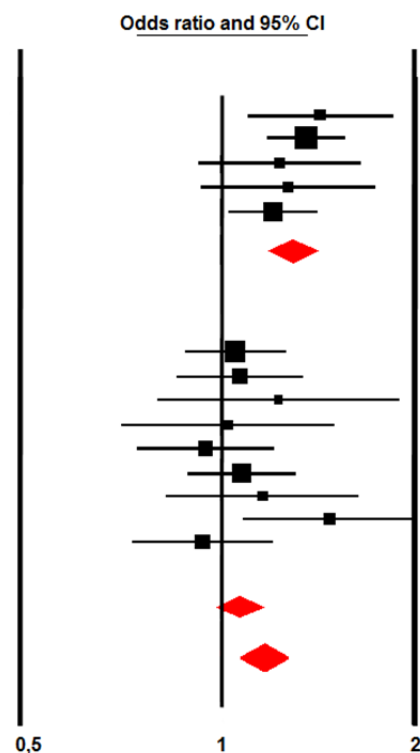


Figure 6.3: Forest plot of the association of rs13361160 SNP with chronic widespread pain (CWP). Study specific estimates and summary association between rs13361160 and CWP are shown.

Meta-analysis of GWAS replication

For the 10 independent SNPs with suggestive evidence, we pursued *in silico* replication data in six studies (stage 2a: 1203 CWP cases and 5032 controls) and performed *de novo* genotyping in subjects from three additional studies (stage 2b: 277 CWP cases and 2957 controls) (a detailed description of the studies is presented in table 6.1 and supplementary methods). The summary results of the stage 1 and 2 meta-analysis are presented in table 6.2. After combining the results of stage 1 and stage 2, the top SNP was rs13361160 (OR=1.17, 95% CI 1.10 to 1.24, $p=4.7 \times 10^{-7}$, $I^2=28.4\%$). Figure 6.3 shows a forest plot of the association of rs13361160 with CWP across the stage 1 and stage 2 studies. The overall effect in the replication studies (stage 2 studies) was in a consistent direction but not significant (OR=1.06, 95% CI 0.98 to 1.16, $p=0.16$). In the combined analysis, moderate heterogeneity was observed ($I^2=28.4\%$). Supplementary table S6.1 shows the different pain assessment methods used in the different studies to define CWP. Since four out of five stage 1 studies included joint-specific pain only (ERF, RS-I, RS-II, and RS-III), we performed a sensitivity analysis in which stage 2 cohorts using non-joint pain were excluded (1958BC, DSDBAG, EPIFUND, HCS, and SHIP). This resulted in a combined OR of 1.23 (95% CI 1.14 to 1.32, $p=3.4 \times 10^{-8}$, $I^2=0\%$). An overview of the results of the combined meta-analysis and the separate stage 1 and stage 2 analyses is presented in table 6.3.

Table 6.2: Association results of the 10 top hits.

SNP ID	SNP information			Gene information		Stage 1			Stage 2			Stage 1 & 2 (combined)			
	CHR	Minor Allele (MA)	Other Allele (OA)	MAF (%)	Nearest gene	Distance to gene (kb)	OR (Minor Allele)	95%CI	P	OR (Minor Allele)	95%CI	P	OR (Minor Allele)	95%CI	P
rs13361160	5	c	t	43.5	FAM173B	56.7	1.30	1.18-1.42	1.18 x10⁻⁸	1.06	0.98-1.16	0.161	1.17	1.10-1.24	4.67 x10⁻⁷
rs8065610	17	a	c	38.7	PMP22	41.9	1.26	1.15-1.38	3.86 x10 ⁻⁷	0.93	0.85-1.02	0.119	1.08	1.02-1.16	1.20 x10 ⁻²
rs12132674	1	a	g	29.5	HMGCS2	0.0	1.28	1.16-1.41	9.29 x10 ⁻⁷	1.07	0.97-1.17	0.165	1.16	1.09-1.24	1.23 x10 ⁻⁵
rs11606304	11	g	t	9.07	TPH1	0.0	0.55	0.43-0.70	1.47 x10 ⁻⁶	0.99	0.81-1.22	0.934	0.78	0.66-0.91	1.64 x10 ⁻³
rs7680363	4	a	t	6.42	PROM1	0.0	1.52	1.28-1.80	1.72 x10 ⁻⁶	1.04	0.86-1.25	0.688	1.27	1.12-1.44	1.52 x10 ⁻⁴
rs4837492	9	c	t	4.51	FREQ	56.2	1.23	1.13-1.34	2.96 x10 ⁻⁶	0.97	0.89-1.07	0.568	1.10	1.03-1.17	2.68 x10 ⁻³
rs524513	18	t	c	18.2	BRUNOL4	0.0	1.29	1.16-1.44	4.00 x10 ⁻⁶	0.96	0.85-1.09	0.537	1.13	1.04-1.23	2.75 x10 ⁻³
rs7835968	8	g	a	12.7	KHDRBS3	175.8	1.34	1.18-1.52	4.26 x10 ⁻⁶	0.98	0.86-1.12	0.787	1.16	1.06-1.27	1.43 x10 ⁻³
rs2249104	11	t	c	8.8	MYOD1	3.7	1.42	1.22-1.64	4.57 x10 ⁻⁶	0.99	0.84-1.17	0.882	1.21	1.08-1.35	8.78 x10 ⁻⁴
rs17796312	19	g	a	33.1	FBL	7.1	1.24	1.13-1.37	9.79 x10 ⁻⁶	1.08	0.97-1.2	0.166	1.17	1.09-1.25	2.56 x10 ⁻⁵

CHR, chromosome; MA, minor allele or effect allele (minor allele = effect allele); MAF, minor allele frequency (%); OA, other allele.

Table 6.3: Top hit association results.

Type of Analysis		Stage 1		Stage 2		Stage 1 & 2 (combined)	
SNP tested	Adjustments	OR (95%CI)	P	OR (95%CI)	P	OR (95%CI)	P
rs13361160	Age, BMI, and 4 PCs (minor allele = C, other allele = T, MAF=43.5%)	1.30 (1.19 -1.42)	1.18x10 ⁻⁸	1.06 (0.98-1.16)	0.16	1.17 (1.10-1.24)	4.67x10 ⁻⁷
SENSITIVITY ANALYSIS – JOINT PAIN ONLY							
rs13361160	Age, BMI, and 4 PCs (minor allele = C, other allele = T, MAF=43.5%)	1.30 (1.19 -1.42)	1.18x10 ⁻⁸	1.10 (0.97-1.25)	0.15	1.23 (1.14-1.32)	3.43x10 ⁻⁸

In both analyses the effect estimates of the models refer to the minor allele (=effect allele). BMI, body mass index; MAF, minor allele frequency.

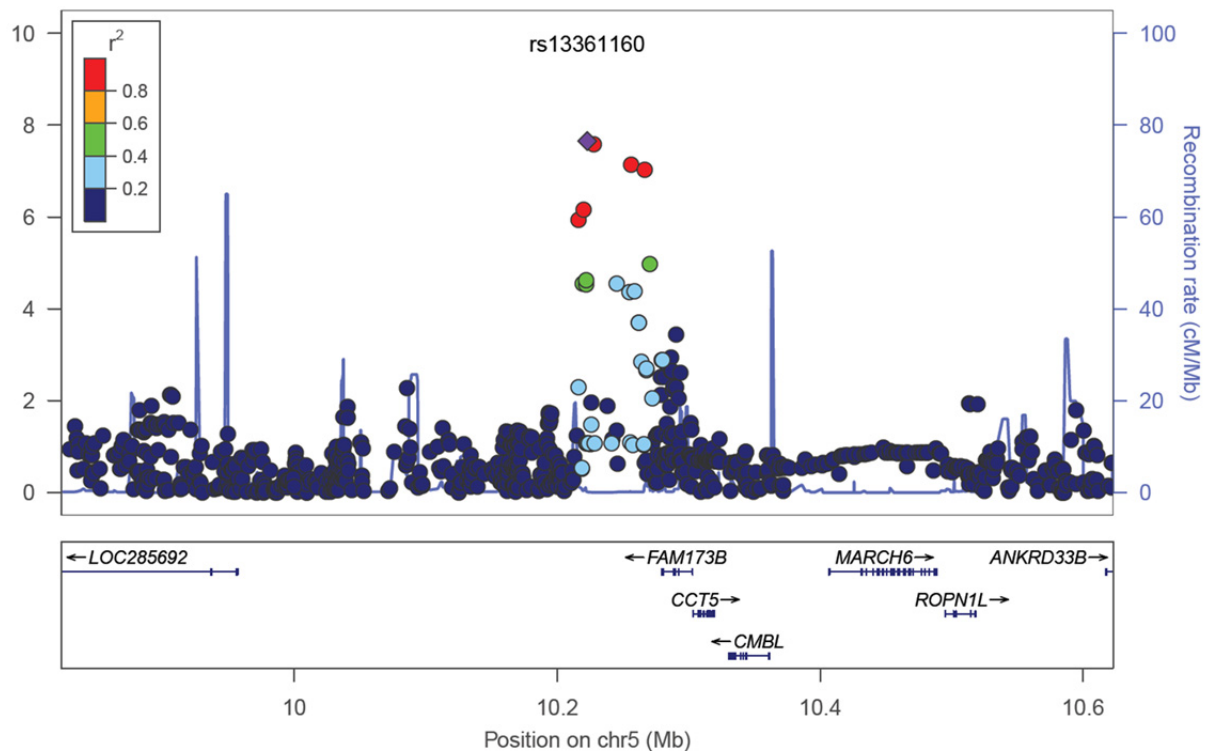


Figure 6.4: Regional plot of locus 5p15.2. On the x-axis, SNPs are plotted according to their position in a 400-kb window around rs13361160. On the y-axis, the association p values with chronic widespread pain are shown (as $-\log_{10} p$ values). The purple diamond highlights the most significant SNP rs13361160. Blue peaks indicate recombination sites, and the SNPs surrounding the most significant SNP are colour coded to identify their strength of linkage disequilibrium with the most significant SNP (pairwise r^2 values of the HapMap CEU samples). Genes and the direction of transcription are shown at the bottom of the plot.

Functional analysis of rs13361160 and rs2386592

The SNPs rs13361160 and rs2386592 ($r^2=0.97$) are annotated to the 5p15.2-region and located 81 kb upstream of CCT5 and 57 kb downstream of FAM173B (figure 6.4). We tested whether rs13361160 and rs2386592 and their linked SNPs ($r^2>0.1$) affected gene expression levels of CCT5 or FAM173B. In total, we identified 130 SNPs in LD with our top SNPs of which two SNPs were located in the coding region: one synonymous SNP rs1042392 in the CCT5 gene ($r^2=0.16$, $D'=0.85$) and one non-synonymous SNP rs2438652 in the FAM173B gene ($r^2=0.17$, $D'=1.0$) (See supplementary table S6.9). The minor allele of rs2438652 causes a threonine-to-methionine substitution (T75M) which is thought to be functionally neutral. SNPs rs13361160 and rs2386592 were not recorded as influencing the expression levels of CCT5 and FAM173B, however, the linked intronic SNP rs2445871 ($r^2=0.14$ for both) had a direct eQTL effect on FAM173B expression levels in liver tissue²¹⁵.

RNA expression analysis in mice

We studied gene expression levels of the two nearest genes Cct5 and Fam173b, in the lumbar spinal cord and the DRG in two independent mouse models of chronic inflammatory pain. In both the carrageenan treated group and the CFA treated group, mice had shorter heat withdrawal latency times than mice injected with saline only, confirming enhanced pain sensitivity ($p<0.001$) (See supplementary figure S6.1).

The results from the multivariate analysis using the two genes (Cct5 and Fam173b examined as dependent variables), the different treatments (saline, carrageenan, and CFA) and the different tissues (DRG and spinal cord) confirmed that there is a significant treatment effect for Cct5 ($F(2,25)=3.399$, $p=0.0049$), as well as for Fam173b ($F(2,25)=4.911$, $p=0.016$). Moreover, both genes showed a significant tissue effect (Cct5: $F(1,25)=13.595$, $p=0.001$, and Fam173b: $F(1,25)=13.522$, $p=0.001$), as well as a significant interaction between tissue and treatment (Cct5: $F(2,25)=6.424$, $p=0.006$, and Fam173b: $F(1,25)=4.196$, $p=0.027$) (figure 6.5). These findings indicate that in spinal cord but not in DRG, both Fam173b and Cct5 expression levels were upregulated in response to two different inducers of inflammatory pain. DRG Fam173b and Cct5 expression levels in CFA/carrageenan-treated mice were indistinguishable from saline-treated mice.

Candidate SNPs previously associated with chronic pain.

We examined whether genetic variants previously described for association with pain were associated with CWP in our large stage 1 meta-analysis. We identified a total of 44 genes of which 136 SNPs had been reported at least twice with any pain phenotype (excluding facial pain, migraine, postoperative pain and response to drug therapy), and we examined the association of these 136 SNPs with CWP in the GWAS stage 1 meta-analysis. Out of 136 candidate SNPs, we were able to check 92 common SNPs ($MAF>5\%$) in 65 independent genetic loci (See supplementary table S6.10). Five SNPs had a too low MAF ($\leq 5\%$) and 39 SNPs were not genotyped or imputed in our meta-analysis. None of the earlier reported SNPs passed the

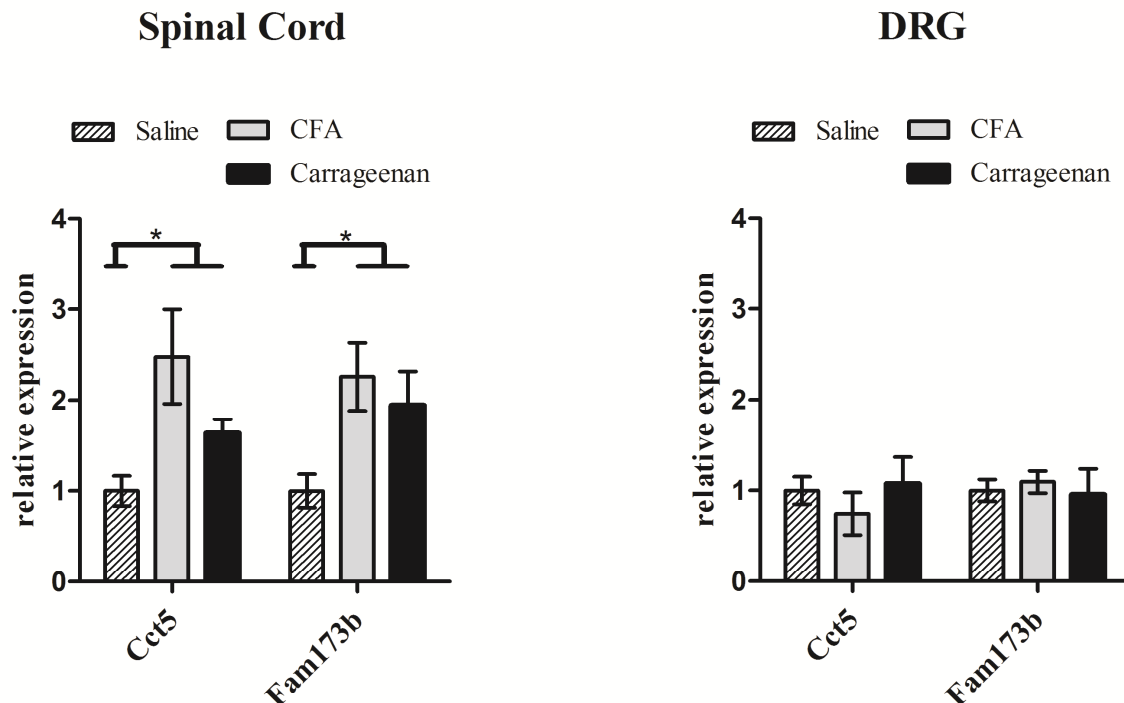


Figure 6.5: Quantitative Polymerase Chain Reaction (PCR) analysis of gene expression levels in the lumbar (L2-L5) spinal cord and the dorsal root ganglions (DRG) of mice after intraplantar saline (n=3), carrageenan (n=4), and Complete Freund's Adjuvant (CFA) (n=4) injection. Spinal cord and DRG were collected and analyzed for RNA levels of Cct5 and Fam173b. Data were normalized for Gapdh and β -actin (housekeeping genes) expression. Data are expressed as means \pm SEM, * = $p < 0.05$.

significance threshold ($p < 8 \times 10^{-4}$). Interestingly, the strongest associated SNPs are located in three genes that have been reported to be associated with pain phenotypes most frequently: COMT, GCH1 (GTP cyclo-hydrolase 1) and OPRM1 (mu opioid receptor). The effects of the SNPs in GCH1 are in the same direction as reported earlier^{24,96,230}: individuals having the minor allele for rs10483639, rs4411417 or rs752688 have 15% less pain than those exhibiting the common alleles. The effect of the SNP rs599548 in OPRM1 is also in the same direction as reported earlier⁹³: those having the minor allele for rs599548 have 19% more pain than those exhibiting the major allele. The two COMT SNPs are in weak linkage disequilibrium with the well-known amino acid changing variant rs4860, but previously have not been reported to be significantly associated with pain^{94,122}. We have found a protective effect for the minor allele of rs2020917 (those having a minor allele have 15% less pain) and an adverse effect for the minor allele of rs5993883: those having the minor allele of rs5993883 have 14% more pain.

Discussion

In this study, we identified a genetic variant near CCT5 and FAM173B to be associated with CWP. Chronic pain coincided with higher RNA-expression of Cct5 and Fam173b in the lumbar spinal cord of mouse models of inflammatory pain. This finding indicates that both genes in the 5p15.2 region are regulated in the context of inflammatory pain.

Interestingly, Bouhouche *et al.*¹⁶ reported a human pedigree in which a CCT5 mutation caused hereditary sensory neuropathy (Online Mendelian Inheritance in Man (OMIM) ID=610150), a syndrome characterized by a sensory deficit in the distal portion of the lower extremities, chronic perforating ulcerations of the feet, and progressive destruction of underlying bones. Symptoms can include pain and numbness, tingling in the hands, legs or feet, and extreme sensitivity to touch. CCT5 is a subunit of the chaperonin containing t-complex polypeptide 1 (TCP-1) which assists in protein folding and assembly in the brain¹³⁰. CCT5 interacts with the serine/threonine-protein phosphatase 4 catalytic subunit PP4C^{29,79,80}. Zhang *et al.*²⁶⁹ confirmed that protein phosphatases like PPP4C may have a regulatory effect on the central sensitization of nociceptive transmission in the spinal cord. Interestingly, sensitization is thought to contribute to chronic inflammatory pain¹³⁴. Since the function of the FAM173B gene is not yet known, it is difficult to postulate the mechanism by which this gene could influence CWP. Further research into the genes in this locus is needed to ascertain whether either or both CCT5 and FAM173B are driving the observed association.

By combining the effects across the different stage 2 studies, moderate heterogeneity was observed in the meta-analysis. This heterogeneity might be caused by different pain assessment methods used by the stage 2 cohorts. In particular, four cohorts asked the participants about joint pain specifically, while the other five also included non-joint pain. When the non-joint pain phenotype were excluded, the heterogeneity across the cohorts reduced to 0% and the overall p value for rs13361160 now reached genome-wide significance by combining the stage 1 and stage 2 effects. This might suggest that indeed phenotype heterogeneity was introduced by including non-joint pain. In general, it is anticipated that pain is a very complex trait, with different aetiological pathways introducing phenotypic heterogeneity.

A limitation of our study is that we were not able to examine possible phenotype subgroups, such as individuals with RA, a chronic systemic inflammatory disorder that principally affects the synovial joints. Stratifying these groups of individuals might serve to increase power to find genetic loci. We here decided to analyse all CWP cases together, based on the hypothesis that several discrete stimuli need to initiate CWP via a common final pathway that involves the

generation of a central pain state through the sensitization of second order spinal neurons. In addition, the prevalence of RA is very low (about 0.5-1%)²¹⁸, and the earlier defined GWAS hits for RA (i.e., the HLA-locus)⁹ were not in our top list. So, we assume the results were not dominated by this small number of individuals with RA.

It would be helpful to dissect the phenotype of pain into quantitative sub-phenotypes, for example by measuring pain sensitivity and pain thresholds for temperature or pressure²⁰⁹, or by examining functional MRIs⁵². The use of quantitative and possibly more objective pain measurements in response to painful stimuli (rather than reported pain) will be of pivotal importance for future pain research. Because we have focused on the clinical pain definition using questionnaires and pain homunculus, we accept that we may have missed true pain susceptibility alleles. However, this study represents the largest genome-wide meta-analysis looking into the genetics of human CWP to date. The experiments in two independent mouse models of chronic inflammatory pain showed that the expression of *Cct5* and *Fam173b* were higher in the lumbar spinal cord of mice with chronic inflammatory pain but not in DRG. In the spinal cord, the expression profiles of both genes were upregulated in response to two different inducers of inflammatory pain. These findings indicate that both genes in the 5p15.2 region are co-regulated in the spinal cord during inflammation-induced pain in both independent pain models, thereby possibly contributing to the neurobiology of pain. In the lumbar DRG, containing the cell bodies of the primary sensory neurons that detect pain signals from the hind paws, *Cct5* and *Fam173b* gene expression levels did not change by inflammation. Because of these complementary results from the two independent tissues (spinal cord and DRG), we hypothesize that the 5p15.2 region is likely to play a role in spinal central pain processing and not in regulating primary sensory neuron responses.

In the study of candidate genes previously reported to be associated with a pain phenotype, we showed that none of the 92 studied variants were significantly associated with CWP in our GWAS meta-analysis. This can be explained by the fact that many of the previous reported loci were studied in relative modest sample sizes and in a large variety of pain phenotypes¹⁶⁹. Power calculations show that we had approximately 80% power to detect an OR as low as 1.22 for SNPs with an allele frequency of 20% or higher. So, even in this large meta-analysis, power was still modest to detect small ORs and we therefore cannot exclude smaller effect sizes of the tested variants, resulting in lack of reproducibility¹⁰⁵. This lack of reproducibility of SNPs in candidate genes in large GWAS meta-analyses has been shown before for other phenotypes such as bone mineral density (BMD)²⁰⁶. It is interesting to note that among the candidate SNPs, the strongest associated ones were located in the three most studied pain genes *COMT*, *GCH1*, and *OPRM1*. The directions of the effects of these SNPs were the same as reported earlier, which would support true associations.

In conclusion, our study reports a GWAS meta-analysis on CWP. We identified the genetic variant rs13361160 at the 5p15.2 locus, located 81kb upstream of the *CCT5* gene and 57kb downstream of the *FAM173B* gene, to be associated with CWP. We showed an increase in expression levels of *Cct5* and *Fam173b* in the spinal cord of inflammatory pain models of mice, and since these genes both seem to influence the central mechanism of sensitization, they may represent a novel pathway involved in pain sensation.

Acknowledgements

For acknowledgements, please see the supplements.

Supplementary Methods:

Full description of the Stage 1 GWAS cohorts.

The ERF study. The ERF study (http://www.epib.nl/research/erf/erf_index.html) is a family-based cohort study that is embedded in the Genetic Research in Isolated Populations Program in the southwest of the Netherlands. The aim of this program was to identify genetic risk factors in the development of complex disorders. For the ERF study, 22 families that had at least five children baptized in the community church between 1850 and 1900 were identified with the help of genealogical records. All living descendants of these couples and their spouses were invited to take part in the study. Data collection started in June 2002 and was finished in February 2005. In this study, we focused on 2,347 participants for whom complete phenotypic, genotypic, and genealogical information was available. The medical ethics committee of Erasmus Medical Center Rotterdam approved the study, and informed consent was obtained from all participants. All participants completed a pain homunculus to report the painful sites in the body (pain during at least half of the days during the last six weeks). Individuals were categorised as CWP cases when they report joint pain in the left side of the body, in the right side of the body, above waist, below waist, and in the axial skeleton. Subjects not being a CWP case were categorised as controls, but subjects using pain medication were excluded from the control group.

The Rotterdam Study. The Rotterdam Study (www.epib.nl/rotterdamstudy) is a prospective, population based cohort study in the district of Rotterdam, the Netherlands. The initial design of the study is straight-forward: a prospective cohort study among, 7,983 persons living in the well-defined Ommoord district in the city of Rotterdam (78% of 10,215 invitees), called Rotterdam Study I (or RS-I). They were all 55 years of age or over and the oldest participant at the start was 106 years. The study started in the second half of 1989. In 1999, 3,011 participants (out of 4,472 invitees) who had become 55 years of age or moved into the study district since the start of the study were added to the cohort, called Rotterdam Study II (or RS-II). In 2006, a further extension of the cohort was initiated in which 3,932 subjects were included, aged 45–54 years (out of 6,057 invited), called Rotterdam Study III (RS-III). The participants were all examined in some detail at baseline. They were interviewed at home and then had an extensive set of examinations in a specially built research facility in the centre of their district. These examinations were repeated every 3–4 years in characteristics that could change over time. The participants in the Rotterdam Study are followed for a variety of diseases that are frequent in the elderly. Informed consent was obtained from each participant, and the medical ethics committee of the Erasmus Medical Center Rotterdam approved the study. In Rotterdam, the participants completed the same pain homunculus as the subjects of ERF. Individuals were categorised as CWP cases when they report joint pain in the left side of the body, in the right side of the body, above waist, below waist, and in the axial skeleton. Subjects not being a CWP case were categorised as controls, but subjects using pain medication were excluded from the control group.

The TwinsUK study. The TwinsUK cohort (www.twinsuk.ac.uk) is a British adult twin registry shown to be representative of singleton populations and the United Kingdom population. 5687 females aged between the ages of 16–88 completed questionnaires related to chronic widespread pain between 2002 - 2008. These questionnaires asked the participants about any pain in muscles, bones or joints lasting at least one week in the past three months.

Full description of the Replication Cohorts

1958BC. The National Child Development Study, also known as the 1958 British Birth Cohort Study is a large, ongoing, prospective cohort study of all children born in England, Scotland, and Wales during one week of March 1958. Detailed methods have been reported previously (Power et al, 2006). Approximately 17,000 participants were recruited at birth and have subsequently been followed up at ages 7, 11, 16, 23, 33, 42 and 45 years. At age 45 years a biomedical survey collected information on health-related factors including the presence of pain. The sample for the current study was 8,572 individuals who responded to a self-complete pain questionnaire at 45yrs (pain was not joint specific), sent in advance of a nurse interview, and who provided blood samples for genetic analysis.

The AGES Study. Age Gene/Environment Susceptibility Reykjavik (AGES-Reykjavik) Study. The Reykjavik Study cohort originally comprised a random sample of 30,795 men and women born in 1907-1935 and living in Reykjavik in 1967. A total of 19,381 people attended, resulting in 71% recruitment rate. The study sample was divided into six groups by birth year and birth date within month. One group was designated for longitudinal follow up and was examined in all stages. One group was designated a control group and was not included in examinations until 1991. Other groups were invited to participate in specific stages of the study. Between 2002 and 2006, the AGES-Reykjavik study re-examined 5764 survivors of the original cohort who had participated before in the Reykjavik Study. Participants came in a fasting state to the clinic and answered questionnaires related to chronic widespread pain. Informed consent was obtained from all participants. Subjects were asked whether they had pain lasting at least one month in the past 12 months. Questions were asked specifically for hand and wrist, hip, knee, shoulder, feet, toes, ankles and back. The AGES Reykjavik Study GWAS was approved by the intra-mural research program of the National Institute on Aging, by the Iceland National Bioethics Committee (VSN: 00-063) and Data Protection Authority.

The Chingford Study. The Chingford Study was established in 1989 when 1003 women, aged 44-67 years, derived from the register of a large general practice in Chingford, North London, were recruited to a prospective population-based longitudinal study of osteoarthritis and osteoporosis. In this study, data on joint and spinal pain, collected as part of the year 4 follow-up visit, was used. Subjects were asked whether they had pain in hand, knee, hip, feet and back during the last year. When they had pain, they were asked for how many days the pain lasted during the last month.

The DSDBAG Study. In 1983, 6542 healthy individuals aged between 42 and 92 years old resident in Newcastle and Greater Manchester were recruited into a longitudinal population-based study of cognition in healthy old age. Pain manikin data was collected via postal questionnaire on subjects remaining in the cohort in 2007, and additionally, subjects were asked whether they have had pain for more than 3 months. Pain was not asked joint specific.

The EPIFUND Study. EPIFUND is a prospective population-based study of functional disorders. Participants, aged 25-65 years old, were recruited from three primary care registers in the North-west of England. Pain manikin data was collected via a postal questionnaire at baseline and at two follow ups. Additionally to the manikins, subjects were asked whether they have had pain for more than 3 months. Pain was not asked joint specific. DNA was collected using buccal swab sampling from 1189 subjects who participated in all three phases.

The FOA Study. The Framingham Osteoarthritis Study is a population-based multigenerational cohort study of over 3500 participants, and is a sub-study of the larger Framingham Heart Study (FHS). In this study, we focused on study participants with information on widespread pain

(collected in FOA) and genetic data (collected in FHS). All participants completed a pain homunculus to report the sites in the body having pain, aching, or stiffness on most days. Individuals were categorised as CWP cases when they report joint pain in the left side of the body, in the right side of the body, above waist, below waist, and in the axial skeleton. Subjects not being a CWP case were categorised as controls, but subjects using pain medication were excluded from the control group.

The GARP Study. The GARP study from Leiden, the Netherlands, consists of 192 sibling pairs concordant for clinical and radiographically (K/L score) confirmed OA at two or more joint sites among hand, spine (cervical or lumbar), knee or hip⁹⁷. Written informed consent was obtained from each subject as approved by the ethical committees of the Leiden University Medical Center. We recorded pain in the GARP questionnaire by asking the question: Have you had pain in and around your joints lasting most days of the last month? Patients could choose: hands (left and/ or right), hips (left and/ or right), knees (left and/ or right), back (cervical, thoracic or lumbar region), shoulders (left and/or right) and other sites as specified. When patients indicated that they had pain in the hands, they could specify the locations in the hand in a drawing. When a patient indicated pain in two sections of two contralateral limbs and in the axial skeleton the patient is defined as a case of CWP. For controls, we used 925 randomly chosen Rotterdam Study participants.

The Hertfordshire Cohort Study (HCS) is a cohort study of men and women born in Hertfordshire, UK during 1931-39 and still living there in adult life. Approximately 3000 participants were recruited in the late 1990s and have subsequently been followed by clinic visit (East Herts only) and postal clinical outcomes questionnaire (all). The sample for the current study was drawn from individuals who completed a pain questionnaire at using a mannequin to report site of pain, and who had previously provided blood samples for genetic analysis. Individuals were categorised having CWP if they reported having pain for at least three months in a detailed pain questionnaire which corresponded pain in the left and right sides of the body, pain both above and below the waist and back pain (pain was not joint specific). Individuals who did not report such pain but reported use of analgesics were excluded from the analysis. All other individuals were categorized as controls resulting in 90 cases and 2117 controls.

The SHIP Study. The SHIP cohort (<http://www.medizin.uni-greifswald.de/cm/fv/ship.html>) is a prospective, population based cohort study among 4,308 subjects aged ≥ 20 years from the West Pomerania, Germany. The study was designed to assess prevalence and incidence of risk factors, subclinical disorders and clinical diseases and to investigate associations among them using extensive medical assessments. In this study, we focused on participants for whom complete phenotypic, genotypic, and genealogical information was available. Informed consent was obtained from each participant, and the medical ethics committee of University of Greifswald approved the study. Subjects were asked to complete questionnaires related to joint pain. These questionnaires asked about pain during the last week, regarding the back, elbow, foot, arms, hands, hip, knee, neck, shoulder, head and facial pain. We decided to exclude head and facial pain, not being joint-related pain. Because no duration was asked for, the pain prevalence in SHIP is one of the highest among the included cohorts.

Genotyping, Quality Control and Imputation

The following sample quality control (QC) criteria were applied in the GWAS of RS-I, RS-II, RS-III and ERF: sample call rate $>97.5\%$, gender mismatch with typed X-linked markers, evidence for DNA contamination in the samples using the mean of the autosomal heterozygosity >0.33 , exclusion of duplicates or first-degree relatives estimated by pairwise IBD, exclusion of ethnic

outliers (>4 SD from population mean using multidimensional scaling (MDS) analysis with 4 principal components (PCs)), and exclusion of samples with missing pain data, age and/or BMI. In the GWAS of TwinsUK, normalised intensity data was pooled, and genotypes were called on the basis of the Illuminus algorithm²³¹. No calls were assigned if the most likely call was less than a posterior probability of 0.95. Validation of pooling was done by visual inspection of 100 random, shared SNPs for overt batch effects; none were observed. SNPs that had a low call rate ($\leq 90\%$), Hardy-Weinberg p values $< 10^{-6}$ and minor allele frequencies $< 1\%$ were excluded. Samples with call rates $< 95\%$ were removed.

Genotype imputation was used to evaluate the association of one and the same SNP across samples typed on different genotyping platforms. Genotypes were imputed for all polymorphic SNPs (minor allele frequency > 0.01) using either MACH¹⁴⁰ or IMPUTE²⁷³ software, based upon phased autosomal chromosomes of the HapMap CEU Phase II panel (release 22, build 36), orientated on the positive strand. Imputation QC metrics from MACH and IMPUTE were used for filtering out SNPs with low-quality data.

Stage 1 GWAS Meta-Analysis

The estimated inflation factors were 1.176, 1.014, 1.008, 1.006, and 0.989 for ERF, RS-I, RS-II, RS-III, and TwinsUK respectively. SNPs with a minor allele frequency < 0.05 , a MACH r^2 -hat < 0.30 , or a SNPTEST *proper_info* < 0.40 were excluded from the meta-analysis. We obtained the combined results of the 2,224,068 autosomal SNPs, pooling the effect sizes by means of a fixed effects inverse variance meta-analysis as implemented in METAL. Estimated heterogeneity variance and forest plots were generated using the Comprehensive Meta-Analysis¹² software. Regional association plots of the meta-analysis results were obtained with LocusZoom¹⁹³.

Sequenom iPLEX and Taqman Allelic Discrimination genotyping

Genotypes for CHINGFORD, EPIFUND, and HCS were generated using Sequenom iPLEX genotyping and Taqman Allelic Discrimination genotyping. Genomic DNA was extracted from samples of peripheral venous blood according to standard procedures. 1-2 ng genomic DNA was dispensed into 384-wells plates using a Caliper Sciclone ALH3000 pipetting robot (Caliper LS, Mountain View, CA, USA).

For Sequenom iPLEX genotyping, multiplex PCR assays were designed using Assay Designer on the website (<https://mysequenom.com/tools/genotyping/default.aspx>). For this, sequences containing the SNP site and at least 100 bp of flanking sequence on either side of the SNP were used. Briefly, 2 ng genomic DNA was amplified in a 5 μ l reaction containing 1 \times Taq PCR buffer (Sequenom), 2 mM MgCl₂, 500 μ M each dNTP, 100 nM each PCR primer, 0.5 U Taq (Sequenom). The reaction was incubated at 94°C for 4 minutes followed by 45 cycles of 94°C for 20 seconds, 56°C for 30 seconds, 72°C for 1 minute, followed by 3 minutes at 72°C. Excess dNTPs were then removed from the reaction by incubation with 0.3 U shrimp alkaline phosphatase (Sequenom) at 37°C for 40 minutes followed by 5 minutes at 85°C to deactivate the enzyme. Single primer extension over the SNP was carried out in a final concentration of between 0.731 μ M and 1.462 μ M for each extension primer (depending on the mass of the probe), iPLEX termination mix (Sequenom), 10x iPLEX Buffer Plus and iPLEX enzyme (Sequenom) and cycled using the following program; 94°C for 30 seconds followed by 94°C for 5 seconds, 5 cycles of 52°C for 5 seconds, and 80°C for 5 seconds, the last three steps were repeated 40 times, then 72°C for 3 minutes. The reaction was then desalted by addition of 6 mg clear resin (Sequenom) followed by mixing (15 minutes) and centrifugation (5 min, 3,000rpm) to settle the contents of the tube. The extension product was then spotted onto a 384 well spectroCHIP using the SEQUENOM

MassARRAY Nanodispenser RS1000 before analysis on the MassARRAY Compact System (Sequenom). Data collection was performed using SpectroACQUIRE 3.3.1.13 and clustering was called using TYPER Analyzer 4.0.3.18 (Sequenom). Additionally to ensure data quality genotypes for each subject were also checked manually.

For Taqman Allelic Discrimination genotyping (Applied Biosystems Inc., Foster City, CA, USA), all SNP assays were available at www.appliedbiosystems.com as pre-designed assays. The PCR reaction mixture included 1-2 ng of genomic DNA in a 2 μ l volume and the following reagents: FAM and VIC probes (200 nM), primers (0.9 μ M), 2x Taqman PCR master mix (Applied Biosystems Inc., Foster City, CA, USA). Reagents were dispensed in a 384-well plate using the Deerac Equator NS808 (Deerac Fluidics, Dublin, Ireland). PCR cycling reaction were performed in 384 wells PCR plates in an ABI 9700 PCR system (Applied Biosystems Inc., Foster City, CA, USA) and consisted of initial denaturation for 15 minutes at 95° C, and 40 cycles with denaturation of 15 seconds at 95° C and annealing and extension for 60 seconds at 60° C. Results were analyzed by the ABI Taqman 7900HT using the sequence detection system 2.22 software (Applied Biosystems Inc., Foster City, CA, USA).

RNA isolation and real-time PCR for mRNA quantitation

Total RNA was isolated with the Trizol (Invitrogen, Paisley, UK) method and 1 μ g of total RNA was used to synthesize cDNA with SuperScript Reverse Transcriptase (Invitrogen; carrageenan experiment) or iScript™ Select cDNA Synthesis Kit (Invitrogen; CFA experiment) using random hexamers.

Using quantitative PCR, mRNA levels of Cct5 and Fam173b were measured in the spinal cord and the DRG. The real-time PCR reaction with SYBR green Master mix (Bio-Rad, Alphen aan den Rijn, the Netherlands) was performed on the iQ5 Real-Time PCR Detection System (BioRad; carrageenan experiment) or Mastercycler ep realplex (Eppendorf; CFA experiment). For both experiments, the gene expression levels were normalized for Gapdh and β -actin expression levels (housekeeping genes). We used the following primers:

- Cct5 forward: GTCTCATGGGGCTTGAGG, reverse: GTCCGCATTGTGTTTGCTAC.
- Fam173b forward: TGGTGTGCCCCAGATGAT, reverse: TGCCCTCTCCAGTGGTGT.
- Gapdh forward: TGAAGCAGGCATCTGAGGG, reverse: CGAAGGTGGAAGAGTGGGAG.
- β -actin forward: AGAGGGAAATCGTGCGTGAC, reverse: CAATAGTGATGACCTGGCCGT.

We designed the primers to be intron-spanning thereby targeting the first two exons of Cct5 and the last two exons of Fam173b. The thermocycling profile of amplification was 10 min at 95°C, 40 cycles of 15s at 95°C and 1 min at 60°C, 1 min at 95°C, and 2 min at 65°C, followed by a final meltcurve analysis.

Supplementary Figures

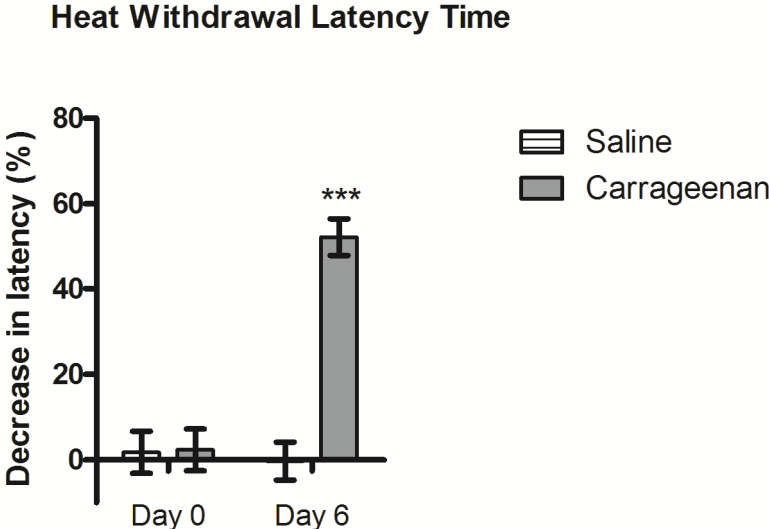


Figure S6.1A: Heat withdrawal latency time measurements at day 0 and day 6 after intraplantar carrageenan (n=4) or saline (n=4) injection. The latency time was measured using the Hargreaves Test. Data are expressed as means ± SEM. *** = p<0.0001.

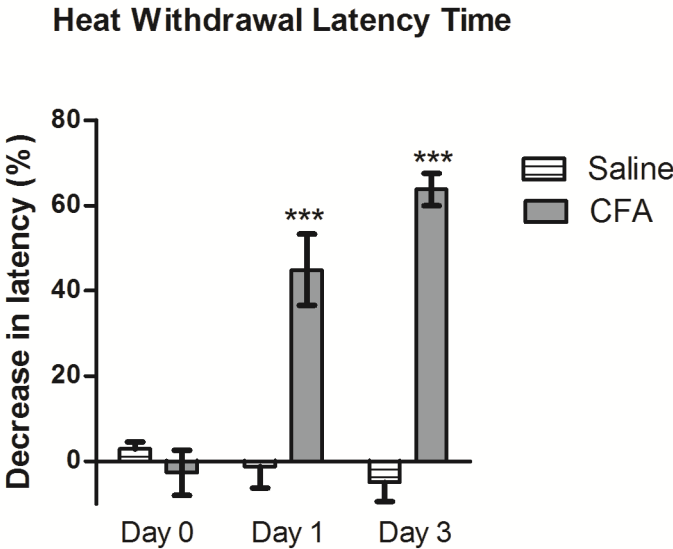


Figure S6.1B: Heat withdrawal latency time measurements at day 0, day 1, and day 3 after intraplantar Complete Freund's Adjuvant (CFA) (n=4) or saline (n=4) injection. The latency time was measured using the Hargreaves Test. Data are expressed as means ± SEM. *** = p<0.0001.

Table S6.1. Pain assessment methods according to the different studies.

Study	Method	Areas of the body checked							Duration of pain*			
		Back	Elbow	Foot	Hand	Hip	Knee	Neck		Shoulder	Others	
Stage 1	ERF study	Homunculus (drawing circles)	yes	yes	yes	yes	yes	yes	yes	no	> half of the days during last 6 wks	
	RS-I	Homunculus (drawing circles)	yes	yes	yes	yes	yes	yes	yes	no	> half of the days during last 6 wks	
	RS-II	Homunculus (drawing circles)	yes	yes	yes	yes	yes	yes	yes	no	> half of the days during last 6 wks	
	RS-III	Homunculus (drawing circles)	yes	yes	yes	yes	yes	yes	yes	no	> half of the days during last 6 wks	
	TWINSUK	Questionnaire	yes [‡]	no [‡]	yes [‡]	yes [‡]	no [‡]	yes [‡]	yes [‡]	yes [‡]	arm, leg, chest [‡]	> 1 week during the last 3 months
Stage 2a	1958BC	Homunculus (shading areas)	yes [‡]	yes [‡]	yes [‡]	yes [‡]	yes [‡]	yes [‡]	yes [‡]	yes [‡]	>=3 months	
	AGES	Questionnaire	yes	no	yes, (not s.s.) [°]	yes, (not s.s.) [°]	yes	yes	no	no	> 1 month during last year	
	DSDBAG	Homunculus (shading areas)	yes [‡]	yes [‡]	yes [‡]	yes [‡]	yes [‡]	yes [‡]	yes [‡]	yes [‡]	>=3 months	
	FOA	Homunculus (shading areas)	yes	yes	yes (incl. indiv. joints) [#]	yes (incl. indiv. joints) [#]	yes	yes	yes	ankle, wrist	"pain on most days" [°]	
	GARP	Questionnaire	yes	yes	no	yes	yes	yes	yes	no	not asked	
	SHIP	Questionnaire	yes [‡]	yes [‡]	yes [‡]	yes [‡]	yes [‡]	yes [‡]	yes [‡]	yes [‡]	head, face, arm, abdomen, pelvic [‡]	not asked
	Stage 2b	CHINGFORD	Joint Symptom Questionnaire	yes	no	no	yes	yes	yes	yes	no	not asked
EPIFUND		Homunculus (shading areas)	yes [‡]	yes [‡]	yes [‡]	yes [‡]	yes [‡]	yes [‡]	yes [‡]	yes [‡]	>=3 months	
HCS		Homunculus (shading areas)	yes [‡]	yes [‡]	yes [‡]	yes [‡]	no [‡]	yes [‡]	yes [‡]	no [‡]	"pain lasting most days of the month over the last year" [°] – extra question: pain lasted > 3 months?	

* If available, the duration of pain criteria was used; # Incl. indiv. joints: the individual joints were scored; ° Not s.s.: information about this joint was not side specific. ‡ Not joint specific.

ERF study = Erasmus Rucphen Family study; RS = Rotterdam Study; TwinsUK = The UK Adult Twin Registry; 1958BC = 1958 Birth Cohort; AGES = Age, Gene/Environment Susceptibility study Reykjavik; CHINGFORD = Chingford 1000 Women Study; DSDBAG = Dyne Steel DNA Bank for Ageing and Cognition; EPIFUND = Epidemiological study of Functional Disorders study; FOA = Framingham Osteoarthritis Study; GARP = Genetics Osteoarthritis and Progression study Leiden; HCS = Hertfordshire Cohort Study. SHIP = Study of Health In Pomerania.

Table S6.2. Study design, number of cases and controls, and sample quality control for the Stage 1 GWAS cohorts.

Study	Study design		Total sample size (N)	Sample QC		Number of samples in the analyses	References
	Short name	Full name		Call rate	Other exclusions		
ERF study	Erasmus Rucphen Family study	Family Based Cohort	2300	> 95%	1) Excess heterozygosity based on FDR 2) Ethnic outliers 3) Gender mismatch 4) Missing phenotype	149 cases, 665 controls	3
RS-I	Rotterdam Study I	Population Based Cohort	7983	≥ 97.5%	1) Gender mismatch with typed Xlinked markers; 2) Excess autosomal heterozygosity > 0.336~FDR>0.1%; 3) Duplicates and/or 1st or 2nd degree relatives using IBS probabilities > 97% from PLINK; 4) Ethnic outliers using IBS distances > 3SD from PLINK; 5) Missing pain, age, and BMI information.	563 cases, 1892 controls	95
RS-II	Rotterdam Study II	Population Based Cohort	3011	≥ 97.5%	1) Gender mismatch with typed X-linked markers; 2) Excess autosomal heterozygosity ($F < -0.055$); 3) Duplicates and/or 1st degree relatives using IBD piHAT >40% from PLINK; 4) Ethnic outliers using IBS distances > 4SD mean HapMap CEU cluster from PLINK; 5) Missing pain, age, and BMI information.	110 cases, 668 controls	95
RS-III	Rotterdam Study III	Population Based Cohort	3932	≥ 97.5%	1) Gender mismatch with typed Xlinked markers; 2) Excess autosomal heterozygosity ($F < -0.055$); 3) Duplicates and/or 1st degree relatives using IBD piHAT >40% from PLINK; 4) Ethnic outliers IBS distances > 4SD mean HapMap CEU cluster from PLINK; 5) Missing pain, age, and BMI information.	85 cases, 868 controls	95
TwinsUK	UK Adult Twin Registry	Twins Based Cohort	5687	≥ 95%	1) Heterozygosity <33% or >67%; 2) Ethnic outliers; 3) Related individuals and duplicates; 4) Missing pain, age, and BMI information.	401 cases, 1698 controls	221,222

ERF study = Erasmus Rucphen Family study; RS = Rotterdam Study; TwinsUK = The UK Adult Twin Registry.

Table S6.3. Information on genotyping methods, quality control of SNPs, and imputation for the Stage 1 GWAS cohorts.

Cohort	Genotyping					Inclusion Criteria			Imputation	
	Platform	Genotype Calling Algorithm	Inclusion Criteria			SNPs that met QC criteria	Imputation Software	Inclusion Criteria		
			MAF	Callrate	P value for HWE			MAF	Imputation Score	Quality
ERF study	Illumina 318K, 370K, Affymetrix 250K	BRLMM, BeadStudio	>0.5%	>95%	>10 ⁻⁰⁶	NA	MACH	>0%	$r^2\text{-hat} \geq 0.30$	
RS-I	Illumina / HumanHap 550K V.3, Illumina / HumanHap 550K V.3 DUO;	BeadStudio Genecall	≥1%	≥97.5%	>10 ⁻⁰⁶	512,349	MACH	≥0%	(O/E) σ^2 ratio≥0.1 $r^2\text{-hat} \geq 0.30$	
RS-II	Illumina / HumanHap 550 V.3 DUO; Illumina / HumanHap 610 QUAD	Genomestudio Genecall	≥1%	≥97.5%	>10 ⁻⁰⁶	466,389	MACH	≥1%	(O/E) σ^2 ratio≥0.1 $r^2\text{-hat} \geq 0.30$	
RS-III	Illumina / HumanHap 610 QU	Genomestudio Genecall	≥1%	≥97.5%	>10 ⁻⁰⁶	514,073	MACH	≥1%	(O/E) σ^2 ratio≥0.1 $r^2\text{-hat} \geq 0.30$	
TwinsUK	Illumina / HumanHap 300 & 550	Illuminus	≥1%	≥95.0%	>10 ⁻⁰⁶	295,702	IMPUTE	>0%	proper-info ≥ 0.40	

ERF study = Erasmus Rucphen Family study; RS = Rotterdam Study; TwinsUK = The UK Adult Twin Registry.

Table S6.4. Study design, number of cases and controls, and sample quality control for the Stage 2 cohorts.

Study	Short name	Full name	Study design	Total sample size (N)	Sample QC		Number of samples in the analyses	References
					Call Rate	Other exclusions		
1958BC		National Child Development (1958 Birth Cohort) Study	Prospective Birth Cohort	4958	≥97%	1) Autosomal heterozygosity 2) Non-Caucasian 3) Average difference in probe intensities across SNPs 4) Individuals with >5% IBD 5) Gender mismatch 6) >10% discordance upon repeated genotyping 7) Missing phenotype	315 cases, 2206 controls	94,191
AGES		Age, Gene Environment Susceptibility Reykjavik Study	Population Based Cohort	3219	≥97%	1) Sample failure 2) Genotype mismatch with reference panel 3) Sex mismatch	173 cases, 1204 controls	90
DSDBAG		Dyne Steel DNA Bank for Ageing and Cognition	Population Based Cohort	6542	>95%	1) Gender mismatch 2) IBD sharing >0.25 3) Non-Caucasians by multi-dimensional scaling	81 cases, 219 controls	196
FOA		The Framingham Osteoarthritis Study	Population Based Cohort	4792	≥97%	1) Subject heterozygosity > ± 5 SDs from the mean 2) Missing pain, age, and BMI information	384 cases, 814 controls	67
GARP		Genetics osteoArthritis and Progression Study	Case Based Cohort	384	>99%	NA	67 cases, 925 RS controls	207
SHIP		Study of Health In Pomerania	Population Based Cohort	4081	>92%	1) Duplicate samples (by IBS) 2) Reported/genotyped gender mismatches	183 cases, 589 controls	113,239
CHINGFORD		Chingford Study	Population Based Cohort	831	NA	1) Missing phenotype information.	48 cases, 337 controls	91,92
EPIFUND		Epidemiological study of FUNCTIONal Disorders	Population Based Cohort	6290	>95%	None	139 cases, 503 controls	97
HCS		Hertfordshire Cohort Study	Population Based Cohort	1073	>95%	Missing phenotype information.	90 cases, 2117 controls	227

Table S6.5. Information on genotyping methods, quality control of SNPs, and imputation for the Stage 2 cohorts.

Cohort	Genotyping				Inclusion Criteria			SNPs that met our replication QC criteria		Imputation	
	Platform	Genotype Calling Algorithm	Inclusion Criteria		p-value for HWE	MAF	Call rate	MAF	Imputation Software	Inclusion Criteria	
			MAF	Call rate						MAF	Imputation Quality Score
1958BC	Affymetrix v6.0 (WTCCC2), Illumina 1.2M chip (WTCCC2), and Illumina 550k (T1DGC)	Chiamo software (adapted for Affymetrix 6.0 SNP data) and Illuminus	>5%	≥ 98%	>0.05	>1%	≥ 97%	2 SNPs + 7 proxy SNPs	NA	NA	NA
AGES	Illumina 370 CNV BeadChip	BeadStudio	≥ 1%	≥97%	>10 ⁻⁶	≥ 1%	≥97%	10	MACH	>0%	r2-hat ≥ 0.30
DSDBAG	Illumina610-Quadv1 chip	Genomestudio	≥1%	≥98%	>10 ⁻³	≥1%	≥98%	10	MACH	>0%	r ² -hat ≥ 0.30
FOA	Affymetrix 500K and	BRLMM	≥1%	≥97%	≥10 ⁻⁶	≥1%	≥97%	10	MACH	≥1%	r2-hat ≥ 0.3
GARP	Illumina Human660W	Genome studio	>5%	>98%	>0.001	>5%	>98%	10	IMPUTE	>5%	proper-info ≥ 0.85
SHIP	Affymetrix SNP Array 6.0	Birdseed2	≥ 0%	≥ 0%	≤ 1	≥ 0%	≥ 0%	10	IMPUTE v0.5.0	≥ 0%	proper_info ≤ 1
CHINGFORD	Sequenom iPLEX and	Taqman / Sequenom	NA	≥95%	>0.05	NA	≥95%	10	NA	NA	NA
EPIFUND	Sequenom iPLEX	Sequenom	NA	≥95%	>0.05	NA	≥95%	1 SNP +	NA	NA	NA
HCS	Taqman Allelic Discrimination	Taqman	NA	NA	NA	NA	NA	5	NA	NA	NA

1958BC = 1958 Birth Cohort; AGES = Age, Gene/Environment Susceptibility study Reykjavik; CHINGFORD = Chingford 1000 Women Study; DSDBAG = Dyne Steel DNA Bank for Ageing and Cognition; EPIFUND = Epidemiological study of Functional Disorders study; FOA = Framingham Osteoarthritis Study; GARP = Genetics Osteoarthritis and Progression study Leiden; HCS = Hertfordshire Cohort Study. SHIP = Study of Health In Pomerania.

Table S6.6. Genotyped SNPs for replication.

Study	rs13361160	rs12132674	rs7680363	rs7835968	rs2249104	rs17796312	rs4837492	rs11606304	rs524513	rs8065610
1958BC	P: rs1508850	P: rs2843016	P: rs12511202	P: rs7830100	P: rs3858511	P: rs12609590	G	NG	P: rs3895875	G
AGES	I	I	I	I	I	I	I	I	I	G
CHINGFORD	G	G	G	G	G	G	G	G	G	G
DSDBAG	I	I	I	I	I	I	G	I	I	G
EPIFUND	G	P: rs2843016	NG	NG	NG	NG	NG	NG	NG	NG
FOA	I	I	I	I	I	I	I	I	I	I
GARP	I	I	I	I	I	I	G	I	I	G
HCS	G	G	G	NG	NG	NG	NG	G	NG	G
SHIP	I	I	G	I	I	I	G	I	I	G

G = Genotyped, I = Imputed, NG = Not Genotyped, P = Proxy Genotyped. The rs-number called behind P gives the used proxy.

1958BC = 1958 Birth Cohort; AGES = Age, Gene/Environment Susceptibility study Reykjavik; CHINGFORD = Chingford 1000 Women Study; DSDBAG = Dyne Steel DNA Bank for Ageing and Cognition; EPIFUND = Epidemiological study of Functional Disorders study; FOA = Framingham Osteoarthritis Study; GARP = Genetics Osteoarthritis and Progression study Leiden; HCS = Hertfordshire Cohort Study. SHIP = Study of Health In Pomerania.

Table S6.7. Mean age and BMI for all participating studies

Cohort	Mean and Standard Deviation of the covariates age and BMI					
	Age (y)			BMI (kg/m ²)		
	Cases	Controls	P-value	Cases	Controls	P-value
ERF study	51.4 (+/- 11.2)	45.3 (+/- 14.3)	1.10E-06	27.1 (+/- 5.1)	26.1 (+/- 4.6)	1.30E-02
RS-I	68.9 (+/- 8.6)	69.5 (+/- 9.0)	1.48E-01	27.4 (+/- 4.3)	26.6 (+/- 4.1)	1.00E-06
RS-II	67.2 (+/- 7.6)	68.0 (+/- 7.5)	2.66E-01	29.0 (+/- 5.0)	27.7 (+/- 4.3)	3.88E-03
RS-III	57.8 (+/- 7.8)	56.2 (+/- 5.8)	1.85E-02	28.6 (+/- 5.2)	27.4 (+/- 5.0)	4.23E-02
TwinsUK	55.4 (+/- 11.6)	51.1 (+/- 13.9)	6.50E-10	26.6 (+/- 5.4)	24.7 (+/- 4.3)	2.70E-11
1958BC	NA	NA	NA	27.7 (+/- 6.1)	26.7 (+/- 5.3)	4.00E-3
AGES	75.7 (+/- 5.2)	76.6 (+/- 5.6)	6.36E-1	28.6 (+/- 4.8)	27.2 (+/- 4.8)	1.44E-5
DSDBAG	79.7 (+/- 4.7)	80.3 (+/- 5.7)	4.09E-1	NA	NA	NA
FOA	61.0 (+/- 11.3)	58.5 (+/- 13.6)	2.00E-3	28.6 (+/- 5.8)	25.6 (+/- 4.8)	2.00E-16
GARP	58.5 (+/- 6.9)	57.7 (+/- 1.4)	7.00E-3	28.1 (+/- 6.1)	26.3 (+/- 5.9)	1.40E-2
SHIP	60.7 (+/- 12.9)	56.7 (+/- 13.4)	1.30E-3	29.3 (+/- 5.41)	27.6 (+/- 5.136)	5.00E-5
CHINGFORD	57.2 (+/- 5.9)	56.5 (+/- 8.7)	5.89E-1	27.1 (+/- 4.6)	26.3 (+/- 4.5)	3.29E-1
EPIFUND	50.9 (+/- 8.8)	48.5 (+/- 10.4)	1.37E-2	NA	NA	NA
HCS	66.8 (+/- 2.7)	66.4 (+/- 2.8)	4.88E-1	29.7 (+/- 6.1)	26.8 (+/- 4.5)	1.69E-5

ERF study = Erasmus Rucphen Family study; RS = Rotterdam Study; TwinsUK = The UK Adult Twin Registry; 1958BC = 1958 Birth Cohort; AGES = Age, Gene/Environment Susceptibility study Reykjavik; CHINGFORD = Chingford 1000 Women Study; DSDBAG = Dyne Steel DNA Bank for Ageing and Cognition; EPIFUND = EPIdemiological study of FUNCTIONal Disorders study; FOA = Framingham Osteoarthritis Study; GARP = Genetics OsteoArthritis and Progression study Leiden; HCS = Hertfordshire Cohort Study. SHIP = Study of Health In Pomerania.

Table S6.8. Information on statistical analysis for the Stage 1 GWAS cohorts.

Cohort	Association Analyses		
	SNPs in meta-analysis	Analysis Software	References Analysis Software
ERF study	2,463,846	ProbABEL	4
RS-I	2,542,336	GRIMP (MACH2DAT)	65,140
RS-II	2,536,671	GRIMP (MACH2DAT)	65,140
RS-III	2,533,563	GRIMP (MACH2DAT)	65,140
TwinsUK	2,460,943	PLINK	194

ERF study = Erasmus Rucphen Family study; RS = Rotterdam Study; TwinsUK = The UK Adult Twin Registry.

Table S6.9: 29 proxy SNPs which are in LD with rs13361160 ($r^2 > 0.1$).

SNP	Proxy	Distance	r^2	D'	Gene Variant	GeneName	Possible eQTL-effect?
rs13361160	rs1045392	56655	0.216	0.892	3'UTR	FAM173B	
rs13361160	rs1045369	57016	0.216	0.892	3'UTR	FAM173B	
rs13361160	rs17294394	58695	0.105	0.329	Intronic	FAM173B	
rs13361160	rs4557374	59018	0.144	1.000	Intronic	FAM173B	
rs13361160	rs7716217	59785	0.216	0.892	Intronic	FAM173B	
rs13361160	rs7716565	60006	0.135	1.000	Intronic	FAM173B	
rs13361160	rs7716851	60151	0.144	1.000	Intronic	FAM173B	
rs13361160	rs7736719	60169	0.144	1.000	Intronic	FAM173B	
rs13361160	rs6887347	61868	0.215	1.000	Intronic	FAM173B	
rs13361160	rs16884328	62099	0.109	0.534	Intronic	FAM173B	
rs13361160	rs6887590	62124	0.144	1.000	Intronic	FAM173B	
rs13361160	rs6888157	62153	0.144	1.000	Intronic	FAM173B	
rs13361160	rs6880482	64235	0.144	1.000	Intronic	FAM173B	
rs13361160	rs2292264	65667	0.186	1.000	Intronic	FAM173B	
rs13361160	rs7710415	65930	0.135	1.000	Intronic	FAM173B	
rs13361160	rs16884348	66129	0.154	1.000	Intronic	FAM173B	yes: r^2 with eQTL-SNP rs2445871 = 0.872
rs13361160	rs12653481	67213	0.186	1.000	Intronic	FAM173B	
rs13361160	rs2438652	69438	0.165	1.000	Non-synonymous coding	FAM173B	yes: r^2 with eQTL-SNP rs2445871 = 0.818
rs13361160	rs2445871	70170	0.135	1.000	Intronic	FAM173B	yes: rs2445871 is an eQTL SNP
rs13361160	rs2607326	70968	0.134	0.851	Intronic	FAM173B	
rs13361160	rs2607328	71623	0.125	1.000	Intronic	FAM173B	
rs13361160	rs2607298	82296	0.104	0.639	Intronic	CCT5	yes: r^2 with eQTL-SNP rs2244964 = 0.953
rs13361160	rs2445867	83341	0.104	0.639	Intronic	CCT5	yes: r^2 with eQTL-SNP rs2244964 = 0.953
rs13361160	rs1042392	86338	0.159	0.854	Synonymous coding	CCT5	yes: r^2 with eQTL-SNP rs2244964 = 0.904
rs13361160	rs2028274	86787	0.104	0.639	Intronic	CCT5	yes: r^2 with eQTL-SNP rs2244964 = 0.953
rs13361160	rs2028272	86899	0.111	0.646	Intronic	CCT5	yes: r^2 with eQTL-SNP rs2244964 = 0.909
rs13361160	rs7710938	87070	0.123	0.732	Intronic	CCT5	yes: r^2 with eQTL-SNP rs2244964 = 0.951
rs13361160	rs7729006	87146	0.123	0.732	Intronic	CCT5	yes: r^2 with eQTL-SNP rs2244964 = 0.951
rs13361160	rs2438653	89550	0.104	0.639	Intronic	CCT5	yes: r^2 with eQTL-SNP rs2244964 = 0.953

Table S6.10. Association results of 92 candidate SNPs in the stage 1 GWAS meta-analysis sorted by gene names and P-values. The strongest associated SNPs ($p < 0.01$) were shaded ($p < 0.01$).

MarkerName	Gene	Allele1	Allele2	Freq A1	OR	95%CI	P-value
rs2020917	COMT	t	c	0.266	0.856	(0.772-0.948)	2.97E-03
rs5993883	COMT	t	g	0.496	1.142	(1.046-1.247)	3.05E-03
rs5746846	COMT	c	g	0.501	1.098	(1.005-1.200)	3.85E-02
rs1544325	COMT	a	g	0.457	1.087	(0.995-1.187)	6.38E-02
rs2239393	COMT	a	g	0.603	1.081	(0.986-1.184)	9.51E-02
rs4818	COMT	c	g	0.604	1.081	(0.986-1.184)	9.66E-02
rs4646312	COMT	t	c	0.604	1.078	(0.984-1.181)	1.07E-01
rs165728	COMT	t	c	0.935	0.812	(0.615-1.071)	1.41E-01
rs4680	COMT	a	g	0.532	1.057	(0.963-1.162)	2.44E-01
rs4633	COMT	t	c	0.536	1.048	(0.957-1.147)	3.09E-01
rs174699	COMT	t	c	0.929	0.860	(0.632-1.172)	3.41E-01
rs2097903	COMT	a	t	0.500	0.961	(0.875-1.056)	4.08E-01
rs165774	COMT	a	g	0.313	1.034	(0.933-1.146)	5.21E-01
rs5993882	COMT	t	g	0.768	1.027	(0.924-1.143)	6.20E-01
rs174674	COMT	a	g	0.274	1.020	(0.917-1.134)	7.19E-01
rs10483639	GCH1	c	g	0.203	0.846	(0.755-0.948)	3.84E-03
rs752688	GCH1	t	c	0.202	0.846	(0.755-0.948)	3.94E-03
rs4411417	GCH1	t	c	0.798	1.181	(1.055-1.323)	4.00E-03
rs8007267	GCH1	t	c	0.178	0.890	(0.790-1.001)	5.23E-02
rs3783641	GCH1	a	t	0.192	0.902	(0.803-1.013)	8.15E-02
rs599548	OPRM1	a	g	0.142	1.189	(1.050-1.346)	6.41E-03
rs558025	OPRM1	a	g	0.739	1.085	(0.979-1.203)	1.19E-01
rs1799971	OPRM1	a	g	0.873	0.907	(0.796-1.033)	1.42E-01
rs563649	OPRM1	t	c	0.091	1.088	(0.934-1.268)	2.78E-01
rs2075572	OPRM1	c	g	0.551	1.051	(0.957-1.154)	3.00E-01
rs10485171	CNR1	a	g	0.530	1.104	(1.009-1.207)	3.09E-02
rs1078602	CNR1	a	g	0.485	0.941	(0.861-1.030)	1.88E-01
rs6454674	CNR1	t	g	0.705	0.957	(0.869-1.055)	3.81E-01
rs2400707	ADRB2	a	g	0.444	0.909	(0.831-0.994)	3.68E-02
rs1042714	ADRB2	c	g	0.548	1.117	(1.000-1.246)	4.90E-02
rs12654778	ADRB2	a	g	0.367	1.072	(0.978-1.175)	1.39E-01
rs1042713	ADRB2	a	g	0.363	1.070	(0.976-1.173)	1.48E-01
rs17778257	ADRB2	a	t	0.630	0.941	(0.859-1.032)	1.96E-01
rs1042718	ADRB2	a	c	0.162	1.027	(0.912-1.156)	6.62E-01

MarkerName (II)	Gene	Allele1	Allele2	Freq A1	OR	95%CI	P-value
rs8192619	TAAR1	a	g	0.056	0.732	(0.517-1.035)	7.77E-02
rs12584920	HTR2A	t	g	0.187	0.903	(0.804-1.015)	8.75E-02
rs4941573	HTR2A	a	g	0.578	0.975	(0.891-1.066)	5.72E-01
rs6313	HTR2A	a	g	0.419	1.019	(0.932-1.114)	6.77E-01
rs17289394	HTR2A	a	g	0.400	0.992	(0.906-1.085)	8.55E-01
rs10502058	GRIA4	t	c	0.884	0.888	(0.774-1.019)	9.18E-02
rs2510177	GRIA4	a	g	0.090	1.140	(0.976-1.331)	9.72E-02
rs10895837	GRIA4	t	c	0.116	1.122	(0.977-1.287)	1.03E-01
rs642544	GRIA4	t	g	0.583	0.960	(0.878-1.051)	3.78E-01
rs17104711	GRIA4	a	g	0.084	1.039	(0.887-1.217)	6.38E-01
rs8065080	TRPV1	t	c	0.618	0.929	(0.848-1.017)	1.09E-01
rs1143623	IL-1B	c	g	0.721	0.923	(0.836-1.019)	1.12E-01
rs16944	IL-1B	a	g	0.344	1.076	(0.980-1.182)	1.25E-01
rs12621220	IL-1B	t	c	0.277	1.080	(0.979-1.192)	1.26E-01
rs1143627	IL-1B	a	g	0.656	0.937	(0.853-1.029)	1.74E-01
rs1143634	IL-1B	a	g	0.244	0.952	(0.856-1.058)	3.61E-01
rs1143643	IL-1B	t	c	0.336	0.987	(0.897-1.086)	7.91E-01
rs1143633	IL-1B	t	c	0.337	0.988	(0.898-1.087)	8.03E-01
rs3917368	IL-1B	t	c	0.335	0.990	(0.901-1.089)	8.42E-01
rs1800469	TGFb	a	g	0.299	0.931	(0.843-1.029)	1.61E-01
rs11661134	MC2R	a	g	0.069	0.859	(0.692-1.067)	1.70E-01
rs11627241	SERPINA6	t	c	0.257	0.931	(0.839-1.033)	1.78E-01
rs746530	SERPINA6	a	g	0.327	0.940	(0.854-1.034)	2.01E-01
rs941601	SERPINA6	t	C	0.135	0.954	(0.837-1.087)	4.76E-01
rs1998056	SERPINA6	c	g	0.413	1.019	(0.931-1.115)	6.86E-01
rs8022616	SERPINA6	a	g	0.892	1.005	(0.867-1.165)	9.48E-01
rs1800871	IL-10	a	g	0.220	0.931	(0.834-1.038)	1.99E-01
rs1800872	IL-10	t	g	0.221	0.931	(0.834-1.039)	2.02E-01
rs1800896	IL-10	t	c	0.492	0.968	(0.886-1.057)	4.73E-01
rs1800890	IL-10	a	t	0.600	1.001	(0.910-1.103)	9.77E-01
rs1875999	CRHBP	t	c	0.683	0.948	(0.863-1.041)	2.61E-01
rs17561	IL-1A	a	c	0.304	0.950	(0.862-1.047)	3.02E-01
rs1800587	IL-1A	a	g	0.304	0.951	(0.862-1.048)	3.08E-01

MarkerName (III)	Gene	Allele1	Allele2	Freq A1	OR	95%CI	P-value
rs3813034	SLC6A4	a	c	0.538	1.044	(0.955-1.141)	3.46E-01
rs11842874	MCF2L	a	g	0.931	1.098	(0.903-1.335)	3.51E-01
rs2239704	TNF / LTA	a	c	0.387	0.957	(0.872-1.050)	3.54E-01
rs6746030	SCN9A	a	g	0.140	1.058	(0.932-1.202)	3.81E-01
rs454078	IL-1RN	a	t	0.730	0.964	(0.874-1.064)	4.72E-01
rs315952	IL-1RN	T	c	0.705	0.990	(0.899-1.090)	8.31E-01
rs1048101	ADRA1A	a	g	0.562	0.971	(0.889-1.061)	5.19E-01
rs1946518	IL-18	t	g	0.397	1.028	(0.940-1.125)	5.38E-01
rs1799945	HFE	c	g	0.858	1.035	(0.910-1.177)	6.01E-01
rs2842003	RGS4	t	g	0.428	1.021	(0.929-1.123)	6.65E-01
rs6280	DRD3	t	c	0.676	1.021	(0.929-1.123)	6.69E-01
rs1020759	NFKb	t	c	0.402	0.980	(0.896-1.073)	6.69E-01
rs4129256	TAAR2	a	g	0.203	1.024	(0.917-1.143)	6.72E-01
rs2745428	TAAR2	a	c	0.788	0.993	(0.892-1.106)	9.03E-01
rs5275	PTGS2	a	g	0.671	1.020	(0.929-1.121)	6.75E-01
rs4906902	GABRB3	a	g	0.827	1.026	(0.910-1.156)	6.80E-01
rs2069827	IL-6	t	g	0.058	0.960	(0.781-1.179)	6.96E-01
rs1800795	IL-6	c	g	0.409	1.004	(0.916-1.099)	9.39E-01
rs1800797	IL-6	a	g	0.399	0.997	(0.909-1.093)	9.44E-01
rs1554606	IL-6	t	g	0.428	0.998	(0.913-1.091)	9.72E-01
rs2069845	IL-6	a	g	0.572	1.001	(0.916-1.095)	9.76E-01
rs7911	GBP1	a	g	0.637	0.994	(0.907-1.090)	9.05E-01
rs6265	BDNF	t	c	0.198	1.006	(0.900-1.124)	9.22E-01

Acknowledgements

This study was funded by the European Commission (HEALTH-F2-2008-201865, GEFOS; HEALTH-F2-2008 35627, TREAT-OA), the Netherlands Organisation for Scientific Research (NWO) Investments (nr. 175.010.2005.011, 911-03-012), the Netherlands Consortium for Healthy Aging (NCHA), the Netherlands Genomics Initiative (NGI) / Netherlands Organisation for Scientific Research (NWO) project nr. 050-060-810 and VIDI grant 917103521, and a Rubicon fellowship; Research Institute for Diseases in the Elderly (RIDE) grant 94800012; The Wellcome Trust and Arthritis Research UK.

1958BC (British 1958 birth cohort) – Phenotype data and sample collection for the Biomedical sweep was supported by the Medical Research Council, UK (Health of the Public initiative grant G0000934). Genotype data was provided by the Wellcome Trust Case-Control Consortium (WTCCC) and the Type 1 Diabetes Genetics Consortium (T1DGC). A full list of the investigators who contributed to generation of the WTCCC data is available from www.wtccc.org.uk; funding was provided by the Wellcome Trust under award 076113. T1DGC is collaborative clinical study sponsored by the National Institute of Diabetes and Digestive and Kidney Diseases (NIDDK), National Institute of Allergy and Infectious Diseases (NIAID), National Human Genome Research Institute (NHGRI), National Institute of Child Health and Human Development (NICHD), and Juvenile Diabetes Research Foundation International (JDRF) and supported by U01 DK062418.

AGES (Age, Gene/Environment Susceptibility-Reykjavik Study) - The AGES Reykjavik Study has been funded by NIH contracts N01-AG-12100 and Z01-AG-007380, the NIA Intramural Research Program, Hjartavernd (the Icelandic Heart Association), and the Althingi (the Icelandic Parliament). The study is approved by the Icelandic National Bioethics Committee, (VSN: 00-063) and the Data Protection Authority. The researchers are indebted to the participants for their willingness to participate in the study.

CHINGFORD (The Chingford Study) - We would like to thank all the participants of the Chingford Women Study and Maxine Daniels and Dr Alan Hakim for their time and dedication and Arthritis Research UK for their funding support to the study and the Oxford NIHR Musculoskeletal Biomedical Research Unit for funding contributions.

DSDBAC (The Dyne Steel DNA Bank for Ageing and Cognition) – Genotyping of this cohort was supported by the BBSRC and the collection of phenotype data used in this study was supported by AgeUK and Arthritis Research UK. Ethical approval was obtained from the University of Manchester.

EPIFUND (The EPIdemiological study of FUNctional Disorderes) – The EPIFUND study was supported by Arthritis Research UK (17552) and was conducted with the approval of the local research ethics committee and the University of Manchester. The researchers would like to thank the participants and staff at the three general practices who contributed to the study and administrative and laboratory staff at the Arthritis Research UK Epidemiology Unit for their contributions to the project.

ERF (Erasmus Rucphen Family) (EUROSPAN) - The genotyping for the ERF study was supported by EUROSPAN (European Special Populations Research Network) and the European Commission FP6 STRP grant (018947; LSHG-CT-2006-01947). The ERF study was further supported by grants from the Netherlands Organisation for Scientific Research, Erasmus MC, the Centre for Medical Systems Biology (CMSB) and the Netherlands Brain Foundation (HersenStichting Nederland). We are grateful to all patients and their relatives, general practitioners and neurologists for their contributions and to Petra Veraart for her help in

genealogy, Jeannette Vergeer for the supervision of the laboratory work and Peter Snijders for his help in data collection.

FOA (The Framingham Osteoarthritis Study) - The study was supported by grants from the National Heart, Lung, and Blood Institute (NHLBI contract N01-HC-25195) and NIH AR47785, AG18393, and AR550127. The researchers thank the study participants and personnel.

GARP (The Genetics osteoarthritis and Progression Study) - This study was supported the Leiden University Medical Centre and the Dutch Arthritis Association. Pfizer Inc., Groton, CT, USA supported the inclusion of the GARP study. The genotypic work was supported by the Netherlands Organization of Scientific Research (MW 904-61-095, 911-03-016, 917 66344 and 911-03-012), Leiden University Medical Centre and the Centre of Medical System Biology and Netherlands Consortium for Healthy Aging both in the framework of the Netherlands Genomics Initiative (NGI). The research leading to these results has received funding from the European Union's Seventh Framework Programme (FP7/2007-2011) under grant agreement n° 259679.

HCS (The Hertfordshire Cohort Study) – This study was funded by the Medical Research Council of Great Britain, Arthritis Research UK, the International Osteoporosis Foundation and the NIHR Nutrition BRU, University of Southampton.

RS (The Rotterdam Study) - The GWA study was funded by the Netherlands Organisation of Scientific Research NWO Investments (nr. 175.010.2005.011, 911-03-012), the Research Institute for Diseases in the Elderly (014-93-015; RIDE2), the Netherlands Genomics Initiative (NGI)/Netherlands Consortium for Healthy Aging (NCHA) project nr. 050-060-810. We thank Pascal Arp, Mila Jhamai, Dr Michael Moorhouse, Marijn Verkerk, and Sander Bervoets for their help in creating the GWAS database. The Rotterdam Study is funded by Erasmus Medical Center and Erasmus University, Rotterdam, Netherlands Organization for the Health Research and Development (ZonMw), the Research Institute for Diseases in the Elderly (RIDE), the Ministry of Education, Culture and Science, the Ministry for Health, Welfare and Sports, the European Commission (DG XII), and the Municipality of Rotterdam. The authors are very grateful to the participants and staff from the Rotterdam Study, the participating general practitioners and the pharmacists. We would like to thank Dr. Tobias A. Knoch, Luc V. de Zeeuw, Anis Abuseiris, and Rob de Graaf as well as their institutions the Erasmus Computing Grid, Rotterdam, The Netherlands, and especially the national German MediGRID and Services@MediGRID part of the German D-Grid, both funded by the German Bundesministerium fuer Forschung und Technology under grants #01 AK 803 A-H and # 01 IG 07015 G for access to their grid resources.

SHIP (The Study of Health in Pomerania) - SHIP is part of the Community Medicine Research net of the University of Greifswald, Germany, which is funded by the Federal Ministry of Education and Research (grants no. 01ZZ9603, 01ZZ0103, and 01ZZ0403), the Ministry of Cultural Affairs as well as the Social Ministry of the Federal State of Mecklenburg-West Pomerania. Genome-wide data have been supported by the Federal Ministry of Education and Research (grant no. 03ZIK012) and a joint grant from Siemens Healthcare, Erlangen, Germany and the Federal State of Mecklenburg- West Pomerania. The University of Greifswald is a member of the 'Center of Knowledge Interchange' program of the Siemens AG. Data analyses were further supported by the DIAB Core project of the German Network of Diabetes.

TwinsUK (The UK Adult Twin Registry) - This study was funded by the Wellcome Trust (Grant ref. 079771); European Community's Seventh Framework Programme (FP7/2007-2013)/grant agreement HEALTH-F2-2008-ENGAGE and the European Union FP-5 GenomEUtwin Project (QLG2-CT-2002-01254) and Framework 6 Project EUroClot. The study also receives support from the National Institute for Health Research (NIHR) comprehensive Biomedical Research

Centre award to Guy's & St Thomas' NHS Foundation Trust in partnership with King's College London. We thank the staff from the TwinsUK, the DNA Collections and Genotyping Facilities at the Wellcome Trust Sanger Institute for sample preparation; Quality Control of the Twins UK cohort for genotyping (in particular Amy Chaney, Radhi Ravindrarajah, Douglas Simpkin, Cliff Hinds, and Thomas Dibling); Paul Martin and Simon Potter of the DNA and Genotyping Informatics teams for data handling; Le Centre National de Génotypage, France, led by Mark Lathrop, for genotyping; Duke University, North Carolina, USA, led by David Goldstein, for genotyping; and the Finnish Institute of Molecular Medicine, Finnish Genome Center, University of Helsinki, led by Aarno Palotie. Nicole Soranzo acknowledges financial support from the Wellcome Trust (Grant 091746/Z/10/Z).

University Medical Center Utrecht - The work of Annemieke Kavelaars is supported by NIH grants RO1 NS074999 and RO1 NS073939.

The authors are very grateful to all study participants, the staff from all studies and the participating physicians and pharmacists.



7

Summary and discussion

Summary

An acute pain response is important to avoid further tissue damage to potentially injurious stimuli. However, after healing of an injury or when an inflammation has resolved, some people develop chronic pain. Chronic pain is present in approximately 19% of the European population²⁰. A recent study has shown that the total number of American people suffering from chronic pain is more than people suffering from diabetes, heart disease and cancer combined¹⁷². Chronic pain is a major clinical problem and there is a great need for effective treatments. Understanding the mechanisms underlying the transition from acute to chronic pain is therefore of great importance. In the studies described in this thesis we investigated various aspects of the transition from acute to chronic inflammatory pain and we specially focused on:

1. GRK2 in microglia/macrophages
2. Underlying neurobiological mechanisms of the transition to chronic pain
3. Potential novel treatments
4. Identification of new potential target genes involved in chronic pain conditions

First, we demonstrated that spinal cord microglia/macrophage GRK2 is reduced during chronic inflammation-induced hyperalgesia. In addition, mice with low GRK2 in peripheral macrophages (LysM-GRK2^{+/-} mice) develop prolonged IL-1 β -induced hyperalgesia. This persistent hyperalgesia is maintained via a loop that involves fractalkine signaling, p38 activation, IL-1 release and persistent spinal microglia/macrophage activity (**chapter 2**). Furthermore, the levels of microRNA-124 (miR-124) in spinal cord microglia from LysM-GRK2^{+/-} mice were decreased after intraplantar IL-1 β . Interestingly, we observed a switch towards a spinal pro-inflammatory M1 phenotype in LysM-GRK2^{+/-} mice. Moreover, miR-124 treatment prevented the transition to IL-1 β -induced persistent pain and normalized the expression of spinal M1/M2 markers in LysM-GRK2^{+/-} mice. In addition, miR-124 treatment reversed persistent carrageenan-induced hyperalgesia and prevented the development of chronic neuropathic pain in wild type (WT) mice. These findings indicate that miR-124 is a novel option for the treatment of chronic pain (**chapter 3**). Next we investigated the contribution of peripheral monocytes/macrophages versus microglia to inflammation-induced hyperalgesia. Surprisingly, GRK2 deficiency in peripheral monocytes/macrophages is sufficient to promote transition from acute to chronic pain, due to the reduced capacity of these cells to produce IL-10 (**chapter 4**). In chapter 5 we developed novel p38 MAPK docking-site targeted inhibitors. Compound FGA-19 yielded the best inhibition of p38 kinase activity *in vitro*. *In vivo*, FGA-19 treatment completely resolved carrageenan-induced persistent hyperalgesia. Thus, FGA-19 is a potential novel candidate for the treatment of persistent inflammatory hyperalgesia (**chapter 5**). In chapter 6, we identified the genomic region encoding CCT5 and FAM173b to be associated with chronic widespread pain. In a murine model of chronic inflammatory pain, we detected increased expression levels of CCT5 and FAM173b in the spinal cord. Overall these data identified CCT5 and FAM173b as potential players in the pathophysiology of chronic pain (**chapter 6**).

Discussion

Activation of microglia in the spinal cord is known to be an important factor in maintaining hyperalgesia. Activated microglia release pro-inflammatory cytokines and chemokines that contribute to central sensitization and consequently to the development of chronic pain^{166,204,250}. Previously, we showed that GRK2 levels are reduced in microglia isolated from spinal cord in rats with neuropathic pain⁶¹. In **chapter 2** we provide evidence that GRK2 is also reduced in spinal microglia in mice with inflammatory-induced hyperalgesia induced by one single injection of a high dose of carrageenan (20 μ l of 2%). Thus in these two models of chronic pain, spinal microglial GRK2 levels are reduced by local injury or inflammation. We hypothesized that the decrease in GRK2 in spinal microglia during ongoing inflammation is associated with the development of chronic pain. To test this hypothesis we used the CRE-Lox system to generate mice with a cell-specific GRK2 reduction. GRK2-lox mice were crossed with mice expressing the Cre enzyme under the specific Lysozyme M (LysM) promoter. The LysM promoter is activated in myeloid cells, like microglia, macrophages and granulocytes. We described that LysM-GRK2^{+/-} mice have a 40%-60% reduction of GRK2 in cultured microglia and freshly isolated macrophages and not in isolated astrocytes (**chapter 2** and ^{61,177}).

In our first experiments we described that a single intraplantar injection of the pro-inflammatory cytokine IL-1 β induces transient hyperalgesia in WT mice (< 24 h), while LysM-GRK2^{+/-} mice develop persistent hyperalgesia for at least 8 days. Subsequently, we demonstrated that granulocytes are not required for the transition from acute to chronic hyperalgesia in LysM-GRK2^{+/-} mice, since granulocyte depletion did not affect inflammation-induced hyperalgesia⁶¹. In addition the prolonged hyperalgesia in LysM-GRK2^{+/-} mice was prevented by an intrathecal injection and reversible by an intraperitoneal injection of the microglia/macrophage inhibitor minocycline (**chapter 2**). On the basis of these results we suggested that GRK2 in microglia/macrophages is crucial for determining the duration of inflammation-induced hyperalgesia. However, recent studies described that resident microglia in the central nervous system (CNS) are in a resting state and that the LysM promoter is not active. Only in activated microglia the LysM gene is upregulated, resulting in the deletion of the preferred lox-targeted gene^{31,157}. In line with the literature, we found that the GRK2 protein and mRNA levels in freshly isolated spinal microglia from WT and LysM-GRK2^{+/-} mice were not different. However, GRK2 levels were reduced for approximately 50% in *peripheral macrophages* from LysM-GRK2^{+/-} mice (**chapter 4**). This was an interesting finding that LysM-GRK2^{+/-} mice have normal microglia GRK2 levels, and we needed to adjust our hypothesis which will be discussed in the paragraph below.

Reduced intracellular GRK2

Peripheral sensory neurons

Many pain signals are first detected by sensory nociceptors. Numerous pain signaling molecules signal through G protein-coupled receptors (GPCRs), such as the chemokine CCL3, the inflammatory stimuli prostaglandin E₂ (PGE₂) and the stress hormone epinephrine (EPI). Mice with reduced GRK2 levels in peripheral sensory neurons (SNS-GRK2^{+/-} mice) have an increased acute pain response after intraplantar carrageenan, CCL3, PGE₂ or EPI injections compared to WT controls^{60,61,245}. However, we demonstrated that the intensity of the acute hyperalgesia after *intraplantar IL-1 β* was not affected in SNS-GRK2^{+/-} mice and, in addition, the duration of hyperalgesia was similar in WT and SNS-GRK2^{+/-} mice (**chapter 2** and ⁶¹). Peripheral IL-1 β injections directly increase the excitability of the neurons via p38 MAPK-dependent activation

downstream of the receptor, leading to a rapid increase in thermal sensitivity via enhancements of TTX-resistant sodium currents. Intraplantar administration of a p38 MAPK inhibitor significantly attenuated the IL-1 β -induced hyperalgesia in WT mice¹¹. Similar results were found in mice with reduced levels of the kinase GRK6. This kinase is also known to play a crucial role in inflammatory pain such as observed in experimental colitis⁵⁹. Moreover, recently we published that IL-1 β -induced hyperalgesia is increased and prolonged in GRK6^{-/-} mice compared to WT mice⁶². Subsequently, the p38 MAPK inhibitor SB239063 also inhibited the magnitude of acute IL-1 β -induced hyperalgesia and partially the duration of hyperalgesia in GRK6^{-/-} mice⁶². Notably, IL-1 β is not a GPCR ligand, so this might explain that we did not see an effect of GRK2 downregulation in sensory neurons on the intensity of acute hyperalgesia.

Next we investigated possible differences between mice with only low GRK2 in sensory neurons or mice with a downregulation of GRK2 in all cells. The duration of carrageenan-, IL-1 β -, CCL3- and PGE2-induced hyperalgesia was shorter in SNS-GRK2^{+/-} mice compared to mice with reduced GRK2 levels in all cell types (GRK2^{+/-}) (reviewed in ¹¹⁹). Only EPI-induced hyperalgesia was prolonged in SNS-GRK2^{+/-} mice to the same extent as in GRK2^{+/-} mice. Interestingly, in LysM-GRK2^{+/-} mice the carrageenan-, IL-1 β - and CCL3-induced hyperalgesia are prolonged to the same extent as in GRK2^{+/-} mice (**chapter 2** and ⁶¹). This indicates that not peripheral sensory neurons, but other cell types have an important role in determining the duration of hyperalgesia.

Astrocytes

The exact role of astrocytes in the regulation of pain is less well studied than in peripheral sensory neurons and microglia. It has been suggested that astrocytes play a role in the maintenance of chronic pain²¹⁰. In **chapter 2**, we examined whether a reduction of GRK2 in GFAP-positive astrocytes (GFAP-GRK2^{+/-}) has an effect on the duration of IL-1 β -induced hyperalgesia. However, there were no differences in the course of IL-1 β -induced hyperalgesia between WT and GFAP-GRK2^{+/-} mice. Similar results were found for the PGE₂-, carrageenan-, EPI- and CCL3- induced hyperalgesia^{61,245}. This suggests that GRK2 in astrocytes does not contribute to the initiation of the prolonged inflammation-induced hyperalgesia. Different results on the role of GRK2 in astrocytes were found by our group in a model of brain damage (hypoxia-ischemia). Here we showed that a 60% reduction of GRK2 in astrocytes significantly reduced the development of brain damage, indicating that low levels of astrocytic GRK2 are beneficial for the neuroprotection of neurons in the developing brain^{176,178}.

Peripheral monocytes/macrophages

Recent findings in models of neuropathic pain suggest that peripheral monocytes/macrophages infiltrate into the CNS where they can exert dual effects: peripheral monocytes/macrophages have been shown to promote repair or to aggravate injury^{120,129,217}. However, the effect of monocyte/macrophage infiltration during inflammation-induced hyperalgesia was still unknown. In **chapter 4**, we described that peripheral monocytes/macrophages regulate inflammation-induced hyperalgesia in a positive way. Depletion of peripheral monocytes/macrophages caused transition from acute to persistent IL-1 β hyperalgesia in WT mice. This finding indicates that monocytes/macrophages are key to preventing the transition to chronic pain after a transient peripheral inflammatory stimulus. In a model of nerve injury-induced allodynia, clodronate-liposome mediated monocyte/macrophage depletion alleviated allodynia¹⁴⁴. However, in other chronic pain models depletion of monocytes/macrophages had no effect^{18,160,211}.

On the basis of our results described above, we hypothesized that normal GRK2 levels in peripheral monocytes/macrophages are crucial to promote resolution of IL-1 β -induced hyperalgesia. In line with our hypothesis we found that adoptive transfer of WT bone marrow-derived monocytes (BMDM), but not of GRK2^{+/-} BMDM, to LysM-GRK2^{+/-} mice prevented development of IL-1 β -induced persistent hyperalgesia. In our search for localization of transplanted BMDM, we detected the transplanted GFP⁺ BMDM in the lumbar DRG, but not in the spinal cord (**chapter 4**). In future experiments we still have to determine more carefully whether these cells can really only be traced in the DRG and not in the spinal cord. How these monocytes/macrophages infiltrate into the DRG during IL-1 β -induced hyperalgesia is still unclear. However, it is known that the chemokine fractalkine is an important chemoattractant for leukocyte trafficking. Recently, it has been described that under inflammatory conditions fractalkine recruits CX3CR1-expressing macrophages to the DRG⁴⁹. Another group described that CX3CR1 is important for the recruitment of CD115⁺Gr1⁺ inflammatory monocytes, which we also used for our adoptive transfer studies². In future experiments we will investigate whether CX3CR1 is important for attraction of the monocytes/macrophages from the periphery to the DRG. Other recent studies described that under conditions of neuropathic pain the chemokine monocyte chemoattractant protein-1 (MCP1) is increased in the DRG^{116,121}. We described in **chapter 4** that CCR2⁺ (receptor for MCP1) monocytes/macrophages are important for the regulation of pain. So it is possible that intraplantar IL-1 β injection up regulates MCP1 expression in the DRGs, which in turn attracts monocytes/macrophages to down regulate the pain response (Figure 7.1).

Next we searched for a pathway via which peripheral monocytes/macrophages promote resolution of transient inflammatory hyperalgesia. We described that intrathecal injection of anti-IL-10 prolonged the IL-1 β -induced hyperalgesia in WT mice, while injection of anti-IL-10 in LysM-GRK2^{+/-} mice did not affect the thermal hyperalgesia. Furthermore, adoptive transfer of IL-10^{-/-} monocytes did not have any effect on the persistent hyperalgesia in LysM-GRK2^{+/-} mice. This indicates that IL-10 signaling is required for spontaneous resolution of hyperalgesia during IL-1 β -induced hyperalgesia. *In vitro* we found that GRK2^{+/-} macrophages produce less IL-10 and more IL-1 β and TNF- α after LPS stimulation. Moreover, after intraplantar IL-1 β the transfer of WT, but not of IL-10-deficient BMDM, reduces the expression of the pro-inflammatory M1 phenotypic marker CD16/CD32 in spinal cord of LysM-GRK2^{+/-} mice (**chapter 4**). Therefore, we suggest that GRK2-deficient macrophages/monocytes have reduced IL-10 expression levels, which in turn are not capable of preventing the downregulation of microglia activity which results in the development of persistent hyperalgesia (Figure 7.1C).

Until now it is still unclear how low GRK2 leads to decreased IL-10 production in monocyte/macrophages. The observation that GRK2 in monocytes/macrophage is crucial for the resolution of inflammatory-induced hyperalgesia sheds a new light on the interpretation of the results described in chapters 2 and 3 and will be discussed in the following paragraph.

Microglia

As described in **chapter 2**, intrathecal injection of minocycline prior to intraplantar IL-1 β significantly reduced the hyperalgesia at 6 and 8 hours after IL-1 β injection in both genotypes. In addition, the chronic phase was completely prevented by pre-treatment of minocycline in LysM-GRK2^{+/-} mice. This indicated to us that in both genotypes spinal microglia or monocyte/macrophage activity in DRG contributes to the late phase of acute hyperalgesia (Figure 7.1).

WT mice

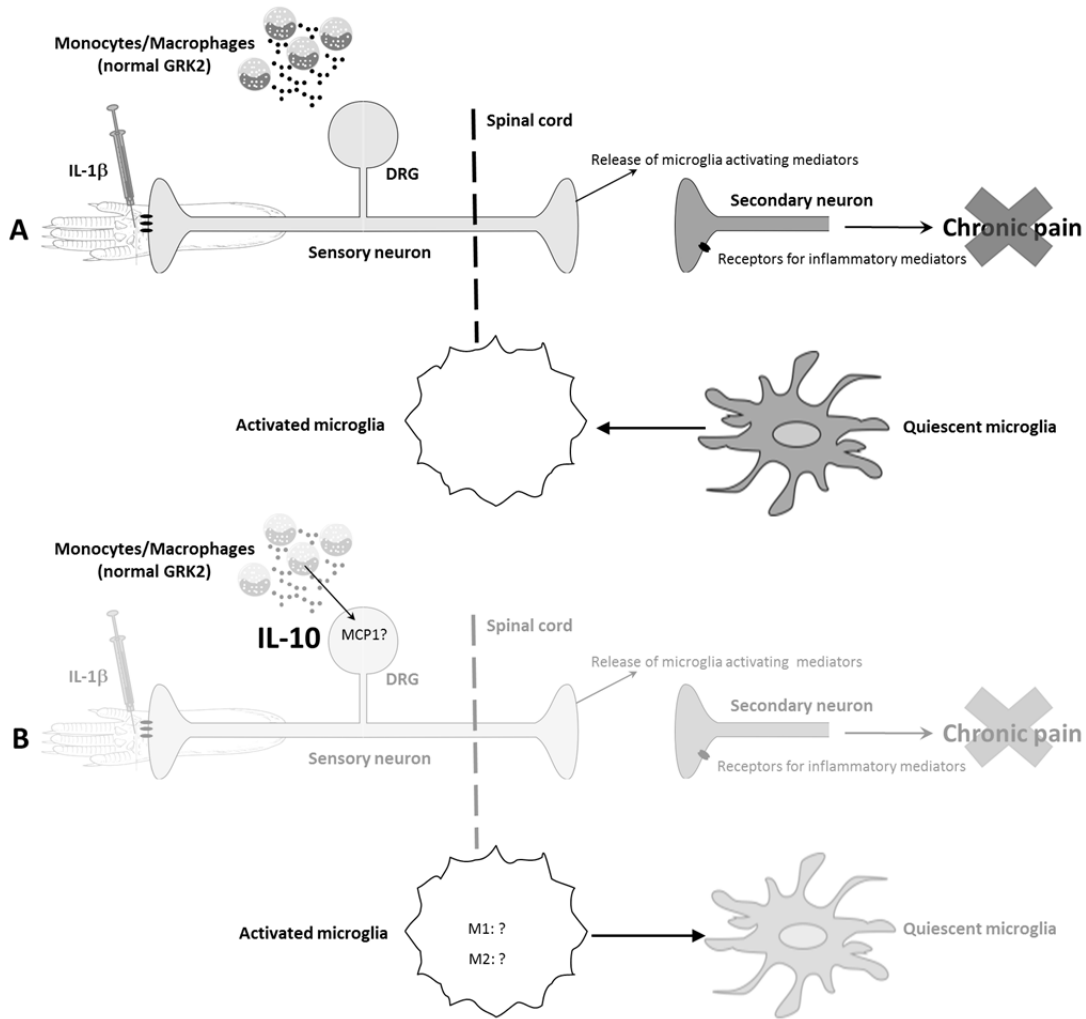
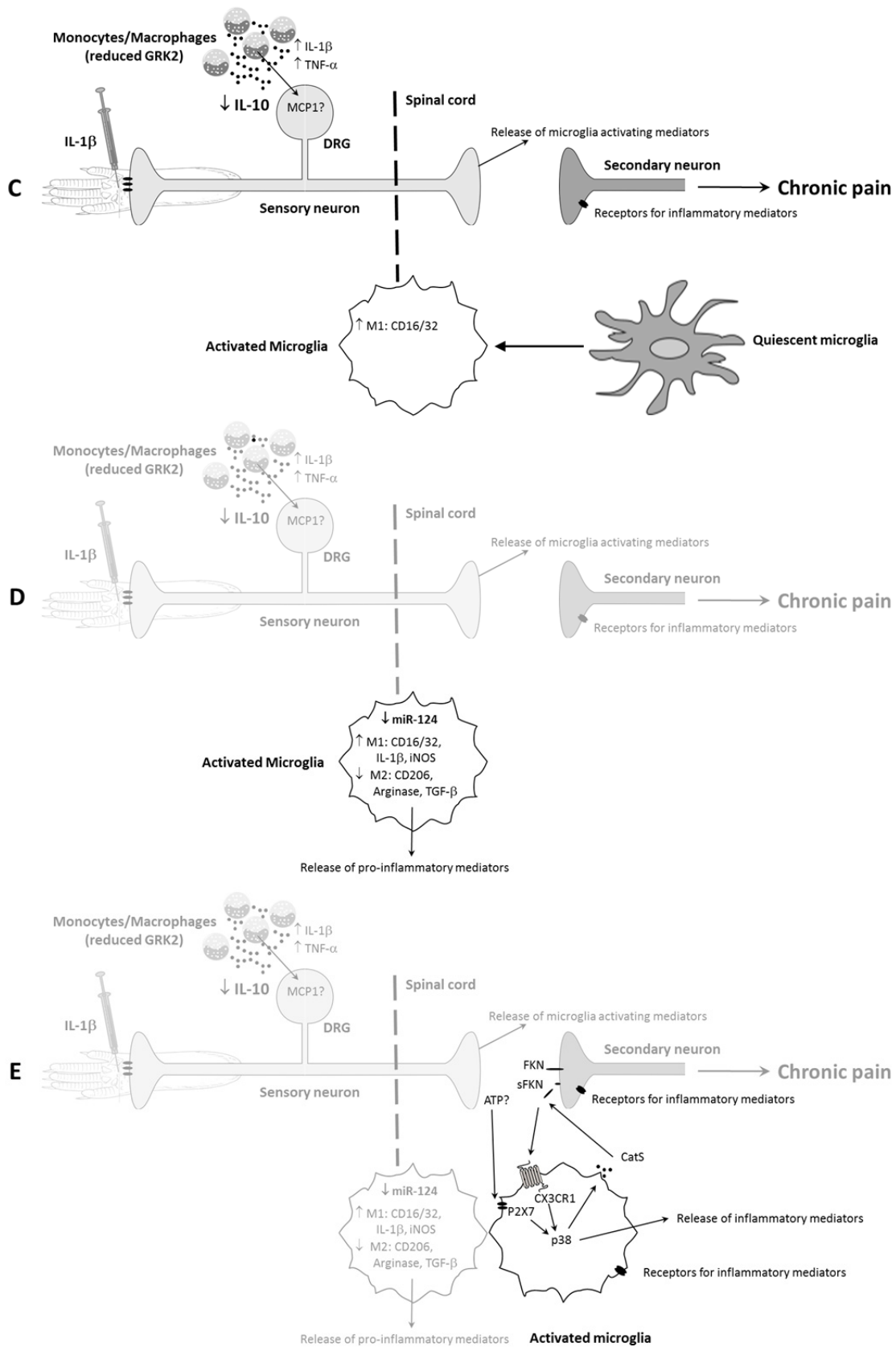


Figure 7.1: Schematic model of the proposed role of GRK2 in IL-1 β -induced hyperalgesia. (A) A single intraplantar injection of IL-1 β induces transient hyperalgesia in WT mice that is associated with transient spinal microglia activation. (B) Bone marrow-derived monocytes (BMDM) migrate towards the DRG, possibly through MCP1 production by sensory neurons in the DRG. The IL-10 producing BMDM attenuate ongoing spinal microglia activation and thereby preventing the development of chronic pain. (C) Conversely, LysM-GRK2^{+/-} mice that have reduced GRK2 levels in macrophages have a reduced capacity to produce IL-10 leading to ongoing hyperalgesia and a microglial M1 phenotype in the spinal cord. (D) In comparison to WT microglia, miR-124 levels are decreased in microglia from LysM-GRK2^{+/-} mice with ongoing hyperalgesia. In addition, M2 type phenotypic markers decrease and pro-inflammatory cytokines increase, which contributes to central sensitization and the development of chronic pain. (E) In LysM-GRK2^{+/-} mice the fractalkine signalling pathway is initiated that contributes to the maintenance of the IL-1 β -induced hyperalgesia.

LysM-GRK2^{+/-} mice



The antibiotic minocycline has been shown to reduce the release of pro-inflammatory mediators from microglia and monocytes/macrophages⁷⁵. Furthermore, we know that normal levels of GRK2 in monocytes/macrophages are important to ensure adequate termination of inflammation-induced hyperalgesia. In addition, as described above, after intraplantar IL-1 β , IL-10 deficient BMDM reduced the expression of the pro-inflammatory M1 phenotypic marker CD16/CD32 in spinal cord of LysM-GRK2^{+/-} mice. So we suggested that GRK2-deficient monocytes/macrophages produces not enough IL-10 to (indirectly) downregulate microglia activity and consequently cannot prevent the development of chronic pain. Moreover, the observed similar effect of minocycline pre-treatment in WT mice (reduction of hyperalgesia 6-8 hr after IL-1 β) indicated to us that the production of IL-10 by peripheral monocytes/macrophages is just not enough to keep microglia in a resting state during acute hyperalgesia and that another factor contributes to down regulate spinal microglia activity. Although we first suggested that GRK2 was down regulated in microglia from LysM-GRK2^{+/-} mice, now we know that they express normal GRK2 levels under basal conditions (**chapter 4**).

In **chapter 3** we aimed at determining the mechanism how spinal cord microglia activity is regulated and terminated during inflammatory pain. It has recently been described that microRNA-124 (miR-124) keeps resident microglia in brain and spinal cord in a quiescent state¹⁸⁹. MicroRNAs have an important role in the regulation of gene expression by promoting degradation of mRNA or by preventing translation of multiple target genes. Ponomarev *et al.* demonstrated that bone marrow-derived macrophages (BMDM) transfected with miR-124 produce less anti-inflammatory mediators and increased levels of pro-inflammatory mediators¹⁸⁹. Thus the authors proposed that miR-124 is involved in defining the activation state of microglia. Interestingly, we observed that isolated microglia from LysM-GRK2^{+/-} mice have a reduction in miR-124 expression after intraplantar IL-1 β injection compared to isolated microglia from WT mice. Next we wanted to know if this difference in miR-124 levels was associated with differences in the expression of spinal microglia activation markers. We investigated the two well-known microglia/macrophage activation subtypes, known as pro-inflammatory or M1 type and anti-inflammatory or M2 type, in the spinal cord after IL-1 β -induced hyperalgesia in control WT and LysM-GRK2^{+/-} mice. In line with our hypothesis, we observed a switch in the M1/M2 balance towards a pro-inflammatory M1 phenotype together with increased pro-inflammatory cytokine production after IL-1 β -induced hyperalgesia in LysM-GRK2^{+/-} mice compared to WT mice (**chapter 3** and figure 7.1D). In addition, intrathecal administration of miR-124 prevented the transition to persistent IL-1 β -induced hyperalgesia and normalized the M1/M2 ratio in LysM-GRK2^{+/-} mice (**chapter 3**). We suggest that miR-124 bypasses the need for IL-10 production by monocytes/macrophages to halt microglia activation. However, the reverse may also be true that IL-10 regulates miR-124 expression in monocytes/macrophages. Future experiments will have to uncover if or how IL-10 and miR-124 interact to regulate microglial activity.

The question arises how intraplantar IL-1 β induces a decrease in spinal microglial miR-124 levels. There is evidence that *in vitro* co-culture of BMDM with primary neurons reduces the level of macrophage miR-124¹⁸⁹. This indicates that neuronal signals can regulate the miR-124 expression in macrophage-like cells. Recently, we described that the GRK2-exchange protein activated by cAMP (Epac1) ratio in nociceptors is important for the regulation of chronic pain. Normally pain signaling is regulated via the classical cAMP/PKA pathway to induce transient hyperalgesia. However, low nociceptor GRK2 protein levels induce a switch from PKA- to an Epac/PKC ϵ -dependent pathway, resulting in markedly prolonged inflammatory-induced chronic pain. GRK2 physically binds to Epac1 and inhibits Epac signaling to its downstream target Rap1.

So reduced GRK2 results in enhanced Rap1 activation, leading to prolongation of hyperalgesia^{60,246}. A recent study described that Rap1 physically binds to the regulatory elements of the miR-124 gene to restrict miR-124 transcription²⁶⁵. Therefore, it might be possible that also in macrophage/microglia with low GRK2 enhances Rap1 activation, leading to a reduction in miR-124 expression. However, most of this research is done in neurons, so it should still be investigated whether this pathway is also present in macrophages or microglial cells.

The fractalkine pathway is an important mechanism for neuro-microglia communication, since fractalkine is expressed on neurons, whereas its receptor CX3CR1 is mainly expressed on microglia/macrophages in the spinal cord. It has been suggested that activation of the fractalkine signaling pathway is critical for the maintenance of chronic pain^{36,249}. During the development of chronic pain several molecules are released in the spinal cord to facilitate central sensitization. An important molecule that regulates microglial activity is ATP²³⁴. It has been suggested that the central terminals of (damaged) primary afferent neurons produce high extracellular ATP levels to induce the release of the lysosomal cysteine protease cathepsin S (CatS) via a p38-mediated pathway, which in turn initiates the fractalkine-pathway³⁶. Clark *et al.* hypothesized that during peripheral tissue damage or nerve injury, ATP is released from sensory neurons in the spinal cord which activates the ATP-receptor (P2X7) on microglia to induce the activation of the p38 MAPK pathway and the release of the CatS. Subsequently, CatS cleaves and liberates fractalkine expressed on neuronal membranes. Soluble fractalkine feeds back onto the microglial cells to bind to its receptor (CX3CR1) to further activate p38 MAPK. This p38 MAPK activation stimulates the release of inflammatory mediators that activates neurons and microglia and in turn the development of chronic pain (³⁸ and Figure 7.1E). Recently, it has been described that during neuropathic pain the fractalkine levels on neurons remained unaltered while CX3CR1 is upregulated in spinal microglia and neutralizing antibodies to CX3CR1 were able to block the pain^{142,226,238,275}. In **chapter 2** we found similar results in LysM-GRK2^{+/-} mice after intraplantar IL-1 β , since a significant increase in spinal CX3CR1, CatS and IL-1 β was measured in LysM-GRK2^{+/-} mice compared to WT mice. Furthermore, the prolonged hyperalgesic state in LysM-GRK2^{+/-} mice was also dependent on spinal cord fractalkine signaling, since i.t. administration of anti-CX3CR1 attenuated ongoing IL-1 β -induced hyperalgesia. As described above, CX3CR1 activation is thought to lead to activation of p38 MAPK signaling and subsequently the release of pro-inflammatory cytokines including IL-1 β ³⁴. Indeed, inhibition of p38 MAPK activity or IL-1 β signaling during prolonged hyperalgesia attenuated the ongoing response in LysM-GRK2^{+/-} mice. We propose that in WT mice the fractalkine signaling pathway is not initiated, since WT peripheral monocytes/macrophages produce high levels of IL-10 and prevent a M1 activation phenotype in the spinal cord. Conversely, mice with reduced levels of GRK2 in macrophages produce low levels of IL-10 and a switch towards an increased ratio of spinal M1/M2 phenotype occurs. Subsequently, the development of prolonged hyperalgesia is maintained via aberrant microglial miR-124 regulation and ongoing fractalkine-induced microglia activity (**chapter 2** and Figure 7.1).

GRK2 is capable to bind and phosphorylate p38 (p-p38), thereby interfering with activation of p38 MAPK^{158,185}. Activated p38 MAPK enhances the production of pro-inflammatory cytokines¹¹⁰. Recently it has been shown *in vitro* that LPS-stimulated macrophages and microglia with a 50% reduction in GRK2 produced significantly more pro-inflammatory cytokines and this increase was p38 MAPK- dependent^{117,177,185}. Thus it is possible that GRK2 binds to p38 MAPK and thereby prevents the development of pro-inflammatory mediators in WT mice which have normal GRK2 expression levels in monocytes/macrophages. Conversely, we suggest that GRK2-

deficient peripheral monocytes/macrophages produce more pro-inflammatory cytokines and less IL-10 due to enhanced p38 MAPK activity, leading to a decrease in spinal microglia miR-124 expression. Activation of microglia stimulates the fractalkine pathway which now contributes to the maintenance of chronic hyperalgesia (Figure 7.1E). From our recent findings we can confirm that mice with low levels of GRK2 in monocytes/macrophages have a more pro-inflammatory phenotype, since intrathecal injections with IL-1ra or p38 inhibitor can prevent the development of persistent IL-1 β -induced hyperalgesia (Figure 7.2A and B).

Normally the persistent hyperalgesia in LysM-GRK2^{+/-} mice resolves in 8-10 days after intraplantar IL-1 β . Interestingly, the magnitude and duration of IL-1 β -induced hyperalgesia in homozygous LysM-GRK2^{-/-} mice (>95% reduction of GRK2 in peripheral macrophages) was

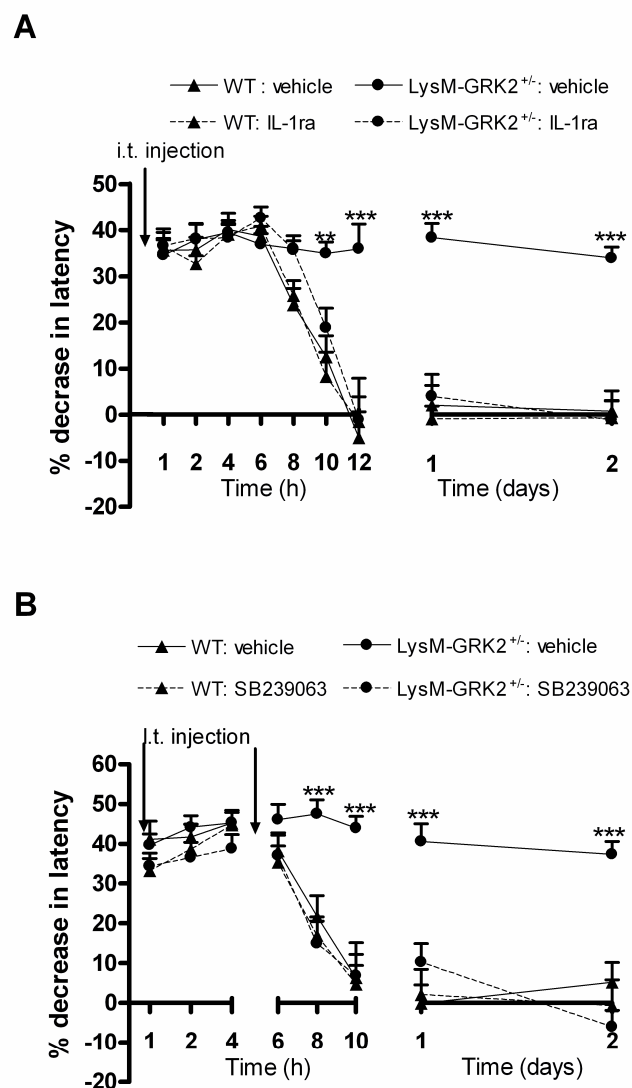


Figure 7.2: Role of p38 and IL-1 in the regulation of IL-1 β -induced hyperalgesia. The percentage decrease in heat withdrawal latency was determined over time after intraplantar IL-1 β in WT and LysM-GRK2^{+/-} mice. Mice received 15 minutes prior to intraplantar IL-1 β an intrathecal injection of (A) 10 ng IL-1ra or vehicle (n = 12) or (B) 5 μ g of the p38-inhibitor SB239063 or vehicle (n = 8) and a second injection at 4 hours after intraplantar IL-1 β . All data are expressed as mean \pm SEM. * p<0.05 ** p<0.01, *** p<0.001.

similar as in heterozygous LysM-GRK2^{+/-} mice (**chapter 2**). This indicates that no gene dose effect of GRK2 exists since in both heterozygous and homozygous LysM-GRK2 mice the IL-1 β -induced hyperalgesia lasts till approximately 8 days and does not differ with respect to severity of hyperalgesia.

One of the intriguing problems is how hyperalgesia around day 8 after intraplantar IL-1 β resolves. In WT mice we know that IL-10 is an important factor to prevent the development of IL-1 β -induced hyperalgesia. We don't know whether this same resolution mechanism takes place during the late phase of IL-1 β -induced hyperalgesia in LysM-GRK2^{+/-} mice. Possibly other cell types or molecules can switch off the pain response, like e.g. regulatory T-cells (Tregs). A recent study described that Tregs can reduce the activation of microglia and the infiltration of T cells in the spinal cord, which in turn results in the reduction of mechanical pain hypersensitivity. Furthermore depletion of Tregs prolonged the neuropathic pain response⁵. In addition, astrocytes may contribute to the termination of hyperalgesia. For example, many astrocytes express several glutamate receptors and glutamate transporter molecules to regulate the concentration of extracellular glutamate in the spinal cord. Xin *et al.* have shown that these receptors are down regulated during the development of chronic pain²⁶³. Moreover, hypoxia-ischemic and ibotenate-induced excitotoxic brain damage decreases the levels of GRK2 in astrocytes. Nijboer *et al.* recently showed that reduced GRK2 in astrocytes leads to an increase in the uptake of glutamate¹⁷⁸. If this mechanism would also be operative in astrocytes in spinal cord or in satellite glial cells in the DRG, it might be that around 8 days after intraplantar IL-1 β , astrocytes will have a low GRK2 level, which may lead to an increase in glutamate uptake which subsequently leads to a termination of the hyperalgesic response. In addition, until now it is unclear whether the ongoing microglia activation in LysM-GRK2^{+/-} mice, due to decreased capacity of GRK2-deficient monocytes/macrophages to produce IL-10, initiates the reduction of microglial GRK2 levels, since most likely the LysM promoter is activated in the later phase of IL-1 β -induced hyperalgesia. Future research is needed to investigate this more in detail.

Pain and genetics

Pain is a complex trait since not only environmental factors but often also genetic factors play a role in the aetiology. Genetic research is important to investigate DNA polymorphisms in genes that can be responsible for expression of the 'pain phenotype'⁷¹. For example, recently it has been described that a polymorphism in the opioid receptor- μ 1 gene is significantly associated with the opioid dosage that is required during neuropathic pain^{33,145}. Another well-known gene in relation to pain is *catechol-O-methyltransferase* gene (COMT). The enzyme COMT controls the breakdown of dopamine, epinephrine and norepinephrine. A SNP in this gene decreases the COMT activity and consequently increases the levels of e.g. epinephrine which in response increases the pain sensitivity^{146,199}.

Genetic studies are often done by hypothesis-driven approaches such as by studying a particular pain-related gene, like COMT, which is important to regulate pain sensitivity. This allows the assumption that a possible SNP in this gene can contribute to altered function of the COMT enzyme and thereby to pain signaling. During the past several years more research has been done to investigate possible SNP's in pain-related genes⁷¹. However, as discussed several times, pain is a complex trait so it is possible that many pain-related genes are still not known. Therefore we investigated in **chapter 6** genetic variants involved in chronic widespread pain (CWP) by a large-scale hypothesis free genome-wide association study (GWAS). We identified genetic variants near the genes CCT5 and FAM173b to be associated with CWP. Next, we tested whether those genetic variants affected gene expression levels of CCT5 and FAM173b. In both

genes we found a SNP in the coding region, however, only the SNP rs2438653 in the FAM173b gene was non-synonymous, thus altering the amino acid sequence in the protein. Moreover, we found a significant increase in both FAM173b and CCT5 expression in the spinal cord (and not DRG) during inflammatory- induced hyperalgesia in mice. The function of FAM173b is still unknown, so it is difficult to propose a mechanism how this gene can influence CWP. In a Moroccan family, a mutation in the CCT5 gene was found to be associated with sensory neuropathy with spastic paraplegia¹⁶. Furthermore, it is known that CCT5 can interact with the phosphatase PP4C and it has been suggested that this phosphatase can regulate central sensitization mechanisms^{29,269}. So both CCT5 and FAM173b are novel genes that are associated with inflammatory pain but the underlying mechanism involving pain sensation should be investigated more in detail.

We also investigated whether patients with CWP have polymorphisms in or nearby the GRK2 gene. However, no significant SNPs were found (unpublished data). It is possible that there are SNPs in downstream targets of GRK2 or in proteases that can regulate the GRK2 expression levels. However, this is pure speculation and should be investigated more in detail in the future.

Possible therapeutic consequences of our observations

As described in **chapter 4**, GRK2-deficient peripheral monocytes/macrophages have an increased production of pro-inflammatory cytokines, like IL-1 β and TNF- α , and a reduced production of anti-inflammatory cytokine IL-10. The p38 MAPK is known to regulate the stability and expression of many mRNAs coding for several inflammatory mediators (e.g. TNF- α , IL-1 β , IL-10)³⁹. Inflammation plays a crucial role in the development of chronic pain and different pharmaceutical companies are investigating effective therapeutics to target p38 MAPK. However, during clinical trials there were some disappointing results, since many of the first and second generation of p38 MAPK inhibitors were designed to target the ATP binding pocket of p38 MAPK. This is a common domain and has high homology with many different kinases and therefore can affect other signaling pathways that are important for e.g. cell survival, proliferation, tumorigenesis⁴⁵. Recently it has been described that direct interaction of GRK2 with p38 MAPK, results in phosphorylation of Thr-123 at the docking domain which reduced binding of upstream kinases (like MM6) and downstream targets¹⁸⁵. With this knowledge we investigated in **chapter 5** the development of a novel p38 MAPK inhibitor. We identified the FGA-19 compound as an effective inhibitor *in vitro* and *in vivo*. We detected that FGA-19 treatment could completely reverse the carrageenan-induced hyperalgesia in WT mice. In addition, FGA-19 is almost ten times as potent as the commercially available SB239063 p38 MAPK inhibitor, since 0.5 μ g of FGA-19 has the same analgesic effect as 5 μ g SB239063. Moreover, FGA-19-treatment results in a long-lasting effect, since the carrageenan-induced hyperalgesia resolved at least during 5 days post-injection of the drug, while SB239063 treatment did not last longer than 6 hours. We know that GRK2 can bind and inhibit p38 MAPK activity, thus we propose that low levels of GRK2 can increase the p38 MAPK activity which results in an increase of pro-inflammatory mediators and the development of chronic pain. Our hypothesis is strengthened by our finding that FGA-19 treatment can completely reverse the carrageenan-induced persistent hyperalgesia in LysM-GRK2^{+/-} mice (**chapter 5**). We suggest that under inflammatory conditions reduced GRK2 levels enhance p38 MAPK activity and that FGA-19 treatment has promising effects to dampen p38 MAPK activity and consequently the development of hyperalgesia. In the future the side-effects of FGA-19 treatment should be investigated, since this drug might represent an attractive therapy in pain management.

It is widely expected that spinal cord microglia activity plays a major role in the maintenance of chronic pain. Most of the therapeutics are not exclusively microglial inhibitors and may target other immune cells or neurons. The fractalkine receptor is exclusively expressed on spinal microglia and several studies identified that blocking of CX3CR1 attenuates neuropathic pain and as we described also inflammatory pain (^{38,163} and **chapter 2**). Recently, it has been demonstrated that rats with bone cancer pain have increased spinal CX3CR1 levels⁹⁹. In addition, intrathecal injection of anti-CX3CR1 suppressed the spinal microglia activation and p38 MAPK activity and subsequently delayed and also attenuated mechanical allodynia. We suggest that anti-CX3CR1 treatment or drugs specifically blocking the CX3CR1 could become beneficial therapeutic agents to treat chronic pain.

As suggested, miR-124 levels are required to keep microglia in a quiescent state¹⁸⁹. We support this suggestion, since during inflammatory hyperalgesia the miR-124 levels are decreased in isolated spinal microglia from LysM-GRK2^{+/-} mice. Furthermore, we presented the first evidence that intrathecal miR-124 treatment can be used to prevent IL-1 β -induced hyperalgesia in LysM-GRK2^{+/-} mice. In addition, miR-124 can also be used to treat persistent inflammatory and neuropathic pain since miR-124 treatment attenuates the existing persistent carrageenan-induced hyperalgesia in WT. The clinical relevance of miR-124 treatment is further supported by the current data showing that miR-124 treatment inhibited the development of hyperalgesia in a mice model of neuropathic pain (**chapter 3**). In conclusion, miR-124 might represent a novel option for the treatment of chronic pain.

In **chapter 4**, we described that normal GRK2 levels in peripheral monocytes/macrophages are crucial to prevent the transition from acute to chronic inflammatory pain. GRK2-deficient peripheral monocytes/macrophages have an impaired capacity to produce IL-10 and are thereby unable to promote resolution of inflammatory pain. These results indicate that the GRK2 and/or IL-10 expression levels in peripheral monocytes/macrophages can be used as biomarker to predict the risk of developing chronic pain after an inflammation.

In **chapter 4** we also described that an i.t. IL-10 injection transiently reduced IL-1 β -induced hyperalgesia in LysM-GRK2^{+/-} mice. Milligan *et al.* also described a transient effect of IL-10 treatment in neuropathic rats, likely due the short half-life of IL-10 in the intrathecal space¹⁶⁴. To overcome the problem of the short half-life of IL-10, some studies described that IL-10 gene therapy in the spinal cord might be better to attenuate chronic hyperalgesia in models of chronic neuropathic pain. These authors used adenoviral vector encoding human IL-10 to treat chronic neuropathic pain. However, the disadvantage is that these viral vectors are short-lived due to recognition by the immune system or due to inefficient cellular specific promoter activity¹⁶⁵. But most of all, the use of systemic viral vector injections can be dangerous since the virus could also infect other cell types. Alternative methods are needed, so a non-viral gene therapy is preferable over the use of viruses that are specifically interacting with or integrating in a specific cell type. Recently it has been described that the use of naked pDNA encoding IL-10 reversed neuropathic pain in rats. High doses of pDNA are required because the uptake of naked DNA is inefficient which makes it an expensive procedure¹³⁷. The same group improved the uptake of pDNA by using microparticle-encapsulated DNA²²⁰. We propose that a relatively simple and save approach to deliver a stable IL-10 protein is needed. At the moment our lab is testing a new stable IL-10 construct with promising results.

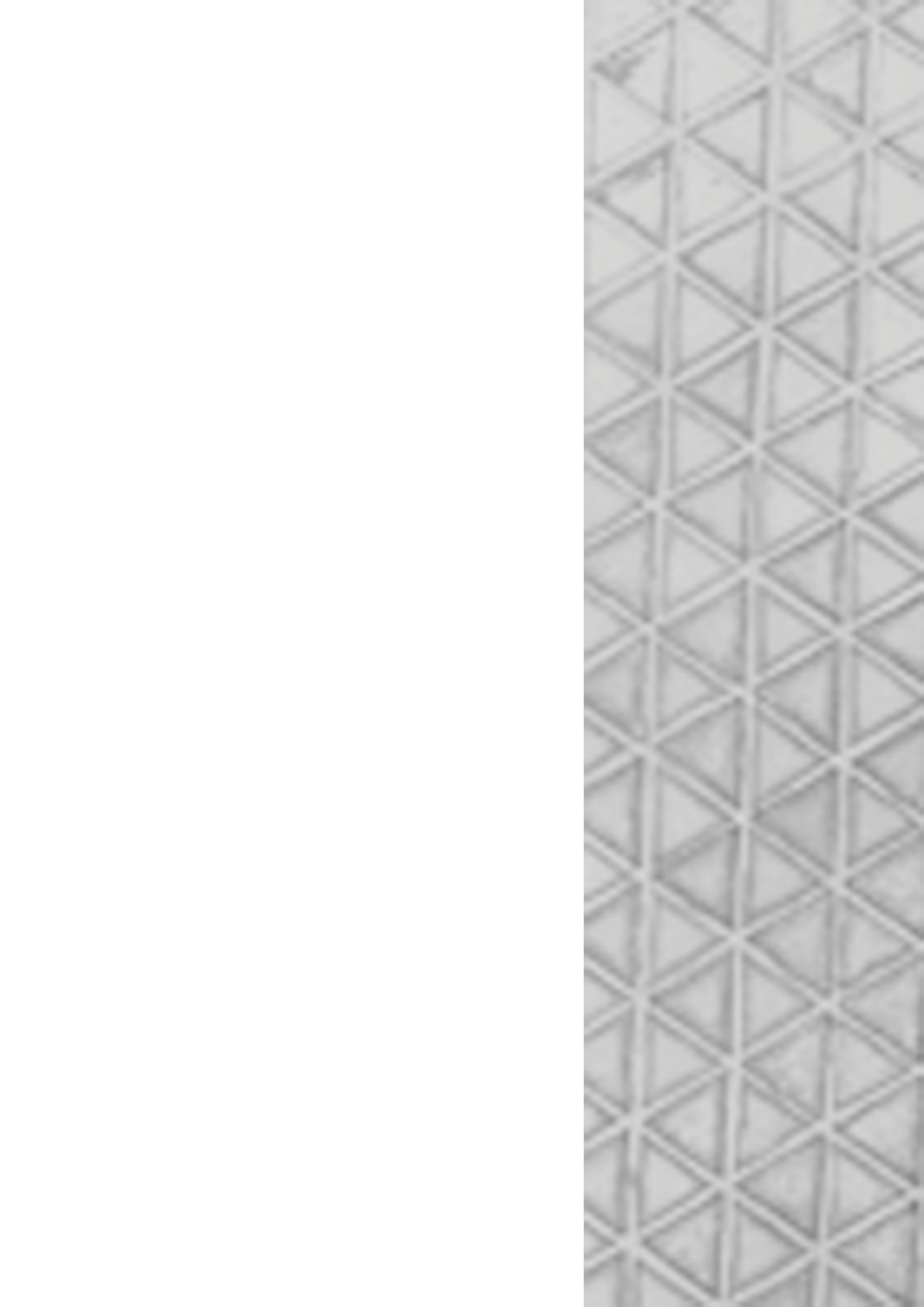
As described in **chapter 6** patients with chronic widespread pain have genetic variants nearby the CCT5 and FAM173b gene. In addition, CCT5 and FAM173b expression are up regulated in the spinal cord of mice with inflammatory pain. Preliminary results identify that FAM173b

reduction enhances the resolution of inflammatory pain. Future research is needed to identify whether FAM173b or CCT5 can be used as potential therapeutic targets to treat chronic pain.

Conclusion

An important finding in this thesis is that **peripheral monocytes/macrophages** have a key role in promoting the resolution of inflammatory hyperalgesia. Mice with a 50% reduction of GRK2 in macrophages (LysM-GRK2^{+/-}) have a decreased capacity to produce IL-10 and thereby are unable to prevent the transition from acute to chronic inflammation-induced hyperalgesia. The observation that LysM-GRK2^{+/-} mice have normal microglial GRK2 levels strengthened our hypothesis that peripheral monocyte/macrophages are crucial to regulate the transition from acute to chronic pain. In addition we found that intraplantar IL-1 β administration in LysM-GRK2^{+/-} mice induces persistent hyperalgesia, decreases the level of miR-124 in spinal cord microglia and increases the expression of spinal M1 type phenotypic markers. In addition, miR-124 treatment reverses persistent carrageenan-induced hyperalgesia and prevents the development of chronic neuropathic pain in WT mice. We identified that the ongoing microglia activity in LysM-GRK2^{+/-} mice is maintained via the fractalkine loop. Taken these data together, we propose that LysM-GRK2^{+/-} mice can be used as a model to investigate mechanisms of chronic pain. In addition, we describe here a novel p38 MAPK inhibitor, FGA-19, which is an effective inhibitor, since FGA-19 treatment can completely reverse the carrageenan-induced persistent hyperalgesia in LysM-GRK2^{+/-} mice. Finally, we found genetic variants nearby CCT5 and FAM173b gene in patients with chronic widespread pain. The expression of these genes are up regulated in the spinal cord of mice with inflammatory pain, thus representing novel target genes that are involved in pathological pain.

In conclusion the studies described in this thesis give more insight into the neurobiological mechanisms of chronic inflammatory pain, leading not only to more fundamental knowledge on the development of chronic pain but also to uncovering of some interesting novel options for the treatment of chronic pain.



References

1. Arriza, JL, Dawson, TM, Simerly, RB, et al. The G-protein-coupled receptor kinases beta ARK1 and beta ARK2 are widely distributed at synapses in rat brain. *J Neurosci*. 1992; 12:4045-4055.
2. Auffray, C, Fogg, DK, Narni-Mancinelli, E, et al. CX3CR1+ CD115+ CD135+ common macrophage/DC precursors and the role of CX3CR1 in their response to inflammation. *J Exp Med*. 2009; 206:595-606.
3. Aulchenko, YS, Heutink, P, Mackay, I, et al. Linkage disequilibrium in young genetically isolated Dutch population. 2004; 2004/04/01:527-534.
4. Aulchenko, YS, Ripke, S, Isaacs, A, et al. GenABEL: an R library for genome-wide association analysis. 2007; 2007/03/27:1294-1296.
5. Austin, PJ, Kim, CF, Perera, CJ, et al. Regulatory T cells attenuate neuropathic pain following peripheral nerve injury and experimental autoimmune neuritis. *Pain*. 2012; 153:1916-1931.
6. Bai, G, Ambalavanar, R, Wei, D, et al. Downregulation of selective microRNAs in trigeminal ganglion neurons following inflammatory muscle pain. *Mol Pain*. 2007; 3:15.
7. Bank, PJ, Peper, CE, Marinus, J, et al. Motor consequences of experimentally induced limb pain: A systematic review. *Eur J Pain*. 2012.
8. Basbaum, AI, Bautista, DM, Scherrer, G, et al. Cellular and molecular mechanisms of pain. *Cell*. 2009; 139:267-284.
9. Bax, M, van Heemst, J, Huizinga, TW, et al. Genetics of rheumatoid arthritis: what have we learned? 2011; 2011/05/11:459-466.
10. Biber, K, Neumann, H, Inoue, K, et al. Neuronal 'On' and 'Off' signals control microglia. *Trends Neurosci*. 2007; 30:596-602.
11. Binshtok, AM, Wang, H, Zimmermann, K, et al. Nociceptors are interleukin-1beta sensors. *J Neurosci*. 2008; 28:14062-14073.
12. Biostat. Comprehensive Meta-Analysis Software. 2011; 2011-03-04.
13. Boettger, MK, Hensellek, S, Richter, F, et al. Antinociceptive effects of tumor necrosis factor alpha neutralization in a rat model of antigen-induced arthritis: evidence of a neuronal target. *Arthritis Rheum*. 2008; 58:2368-2378.
14. Bogoyevitch, MA and Fairlie, DP. A new paradigm for protein kinase inhibition: blocking phosphorylation without directly targeting ATP binding. *Drug Discov Today*. 2007; 2007/08/21:622-633.
15. Bondy, B, Spaeth, M, Offenbaecher, M, et al. The T102C polymorphism of the 5-HT2A-receptor gene in fibromyalgia. 1999; 1999/10/21:433-439.
16. Bouhouche, A, Benomar, A, Bouslam, N, et al. Mutation in the epsilon subunit of the cytosolic chaperonin-containing t-complex peptide-1 (Cct5) gene causes autosomal recessive mutilating sensory neuropathy with spastic paraplegia. 2006; 2006/01/10:441-443.
17. Bourlier, V, Zakaroff-Girard, A, Miranville, A, et al. Remodeling phenotype of human subcutaneous adipose tissue macrophages. *Circulation*. 2008; 117:806-815.
18. Brack, A, Labuz, D, Schiltz, A, et al. Tissue monocytes/macrophages in inflammation: hyperalgesia versus opioid-mediated peripheral antinociception. *Anesthesiology*. 2004; 101:204-211.
19. Brandenburger, T, Castoldi, M, Brendel, M, et al. Expression of spinal cord microRNAs in a rat model of chronic neuropathic pain. *Neurosci Lett*. 2012; 506:281-286.
20. Breivik, H, Collett, B, Ventafridda, V, et al. Survey of chronic pain in Europe: prevalence, impact on daily life, and treatment. *Eur J Pain*. 2006; 10:287-333.
21. Buskila, D, Cohen, H, Neumann, L, et al. An association between fibromyalgia and the dopamine D4 receptor exon III repeat polymorphism and relationship to novelty seeking personality traits. 2004; 2004/03/31:730-731.
22. Buskila, D and Mader, R. Trauma and work-related pain syndromes: Risk factors, clinical picture, insurance and law interventions. *Best Pract Res Cl Rh*. 2011; 25:199-207.
23. Cabrera, AC, Gil-Redondo, R, Perona, A, et al. VSDMIP 1.5: an automated structure-and ligand-based virtual screening platform with a PyMOL graphical user interface. 2011;1-12.
24. Campbell, CM, Edwards, RR, Carmona, C, et al. Polymorphisms in the GTP cyclohydrolase gene

- (GCH1) are associated with ratings of capsaicin pain. 2009; 2008/12/17:114-118.
25. Cao, FL, Liu, MG, Hao, J, et al. Different roles of spinal p38 and c-Jun N-terminal kinase pathways in bee venom-induced multiple pain-related behaviors. *Neurosci Lett*. 2007; 427:50-54.
 26. Case, DA, Darden, TA, Cheatham, TE, et al. AMBER 8, University of California, San Francisco. 2004.
 27. Chang, CI, Xu, BE, Akella, R, et al. Crystal structures of MAP kinase p38 complexed to the docking sites on its nuclear substrate MEF2A and activator MKK3b. *Mol Cell*. 2002; 9:1241-1249.
 28. Chaplan, SR, Bach, FW, Pogrel, JW, et al. Quantitative assessment of tactile allodynia in the rat paw. *J Neurosci Methods*. 1994; 53:55-63.
 29. Chen, GI, Tisayakorn, S, Jorgensen, C, et al. PP4R4/KIAA1622 forms a novel stable cytosolic complex with phosphoprotein phosphatase 4. 2008; 2008/08/22:29273-29284.
 30. Cheung, PC, Campbell, DG, Nebreda, AR, et al. Feedback control of the protein kinase TAK1 by SAPK2a/p38alpha. *Embo J*. 2003; 2003/11/01:5793-5805.
 31. Cho, IH, Hong, J, Suh, EC, et al. Role of microglial IKKbeta in kainic acid-induced hippocampal neuronal cell death. *Brain*. 2008; 131:3019-3033.
 32. Choi, JI, Svensson, CI, Koehn, FJ, et al. Peripheral inflammation induces tumor necrosis factor dependent AMPA receptor trafficking and Akt phosphorylation in spinal cord in addition to pain behavior. *Pain*. 2010; 149:243-253.
 33. Chou, WY, Wang, CH, Liu, PH, et al. Human opioid receptor A118G polymorphism affects intravenous patient-controlled analgesia morphine consumption after total abdominal hysterectomy. *Anesthesiology*. 2006; 105:334-337.
 34. Clark, AK, Gentry, C, Bradbury, EJ, et al. Role of spinal microglia in rat models of peripheral nerve injury and inflammation. *Eur J Pain*. 2007; 11:223-230.
 35. Clark, AK, Yip, PK, Grist, J, et al. Inhibition of spinal microglial cathepsin S for the reversal of neuropathic pain. *Proc Natl Acad Sci U S A*. 2007; 104:10655-10660.
 36. Clark, AK, Yip, PK, and Malcangio, M. The liberation of fractalkine in the dorsal horn requires microglial cathepsin S. *J Neurosci*. 2009; 29:6945-6954.
 37. Clark, AK, Grist, J, Al-Kashi, A, et al. Spinal cathepsin S and fractalkine contribute to chronic pain in collagen induced arthritis. *Arthritis Rheum*. 2011.
 38. Clark, AK and Malcangio, M. Microglial signalling mechanisms: Cathepsin S and Fractalkine. *Exp Neurol*. 2012; 234:283-292.
 39. Clark, AR and Dean, JL. The p38 MAPK Pathway in Rheumatoid Arthritis: A Sideways Look. *Open Rheumatol J*. 2012; 6:209-219.
 40. Cohen, H, Buskila, D, Neumann, L, et al. Confirmation of an association between fibromyalgia and serotonin transporter promoter region (5-HTTLPR) polymorphism, and relationship to anxiety-related personality traits. 2002; 2002/03/29:845-847.
 41. Cohen, H, Neumann, L, Glazer, Y, et al. The relationship between a common catechol-O-methyltransferase (COMT) polymorphism val(158) met and fibromyalgia. 2009; 2010/03/12:S51-S56.
 42. Cohen, P. Targeting protein kinases for the development of anti-inflammatory drugs. *Curr Opin Cell Biol*. 2009; 2009/02/17:317-324.
 43. Consortium, UKP, Wellcome Trust Case Control, C, Spencer, CC, et al. Dissection of the genetics of Parkinson's disease identifies an additional association 5' of SNCA and multiple associated haplotypes at 17q21. 2011; 2010/11/04:345-353.
 44. Correale, J, Farez, MF, and Ysraelit, MC. Increase in multiple sclerosis activity after assisted reproduction technology. *Ann Neurol*. 2012.
 45. Coulthard, LR, White, DE, Jones, DL, et al. p38(MAPK): stress responses from molecular mechanisms to therapeutics. *Trends Mol Med*. 2009; 2009/08/12:369-379.
 46. Craig, AD. Distribution of trigeminothalamic and spinothalamic lamina I terminations in the cat. *Somatosens Mot Res*. 2003; 20:209-222.
 47. Croft, P, Schollum, J, and Silman, A. Population study of tender point counts and pain as evidence of fibromyalgia. 1994; 1994/09/17:696-699.

48. Cuadrado, A and Nebreda, AR. Mechanisms and functions of p38 MAPK signalling. *Biochem J.* 2010; 2010/07/16:403-417.
49. D'Haese, JG, Demir, IE, Friess, H, et al. Fractalkine/CX3CR1: why a single chemokine-receptor duo bears a major and unique therapeutic potential. *Expert Opin Ther Targets.* 2010; 14:207-219.
50. Darden, T, York, D, and Pedersen, L. Particle mesh Ewald: An $N \log(N)$ method for Ewald sums in large systems. 1993; 98:10089-10092.
51. De Leo, JA, Tawfik, VL, and LaCroix-Fralish, ML. The tetrapartite synapse: path to CNS sensitization and chronic pain. *Pain.* 2006; 122:17-21.
52. deCharms, RC, Maeda, F, Glover, GH, et al. Control over brain activation and pain learned by using real-time functional MRI. 2005; 2005/12/15:18626-18631.
53. Decosterd, I and Woolf, CJ. Spared nerve injury: an animal model of persistent peripheral neuropathic pain. *Pain.* 2000; 87:149-158.
54. DeLano, WL. The PyMOL molecular graphics system. 2002. Schrodinger Inc. 16-5-2011.
55. DeLeo, JA and Yeziarski, RP. The role of neuroinflammation and neuroimmune activation in persistent pain. *Pain.* 2001; 90:1-6.
56. Devlin, B and Roeder, K. Genomic control for association studies. 1999; 2001/04/21:997-1004.
57. Dray, A. Inflammatory mediators of pain. *Br J Anaesth.* 1995; 75:125-131.
58. Echeverry, S, Shi, XQ, Rivest, S, et al. Peripheral nerve injury alters blood-spinal cord barrier functional and molecular integrity through a selective inflammatory pathway. *J Neurosci.* 2011; 31:10819-10828.
59. Eijkelkamp, N, Heijnen, CJ, Lucas, A, et al. G protein-coupled receptor kinase 6 controls chronicity and severity of dextran sodium sulphate-induced colitis in mice. *Gut.* 2007; 56:847-854.
60. Eijkelkamp, N, Wang, H, Garza-Carbajal, A, et al. Low nociceptor GRK2 prolongs prostaglandin E2 hyperalgesia via biased cAMP signaling to Epac/Rap1, protein kinase Cepsilon, and MEK/ERK. *J Neurosci.* 2010; 30:12806-12815.
61. Eijkelkamp, N, Heijnen, CJ, Willemen, HL, et al. GRK2: a novel cell-specific regulator of severity and duration of inflammatory pain. *J Neurosci.* 2010; 30:2138-2149.
62. Eijkelkamp, N, Heijnen, CJ, Carbajal, AG, et al. GRK6 acts as a critical regulator of cytokine-induced hyperalgesia by promoting PI3kinase- and inhibiting p38-signaling. *Mol Med.* 2012.
63. Ekberg, J and Adams, DJ. Neuronal voltage-gated sodium channel subtypes: key roles in inflammatory and neuropathic pain. *Int J Biochem Cell Biol.* 2006; 38:2005-2010.
64. Erdtmann-Vourliotis, M, Mayer, P, Ammon, S, et al. Distribution of G-protein-coupled receptor kinase (GRK) isoforms 2, 3, 5 and 6 mRNA in the rat brain. *Brain Res Mol Brain Res.* 2001; 95:129-137.
65. Estrada, K, Abuseiris, A, Grosveld, FG, et al. GRIMP: a web- and grid-based tool for high-speed analysis of large-scale genome-wide association using imputed data. 2009; 2009/08/25:2750-2752.
66. Fan, J and Malik, AB. Toll-like receptor-4 (TLR4) signaling augments chemokine-induced neutrophil migration by modulating cell surface expression of chemokine receptors. *Nat Med.* 2003; 9:315-321.
67. Felson, DT, Zhang, Y, Hannan, MT, et al. The incidence and natural history of knee osteoarthritis in the elderly. The Framingham Osteoarthritis Study. 1995; 1995/10/01:1500-1505.
68. Feng, R, Desbordes, SC, Xie, H, et al. PU.1 and C/EBPalpha/beta convert fibroblasts into macrophage-like cells. *Proc Natl Acad Sci U S A.* 2008; 105:6057-6062.
69. Fenn, AM, Henry, CJ, Huang, Y, et al. Lipopolysaccharide-induced interleukin (IL)-4 receptor-alpha expression and corresponding sensitivity to the M2 promoting effects of IL-4 are impaired in microglia of aged mice. *Brain Behav Immun.* 2011.
70. Ferguson, SS. Evolving concepts in G protein-coupled receptor endocytosis: the role in receptor desensitization and signaling. *Pharmacol Rev.* 2001; 53:1-24.
71. Fernandez Robles, CR, Degnan, M, and Candiotti, KA. Pain and genetics. *Curr Opin Anaesthesiol.* 2012; 25:444-449.
72. Foulkes, T and Wood, JN. Pain genes. *PLoS Genet.* 2008; 4:e1000086.

73. Frank, B, Niesler, B, Bondy, B, et al. Mutational analysis of serotonin receptor genes: HTR3A and HTR3B in fibromyalgia patients. 2004; 2004/08/05:338-344.
74. Fujiu, K, Manabe, I, and Nagai, R. Renal collecting duct epithelial cells regulate inflammation in tubulointerstitial damage in mice. *J Clin Invest*. 2011; 121:3425-3441.
75. Garrido-Mesa, N, Utrilla, P, Comalada, M, et al. The association of minocycline and the probiotic *Escherichia coli* Nissle 1917 results in an additive beneficial effect in a DSS model of reactivated colitis in mice. *Biochem Pharmacol*. 2011; 82:1891-1900.
76. Garry, EM, Delaney, A, Anderson, HA, et al. Varicella zoster virus induces neuropathic changes in rat dorsal root ganglia and behavioral reflex sensitisation that is attenuated by gabapentin or sodium channel blocking drugs. *Pain*. 2005; 118:97-111.
77. Genomes Project, C. A map of human genome variation from population-scale sequencing. 2010; 2010/10/29:1061-1073.
78. Gil-Redondo, R, Master, T, and UNED. 2006.
79. Gingras, AC, Caballero, M, Zarske, M, et al. A novel, evolutionarily conserved protein phosphatase complex involved in cisplatin sensitivity. 2005; 2005/08/09:1725-1740.
80. Glatter, T, Wepf, A, Aebersold, R, et al. An integrated workflow for charting the human interaction proteome: insights into the PP2A system. 2009; 2009/01/22:237.
81. Gold, MS and Gebhart, GF. Nociceptor sensitization in pain pathogenesis. *Nat Med*. 2010; 16:1248-1257.
82. Gordon, JC, Myers, JB, Folta, T, et al. H++: a server for estimating pKas and adding missing hydrogens to macromolecules. *Nucleic Acids Res*. 2005; 2005/06/28:W368-W371.
83. Gosselin, RD, Suter, MR, Ji, RR, et al. Glial cells and chronic pain. *Neuroscientist*. 2010; 16:519-531.
84. Gursoy, S, Erdal, E, Herken, H, et al. Association of T102C polymorphism of the 5-HT_{2A} receptor gene with psychiatric status in fibromyalgia syndrome. 2001; 2001/12/06:58-61.
85. Gursoy, S. Absence of association of the serotonin transporter gene polymorphism with the mentally healthy subset of fibromyalgia patients. 2002; 2002/07/12:194-197.
86. Gursoy, S, Erdal, E, Herken, H, et al. Significance of catechol-O-methyltransferase gene polymorphism in fibromyalgia syndrome. 2003; 2003/05/10:104-107.
87. Hagen, K, Pettersen, E, Stovner, LJ, et al. No association between chronic musculoskeletal complaints and Val158Met polymorphism in the Catechol-O-methyltransferase gene. *The HUNT study*. 2006; 2006/05/06:40.
88. Hammaker, D and Firestein, GS. "Go upstream, young man": lessons learned from the p38 saga. *Ann Rheum Dis*. 2010; 2010/01/09:i77-i82.
89. Hargreaves, K, Dubner, R, Brown, F, et al. A new and sensitive method for measuring thermal nociception in cutaneous hyperalgesia. 1988; 1988/01/01:77-88.
90. Harris, TB, Launer, LJ, Eiriksdottir, G, et al. Age, Gene/Environment Susceptibility-Reykjavik Study: multidisciplinary applied phenomics. 2007; 2007/03/14:1076-1087.
91. Hart, DJ and Spector, TD. Cigarette smoking and risk of osteoarthritis in women in the general population: the Chingford study. 1993; 1993/02/01:93-96.
92. Hart, DJ and Spector, TD. The relationship of obesity, fat distribution and osteoarthritis in women in the general population: the Chingford Study. 1993; 1993/02/01:331-335.
93. Hayashida, M, Nagashima, M, Satoh, Y, et al. Analgesic requirements after major abdominal surgery are associated with OPRM1 gene polymorphism genotype and haplotype. 2008; 2008/11/21:1605-1616.
94. Hocking, LJ, Smith, BH, Jones, GT, et al. Genetic variation in the beta2-adrenergic receptor but not catecholamine-O-methyltransferase predisposes to chronic pain: results from the 1958 British Birth Cohort Study. 2010; 2010/02/20:143-151.
95. Hofman, A, van Duijn, CM, Franco, OH, et al. The Rotterdam Study: 2012 objectives and design update. 2011; 2011/08/31:657-686.
96. Holliday, KL, Nicholl, BI, Macfarlane, GJ, et al. Do genetic predictors of pain sensitivity associate with persistent widespread pain? 2009; 2009/09/25:56.

97. Holliday, KL, Nicholl, BI, Macfarlane, GJ, et al. Genetic variation in the hypothalamic-pituitary-adrenal stress axis influences susceptibility to musculoskeletal pain: results from the EPIFUND study. 2010; 2009/09/03:556-560.
98. Honore, P, Wade, CL, Zhong, C, et al. Interleukin-1alpha gene-deficient mice show reduced nociceptive sensitivity in models of inflammatory and neuropathic pain but not post-operative pain. *Behav Brain Res.* 2006; 167:355-364.
99. Hu, JH, Yang, JP, Liu, L, et al. Involvement of CX3CR1 in bone cancer pain through the activation of microglia p38 MAPK pathway in the spinal cord. *Brain Res.* 2012; 1465:1-9.
100. Hucho, T and Levine, JD. Signaling pathways in sensitization: toward a nociceptor cell biology. *Neuron.* 2007; 55:365-376.
101. Hudspith M.J, Siddall P.J., and Munglani R. *Physiology and Pain.*, 2006.
102. Hwang, HJ, Lee, HJ, Kim, CJ, et al. Inhibitory effect of amygdalin on lipopolysaccharide-inducible TNF-alpha and IL-1beta mRNA expression and carrageenan-induced rat arthritis. *J Microbiol Biotechnol.* 2008; 18:1641-1647.
103. Hylden, JL and Wilcox, GL. Intrathecal morphine in mice: a new technique. *Eur J Pharmacol.* 1980; 67:313-316.
104. Imamura, M, Imamura, ST, Kaziyama, HHS, et al. Impact of Nervous System Hyperalgesia on Pain, Disability, and Quality of Life in Patients With Knee Osteoarthritis: A Controlled Analysis. *Arthrit Rheum-Arthr.* 2008; 59:1424-1431.
105. Ioannidis, JP. Why most published research findings are false. 2005; 2005/08/03:e124.
106. Irwin, JJ and Shoichet, BK. ZINC--a free database of commercially available compounds for virtual screening. 2005; 2005/01/26:177-182.
107. Jaber, M, Koch, WJ, Rockman, H, et al. Essential role of beta-adrenergic receptor kinase 1 in cardiac development and function. *Proc Natl Acad Sci U S A.* 1996; 93:12974-12979.
108. Jancalek, R, Svizenska, I, Klusakova, I, et al. Bilateral changes of IL-10 protein in lumbar and cervical dorsal root ganglia following proximal and distal chronic constriction injury of peripheral nerve. *Neurosci Lett.* 2011; 501:86-91.
109. Ji, RR, Samad, TA, Jin, SX, et al. p38 MAPK activation by NGF in primary sensory neurons after inflammation increases TRPV1 levels and maintains heat hyperalgesia. *Neuron.* 2002; 36:57-68.
110. Ji, RR and Suter, MR. p38 MAPK, microglial signaling, and neuropathic pain. *Mol Pain.* 2007; 3:33.
111. Ji, RR, Gereau, RW, Malcangio, M, et al. MAP kinase and pain. *Brain Res Rev.* 2009; 60:135-148.
112. Jimenez-Sainz, MC, Murga, C, Kavelaars, A, et al. G protein-coupled receptor kinase 2 negatively regulates chemokine signaling at a level downstream from G protein subunits. *Mol Biol Cell.* 2006; 17:25-31.
113. John, U, Greiner, B, Hensel, E, et al. Study of Health In Pomerania (SHIP): a health examination survey in an east German region: objectives and design. 2001; 2001/09/22:186-194.
114. Johnson, AD, Handsaker, RE, Pulit, SL, et al. SNAP: a web-based tool for identification and annotation of proxy SNPs using HapMap. 2008; 2008/11/01:2938-2939.
115. Jorgensen, WL, Chandrasekhar, J, Madura, JD, et al. Comparison of simple potential functions for simulating liquid water. 1983; 79:926-935.
116. Jung, H, Bhangoo, S, Banisadr, G, et al. Visualization of chemokine receptor activation in transgenic mice reveals peripheral activation of CCR2 receptors in states of neuropathic pain. *J Neurosci.* 2009; 29:8051-8062.
117. Jurado-Pueyo, M, Campos, PM, Mayor, F, et al. GRK2-dependent desensitization downstream of G proteins. *J Recept Signal Transduct Res.* 2008; 28:59-70.
118. Kato, K, Sullivan, PF, Evengard, B, et al. Importance of genetic influences on chronic widespread pain. 2006; 2006/04/29:1682-1686.
119. Kavelaars, A, Eijkelkamp, N, Willemen, HL, et al. Microglial GRK2: a novel regulator of transition from acute to chronic pain. *Brain Behav Immun.* 2011; 2011/04/09:1055-1060.
120. Kigerl, KA, Gensel, JC, Ankeny, DP, et al. Identification of two distinct macrophage subsets with divergent effects causing either neurotoxicity or regeneration in the injured mouse spinal cord. *J Neurosci.* 2009; 29:13435-13444.

121. Kim, D, You, B, Lim, H, et al. Toll-like receptor 2 contributes to chemokine gene expression and macrophage infiltration in the dorsal root ganglia after peripheral nerve injury. *Mol Pain*. 2011; 7:74.
122. Kim, H, Lee, H, Rowan, J, et al. Genetic polymorphisms in monoamine neurotransmitter systems show only weak association with acute post-surgical pain in humans. 2006; 2006/07/20:24.
123. Kleibeuker, W, Ledebouer, A, Eijkelkamp, N, et al. A role for G protein-coupled receptor kinase 2 in mechanical allodynia. *Eur J Neurosci*. 2007; 25:1696-1704.
124. Kleibeuker, W, Jurado-Pueyo, M, Murga, C, et al. Physiological changes in GRK2 regulate CCL2-induced signaling to ERK1/2 and Akt but not to MEK1/2 and calcium. *J Neurochem*. 2008; 104:979-992.
125. Kleibeuker, W, Gabay, E, Kavelaars, A, et al. IL-1 beta signaling is required for mechanical allodynia induced by nerve injury and for the ensuing reduction in spinal cord neuronal GRK2. *Brain Behav Immun*. 2008; 22:200-208.
126. Kohno, T, Wang, H, Amaya, F, et al. Bradykinin enhances AMPA and NMDA receptor activity in spinal cord dorsal horn neurons by activating multiple kinases to produce pain hypersensitivity. *J Neurosci*. 2008; 28:4533-4540.
127. Kohout, TA and Lefkowitz, RJ. Regulation of G protein-coupled receptor kinases and arrestins during receptor desensitization. *Mol Pharmacol*. 2003; 63:9-18.
128. Kollman, PA, Massova, I, Reyes, C, et al. Calculating Structures and Free Energies of Complex Molecules: Combining Molecular Mechanics and Continuum Models. 2000; 33:889-897.
129. Komori, T, Morikawa, Y, Inada, T, et al. Site-specific subtypes of macrophages recruited after peripheral nerve injury. *Neuroreport*. 2011; 22:911-917.
130. Kubota, H, Hynes, G, and Willison, K. The chaperonin containing t-complex polypeptide 1 (TCP-1). Multisubunit machinery assisting in protein folding and assembly in the eukaryotic cytosol. 1995; 1995/05/15:3-16.
131. Kumar, P, Henikoff, S, and Ng, PC. Predicting the effects of coding non-synonymous variants on protein function using the SIFT algorithm. 2009; 2009/06/30:1073-1081.
132. Kumar, S, Boehm, J, and Lee, JC. p38 MAP kinases: key signalling molecules as therapeutic targets for inflammatory diseases. 2003; 2:717-726.
133. Kunori, S, Matsumura, S, Okuda-Ashitaka, E, et al. A novel role of prostaglandin E2 in neuropathic pain: blockade of microglial migration in the spinal cord. *Glia*. 2011; 59:208-218.
134. Latremoliere, A and Woolf, CJ. Central sensitization: a generator of pain hypersensitivity by central neural plasticity. 2009; 2009/08/29:895-926.
135. Laughlin, TM, Bethea, JR, Yezierski, RP, et al. Cytokine involvement in dynorphin-induced allodynia. *Pain*. 2000; 84:159-167.
136. Ledebouer, A, Sloane, EM, Milligan, ED, et al. Minocycline attenuates mechanical allodynia and proinflammatory cytokine expression in rat models of pain facilitation. *Pain*. 2005; 115:71-83.
137. Ledebouer, A, Jekich, BM, Sloane, EM, et al. Intrathecal interleukin-10 gene therapy attenuates paclitaxel-induced mechanical allodynia and proinflammatory cytokine expression in dorsal root ganglia in rats. *Brain Behav Immun*. 2007; 21:686-698.
138. Lee, MK, Han, SR, Park, MK, et al. Behavioral evidence for the differential regulation of p-p38 MAPK and p-NF-kappaB in rats with trigeminal neuropathic pain. *Mol Pain*. 2011; 7:57.
139. Leffler, AS, Kosek, E, Lerndal, T, et al. Somatosensory perception and function of diffuse noxious inhibitory controls (DNIC) in patients suffering from rheumatoid arthritis. *Eur J Pain-London*. 2002; 6:161-176.
140. Li, Y, Willer, CJ, Ding, J, et al. MaCH: using sequence and genotype data to estimate haplotypes and unobserved genotypes. 2010; 2010/11/09:816-834.
141. Limer, KL, Nicholl, BI, Thomson, W, et al. Exploring the genetic susceptibility of chronic widespread pain: the tender points in genetic association studies. 2008; 2008/03/07:572-577.
142. Lindia, JA, McGowan, E, Jochowitz, N, et al. Induction of CX3CL1 expression in astrocytes and CX3CR1 in microglia in the spinal cord of a rat model of neuropathic pain. *J Pain*. 2005; 6:434-438.

143. Lipinski, CA, Lombardo, F, Dominy, BW, et al. Experimental and computational approaches to estimate solubility and permeability in drug discovery and development settings. 1997; 23:3-25.
144. Liu, T, van, RN, and Tracey, DJ. Depletion of macrophages reduces axonal degeneration and hyperalgesia following nerve injury. *Pain*. 2000; 86:25-32.
145. Liu, YC and Wang, WS. Human mu-opioid receptor gene A118G polymorphism predicts the efficacy of tramadol/acetaminophen combination tablets (ultracet) in oxaliplatin-induced painful neuropathy. *Cancer*. 2012; 118:1718-1725.
146. Loggia, ML, Jensen, K, Gollub, RL, et al. The catechol-O-methyltransferase (COMT) val158met polymorphism affects brain responses to repeated painful stimuli. *PLoS One*. 2011; 6:e27764.
147. Lombardi, MS, Kavelaars, A, Schedlowski, M, et al. Decreased expression and activity of G-protein-coupled receptor kinases in peripheral blood mononuclear cells of patients with rheumatoid arthritis. *FASEB J*. 1999; 13:715-725.
148. Lombardi, MS, Kavelaars, A, Cobelens, PM, et al. Adjuvant arthritis induces down-regulation of G protein-coupled receptor kinases in the immune system. *J Immunol*. 2001; 166:1635-1640.
149. Lombardi, MS, Kavelaars, A, Penela, P, et al. Oxidative stress decreases G protein-coupled receptor kinase 2 in lymphocytes via a calpain-dependent mechanism. *Mol Pharmacol*. 2002; 62:379-388.
150. Lombardi, MS, Vroon, A, Sooda, P, et al. Down-regulation of GRK2 after oxygen and glucose deprivation in rat hippocampal slices: role of the PI3-kinase pathway. *J Neurochem*. 2007; 102:731-740.
151. Loudon, RP, Perussia, B, and Benovic, JL. Differentially regulated expression of the G-protein-coupled receptor kinases, betaARK and GRK6, during myelomonocytic cell development in vitro. *Blood*. 1996; 88:4547-4557.
152. Luo, XG and Chen, SD. The changing phenotype of microglia from homeostasis to disease. *Transl Neurodegener*. 2012; 1:9.
153. Lyons, A, Lynch, AM, Downer, EJ, et al. Fractalkine-induced activation of the phosphatidylinositol-3 kinase pathway attenuates microglial activation in vivo and in vitro. *J Neurochem*. 2009; 110:1547-1556.
154. Mack, M, Cihak, J, Simonis, C, et al. Expression and characterization of the chemokine receptors CCR2 and CCR5 in mice. *J Immunol*. 2001; 166:4697-4704.
155. Marchand, F, Perretti, M, and McMahon, SB. Role of the immune system in chronic pain. *Nat Rev Neurosci*. 2005; 6:521-532.
156. Matkovich, SJ, Diwan, A, Klanke, JL, et al. Cardiac-specific ablation of G-protein receptor kinase 2 redefines its roles in heart development and beta-adrenergic signaling. *Circ Res*. 2006; 99:996-1003.
157. Mawhinney, LA, Thawer, SG, Lu, WY, et al. Differential detection and distribution of microglial and hematogenous macrophage populations in the injured spinal cord of lys-EGFP-ki transgenic mice. *J Neuropathol Exp Neurol*. 2012; 71:180-197.
158. Mayor, F, Jr., Jurado-Pueyo, M, Campos, PM, et al. Interfering with MAP kinase docking interactions: implications and perspective for the p38 route. *Cell Cycle*. 2007; 6:528-533.
159. Meerding, WJ, Bonneux, L, Polder, JJ, et al. Demographic and epidemiological determinants of healthcare costs in Netherlands: cost of illness study. 1998; 1998/07/10:111-115.
160. Mert, T, Gunay, I, Ocal, I, et al. Macrophage depletion delays progression of neuropathic pain in diabetic animals. *Naunyn Schmiedebergs Arch Pharmacol*. 2009; 379:445-452.
161. Michelucci, A, Heurtaux, T, Grandbarbe, L, et al. Characterization of the microglial phenotype under specific pro-inflammatory and anti-inflammatory conditions: Effects of oligomeric and fibrillar amyloid-beta. *J Neuroimmunol*. 2009; 210:3-12.
162. Miller, RJ, Jung, H, Bhangoo, SK, et al. Cytokine and chemokine regulation of sensory neuron function. *Handb Exp Pharmacol*. 2009; 417-449.
163. Milligan, ED, Zapata, V, Chacur, M, et al. Evidence that exogenous and endogenous fractalkine can induce spinal nociceptive facilitation in rats. *Eur J Neurosci*. 2004; 20:2294-2302.
164. Milligan, ED, Langer, SJ, Sloane, EM, et al. Controlling pathological pain by adenovirally driven spinal production of the anti-inflammatory cytokine, interleukin-10. *Eur J Neurosci*. 2005;

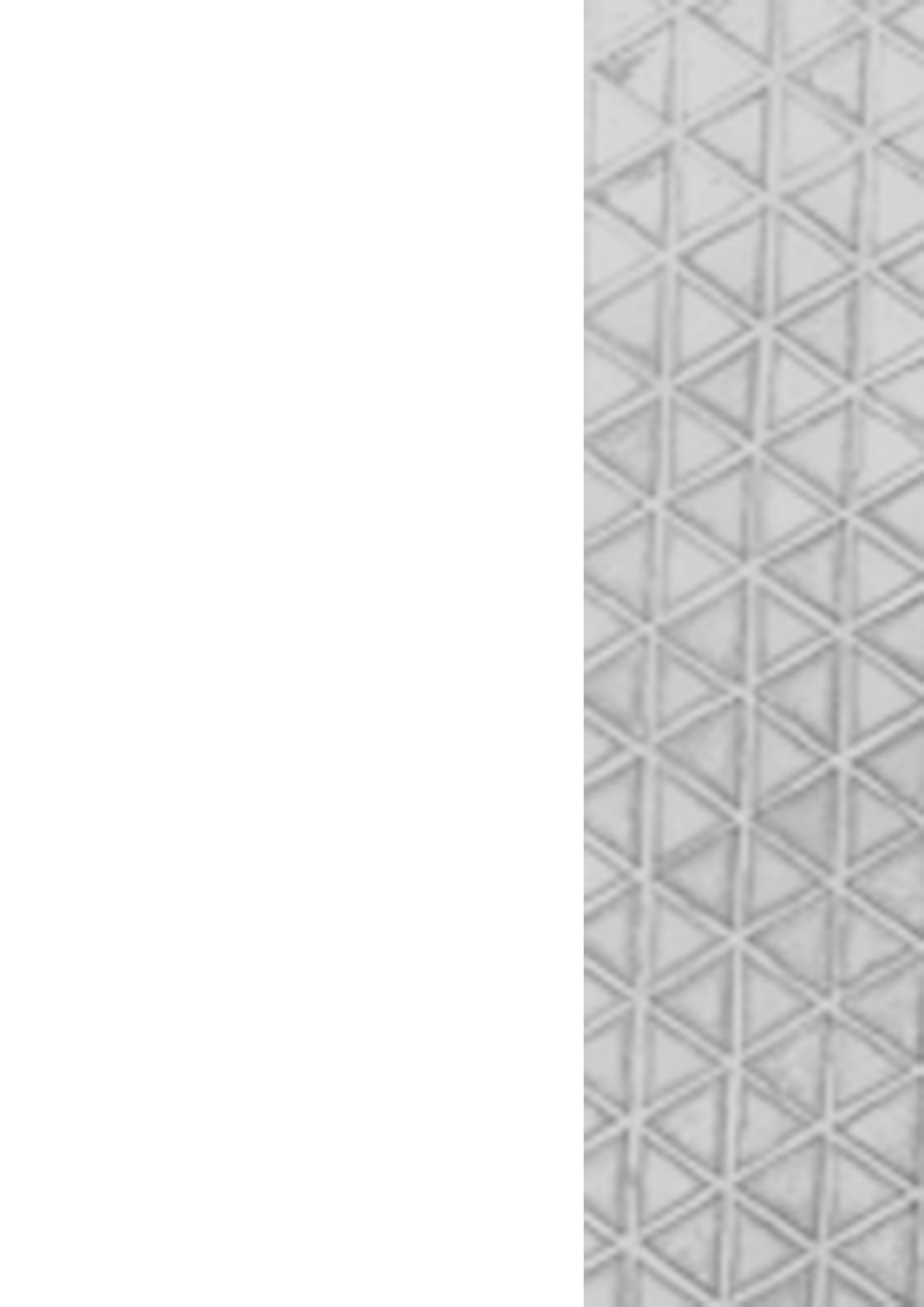
- 21:2136-2148.
165. Milligan, ED, Soderquist, RG, Malone, SM, et al. Intrathecal polymer-based interleukin-10 gene delivery for neuropathic pain. *Neuron Glia Biol.* 2006; 2:293-308.
 166. Milligan, ED and Watkins, LR. Pathological and protective roles of glia in chronic pain. *Nat Rev Neurosci.* 2009; 10:23-36.
 167. Milligan, ED, Penzkover, KR, Soderquist, RG, et al. Spinal Interleukin-10 Therapy to Treat Peripheral Neuropathic Pain. *Neuromodulation.* 2012.
 168. Moelants, EA, Mortier, A, Grauwen, K, et al. Citrullination of TNF-alpha by peptidylarginine deiminases reduces its capacity to stimulate the production of inflammatory chemokines. *Cytokine.* 2013; 61:161-167.
 169. Moller, AT and Jensen, TS. Pain and genes: Genetic contribution to pain variability, chronic pain and analgesic responses. 2010; 2010/09/10:197-201.
 170. Morreale, A, Gil-Redondo, R, and Ortiz, AR. A new implicit solvent model for protein-ligand docking. 2007; 2007/03/03:606-616.
 171. Muralidharan, A and Smith, MT. Pain, analgesia and genetics. *J Pharm Pharmacol.* 2011; 63:1387-1400.
 172. National Center for Health Statistics Hyattsville. Health, United States., 2006.
 173. Ndong, C, Landry, RP, Deleo, JA, et al. Mitogen activated protein kinase phosphatase-1 prevents the development of tactile sensitivity in a rodent model of neuropathic pain. *Mol Pain.* 2012; 2012/05/01:34.
 174. Nicholl, BI, Holliday, KL, Macfarlane, GJ, et al. No evidence for a role of the catechol-O-methyltransferase pain sensitivity haplotypes in chronic widespread pain. 2010; 2010/06/24:2009-2012.
 175. Nicholl, BI, Holliday, KL, Macfarlane, GJ, et al. Association of HTR2A polymorphisms with chronic widespread pain and the extent of musculoskeletal pain: results from two population-based cohorts. 2011; 2011/02/10:810-818.
 176. Nijboer, CH, Kavelaars, A, Vroon, A, et al. Low endogenous G-protein-coupled receptor kinase 2 sensitizes the immature brain to hypoxia-ischemia-induced gray and white matter damage. *J Neurosci.* 2008; 28:3324-3332.
 177. Nijboer, CH, Heijnen, CJ, Willemsen, HL, et al. Cell-specific roles of GRK2 in onset and severity of hypoxic-ischemic brain damage in neonatal mice. *Brain Behav Immun.* 2010; 24:420-426.
 178. Nijboer, CH, Gressens, P, Willemsen, HLDM, et al. Astrocyte GRK2 as a novel regulator of glutamate transport and brain damage. 2012.
 179. Nikolic, T, Geutskens, SB, van, RN, et al. Dendritic cells and macrophages are essential for the retention of lymphocytes in (peri)-insulinitis of the nonobese diabetic mouse: a phagocyte depletion study. *Lab Invest.* 2005; 85:487-501.
 180. O'Callaghan, JP and Miller, DB. Spinal glia and chronic pain. *Metabolism.* 2010; 59 Suppl 1:S21-S26.
 181. Offenbaecher, M, Bondy, B, de Jonge, S, et al. Possible association of fibromyalgia with a polymorphism in the serotonin transporter gene regulatory region. 1999; 1999/11/11:2482-2488.
 182. Oppermann, M, Mack, M, Proudfoot, AE, et al. Differential effects of CC chemokines on CC chemokine receptor 5 (CCR5) phosphorylation and identification of phosphorylation sites on the CCR5 carboxyl terminus. *J Biol Chem.* 1999; 274:8875-8885.
 183. Panagiotou, OA, Ioannidis, JP, and for the Genome-Wide Significance, P. What should the genome-wide significance threshold be? Empirical replication of borderline genetic associations. 2011; 2012/01/19.
 184. Pasero, C. Pathophysiology of neuropathic pain. *Pain Manag Nurs.* 2004; 5:3-8.
 185. Peregrin, S, Jurado-Pueyo, M, Campos, PM, et al. Phosphorylation of p38 by GRK2 at the docking groove unveils a novel mechanism for inactivating p38MAPK. *Curr Biol.* 2006; 16:2042-2047.
 186. Pérez, C and Ortiz, AR. Evaluation of docking functions for protein-ligand docking. 2001; 44:3768-3785.

187. Perl, ER. Ideas about pain, a historical view. *Nat Rev Neurosci.* 2007; 8:71-80.
188. Pitcher, JA, Freedman, NJ, and Lefkowitz, RJ. G protein-coupled receptor kinases. *Annu Rev Biochem.* 1998; 67:653-692.
189. Ponomarev, ED, Veremeyko, T, Barteneva, N, et al. MicroRNA-124 promotes microglia quiescence and suppresses EAE by deactivating macrophages via the C/EBP-alpha-PU.1 pathway. *Nat Med.* 2011; 17:64-70.
190. Potvin, S, Larouche, A, Normand, E, et al. DRD3 Ser9Gly polymorphism is related to thermal pain perception and modulation in chronic widespread pain patients and healthy controls. 2009; 2009/05/26:969-975.
191. Power, C, Atherton, K, and Manor, O. Co-occurrence of risk factors for cardiovascular disease by social class: 1958 British birth cohort. 2008; 2008/11/15:1030-1035.
192. Premont, RT and Gainetdinov, RR. Physiological roles of G protein-coupled receptor kinases and arrestins. *Annu Rev Physiol.* 2007; 69:511-534.
193. Pruim, RJ, Welch, RP, Sanna, S, et al. LocusZoom: regional visualization of genome-wide association scan results. 2010; 2010/07/17:2336-2337.
194. Purcell, S, Neale, B, Todd-Brown, K, et al. PLINK: a tool set for whole-genome association and population-based linkage analyses. 2007; 2007/08/19:559-575.
195. Raake, PW, Vinge, LE, Gao, E, et al. G protein-coupled receptor kinase 2 ablation in cardiac myocytes before or after myocardial infarction prevents heart failure. *Circ Res.* 2008; 103:413-422.
196. Rabbitt, P, McInnes, L, Diggle, P, et al. The University of Manchester longitudinal study of cognition in normal healthy old age, 1983 through 2003. 2004; 11:245-279.
197. Racine, M, Tousignant-Laflamme, Y, Kloda, LA, et al. A systematic literature review of 10years of research on sex/gender and experimental pain perception - Part 1: Are there really differences between women and men? 2011; 2011/12/24.
198. Raghavendra, V, Tanga, F, and DeLeo, JA. Inhibition of microglial activation attenuates the development but not existing hypersensitivity in a rat model of neuropathy. *J Pharmacol Exp Ther.* 2003; 306:624-630.
199. Rakvag, TT, Klepstad, P, Baar, C, et al. The Val158Met polymorphism of the human catechol-O-methyltransferase (COMT) gene may influence morphine requirements in cancer pain patients. *Pain.* 2005; 116:73-78.
200. Ramos-Ruiz, R, Penela, P, Penn, RB, et al. Analysis of the human G protein-coupled receptor kinase 2 (GRK2) gene promoter: regulation by signal transduction systems in aortic smooth muscle cells. *Circulation.* 2000; 101:2083-2089.
201. Ré, DB and Przedborski, S. Fractalkine: moving from chemotaxis to neuroprotection. *Nat Neurosci.* 2006; 9:859-861.
202. Reiter, E and Lefkowitz, RJ. GRKs and beta-arrestins: roles in receptor silencing, trafficking and signaling. *Trends Endocrinol Metab.* 2006; 17:159-165.
203. Remmers, AE, Martinez, C, and Daniels, S. 2008; 58:Suppl.
204. Ren, K and Dubner, R. Interactions between the immune and nervous systems in pain. *Nat Med.* 2010; 16:1267-1276.
205. Ribas, C, Penela, P, Murga, C, et al. The G protein-coupled receptor kinase (GRK) interactome: role of GRKs in GPCR regulation and signaling. *Biochim Biophys Acta.* 2007; 1768:913-922.
206. Richards, JB, Kavvoura, FK, Rivadeneira, F, et al. Collaborative meta-analysis: associations of 150 candidate genes with osteoporosis and osteoporotic fracture. 2009; 2009/10/21:528-537.
207. Riyazi, N, Meulenbelt, I, Kroon, HM, et al. Evidence for familial aggregation of hand, hip, and spine but not knee osteoarthritis in siblings with multiple joint involvement: the GARP study. 2005; 2004/10/02:438-443.
208. ROCS. ROCS. OpenEye Scientific Software, Santa Fe, NM.
209. Rolke, R, Baron, R, Maier, C, et al. Quantitative sensory testing in the German Research Network on Neuropathic Pain (DFNS): standardized protocol and reference values. 2006; 2006/05/16:231-243.

210. Romero-Sandoval, A, Chai, N, Nutile-McMenemy, N, et al. A comparison of spinal Iba1 and GFAP expression in rodent models of acute and chronic pain. *Brain Res.* 2008; 1219:116-126.
211. Rutkowski, MD, Pahl, JL, Sweitzer, S, et al. Limited role of macrophages in generation of nerve injury-induced mechanical allodynia. *Physiol Behav.* 2000; 71:225-235.
212. Ryckaert, JP, Ciccotti, G, and Berendsen, HJC. Numerical integration of the cartesian equations of motion of a system with constraints: molecular dynamics of n-alkanes. 1977; 23:327-341.
213. Saeij, JP, Wiegertjes, GF, and Stet, RJ. Identification and characterization of a fish natural resistance-associated macrophage protein (NRAMP) cDNA. *Immunogenetics.* 1999; 50:60-66.
214. Sandrini, G, Serrao, M, Rossi, P, et al. The lower limb flexion reflex in humans. *Prog Neurobiol.* 2005; 77:353-395.
215. Schadt, EE, Molony, C, Chudin, E, et al. Mapping the genetic architecture of gene expression in human liver. 2008; 2008/05/09:e107.
216. Scholz, J and Woolf, CJ. The neuropathic pain triad: neurons, immune cells and glia. *Nat Neurosci.* 2007; 10:1361-1368.
217. Shechter, R, London, A, Varol, C, et al. Infiltrating blood-derived macrophages are vital cells playing an anti-inflammatory role in recovery from spinal cord injury in mice. *PLoS Med.* 2009; 6:e1000113.
218. Silman, AJ and Pearson, JE. Epidemiology and genetics of rheumatoid arthritis. 2002; 2002/07/12:S265-S272.
219. Skrbo, A, Begovic, B, and Skrbo, S. [Classification of drugs using the ATC system (Anatomic, Therapeutic, Chemical Classification) and the latest changes] Klasificiranje lijekova po ATC sistemu i najnovije izmjene. 2004; 2004/05/13:138-141.
220. Sloane, EM, Soderquist, RG, Maier, SF, et al. Long-term control of neuropathic pain in a non-viral gene therapy paradigm. *Gene Ther.* 2009; 16:470-475.
221. Spector, TD and MacGregor, AJ. The St. Thomas' UK Adult Twin Registry. 2002; 2003/01/23:440-443.
222. Spector, TD and Williams, FM. The UK Adult Twin Registry (TwinsUK). 2006; 2007/01/27:899-906.
223. Stewart, JJ. MOPAC: a semiempirical molecular orbital program. 1990; 4:1-105.
224. Stirling, LC, Forlani, G, Baker, MD, et al. Nociceptor-specific gene deletion using heterozygous NaV1.8-Cre recombinase mice. *Pain.* 2005; 113:27-36.
225. Su, SY, Chen, JJ, Lai, CC, et al. The association between fibromyalgia and polymorphism of monoamine oxidase A and interleukin-4. 2007; 2006/03/21:12-16.
226. Sun, S, Cao, H, Han, M, et al. New evidence for the involvement of spinal fractalkine receptor in pain facilitation and spinal glial activation in rat model of monoarthritis. *Pain.* 2007; 129:64-75.
227. Syddall, HE, Aihie Sayer, A, Dennison, EM, et al. Cohort profile: the Hertfordshire cohort study. 2005; 2005/06/21:1234-1242.
228. Syvanen, AC, Tilgmann, C, Rinne, J, et al. Genetic polymorphism of catechol-O-methyltransferase (COMT): correlation of genotype with individual variation of S-COMT activity and comparison of the allele frequencies in the normal population and parkinsonian patients in Finland. 1997; 1997/02/01:65-71.
229. Tander, B, Gunes, S, Boke, O, et al. Polymorphisms of the serotonin-2A receptor and catechol-O-methyltransferase genes: a study on fibromyalgia susceptibility. 2008; 2008/01/16:685-691.
230. Tegeder, I, Costigan, M, Griffin, RS, et al. GTP cyclohydrolase and tetrahydrobiopterin regulate pain sensitivity and persistence. 2006; 2006/10/24:1269-1277.
231. Teo, YY, Inouye, M, Small, KS, et al. A genotype calling algorithm for the Illumina BeadArray platform. 2007; 2007/09/12:2741-2746.
232. Tetko, IV, Gasteiger, J, Todeschini, R, et al. Virtual computational chemistry laboratory--design and description. 2005; 2005/10/19:453-463.
233. Tikka, T, Fiebich, BL, Goldsteins, G, et al. Minocycline, a tetracycline derivative, is neuroprotective against excitotoxicity by inhibiting activation and proliferation of microglia. *J Neurosci.* 2001; 21:2580-2588.

234. Trang, T, Beggs, S, and Salter, MW. ATP receptors gate microglia signaling in neuropathic pain. *Exp Neurol*. 2012; 234:354-361.
235. van Meurs, JB, Uitterlinden, AG, Stolck, L, et al. A functional polymorphism in the catechol-O-methyltransferase gene is associated with osteoarthritis-related pain. 2009; 2009/01/31:628-629.
236. van Rooijen, N and Sanders, A. Liposome mediated depletion of macrophages: mechanism of action, preparation of liposomes and applications. *J Immunol Methods*. 1994; 174:83-93.
237. Vargas-Alarcon, G, Fragoso, JM, Cruz-Robles, D, et al. Catechol-O-methyltransferase gene haplotypes in Mexican and Spanish patients with fibromyalgia. 2007; 2007/10/27:R110.
238. Verge, GM, Milligan, ED, Maier, SF, et al. Fractalkine (CX3CL1) and fractalkine receptor (CX3CR1) distribution in spinal cord and dorsal root ganglia under basal and neuropathic pain conditions. *Eur J Neurosci*. 2004; 20:1150-1160.
239. Volzke, H, Alte, D, Schmidt, CO, et al. Cohort profile: the study of health in Pomerania. 2011; 2010/02/20:294-307.
240. Vroon, A, Lombardi, MS, Kavelaars, A, et al. Changes in the G-protein-coupled receptor desensitization machinery during relapsing-progressive experimental allergic encephalomyelitis. *J Neuroimmunol*. 2003; 137:79-86.
241. Vroon, A, Heijnen, CJ, Lombardi, MS, et al. Reduced GRK2 level in T cells potentiates chemotaxis and signaling in response to CCL4. *J Leukoc Biol*. 2004; 75:901-909.
242. Vroon, A, Kavelaars, A, Limmroth, V, et al. G protein-coupled receptor kinase 2 in multiple sclerosis and experimental autoimmune encephalomyelitis. *J Immunol*. 2005; 174:4400-4406.
243. Vroon, A, Heijnen, CJ, and Kavelaars, A. GRKs and arrestins: regulators of migration and inflammation. *J Leukoc Biol*. 2006; 80:1214-1221.
244. Vroon, A, Lombardi, MS, Kavelaars, A, et al. Taxol normalizes the impaired agonist-induced beta2-adrenoceptor internalization in splenocytes from GRK2+/- mice. *Eur J Pharmacol*. 2007; 560:9-16.
245. Wang, H, Heijnen, CJ, Eijkelkamp, N, et al. GRK2 in sensory neurons regulates epinephrine-induced signalling and duration of mechanical hyperalgesia. *Pain*. 2011; 152:1649-1658.
246. Wang, H, Heijnen, CJ, Velthoven, vCTJ, et al. Targeting the GRK2-Epac1 ratio to prevent transition to chronic pain. 2012.
247. Wang, J, Cieplak, P, and Kollman, PA. How well does a restrained electrostatic potential (RESP) model perform in calculating conformational energies of organic and biological molecules? 2000; 21:1049-1074.
248. Wang, K, Murcia, M, Constans, P, et al. Gaussian mapping of chemical fragments in ligand binding sites. 2004; 2004/08/04:101-118.
249. Watkins, LR and Maier, SF. Glia: a novel drug discovery target for clinical pain. *Nat Rev Drug Discov*. 2003; 2:973-985.
250. Watkins, LR, Hutchinson, MR, Ledebor, A, et al. Norman Cousins Lecture. Glia as the "bad guys": implications for improving clinical pain control and the clinical utility of opioids. *Brain Behav Immun*. 2007; 21:131-146.
251. Weininger, D. SMILES, a chemical language and information system. 1. Introduction to methodology and encoding rules. 1988; 28:31-36.
252. Wellcome Trust Case Control, C. Genome-wide association study of 14,000 cases of seven common diseases and 3,000 shared controls. 2007; 2007/06/08:661-678.
253. Weng, HR, Chen, JH, and Cata, JP. Inhibition of glutamate uptake in the spinal cord induces hyperalgesia and increased responses of spinal dorsal horn neurons to peripheral afferent stimulation. *Neuroscience*. 2006; 138:1351-1360.
254. Wettschureck, N and Offermanns, S. Mammalian G proteins and their cell type specific functions. *Physiol Rev*. 2005; 85:1159-1204.
255. Wieseler-Frank, J, Maier, SF, and Watkins, LR. Glial activation and pathological pain. *Neurochem Int*. 2004; 45:389-395.
256. Wilkerson, JL, Gentry, KR, Dengler, EC, et al. Intrathecal cannabidiol CB(2)R agonist, AM1710,

- controls pathological pain and restores basal cytokine levels. *Pain*. 2012; 153:1091-1106.
257. Willemen, HL, Eijkelkamp, N, Wang, H, et al. Microglial/macrophage GRK2 determines duration of peripheral IL-1 β -induced hyperalgesia: contribution of spinal cord CX3CR1, p38 and IL-1 signaling. *Pain*. 2010; 150:550-560.
 258. Willemen, HL, Huo, XJ, Mao-Ying, QL, et al. MicroRNA-124 as a novel treatment for persistent hyperalgesia. *J Neuroinflammation*. 2012; 9:143.
 259. Willer, CJ, Li, Y, and Abecasis, GR. METAL: fast and efficient meta-analysis of genomewide association scans. 2010; 2010/07/10:2190-2191.
 260. Wolfe, F, Smythe, HA, Yunus, MB, et al. The American College of Rheumatology 1990 Criteria for the Classification of Fibromyalgia. Report of the Multicenter Criteria Committee. 1990; 1990/02/01:160-172.
 261. Woolf, CJ. Pain: moving from symptom control toward mechanism-specific pharmacologic management. *Ann Intern Med*. 2004; 140:441-451.
 262. Woolf, CJ and Ma, Q. Nociceptors--noxious stimulus detectors. *Neuron*. 2007; 55:353-364.
 263. Xin, WJ, Weng, HR, and Dougherty, PM. Plasticity in expression of the glutamate transporters GLT-1 and GLAST in spinal dorsal horn glial cells following partial sciatic nerve ligation. *Mol Pain*. 2009; 5:15.
 264. Xu, JT, Tu, HY, Xin, WJ, et al. Activation of phosphatidylinositol 3-kinase and protein kinase B/Akt in dorsal root ganglia and spinal cord contributes to the neuropathic pain induced by spinal nerve ligation in rats. *Exp Neurol*. 2007; 206:269-279.
 265. Yang, Y, Shu, X, Liu, D, et al. EPAC null mutation impairs learning and social interactions via aberrant regulation of miR-124 and Zif268 translation. *Neuron*. 2012; 73:774-788.
 266. Yu, W, Clyne, M, Khoury, MJ, et al. Phenopedia and Genopedia: disease-centered and gene-centered views of the evolving knowledge of human genetic associations. 2010; 2009/10/30:145-146.
 267. Yudoh, K, Matsuno, H, Nakazawa, F, et al. Reduced expression of the regulatory CD4⁺ T cell subset is related to Th1/Th2 balance and disease severity in rheumatoid arthritis. *Arthritis Rheum*. 2000; 43:617-627.
 268. Zhang, P, Iwasaki-Arai, J, Iwasaki, H, et al. Enhancement of hematopoietic stem cell repopulating capacity and self-renewal in the absence of the transcription factor C/EBP α . *Immunity*. 2004; 21:853-863.
 269. Zhang, X, Ozawa, Y, Lee, H, et al. Histone deacetylase 3 (HDAC3) activity is regulated by interaction with protein serine/threonine phosphatase 4. *Genes Dev*. 2005; 19:827-839.
 270. Zhang, X, Li, L, and McNaughton, PA. Proinflammatory mediators modulate the heat-activated ion channel TRPV1 via the scaffolding protein AKAP79/150. *Neuron*. 2008; 59:450-461.
 271. Zhao, J, Yuan, G, Cendan, CM, et al. Nociceptor-expressed ephrin-B2 regulates inflammatory and neuropathic pain. 2010; 2010/11/10:77.
 272. Zhao, J, Lee, MC, Momin, A, et al. Small RNAs control sodium channel expression, nociceptor excitability, and pain thresholds. *J Neurosci*. 2010; 30:10860-10871.
 273. Zhao, Z, Timofeev, N, Hartley, SW, et al. Imputation of missing genotypes: an empirical evaluation of IMPUTE. 2008; 2008/12/17:85.
 274. Zheng, W, Ouyang, H, Zheng, X, et al. Glial TNF α in the spinal cord regulates neuropathic pain induced by HIV gp120 application in rats. *Mol Pain*. 2011; 7:40.
 275. Zhuang, ZY, Kawasaki, Y, Tan, PH, et al. Role of the CX3CR1/p38 MAPK pathway in spinal microglia for the development of neuropathic pain following nerve injury-induced cleavage of fractalkine. *Brain Behav Immun*. 2007; 21:642-651.
 276. Zin, CS, Nissen, LM, O'Callaghan, JP, et al. Preliminary study of the plasma and cerebrospinal fluid concentrations of IL-6 and IL-10 in patients with chronic pain receiving intrathecal opioid infusions by chronically implanted pump for pain management. *Pain Med*. 2010; 11:550-561.
 277. Zubieta, JK, Heitzeg, MM, Smith, YR, et al. COMT val158met genotype affects mu-opioid neurotransmitter responses to a pain stressor. 2003; 2003/02/22:1240-1243.



Nederlandse samenvatting

Pijn is een belangrijk beschermend signaal. Specifieke receptoren in perifere zenuwcellen (neuronen), zogenoemde nociceptoren, detecteren en reageren op de aanwezigheid van mogelijk schadelijke stimuli, zoals hitte, druk, weefselschade of een ontsteking, om mogelijke (verdere) weefselbeschadiging te voorkomen. De ontstekingsmediatoren die geproduceerd worden tijdens weefselschade en/of ontsteking kunnen de gevoeligheid voor signalering van de nociceptoren veranderen. Bijvoorbeeld een verhoogde gevoeligheid voor pijnlijke prikkels (hyperalgesie) of voor prikkels die normaal gesproken geen pijn zouden veroorzaken (allodynia). Pijnprikkels kunnen lokaal gedetecteerd worden door perifere neuronen of door neuronen in het centrale zenuwstelsel, zoals in het ruggenmerg, waar de pijnprikkels uiteindelijk naar de hersenen worden geleid. In het ruggenmerg zijn naast neuronen ook microglia en astrocyten (ontstekingscellen) aanwezig, die de gevoeligheid van neuronen kunnen reguleren en dus ook een belangrijke rol spelen tijdens hyperalgesie. Normaal zijn de fysiologische veranderingen van de nociceptoren van tijdelijke aard en kunnen zo beschermen tegen verdere weefselschade. Echter, in sommige gevallen kan, nadat de weefselbeschadiging is genezen of de ontsteking voorbij is, een verhoogde gevoeligheid van de nociceptoren blijven bestaan hetgeen zich vertaalt in de ontwikkeling van chronische pijn. Het ontstaan van chronische pijn is een groot klinisch probleem omdat de huidige therapieën nog niet effectief genoeg zijn om chronische pijn te voorkomen of te bestrijden. Daarom is er een grote behoefte om nieuwe therapeutische targets te identificeren. Om deze therapeutische targets te ontdekken, moeten we het mechanisme ontrafelen dat verantwoordelijk is voor het ontstaan en onderhouden van chronische pijn.

Veel ontstekingsmediatoren (zoals chemokines, cytokines en neurotransmitters) binden aan een specifieke familie van receptoren, genaamd G proteïne-gekoppelde-receptoren (GPCRs). GPCRs zijn aanwezig aan de oppervlakte van cellen en spelen een rol bij het doorgeven van signalen. Wanneer een ontstekingsmediator bindt aan de GPCR worden G proteïne-gekoppelde-receptoren-kinases (GRKs) geactiveerd. GRKs fosforyleren de receptor waardoor de GPCR ongevoelig wordt gemaakt. Tevens wordt de GPCR verwijderd van de oppervlakte van de cel (internalisatie), zodat de receptor niet meer geactiveerd kan worden. GRKs hebben dus een belangrijke functie in het reguleren van de gevoeligheid van de GPCR en zijn essentieel om GPCR signalering te beëindigen, een proces dat overstimulatie van cellen voorkomt. Recent onderzoek heeft uitgewezen dat GRKs niet alleen GPCRs reguleren, maar dat GRKs ook aan andere eiwitten kunnen binden om signalering van de cel te beïnvloeden.

Recent heeft onze onderzoeksgroep aangetoond dat het gehalte van een bepaald GRK-subtype, namelijk GRK2, is verlaagd in witte bloedcellen van patiënten met een chronische ontstekingsziekte, zoals reumatoïde artritis of multiple sclerose. Hetzelfde geldt in diermodellen voor deze ziektes. In verschillende celkweken is aangetoond dat ontstekingsmediatoren het gehalte van GRK2 verlagen. Dit geeft aan dat tijdens chronische ontsteking GRK2 verlaagd wordt door de geproduceerde ontstekingsmediatoren. Recent heeft onze onderzoeksgroep aangetoond dat in het ruggenmerg van ratten met neuropatische pijn (zenuwpijn) het GRK2 gehalte met 35-55% verlaagd was. Vervolgens is bestudeerd wat de gevolgen zijn van een laag GRK2-gehalte voor het ontstaan van ontstekings-geïnduceerde chronische pijn. Hiervoor is gebruik gemaakt van knock-out muizen met een partiële deletie van het GRK2-gen, ook wel GRK2^{+/-} muizen genoemd (ongeveer 50% reductie in het GRK2 eiwit) en als controle werden wild type (WT) muizen gebruikt. Een ontsteking werd geïnduceerd door het toedienen van carrageenan (stofje geïsoleerd uit zeewier) in de poot van de muis en vervolgens werd de thermische gevoeligheid van de muis getest met de "Hargreaves Test". In deze test wordt een warmtebron op de poot van de muis gericht en gemeten wordt hoe snel de muis zijn pootje wegtrekt. Hoe eerder de muis

reageert, hoe gevoeliger het dier is voor de thermische prikkel. Carrageenan injectie in de poot van WT muizen induceert gedurende 2-3 dagen thermische hyperalgesie in WT muizen, terwijl GRK2^{+/-} muizen een verhoogde en langdurige hyperalgesia ontwikkelen die drie weken duurt. Ook andere ontstekingsstofjes (zoals PGE2, CCL3, adrenaline) induceren chronische hyperalgesie in GRK2^{+/-} muizen. Door het gebruik van celspecifieke knock-out muizen, kan onderzocht worden welke celtypen een rol spelen in het ontstaan van chronische pijn. Recent heeft onze onderzoeksgroep beschreven dat muizen met een verlaagd GRK2-gehalte in LysM-positieve cellen (zoals microglia/macrofagen/granulocyten), ook wel LysM-GRK2^{+/-} muizen genoemd, chronische hyperalgesie ontwikkelen na een carrageenan injectie in de poot. Daarbij is aangetoond dat in GRK2^{+/-} muizen de ontstekings-geïnduceerde chronische pijn geremd kan worden door microglia/macrofagen activiteit in het ruggenmerg te dempen. Deze eerdere bevindingen suggereren dat GRK2 in microglia/macrofagen een cruciale factor is voor het regelen van ontstekingsgeïnduceerde hyperalgesie. Het hoofddoel van de studies, welke zijn beschreven in dit proefschrift, was om de rol van GRK2 tijdens ontstekingsgeïnduceerde chronische hyperalgesie te bestuderen en nieuwe neurobiologische mechanismes te ontrafelen.

Hoofdstuk 2 laat zien dat het GRK2-gehalte verlaagd is (ongeveer met 40%) in microglia/macrofagen geïsoleerd uit het ruggenmerg van muizen met ontstekingsgeïnduceerde chronische hyperalgesie. De rol van GRK2 in microglia/macrofagen is vervolgens bestudeerd in muizen met chronische hyperalgesie. Hyperalgesie werd geïnduceerd door een injectie met het pro-inflammatoire cytokine IL-1 β in de poot van WT en LysM-GRK2^{+/-} muizen. Een sterke verlenging van de hyperalgesie werd waargenomen in LysM-GRK2^{+/-} muizen (> 8 dagen) in vergelijking tot WT muizen (< 1 dag). Een laag GRK2-gehalte in neuronen of in astrocyten gaf geen verschil in de intensiteit en de duur van de hyperalgesie. De chronische hyperalgesie in LysM-GRK2^{+/-} muizen kan geremd worden door de microglia/macrofagen activiteit in het ruggenmerg te dempen. Dit geeft aan dat microglia/macrofaag activiteit een cruciale rol speelt in het onderhouden van de chronische hyperalgesie in LysM-GRK2^{+/-} muizen. Daarnaast bleek dat de chronische hyperalgesie wordt onderhouden door het activeren van de fractalkine signaleringsroute in het ruggenmerg van LysM-GRK2^{+/-} muizen. Door het remmen van deze route en van specifieke signaleringseiwitten p38 en IL-1 kunnen we namelijk de chronische hyperalgesie opheffen in LysM-GRK2^{+/-} muizen. De resultaten in dit hoofdstuk suggereren dat een chronische ontsteking het GRK2-gehalte in microglia/macrofagen doet verlagen, waardoor microglia/macrofaag activiteit in het ruggenmerg niet gedempt wordt. Hierbij wordt de fractalkine signaleringsroute wordt geïnitieerd, wat vervolgens bijdraagt aan het ontstaan van IL-1 β -geïnduceerde chronische hyperalgesie.

In hoofdstuk 3 beschrijven we hoe de microglia/macrofaag activiteit in het ruggenmerg gereguleerd wordt en welk signaal ervoor kan zorgen dat deze activiteit geremd kan worden. Recent is beschreven dat microRNA-124 (miR-124) microglia activiteit kan dempen. Ons genetisch materiaal is opgeslagen in DNA. RNA kopieert de genetische informatie en kan vervolgens de eiwitsynthese regelen. MicroRNA is een niet-coderend stuk RNA maar het kan wel de expressie van genen reguleren door bijvoorbeeld stukjes coderend RNA af te breken of te voorkomen dat eiwitsynthese plaatsvindt. Hoofdstuk 3 laat zien dat miR-124 expressie significant verlaagd is in microglia van LysM-GRK2^{+/-} muizen in vergelijking tot geïsoleerde microglia van WT muizen na IL-1 β injectie in de poot. Na injectie van IL-1 β in de poot is er een meer pro-inflammatoire fenotype, zogenaamd M1-type, en minder anti-inflammatoire fenotype, zogenaamd M2-type, zichtbaar in het ruggenmerg van LysM-GRK2^{+/-} muizen. Als LysM-GRK2^{+/-} muizen een miR-124 injectie in het ruggenmerg krijgen, voorafgaand aan injectie van IL-1 β in de poot, wordt de M1/M2 ratio genormaliseerd. Daarbij hebben we de belangrijke bevinding

gedaan dat miR-124 het ontwikkelen van de chronische hyperalgesie voorkomt. Daarnaast zien we in WT muizen dat miR-124 injectie carrageenan-geïnduceerde hyperalgesie remt en dat chronische neuropatische pijn voorkomen wordt na zenuw schade. Dit geeft aan dat miR-124 behandeling een nieuwe methode kan worden voor het behandelen van chronische pijn.

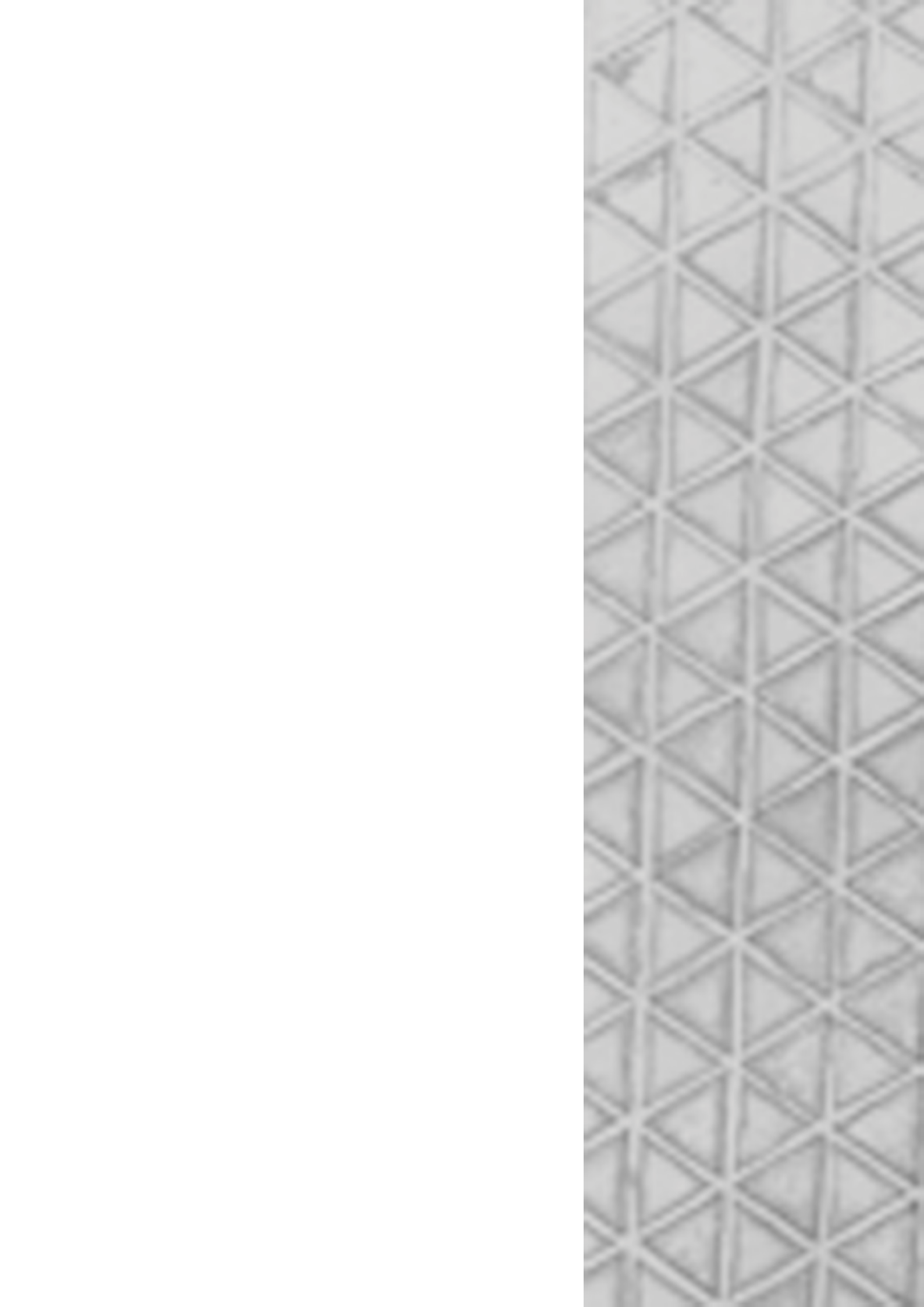
In hoofdstuk 4 beschrijven we of specifieke perifere cellen, namelijk macrofagen/monocyten, bijdragen aan het ontstaan van chronische pijn. Als we deze cellen depletieren ontstaat er chronische hyperalgesie in WT muizen (> 1 week) na injectie van IL-1 β , terwijl WT muizen normaalgesproken alleen acute hyperalgesie ontwikkelen (< 1 dag). Daarentegen heeft depletie van macrofagen/monocyten in LysM-GRK2^{+/-} muizen geen effect op het verloop van de hyperalgesie en deze blijft dus chronisch. Deze bevinding geeft aan dat perifere monocyten/macrofagen een cruciale rol spelen in het voorkomen van de transitie van acute naar chronische hyperalgesie. Vervolgens hebben we vooraf aan IL-1 β in de poot, WT monocyten overgebracht naar LysM-GRK2^{+/-} muizen wat het ontstaan van chronische pijn voorkomt. Daarentegen heeft het overbrengen van GRK2^{+/-} monocyten in LysM-GRK2^{+/-} muizen geen effect op het verloop van de hyperalgesie en blijft deze dus chronisch. Dit suggereert dat WT monocyten een bepaalde stof produceren die de transitie van acute naar chronische hyperalgesia kan voorkomen. Op celniveau vonden we dat GRK2^{+/-} macrofagen minder het anti-inflammatoire cytokine IL-10 produceren dan WT macrofagen. Daarbij geeft IL-10 behandeling een tijdelijke remming van IL-1 β -geïnduceerde chronische hyperalgesie in LysM-GRK2^{+/-} muizen. Als we IL-10 wegvangen in WT muizen, ontwikkelen deze muizen chronische hyperalgesie na IL-1 β in de poot. Daarnaast hebben we in hoofdstuk 4 beschreven dat het overbrengen van IL10^{-/-} monocyten (deze brengen geen IL-10 tot expressie) naar LysM-GRK2^{+/-} muizen het ontstaan van IL-1 β -geïnduceerde chronische hyperalgesie niet kan voorkomen. Dit geeft aan dat IL-10 een belangrijk anti-inflammatoir cytokine is dat de transitie van acute naar chronische hyperalgesie kan reguleren. Wij suggereren dat perifere macrofagen/monocyten met laag GRK2 een verlaagde IL-10 expressie hebben, wat ertoe leidt dat de microglia-activiteit in het ruggenmerg niet gedempt wordt en zo chronische hyperalgesie ontstaat. De suggestie dat perifere macrofagen/monocyten cruciaal zijn voor de regulatie van ontstekings-geïnduceerde pijn wordt versterkt door de interessante bevinding dat LysM-GRK2^{+/-} muizen een verlaagd GRK2 gehalte hebben in perifere macrofagen, maar normale GRK2 gehalten hebben in geïsoleerde microglia uit het ruggenmerg (hoofdstuk 4).

In hoofdstuk 5 beschrijven we de ontwikkeling van een nieuwe potentieel medicijn om chronische pijn te bestrijden. Het signaleringsmolecuul p38 MAPK is een belangrijk molecuul dat de productie van verschillende ontstekingsmediatoren reguleert. In verschillende diermodellen is aangetoond dat p38 MAPK verhoogd is tijdens chronische pijn en dat een p38 MAPK remmer de pijn tijdelijk kan remmen. Verschillende academische groepen en farmaceutische bedrijven hebben onderzoek verricht naar het ontwikkelen van een p38 MAPK remmer. Zelfs is een aantal van deze remmers al getest op patiënten, met bijvoorbeeld reumatoïde artritis, maar helaas waren de resultaten teleurstellend. De meeste van deze p38 MAPK remmers zijn gemaakt tegen een bepaalde plek op het p38 MAPK molecuul, maar deze plek komt ook voor op verschillende andere eiwitten, en is dus niet uniek. Dit is zeer nadelig, want hierdoor kan ook de activiteit van andere eiwitten beïnvloed worden. Daarom is er een grote behoefte om nieuwe meer specifieke p38 MAPK remmers te ontwikkelen. Recent is beschreven dat een nieuwe, meer specifieke plek op het p38 MAPK molecuul gevonden is en door het blokkeren van deze plek het p38 MAPK molecuul minder activiteit heeft. Met deze kennis hebben we in hoofdstuk 5 onderzocht of we een nieuwe remmer tegen deze mogelijk specifiekere plek op het p38 MAPK molecuul kunnen ontwikkelen. We hebben verschillende moleculen ontwikkeld en getest, waarvan molecuul FGA-

19 het meest potentieel bleek te hebben. We vonden namelijk op celniveau dat een verlaagde p38 MAPK activiteit ontstaat na een FGA-19 behandeling. Daarnaast kunnen we carrageenan-geïnduceerde chronische hyperalgesie remmen met een FGA-19 injectie in het ruggenmerg van WT muizen. Het pijnstillend effect van FGA-19 is duidelijk langduriger (> 5 dagen) in vergelijking tot de commercieel verkrijgbare p38 MAPK remmer, SB239063 (< 6 uur). In de toekomst zullen we verder onderzoeken of een FGA-19 behandeling geen nadelige specifieke bijwerkingen heeft. We suggereren dat FGA-19 een potentieel nieuw medicijn kan zijn voor het behandelen van chronische hyperalgesie.

In hoofdstuk 6 hebben we een genetisch onderzoek uitgevoerd in patiënten met “chronic widespread pain (CWP)”, ook wel bekend als fibromyalgie. Het doel hiervan is om eventuele nieuwe genen te ontdekken die betrokken kunnen zijn bij het ontstaan van chronische pijn. Het DNA is uit bloed geïsoleerd van 1308 patiënten met CWP en 5791 controles. Het DNA is gebruikt om een enkel-nucleotide polymorfisme te ontdekken (Engels: Single nucleotide polymorphism, afgekort als SNP), wat betekent dat één bouwsteen (nucleotide) op één specifieke plaats in het DNA veranderd is. Van elke persoon zitten in het DNA grote hoeveelheden SNP's (> 5 miljoen), doordat er kleine foutjes ontstaan bij het kopiëren van het DNA. Meestal heeft dit geen nadelig effect. In sommige gevallen, echter, kan een bepaalde SNP de functie van een gen beïnvloeden. In hoofdstuk 6 vinden we dat één bepaalde SNP significant vaker voorkomt in patiënten met CWP in vergelijking met controledonoren zonder chronische pijn. Deze SNP ligt in de buurt van twee verschillende genen, namelijk CCT5 en FAM173b. We hebben aangetoond dat muizen met chronische pijn een verhoging hebben van het CCT5 en FAM173b eiwit. Dit is een interessante bevinding en kan klinisch zeer interessant zijn om nieuwe aanknopingspunten te vinden om chronische pijn te bestrijden.

De resultaten beschreven in dit proefschrift laten zien dat perifere monocyten/macrofagen een cruciale rol spelen in het voorkomen van ontstekings-geïnduceerde chronische hyperalgesie. We suggereren dat een laag GRK2-gehalte in perifere macrofagen ertoe leidt dat er een verlaagde IL-10 productie is, wat er vervolgens toe leidt dat microglia en de fractalkine signaleringsroute in het ruggenmerg geactiveerd worden, wat bijdraagt aan het ontstaan van chronische hyperalgesie. Daarnaast suggereren we dat een afwijkende miR-124 productie ervoor kan zorgen dat microglia activatie niet wordt uitgeschakeld. Verder zijn in dit proefschrift mogelijke nieuwe opties weergegeven voor het bestrijden van chronische pijn. De studies die zijn uitgevoerd geven nieuwe inzichten in welke mechanismes betrokken kunnen zijn bij het ontstaan van chronische ontstekingspijn. Deze nieuwe gegevens kunnen helpen bij het ontwikkelen van nieuwe medicijnen die chronische pijn kunnen bestrijden.



Dankwoord - Acknowledgements

Jeetje, mijn proefschrift is af! Wie had dat ooit gedacht? Ik in ieder geval niet, aangezien een paar jaar geleden promoveren niet echt mijn doel was. Na 1,5 jaar als research analist gewerkt te hebben, begon ik het research gedeelte toch wel echt interessanter te vinden. Ik ben dan ook als allereerste mijn twee promotoren bijzonder dankbaar voor het vertrouwen en de stimulans om het promotietraject in te gaan.

Hooggeleerde Professor Heijnen, beste Cobi, bedankt voor alles wat je me afgelopen jaren geleerd hebt. Ik heb veel geleerd van alle werkbeprekingen en de ideeën voor experimenten. Je hebt kennis over heel veel verschillende onderzoeksgebieden. Daarnaast ben je erg begaan met iedereen, waardoor iedereen zich snel thuis voelt in het NIDOD-lab. Ik wilde graag mijn proefschrift in 2012 afronden en ik wil je dan ook bedanken voor je inzet om dat te laten lukken. Ik vind het erg bijzonder dat je je carrière voortzet in Houston. Ik hoop dat je er snel thuis voelt en ik ben blij dat we je nog regelmatig in het lab of via skype zien. Fijn dat ik mijn onderzoek in het NIDOD-lab kan voortzetten!

Hooggeleerde Professor Kavelaars, beste Annemieke, bedankt voor alles! Ik heb veel geleerd over hoe je nou eigenlijk goed onderzoek doet. Naast de vele theoretische kennis had je ook altijd veel tips en ideeën over hoe je een experiment goed kunt uitvoeren. Jouw kritische blik heeft er mede toe bijgedragen dat er een paar mooie publicaties de deur uit zijn gegaan. Jouw snelle reacties hebben er ook zeker aan bijgedragen dat ik mijn proefschrift in december bij de commissie heb kunnen inleveren. Ik vind het leuk dat ik je eerste Nederlandse promovendus ben; met ook jou als promotor, heb ik er nu gewoon twee! Ik wil je veel succes wensen in Houston, maar volgens mij heb je je plek daar al goed gevonden. Ik hoop dat we nog een lange tijd kunnen samenwerken.

Zeergeleerde Dr. Eijkelkamp, beste Niels, leuk dat jij mijn co-promotor bent! Als pijngoeroe heb je me de beginselen van het pijnonderzoek geleerd, bedankt daarvoor! Ik kan me nog goed herinneren dat jij me introduceerde op het GDL om voor het eerst met muizen te werken, dat was even wennen! Je bent een erg gezellige collega en we hebben veel leuke borrels, uitjes en feestjes gehad. Twee jaar heb je in Londen gezeten en nu ben je alweer bijna een jaar terug op het NIDOD-lab. Nu heb je een belangrijke verantwoordelijke functie gekregen, wat erg spannend is, maar ik weet zeker dat je snel je draai daarin zult vinden. Ik vind het een hele leuke uitdaging om samen met het pijnonderzoek verder te gaan en hopelijk kunnen we de groep snel wat uitbreiden. Op naar spannende nieuwe publicaties!

Next I like to thank my ex-colleagues in the pain group: Dear Huijing, it was really nice working together with you! You helped me a lot with the animal experiments and you are the expert in DRG-isolation and intrathecal injections. During our work we also laughed a lot, since often it was a mess, but finally we got some nice results. Thank you for all your help! You are not only a great researcher but also a nice person to have around. I really miss you but I am very glad for you that you are back in China with your husband, daughter, family and friends. Best of luck with your career and we keep in touch! Dear Anibal, it was nice to collaborate with you on the pain projects. But next to work, it was even nicer to have you as a colleague, since you are a person with a good sense of humor. We laughed a lot! With our Spanglish, Dungleish and hands we understood each other quite well. When you left to Germany it became a little bit quiet in the PhD-room... Good luck with everything! Ilona, bedankt voor alle hulp bij mijn dierexperimenten! Veel succes met je carrière in Amsterdam.

Dan mijn paranimfen, Debby en Chantal: lieve Debby, super leuk dat jij mijn paranimf wilt zijn! Ook al behoorde je tot de RSV-groep, je was gewoon een echte collega. Je was een erg gezellige buurvrouw, we hebben veel gelachen op het werk en daarbuiten. Ik miste wel een beetje jouw

vrolijkheid en gezelligheid toen jij een nieuwe baan kreeg en niet meer naast me zat. Leuk dat we elkaar nog regelmatig zien! Erg speciaal dat ik jouw zwangere paranimf was en dat het nu andersom is. Ik hoop dat we nog regelmatig gezellige dates hebben, binnenkort met z'n zessen! Lieve Chantal, bedankt dat jij mijn paranimf wilt zijn! Naast die mooie foto van Elmar in het academiegebouw, komt nu een mooie foto van jou te hangen. We zijn al 29 jaar vriendinnetjes, het voelt eigenlijk meer als familie, en we hebben al veel mooie en moeilijke momenten gedeeld. Eén van de mooie momenten was samen zwanger zijn en dat jij zo'n mooie lieve Tijme op de wereld heb gezet. Ik vind het heel fijn dat jij bij dit speciale moment voor mij bent. Ik hoop dat we nog ons hele leven veel gezellige dagjes-uit, etentjes, weekendjes-weg met z'n zessen (of meer) mogen hebben.

Dan de post-docs van het NIDOD-lab. Lieve Cora en Cindy, al heel wat jaartjes zijn we collega's. Op het werk, maar ook vooral daarbuiten is het altijd erg gezellig met jullie, bedankt! Cindy, heel veel succes in de VS! Ik hoop dat je je er snel thuis voelt en je gaat daar vast een hele mooie tijd tegemoet. We zullen al jouw kennis zeker gaan missen en natuurlijk ook jou als persoon. Cora, de nieuwe "mama" van de groep ☺. Ik heb er bewondering voor dat je begaan bent met iedereen en je zorgt daardoor ook mede voor een goede sfeer op het NIDOD-lab. Daarnaast vind ik het knap dat jij nu je eigen groepje aan het creëren bent. Ik weet zeker dat er voor jou behalve een spannende ook een mooie tijd aankomt. Ik hoop dat we nog lang collegaatjes zijn!

Lieve kamergenootjes, Hilde, Marcel, Elke, Vanessa, Emiel en Luca. Ik wens jullie veel succes met het afronden van jullie promotieonderzoek. Jullie zijn leuke collega's! Hilde, je bent een erg leuke en gezellige buurvrouw, hopelijk blijven we dat nog even. Je bent een slimme dokter en over een tijdje ook nog eens doctor! Succes met alles! Marcel, ook al ben je in je eentje de RSV-groep, wij zijn blij dat we je een beetje geadopteerd hebben met het NIDOD-lab. Succes met de laatste loodjes! Lieve Marijke en Lotte, ex-kamergenootjes, bedankt voor jullie interesse en gezelligheid. Marijke, bedankt voor het helpen met allerlei dingen; bestellingen, antibodies overzicht maken, promotiezaken regelen etc. Lotte, veel succes in het St. Antonius, nu lekker als doctor dokteren.

Lieve Jitske, Karima en Mirjam, al lange tijd dé analisten van het lab. Bedankt voor al jullie hulp! Jitske, jou mogen we wel de labgoeroe noemen! Je weet zoveel van bijna alle technieken en ook regelingen. Jij hebt mij wegwijs gemaakt op het lab en ik heb veel van je geleerd, enorm bedankt daarvoor! Bedankt voor alle kleuringen, er staan een aantal mooie door jouw gemaakte foto's in dit proefschrift. Nog eventjes en dan ga je genieten van je pensioen; wat zullen we jouw kennis en jou als persoon enorm gaan missen! Karima, wij zijn ongeveer tegelijk op het NIDOD-lab begonnen, dus ook wij zijn al een hele tijd collegaatjes, dat scheidt een bijzondere band! Je bent een leuke collega en ook regelmatig een gezellig reisgenootje. Mirjam, de laatste tijd ben je steeds vaker betrokken bij experimenten voor het pijnonderzoek. Bedankt dat je kunt helpen met de celkweken, transfecties, microscopie etc.

Ik heb aardig wat uurtjes doorgebracht op het GDL, iedereen bedankt voor het bijhouden van fokken, dieren verzorgen, bestellingen doen en helpen bij al mijn vragen. Vooral Anja, Manuela, Helma, Tamara, Herma en Sabine bedankt voor alles! Sabine, leuk dat jij nu mijn directe collega bent geworden. We zijn blij dat je nu op het NIDOD-lab werkt, hopelijk gaan we flink wat jaartjes samenwerken. Bedankt voor al jouw hulp!

Dan mijn ex-collegaatjes: lieve Jessica, je was een leuke en gezellige collega. Ik vind het daarom ook fijn dat we elkaar nog af en toe zien. Veel succes met je nieuwe baan! Beste Michael, wat was jij een goede sfeermaker in de groep! Wat heb ik veel met je gelachen! Volgens mij heb jij het goed naar je zin in Lausanne. Hopelijk zie ik je weer eens een keertje! Lieve Maike en Mirjam, dé psychologen van de groep, bedankt voor de leuke gesprekken en de gezellige tijd. Leuk dat ik

jullie nog soms tegenkom! Alle andere ex-collega's: Pieter, Mariska, Moniek, Noëline, Margarida, Linda, Esther, Michaël, Zabi, Anne, Paula en de rest, bedankt voor de gezelligheid op het werk, maar ook tijdens borrels, etentjes, bowlen, feestjes en de leuke ski-trip!

Koos, Pirkko, Nathalie, Wil, Gerda en Grada bedankt voor jullie interesse en de gezellige koffiepauzes.

Beste Joyce en Marjolein, bedankt voor de goede samenwerking. Er zijn interessante bevindingen gedaan en daardoor is er een mooie publicatie uitgekomen. Marjolein, succes met de laatste loodjes!

Dear Federico, Cristina, Rocio and Elisa, thank you for the nice collaboration! Cristina, I really appreciate that you are one of the opponents during my defence. Rocio, you are a nice colleague abroad. I enjoyed the times when you were in the Netherlands. I hope that everything goes well, and I wish you the best of luck with your research.

Dear XiaoJiao, Pooja, Mao, Benedict and Wenjun, thank you for the nice time in Urbana. Good luck with your scientific career in Houston! XiaoJiao and Mao, thank you for the good collaboration on the miR-124 manuscript.

Beste Mark en Stella, hopelijk heb ik jullie wat kunnen leren tijdens jullie stages. Naast het harde werken waren jullie ook erg sociale en gezellige studenten om in het lab te hebben. Succes met jullie verdere wetenschappelijke carrière.

Lieve vriendinnen, vrienden, familie en schoonfamilie, bedankt voor jullie interesse en de gezellige afspraken en gesprekken over ook niet werk gerelateerde dingen. Lieve ome Ad, door de vele gezellige werkbezoekjes in je atelier ben je voor mij een extra speciale oom. De ets v./v. V.V.? zie ik dagelijks en doet me denken aan allerlei verbanden uit mijn onderzoek. Bedankt dat ik deze mooie ets heb mogen gebruiken voor de omslag van mijn proefschrift.

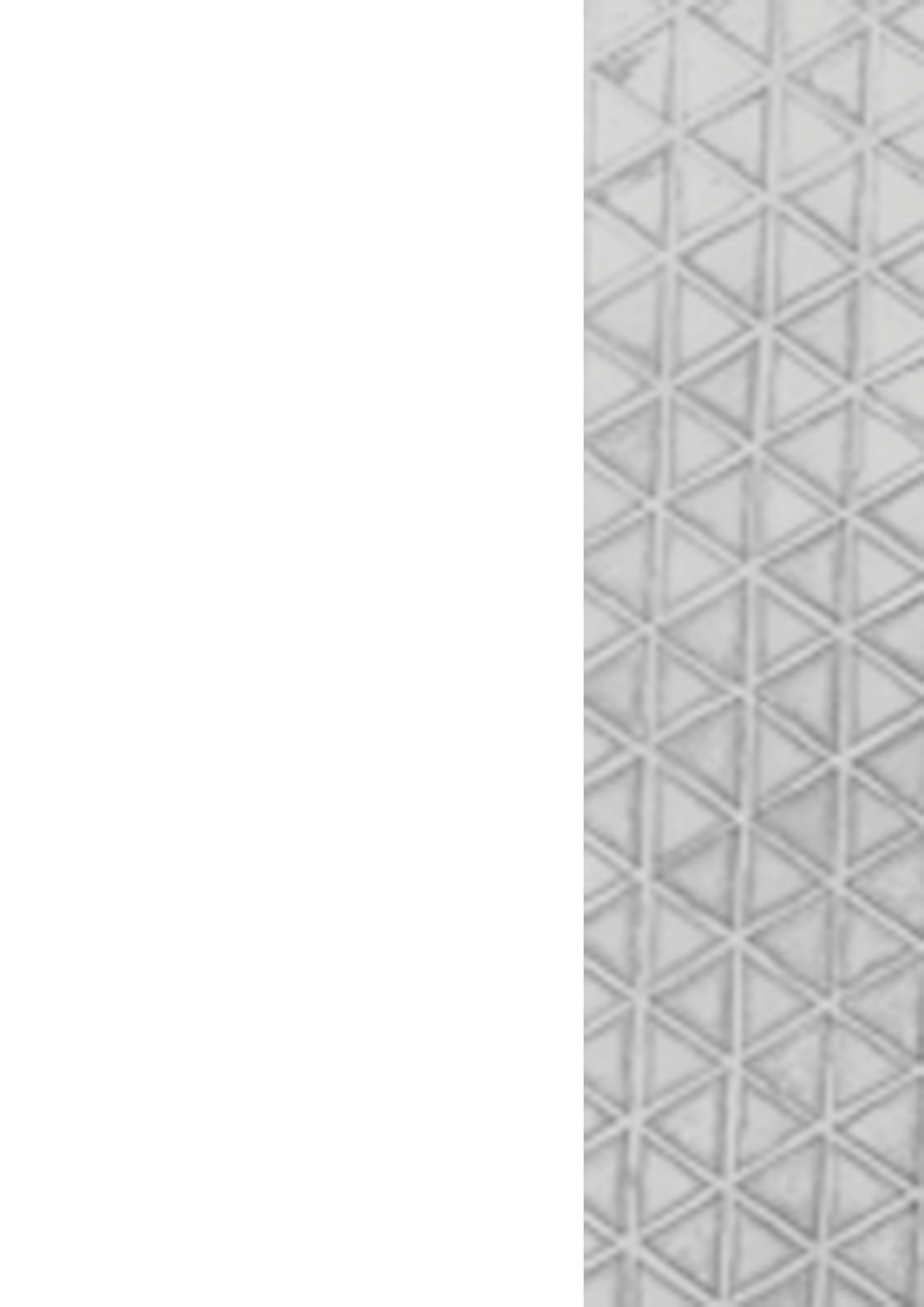
Wat heb ik een lieve en leuke broer en zus! Wieteke, ook al ben je altijd ver weg, ik spreek je gelukkig vaak via skype, zodat ik toch veel met je kan bespreken en wat promotietips kan krijgen. Zo blijven we toch goed op de hoogte van elkaar. Ik heb bewondering voor hoe je heel de wereld over reist en dat je van elke plek weer een thuis weet te maken. Joost, dan heb je dadelijk twee gepromoveerde zusjes, dat is wel heel apart! Maar eigenlijk ben jij natuurlijk de slimste van ons drietjes ☺. Schoonzusje Diana, het is altijd erg gezellig als ik jou en Joost weer zie, leuk dat jullie een mooi nestje gevonden hebben. Bedankt voor de indirecte connecties die je hebt gelegd met Harlan laboratories ☺.

Lieve pap en mam, bedankt dat jullie het mogelijk hebben gemaakt dat ik heb kunnen studeren. Eerst HBO daarna Universiteit, jullie vonden het allemaal goed en stimuleerden het alleen maar. Bedankt voor het zelfvertrouwen dat jullie mij hebben geven en voor de interesse in mijn onderzoek. Ik weet dat jullie trots op me zijn en dat geeft een fijn gevoel. Jullie zijn hele lieve (o)ma en (o)pa! Pap, in het bijzonder wil ik jou nog bedanken. Op school was ik er niet altijd met mijn gedachten bij, maar jij legde het een en ander thuis gewoon nog eens uit. Van Engels tot biologie; overal kon je mij wat over leren. Wat heb ik toch een slimme pap. Ook niet te vergeten zijn de overhoringen over aardrijkskunde; zonder jou zou het nu nog steeds mis gaan met "elders zijn woestijnen... ". Pap, je hebt een hele belangrijke rol gespeeld in mijn basiskennis op vele vlakken. Zelfs nu ik bijna gepromoveerd ben, ben je nog steeds een hele goede helpdesk, vooral op taalgebied. Bedankt!

Lieve Elise, wat is het leven nog mooier nu jij er bent! Na het harde werken is het heel fijn om thuis te komen en jouw mooie lach te zien. Ga maar alvast oefenen met je eerste woordjes: dr. Papa & dr. Mama.

Lieve Ruud, wat heb ik het getroffen met zo'n leuke en lieve man! Ook jij hebt me gestimuleerd om te promoveren, want jij vond dat toen zo'n geweldige periode. Bedankt dat je de laatste weekjes met mijn proefschrift hebt geholpen door teksten na te kijken, mee te helpen met de discussiefiguur en uiteindelijk alles te lay-outen! Vooral de laatste avondjes en weekenden waren druk, maar het resultaat is mooi geworden! Super bedankt en jij hebt het zeker verdiend om in mijn dankwoord te staan 😊. Bedankt voor al jouw liefde en steun! Kouvanjou!

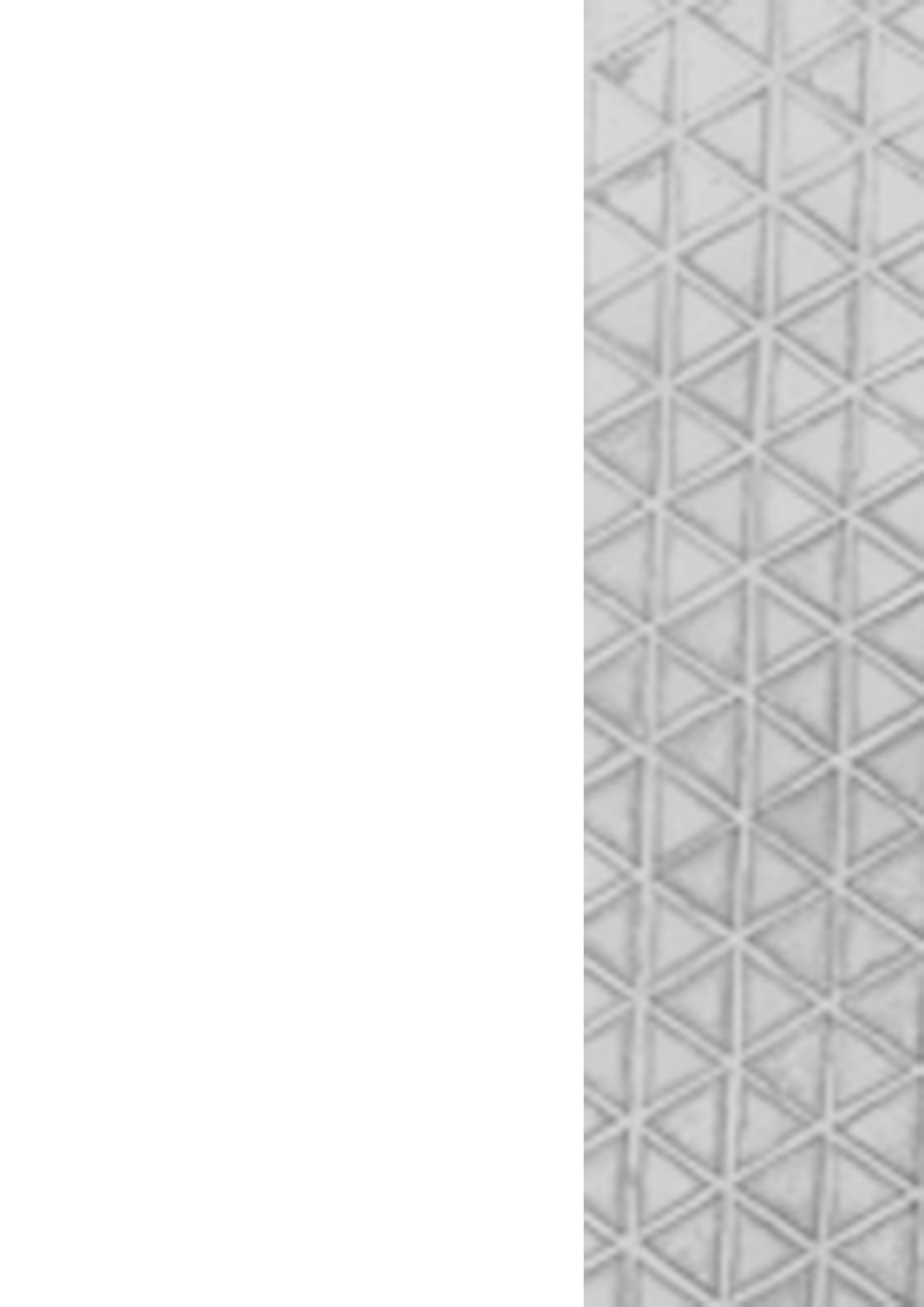
Hanneke, februari 2013



List of publications

1. Brouns SJ, Turnbull AP, **Willemen HLDM**, Akerboom J, van der OJ: Crystal structure and biochemical properties of the D-arabinose dehydrogenase from *Sulfolobus solfataricus*. *J Mol Biol* 2007, 371:1249-1260.
2. Brouns SJ, Walther J, Snijders AP, van de Werken HJ, **Willemen HLDM**, Worm P, de Vos MG, Andersson A, Lundgren M, Mazon HF et al.: Identification of the missing links in prokaryotic pentose oxidation pathways: evidence for enzyme recruitment. *J Biol Chem* 2006, 281:27378-27388.
3. Eijkelkamp N, Heijnen CJ, Carbajal AG, **Willemen HLDM**, Wang H, Minett MS, Wood JN, Schedlowski M, Dantzer R, Kelley KW et al.: GRK6 acts as a critical regulator of cytokine-induced hyperalgesia by promoting PI3kinase- and inhibiting p38-signaling. *Mol Med* 2012.
4. Eijkelkamp N, Heijnen CJ, **Willemen HLDM**, Deumens R, Joosten EAJ, Kleibeuker W, den Hartog IJM, van Velthoven CTJ, Nijboer CH, Nassar MA et al.: GRK2: a Novel Cell Specific Regulator of Severity and Duration of Inflammatory Pain. *J Neurosci* 2010.
5. Eijkelkamp N, Wang H, Garza-Carbajal A, **Willemen HLDM**, Zwartkruis FJ, Wood JN, Dantzer R, Kelley KW, Heijnen CJ, Kavelaars A: Low nociceptor GRK2 prolongs prostaglandin E2 hyperalgesia via biased cAMP signaling to Epac/Rap1, protein kinase Cepsilon, and MEK/ERK. *J Neurosci* 2010, 30:12806-12815.
6. Kavelaars A, Eijkelkamp N, **Willemen HLDM**, Wang H, Carbajal AG, Heijnen CJ: Microglial GRK2: a novel regulator of transition from acute to chronic pain. *Brain Behav Immun* 2011, 25:1055-1060.
7. Nijboer CH, Gressens P, **Willemen HLDM**, Degos V, Heijnen CJ, Kavelaars A. Astrocyte GRK2 as a novel regulator of glutamate transport and brain damage. *Neurobiology of Disease*, 2013.
8. Nijboer CH, Heijnen CJ, **Willemen HLDM**, Groenendaal F, Dorn GW, van BF, Kavelaars A: Cell-specific roles of GRK2 in onset and severity of hypoxic-ischemic brain damage in neonatal mice. *Brain Behav Immun* 2010, 24:420-426.
9. Riether C, Kavelaars A, Wirth T, Pacheco-Lopez G, Doenlen R, **Willemen HLDM**, Heijnen CJ, Schedlowski M, Engler H: Stimulation of beta-adrenergic receptors inhibits calcineurin activity in CD4(+) T cells via PKA-AKAP interaction. *Brain Behav Immun* 2011, 25:59-66.
10. van Velthoven CTJ, Sheldon RA, Kavelaars A, Derugin N, Vexler ZS, **Willemen HLDM**, Maas MM, Heijnen CJ, Ferriero DM. Mesenchymal stem cell transplantation attenuates brain injury after neonatal stroke. 2013. Submitted
11. van Zuiden M, Geuze E, **Willemen HLDM**, Vermetten E, Maas M, Amarouchi K, Kavelaars A, Heijnen CJ: Glucocorticoid receptor pathway components predict posttraumatic stress disorder symptom development: a prospective study. *Biol Psychiatry* 2012, 71:309-316.
12. van Zuiden M, Geuze E, **Willemen HLDM**, Vermetten E, Maas M, Heijnen CJ, Kavelaars A: Pre-existing high glucocorticoid receptor number predicting development of posttraumatic stress symptoms after military deployment. *Am J Psychiatry* 2011, 168:89-96.

13. Wang H, Heijnen CJ, van Velthoven CTJ, **Willemen HLDM**, Ishikawa Y, Vroon A, Eijkelkamp N, Kavelaars A. Targeting the GRK2-Epac1 ratio to prevent transition to chronic pain. 2013. Submitted
14. **Willemen HLDM**, Campos PM, Lucas E, Morreale A, Gil-Redondo R, Agut J, Gonzalez F, Ramos P, Mayor F, Jr., Heijnen CJ et al.. A novel p38 MAPK docking groove-targeted compound is a potent inhibitor of inflammatory hyperalgesia. 2013. Submitted
15. **Willemen HLDM**, Eijkelkamp N, Carbajal AG, Wang H, Mack M, Zijlstra J, Heijnen CJ, Kavelaars A. Peripheral monocytes/macrophages control resolution of inflammatory pain. 2013. Submitted
16. **Willemen HLDM**, Eijkelkamp N, Wang H, Dantzer R, Dorn GW, Kelley KW, Heijnen CJ, Kavelaars A: Microglial/macrophage GRK2 determines duration of peripheral IL-1beta-induced hyperalgesia: contribution of spinal cord CX3CR1, p38 and IL-1 signaling. *Pain* 2010, 150:550-560.
17. **Willemen HLDM**, Huo XJ, Mao-Ying QL, Zijlstra J, Heijnen CJ, Kavelaars A: MicroRNA-124 as a novel treatment for persistent hyperalgesia. *J Neuroinflammation* 2012, 9:143.
18. **Willemen HLDM**, Peters MJ, Broer L, Eiriksdottir G, Hocking LJ, Holliday KL, Horan MA, Meulenbelt I, Neogi T, Popham M et al.: Genome-wide association study meta-analysis of chronic widespread pain: evidence for involvement of the 5p15.2 region. *Ann Rheum Dis* 2012.



| Curriculum Vitae

Hanneke Willemen was born on March 21th, 1982 in Den Bosch, the Netherlands. In 2000 she graduated secondary school (HAVO) at the Sint-Janslyceum in 's-Hertogenbosch and started studying Laboratory science at Larenstein University of professional education in Velp. An internship was done to investigate novel proteins in vegetables and fruit (confidential) at ATO Institute in Wageningen under supervision of Ing. Mark Sanders. For her Bachelor thesis she studied D-arabinose metabolism of *Sulfolobus solfataricus* at the department Microbiology at the University of Wageningen under supervision of Dr. Ir. Stan Brouns. In 2004, she obtained her Bachelor of Science degree with specializations in Biotechnology. In the same year she started the Master Biotechnology at Wageningen University. For her Master's thesis she investigated the functional analysis of six unique genes of *Helicoverpa armigera* nucleopolyhedrovirus at the department of Virology at the University of Wageningen under the supervision of Dr. Ir. Marcel Westenberg. In June 2006 she received her Master's degree with specialization Cellular/molecular research.

In May 2006 she started working as a research technician at the Laboratory of Neuroimmunology and Developmental Origins of Disease (NIDOD) at the Wilhelmina Children's Hospital, part of University Medical Centre Utrecht. After 1.5 year working as research technician she started her PhD-project to study neurobiological mechanisms underlying the transition from acute to chronic inflammation-induced pain under supervision of Prof. Dr. Cobi Heijnen, Prof. Dr. Annemieke Kavelaars, and Dr. Niels Eijkelkamp. The results of her PhD-project are described in this PhD-thesis and have been published in various international scientific journals.

